ISSN 1949-8454 (online)

World Journal of *Biological Chemistry*

World J Biol Chem 2022 January 27; 13(1): 1-34

Published by Baishideng Publishing Group Inc

WJBC

World Journal of Biological Chemistry

Contents

Bimonthly Volume 13 Number 1 January 27, 2022

MINIREVIEWS

ORIGINAL ARTICLE

Basic Study

World Journal of Biological Chemistry

Bimonthly Volume 13 Number 1 January 27, 2022

Contents

ABOUT COVER

Editorial Board Member of *World Journal of Biological Chemistry*, Jean Demarquoy, PhD, Professor, Department of Physiology, Université de Bourgogne, UMR PAM université de Bourgogne/Agrosup Dijon, 21000 Dijon, France. jean.demarquoy@u-bourgogne.fr

AIMS AND SCOPE

The primary aim of the *World Journal of Biological Chemistry* (*WJBC*, *World J Biol Chem*) is to provide scholars and readers from various fields of biological chemistry a platform to publish high-quality basic and clinical research articles and communicate their research findings online.

WJBC mainly publishes articles reporting research results and findings obtained in the field of biological chemistry and covering a wide range of topics including bioenergetics, cell biology, chromosomes, developmental biology, DNA, enzymology, extracellular matrices, gene regulation, genomics, glycobiology, immunology, lipids, membrane biology, metabolism, molecular bases of disease, molecular biophysics, neurobiology, plant biology, protein structure and folding, protein synthesis and degradation, proteomics, and signal transduction.

INDEXING/ABSTRACTING

The *WJBC* is now abstracted and indexed in PubMed, PubMed Central, China National Knowledge Infrastructure (CNKI), China Science and Technology Journal Database (CSTJ), and Superstar Journals Database.

RESPONSIBLE EDITORS FOR THIS ISSUE

NAME OF JOURNAL
World Journal of Biological Chemistry

ISSN
ISSN 1949-8454 (online)

LAUNCH DATE
July 26, 2010

FREQUENCY
Bimonthly

PUBLICATION DATE
January 27, 2022

World Journal of Biological Chemistry

Submit a Manuscript: https://www.f6publishing.com

World J Biol Chem 2022 January 27; 13(1): 1-14

DOI: 10.4331/wjbc.v13.i1.1

ISSN 1949-8454 (online)

MINIREVIEWS

Current understanding of the role of tyrosine kinase 2 signaling in immune responses

Ryuta Muromoto, Kenji Oritani, Tadashi Matsuda

ORCID number: Ryuta Muromoto 0000-0002-7474-493X; Kenji Oritani 0000-0002-5571-2457; Tadashi Matsuda 0000-0002-3089-3757.

Author contributions: Muromoto R, Oritani K and Matsuda T participated sufficiently in this work of drafting the article and/or revising the article for the important rational content; all authors gave final approval of the version to be submitted.

Conflict-of-interest statement: Authors declare no conflict of interests for this article.

Supported by Grant-in-Aid for scientific research from Ministry of Education, Culture, Sports, Science and Technology of Japan, No. 19H03364 and No. 20K07010.

Country/Territory of origin: Japan

Specialty type: Immunology

Provenance and peer review: Invited article; Externally peer reviewed.

Peer-review model: Single blind

Peer-review report's scientific quality classification

Grade A (Excellent): 0
Grade B (Very good): 0
Grade C (Good): C
Grade D (Fair): 0

Ryuta Muromoto, Tadashi Matsuda, Department of Immunology, Graduate School of Pharmaceutical Sciences, Hokkaido University, Sapporo 060-0812, Japan

Kenji Oritani, Department of Hematology, International University of Health and Welfare, Narita 286-8686, Japan

Corresponding author: Tadashi Matsuda, PhD, Professor, Department of Immunology, Graduate School of Pharmaceutical Sciences, Hokkaido University, Kita-ku Kita12 Nishi 6, Sapporo 060-0812, Japan. tmatsuda@pharm.hokudai.ac.jp

Abstract

Immune system is a complex network that clears pathogens, toxic substrates, and cancer cells. Distinguishing self-antigens from non-self-antigens is critical for the immune cell-mediated response against foreign antigens. The innate immune system elicits an early-phase response to various stimuli, whereas the adaptive immune response is tailored to previously encountered antigens. During immune responses, B cells differentiate into antibody-secreting cells, while naïve T cells differentiate into functionally specific effector cells [T helper 1 (Th1), Th2, Th17, and regulatory T cells]. However, enhanced or prolonged immune responses can result in autoimmune disorders, which are characterized by lymphocyte-mediated immune responses against self-antigens. Signal transduction of cytokines, which regulate the inflammatory cascades, is dependent on the members of the Janus family of protein kinases. Tyrosine kinase 2 (Tyk2) is associated with receptor subunits of immune-related cytokines, such as type I interferon, interleukin (IL)-6, IL-10, IL-12, and IL-23. Clinical studies on the therapeutic effects and the underlying mechanisms of Tyk2 inhibitors in autoimmune or chronic inflammatory diseases are currently ongoing. This review summarizes the findings of studies examining the role of Tyk2 in immune and/or inflammatory responses using *Tyk2*-deficient cells and mice.

Key Words: Tyrosine kinase 2; Cytokines; Signal transduction; Immune system; Inflammation

Grade E (Poor): 0

Received: March 27, 2021
Peer-review started: March 27, 2021
First decision: July 27, 2021
Revised: August 6, 2021
Accepted: December 22, 2021
Article in press: December 22, 2021
Published online: January 27, 2022

P-Reviewer: Todorovic-Rakovic N
S-Editor: Liu M
L-Editor: A
P-Editor: Liu M

Core Tip: Studies on murine *tyrosine kinase 2 (Tyk2)*-deficient models were reviewed to examine the role of Tyk2 dysregulation in human diseases. *Tyk2*-deficient mice exhibit reduced responses in several interleukin-12 (IL-12)/Th1- and IL-23/Th17-mediated models of diseases, including rheumatoid arthritis, multiple sclerosis, inflammatory bowel diseases, psoriasis, sarcoidosis, and delayed-type hypersensitivity. These findings demonstrate a broad contribution of Tyk2 to immune responses. Tyk2 represents a candidate for drug development by targeting both the IL-12/Th1 and IL-23/Th17 axes.

Citation: Muromoto R, Oritani K, Matsuda T. Current understanding of the role of tyrosine kinase 2 signaling in immune responses. *World J Biol Chem* 2022; 13(1): 1-14
URL: https://www.wjgnet.com/1949-8454/full/v13/i1/1.htm
DOI: https://dx.doi.org/10.4331/wjbc.v13.i1.1

INTRODUCTION

Cytokines function as effectors and regulate the proliferation, differentiation, and functions of immune cells and consequently aid in the clearance of invading pathogens. However, cytokines are also involved in the onset and development of autoimmune diseases[1]. Cytokine-specific cell surface receptors exhibit conformational changes upon activation, which result in activation of the Janus family of protein tyrosine kinases (Jaks). Activated Jaks promote the recruitment and phosphorylation of the transcription factor signal transducer and activator of transcription (STAT). Nuclear translocation of activated STATs induces the expression of cytokine-responsive genes. Thus, the Jak-STAT pathway transduces signals from various cytokine receptor superfamily members[2-4].

The Jak family comprises Jak1, Jak2, Jak3, and tyrosine kinase 2 (Tyk2), which are activated by distinct cytokines[2-4]. Jak1 binds to interferon (IFN), interleukin (IL)-6, and IL-10 receptors that contain a common γ chain and gp130 subunit, while Jak2 binds to IL-3 and erythropoietin, growth hormone, and prolactin hormone-like receptors. Tyk2 binds to IFN, IL-12, and IL-23 receptors. Jak3, whose expression is localized to hematopoietic cells, binds exclusively to receptors that contain common γ chains along with Jak1. Moreover, *Jak1* deficiency in mice results in perinatal lethality and impaired lymphocyte development[5]. The embryonic lethality in *Jak2*-deficient mice is attributed to insufficient definitive erythropoiesis[6]. *Jak3* deficiency results in dysfunctional mature T and B lymphocytes and leads to severe combined immunodeficiency[7,8]. Although *Tyk2*-deficient mice are viable, they are susceptible to viral infections[9,10].

Previous studies using experimental models, such as *Tyk2*-deficient mice have demonstrated that Tyk2 primarily functions in the IL-12 and IFN-α/β signaling pathways[9,10]. In humans, a mutation in *TYK2*, which causes an autosomal recessive form of hyper IgE syndrome (AR-HIES), affects the IL-23, IL-10, and IL-6 signal transduction pathways (Figure 1)[11]. Tyk2 is involved in both innate and acquired immunity. Here, the current knowledge on the involvement of Tyk2 in immune responses has been reviewed, and the potential clinical applications of Tyk2 inhibitors have been discussed.

ROLE OF TYK2 IN INFLAMMATORY RESPONSES

IFN system

Tyk2 was originally identified as a protein kinase that can compensate for the loss of IFN response in mutant fibroblasts[12]. IFN-α specifically activates Tyk2 and Jak1, which leads to the phosphorylation of STAT1 and STAT2 and the dimerization of activated STATs. The nuclear translocation of dimerized STATs induces the expression of target genes[3,13].

Type I IFNs are constitutively expressed in various cells, including macrophages. Although the constitutive expression of type I IFNs is low, they can regulate physiological cellular functions in an autocrine or a paracrine manner[14,15]. Tyk2

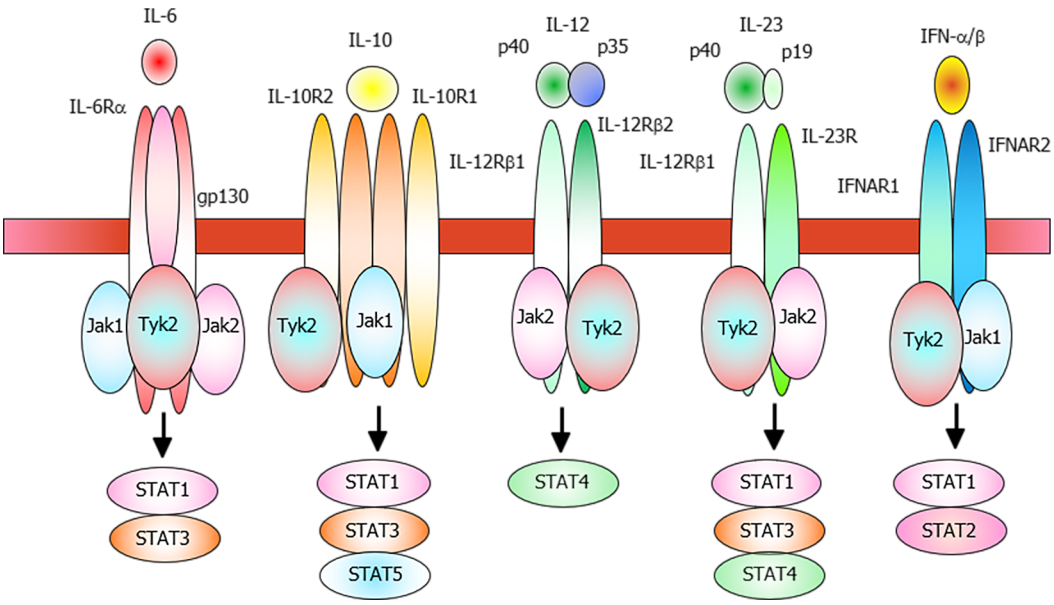

Figure 1 Schematic representation of the tyrosine kinase 2-related cytokine receptors. The IL-6 receptor, which comprises IL6RA (gp80) and IL6RB (gp130) subunits, activates signal transducer and activator of transcription (STAT)1 and STAT3 through interactions with Tyrosine kinase 2 (Tyk2), Janus family of protein tyrosine kinases 1 (Jak1), and Jak2. The IL-10 receptor, which comprises IL-10R1 and IL10-R2 subunits, activates STAT1, STAT3, and STAT5 through interactions with Tyk2 and Jak1. IL-12 is a heterodimeric cytokine comprising the IL-12p35 and IL-12p40 subunits. The IL-12 receptor, which comprises IL-12Rβ1 and IL-12Rβ2, mainly activates STAT4 through interactions with Tyk2 and Jak2. The IL-12p40 component of IL-23 can dimerize with IL-23p19 to form IL-23. The IL-23 receptor, which comprises IL-12Rβ1 and IL-23R subunits, activates STAT1, STAT3, and STAT4 through interactions with Tyk2 and Jak2. The type I IFN receptor, which comprises IFNAR1 and IFNAR2 subunits, activates STAT1 and STAT2 through interactions with Tyk2 and Jak1. STAT: Signal transducer and activator of transcription; Tyk2: Tyrosine kinase 2; Jak1: Janus family of protein tyrosine kinases 1.

promotes the constitutive production of type I IFNs in macrophages under steady-state conditions, as well as during the innate immune responses against bacterial components. The basal and lipopolysaccharide (LPS)-induced expression levels of type I IFN are dysregulated in *Tyk2*-deficient macrophages[16]. Moreover, *Tyk2*-deficient and *Ifnb*-deficient mice are resistant to high-dose LPS-induced lethal septic shock[16, 17]. Additionally, the expression of type I IFN-responsive genes, especially under steady-state conditions, was downregulated in *Tyk2*-deficient macrophages[18]. Therefore, Tyk2 is partially involved in macrophage activation by regulating autocrine and/or exogenous IFN production in the neighboring immune cells.

IL-12 and IL-23 systems

Helper T cells can be classified into the following two subsets based on their cytokine profiles: T helper 1 (Th1) and Th2 cells[19]. IL-12 and IL-4 promote the differentiation of naïve $CD4^+$ T cells into Th1 cells and Th2 cells, respectively. Heterodimeric IL-12 comprises covalently linked p35 and p40 subunits. Both IL-12 and IL-23 comprise the p40 subunit[20]. IL-23 (comprising p40 and unique p19 subunits) promotes the differentiation of Th17 cells, which secrete the effector cytokines IL-17, IL-21, and IL-22[21, 22]. Th17 cells can promote enhanced inflammatory responses to eliminate microbial pathogens. However, Th17 cells are considered highly pathogenic as excessive and prolonged activation of Th17 cells can result in autoimmune and inflammatory disorders, including inflammatory bowel diseases (IBD) and rheumatoid arthritis (RA), in humans (Figure 2)[21,22].

The activation of IL-12 receptor, which is associated with Tyk2 and Jak2, activates STAT4[23,24]. Phosphorylated Stat4 along with signals from the activated T cell receptor induces the expression of T-bet, which is a master transcriptional factor for Th1 differentiation[25]. IL-23, whose receptor is associated with Tyk2, induces the proliferation, survival, and functional maturation of Th17 cells[22,26] although Th17 cell differentiation is dependent on signals from TGF-β and IL-6 (Figure 3)[22]. STAT3, a major downstream effector of the Th17-related cytokine pathway, is critical for commitment to the Th17 Lineage, whereas STAT4 and STAT6 are essential for commitment to the Th1 and Th2 Lineages, respectively[27,28]. Additionally, *Tyk2*-deficient macrophages do not produce nitric oxide in response to LPS stimulation[16]. *Tyk2*-deficient dendritic cells do not produce IL-12 and IL-23 upon stimulation with CpG oligodeoxynucleotides and consequently cannot induce Th1 cell differentiation

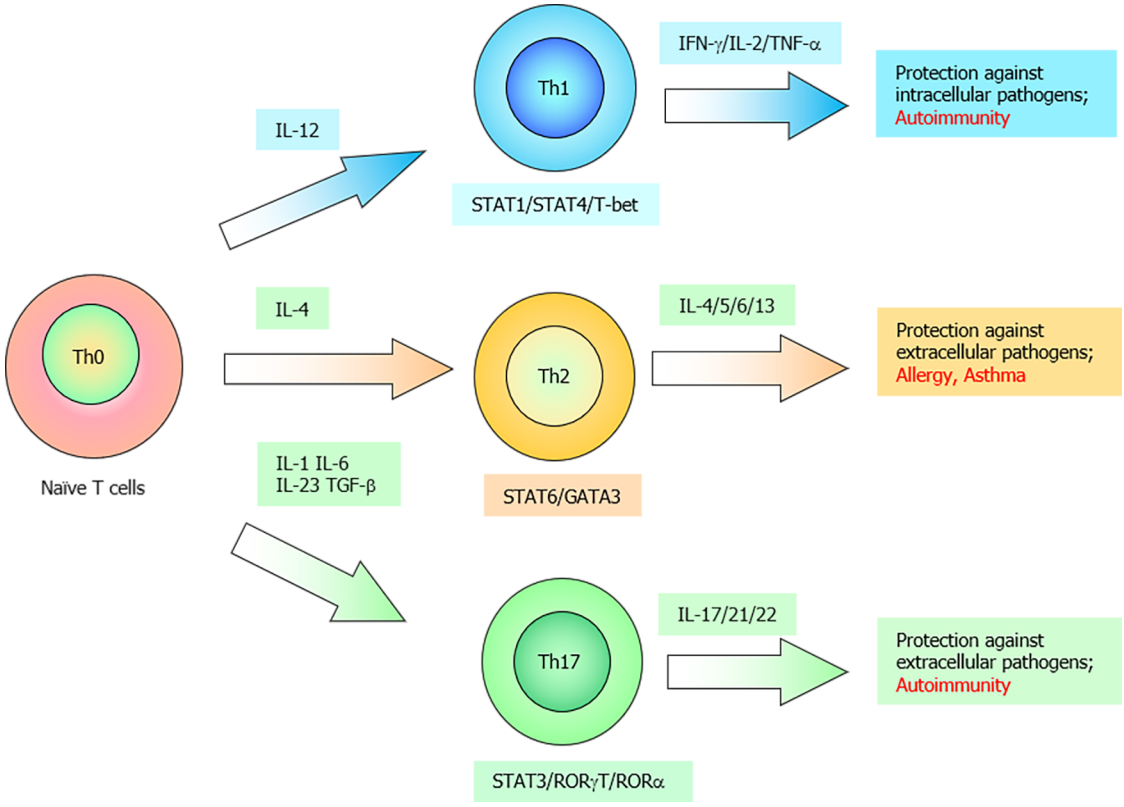

Figure 2 Schematic representation of naïve T cell differentiation into T helper 1, T helper 2, or T helper 17 cells depending on the cytokine profile. IL-12 promotes the differentiation of naïve T cells into Th1 cells. Th1 cells promote the clearance of intracellular pathogens and induce autoimmunity through the production of IFN-γ, IL-2, and TNF-α. Th1 differentiation is regulated by transcription factors such as signal transducer and activator of transcription (STAT)1, STAT4, and T-bet. IL-4 promotes the differentiation of naïve T cells into Th2 cells. Th2 cells promote the clearance of extracellular pathogens and induce allergic responses through the production of IL-4, IL-5, IL-6, and IL-13. Th2 differentiation is regulated by transcription factors such as STAT6 and GATA3. TGF-β, IL-6, and IL1 promote the differentiation of naïve T cells into Th17 cells, while IL-23 can maintain the Th17 phenotype. Th17 cells promote the clearance of extracellular pathogens and induce autoimmunity through the production of IL-17, IL-21, and IL-22. Th2 differentiation is regulated by transcription factors, such as STAT3, RORγt and RORα.

[29]. Therefore, Tyk2 is involved in the host defense response by regulating the production and function of both Th1 and Th17 cells.

Inhibitory effects of type I IFNs on B lymphopoiesis are mediated through the TYK2-DAXX axis

Interactions between IFN-α and its receptor promote potent antiviral and antiproliferative activities against the target cells[3,4]. IFN-α stimulation specifically activates Tyk2 and Jak1, which leads to the phosphorylation of STAT1 and STAT2. Nuclear translocation of phosphorylated STATs (in the form of homodimers or heterodimers) promotes target gene expression[3,4]. *Jak1*-deficient cells are not responsive to IFN-α stimulation[30], whereas *Tyk2*-deficient cells cannot inhibit lymphocyte growth[31]. Additionally, *Stat1*-deficient mice do not respond to IFN-α simulation[32,33], while *Stat2*-deficient mice are highly susceptible to viral infections[34].

Analysis of the colony forming unit (CFU) of bone marrow cells in the presence of IL-7 is a powerful tool to evaluate the growth capacity of B lymphocyte progenitors [35]. The CFU values of bone marrow cells in the presence of IL-7 were not markedly different between wild-type (WT) and *Tyk2*-deficient mice, which indicated that Tyk2 did not affect the number of IL-7-responsive B lymphocyte progenitors under steady-state conditions[31]. IFN-α, which is a potent inhibitor of IL-7-dependent growth of B lymphocyte progenitors, effectively inhibits B lymphocyte differentiation at the pro-B cell stage[36]. The CFU values of WT bone marrow cells in the presence of IL-7 markedly decreased upon stimulation with IFN-α. In contrast, the CFU values of *Tyk2*-deficient bone marrow cells in the presence of IL-7 did not decrease upon stimulation with IFN-α[31]. The knockout of *Tyk2* completely inhibited the IFN-α -induced elevation and nuclear accumulation of death-associated protein (Daxx)[31]. Daxx was originally identified as a Fas-binding protein[37] and it plays crucial roles in the type I IFN-induced growth suppression of B lymphocyte progenitors[38]. One study used the

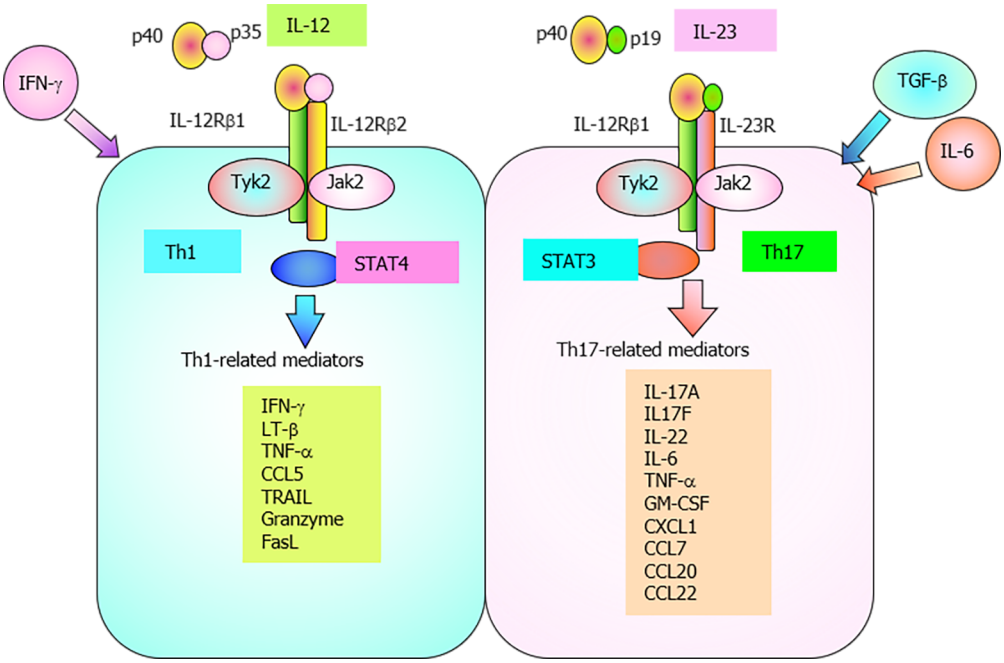

Figure 3 Illustration of interleukin-12 and interleukin-23, as well as their receptors and downstream signaling pathways. IL-12 and IL-23 share the p40 subunit, while their receptors share the IL-12Rβ1 subunit. The binding of IL-12 to its receptor induces the activation of Jak2 and Tyrosine kinase 2 (Tyk2), which results in signal transducer and activator of transcription (STAT)4 phosphorylation. Activated STAT4 promotes the differentiation of naïve Th cells into Th1 cells, which subsequently produce IFN-γ that is required for the development of Th1 immune response. The binding of IL-23 to its receptor induces the activation of Jak2 and Tyk2, which results in STAT3 phosphorylation. IL-23 induces the expression of IL-17A, IL-17F, and/or IL-22 and stabilizes Th17 cells. STAT: Signal transducer and activator of transcription.

sumoylation-defective Daxx KA mutant (Daxx K630/631A) to investigate the involvement of Daxx in decreasing the growth of Ba/F3 pro-B cells in the presence of IL-7 through IFN-α. The study demonstrated that Daxx KA is localized to the cytoplasm, whereas Daxx WT is localized to the nucleus[39]. Moreover, overexpression of Daxx KA conferred resistance to IFN-α -induced growth inhibition in a murine pro-B cell line Ba/F3. Treating Daxx KA-expressing Ba/F3 cells with leptomycin B, an exportin inhibitor, enhanced the nuclear localization of Daxx KA, and the growth of the cells was suppressed upon stimulation with IFN-α. Additionally, Daxx KA binds only weakly to promyelocytic leukemia protein (PML), which aids in the nuclear localization of Daxx. Conversely, overexpression of PML promotes the recruitment of Daxx to the PML nuclear bodies. A fusion protein comprising Daxx and a small ubiquitin-related modifier enhances the nuclear localization of Daxx and inhibits Ba/F3 cell growth. This indicates that IFN-α -induced inhibition of B lymphocyte progenitor growth requires nuclear localization of Daxx, which is dependent on sumoylation and interactions with PML. Therefore, the Tyk2-Daxx axis plays an essential role in IFN-α -induced growth inhibition of B lymphocyte progenitors.

PATHOLOGICAL SIGNIFICANCE OF TYK2 IN IMMUNE AND INFLAMMATORY DISEASES: DATA FROM MURINE EXPERIMENTAL MODELS

RA

RA is associated with joint inflammation and pain owing to a runaway immune system that elicits immune responses against the synovium of the joints of the hands, knees, or ankles. Murine experimental models for arthritis have provided useful information on various cellular and molecular mechanisms associated with RA[40].

Collagen-induced arthritis (CIA) mice are widely utilized as an experimental model for human RA[41]. Development of arthritis involves the production of autoantibodies in response to collagen and the subsequent inflammatory response against joints. Mice harboring *Tyk2* polymorphisms exhibit differential susceptibility to CIA[42,43]. B10.Q/Ai mice are highly susceptible to CIA, whereas B10.D1 mice are resistant. This suggests that *Tyk2* deficiency results in the defined clinical RA.

Monitoring of the inflammatory response in the anti-type II collagen (CII) antibody-induced arthritis (CAIA) experimental model provides useful information on the mechanisms of RA[44]. *Tyk2*-deficient mice are highly resistant to the development of CAIA. Histological analysis has revealed that *Tyk2* deficiency downregulated the inflammatory cell infiltration into the synovium[45]. Additionally, the production of IFN-γ, tumor necrosis factor (TNF)-α, IL-6, and matrix metalloproteinases (MMPs) was severely impaired in *Tyk2*-deficient mice[45]. TNF-α and IL-6, which are secreted by macrophages, function as pro-inflammatory cytokines in the CAIA model. MMPs, which are expressed in chondrocytes, synoviocytes, and macrophages, are reported to be involved in the degradation and damage of articular cartilage[46,47]. *Tyk2*-deficient macrophages cannot produce nitric oxide in response to LPS stimulation. Meanwhile, *Tyk2*-deficient dendritic cells cannot produce IL-12 and IL-23 in response to CpG oligodeoxynucleotides[29]. The potential mechanisms were analyzed using the anti-CII monoclonal antibody, which induced the phosphorylation of STAT3 and STAT4 in the draining lymph node cells. Phosphorylated STAT3 and STAT4 were detected in WT but not in *Tyk2*-deficient mice[45]. This suggests that Tyk2 promotes the production and downstream signaling of Th1/Th17-related cytokines, which are activated through STAT3 and STAT4.

Tyk2 deficiency markedly decreased the susceptibility to arthritis development in both CIA and CAIA murine models, which indicated that Tyk2 plays an important role in adaptive autoimmunity and inflammatory responses. Therefore, Tyk2 regulates multiple steps involved in the onset and development of RA.

Multiple sclerosis

Multiple sclerosis (MS) is characterized by the lack of myelin, a protective sheath covering nerve fibers, which leads to disruption of the communication between the brain and other tissues[48]. Patients with MS exhibit various symptoms, such as difficulty in walking and balancing, muscle weakness and spasticity, and loss of concentration and memory. The murine experimental autoimmune encephalomyelitis (EAE) model, which is an animal model for human MS, is triggered by immunization with myelin antigens or by the adoptive transfer of myelin-specific $CD4^+$ effector cells [49]. *Tyk2*-deficient mice exhibit decreased clinical scores and limited lymphocyte infiltration into the inflamed central nervous system[50]. The involvement of Tyk2 in EAE was confirmed using mice harboring different *Tyk2* polymorphisms. B10.D1 mice, which harbor the *Tyk2A* allele, are resistant to EAE development. The insufficient responses can be compensated by one copy of the *Tyk2G* allele from B10.Q/Ai mice [51].

IBD

Crohn's disease is characterized by inflammation of the digestive tract. Patients with Crohn's disease exhibit severe diarrhea, abdominal pain, fatigue, weight loss, and malnutrition[52]. Dextran sulfate sodium (DSS)-induced colitis, a mouse model for human Crohn's disease, is generated by supplementing mice with DSS through drinking water. The disease activity index and histological score were assessed using the combined scores of weight loss, consistency, and bleeding and acute clinical symptoms with diarrhea and/or extremely bloody stools[53]. Compared with that in WT DSS-induced colitis mice, disease development was delayed in *Tyk2*-deficient DSS-induced colitis mice[45]. Oral supplementation of DSS activates intestinal macrophages, which leads to enhanced production of inflammatory cytokines and chemokines. Subsequently, lymphocytes are recruited to the inflammatory sites and elicit Th1 and/or Th17 responses. During this inflammatory process, Tyk2 can regulate the functions of macrophages and dendritic cells, as well as the Th1 and Th17 responses. Indeed, the mRNA levels of DSS-induced Th1 cell-related or Th17 cell-related cytokines were significantly downregulated in the colon tissues of *Tyk2*-deficient mice [45]. A genome-wide association study identified *Tyk2* as a Crohn's disease susceptibility locus[54].

Ulcerative colitis is characterized by inflammation and ulcers in the large intestine and rectum. Patients with ulcerative colitis exhibit diarrhea with bloody stool, abdominal pain, fever, and body weight loss[55]. To model human ulcerative colitis in mice, 2,4,6-trinitrobenzene sulfonic acid (TNBS) is used[45]. WT mice treated with TNBS die within 3 days due to the induction of massive colitis. However, approximately 50% of *Tyk2*-deficient mice survive after treatment with TNBS. Additionally, the bodyweight of the surviving mice returned to the physiological range after recovery from diarrhea[45].

Therefore, Tyk2 is a key molecule for the development of IBD.

Psoriasis

Psoriasis is characterized by scaly erythematous lesions in the skin, epidermal hyperplasia, parakeratosis, and accumulation of inflammatory cells[56]. The inflammatory response is mediated by several cytokines, such as TNF-α, IL-17, and IL-23. The mouse model for human psoriasis was developed by treatment with imiquimod (IMQ), a ligand for TLR7[57]. *Il23p19*-deficient and *Il17a*–deficient mice exhibit decreased scores for erythema, scaling, and thickness upon treatment with IMQ, which suggests that the IL-23/Th17 axis and the Th17 cell-produced cytokines are essential for the development of skin abnormalities[57]. A genome-wide association study identified *Tyk2* as a psoriasis susceptibility locus[54]. *Tyk2* deficiency mitigates IMQ-induced enhanced ear thickness, which results from epidermal hyperplasia and inflammatory cell infiltration[45]. *Tyk2*-deficient mice exhibit markedly decreased numbers of $CD4^+IL\text{-}17^+$ or $CD4^+IFN\text{-}\gamma^+$ T cells in the draining lymph nodes and downregulated mRNA levels of Th17 cell-related cytokines upon treatment with IMQ [45].

The IL-23-induced skin inflammation mouse model is another promising model for human psoriasis[58]. In this IL-23-induced model, *Tyk2*-deficient mice exhibited reduced ear skin swelling, epidermal hyperplasia, Th17 and IL-22-producing Th22 cell infiltration compared with wild-type mice[45]. *Tyk2* deficiency downregulates the production of pro-inflammatory cytokines and psoriasis-related anti-microbial peptides.

IL-23 and IL-22 coordinate to promote skin inflammation[58,59]. Tyk2-mediated signals are essential for the induction of enhanced leukocyte infiltration and inflammatory cytokine production. Enhanced keratinocyte proliferation and differentiation are highly dependent on IL-17 and IL-22. Previous studies have reported that Tyk2 directly regulates IL-22-dependent processes as evidenced by the downregulation of STAT3 phosphorylation in *Tyk2* knockdown human keratinocyte HaCaT cells after IL-22 stimulation[45]. Therefore, Tyk2 has a critical role in the IL-22 signaling cascade that is involved in inducing epidermal hyperplasia.

IκB-ζ, an IL-17-induced protein encoded by *NFKBIZ*[60], is upregulated in the epidermal keratinocytes of psoriatic lesions[61]. *NFKBIZ* is located in the psoriasis susceptibility locus at 3q12.3[62]. IκB-ζ, a nuclear IκB family protein, positively or negatively modulates NF-κB-dependent and/or STAT3-dependent transcription[63-65]. Tyk2 is involved in IL-17–induced IκB-ζ expression in keratinocytes[66]. *Tyk2*-deficient mice exhibited only slight inflammation and downregulated mRNA levels of *Nfkbiz* upon treatment with IMQ. The catalytic activities of Tyk2 and STAT3 are required for IκB-ζ promoter activity in the HaCaT cells. The signaling pathways activated by IL-17 regulate mRNA stability[66-70]. ZC3H12A, which exhibits endoribonuclease activity, functions as a negative feedback regulator for inflammatory signaling[71-74]. The ubiquitin-proteasome pathway rapidly degrades ZC3H12A in IL-17-treated, IL-1β-treated, or IL-36–treated keratinocytes[72,74], which suggests that the stimulus-induced ZC3H12A downregulation can markedly suppress the inhibitory effects on mRNA expression.

Therefore, Tyk2 promotes the development of psoriasis by transducing IL-22 and IL-23 signals and regulating NFKBIZ along with the IL-17/ZC3H12A axis.

Sarcoidosis

Sarcoidosis is characterized by the aberrant accumulation of inflammatory cells, which typically form granulomas. Sarcoidosis usually begins in the lungs, skin, lymph nodes, eyes, heart, or other organs[75]. The murine model for human sarcoidosis is developed by intraperitoneally administering mice with heat-killed *Propionibacterium acnes* (*P. acnes*), which induces dense granulomas in the liver[76]. IL-12-IFN-γ axis is required for the induction since neither *Ifngr*-deficient nor *Il12p40*-deficient mice form hepatic granulomas after *P. acnes* injection[76]. *Tyk2*-deficient mice injected with *P. acnes* exhibit reduced serum IFN-γ level and decreased formation of hepatic granulomas compared with wild-type mice[45], indicating that Tyk2 has a role in *P. acnes*-induced granuloma formation.

Delayed-type hypersensitivity

Delayed-type hypersensitivity (DTH), which protects against various pathogens, such as mycobacteria, fungi, and parasites, contributes to transplant rejection and tumor immunity[77]. DTH is mainly dependent on T cells and develops 24–72 h after exposure to a foreign antigen. The DTH response analysis is based on a Th1/Th17 type model as the hypersensitivity response is defective in *Il12p40*-deficient and *Il23p19*-

deficient mice[78]. The sensitization phase is triggered by immunizing mice with a specific protein antigen (methylated BSA). The elicitation phase, which is initiated by the second injection of methylated BSA into the rear footpad of the pre-immunized mice, results in footpad swelling. Footpad swelling was significantly alleviated in *Tyk2* -deficient mice, which indicated the role of Tyk2 in DTH responses[45].

HIES

Tyk2 AR-HIES is a hereditary (autosomal recessive) disease involving a *Tyk2* mutation [79]. Patients with Tyk2 AR-HIES are characterized by repeated viral and mycobacterial infections, atopic dermatitis, and enhanced levels of IgE[11]. Therefore, Tyk2 may have a broader and more important role in immunological responses than expected from studies conducted using *Tyk2*-deficient mice.

POTENTIAL CLINICAL APPLICATIONS OF TYK2 INHIBITORS

The first *in vivo* evidence for the roles of Jaks in cytokine signaling originated from a human case study of severe combined immunodeficiency. Mutations in Jak3 or its receptor (a common g cytokine receptor chain) were detected in this case[80,81]. Another example is a somatic Jak2 valine-to-phenylalanine mutation (V617F), which is detected in more than 90% of the patients with polycythemia and some patients with essential thrombocythemia and primary myelofibrosis[82]. Activating point mutations in *Jak1* are detected in DNA samples from patients with acute lymphoblastic leukemia and are rarely observed in patients with acute myeloid leukemia[83]. Thus, dysregulation of the Jak-mediated signaling pathway is associated with the pathogenesis of different diseases, including hematological malignancies, autoimmune diseases, and immune-disrupted conditions. Studies on *Tyk2*-deficient mice or human patients with mutated *Tyk2* alleles have revealed that Tyk2 is a key player in the pathogenesis of autoimmune and/or inflammatory diseases.

Imatinib, a Bcr-Abl kinase inhibitor, exerts potent therapeutic effects in patients with chronic myelocytic leukemia[84]. Hence, various kinase inhibitors with strict selectivity and potency have been developed[85]. Jak inhibitors exert potent therapeutic effects by mitigating high levels of circulating immune/inflammatory cytokines. These results strongly suggest that Tyk2 is a potential therapeutic target for patients with immune and/or inflammatory diseases.

First-generation Jak inhibitors typically target two or three Jak types. Therefore, first-generation Jak inhibitors are associated with broader effects and more adverse events than the new-generation drugs, which specifically target one Jak type. Currently, several Jak inhibitors are used to treat various human diseases[86]. For example, ruxolitinib, an inhibitor of Jak1 and Jak2, has been approved to treat patients with myelofibrosis and polycythemia vera[87]. Tofacitinib, an inhibitor of Jak1, Jak2, and Jak3, has been approved to treat patients with RA, psoriatic arthritis, and ulcerative colitis[88]. Baricitinib, an inhibitor of Jak1 and Jak2, is used to treat patients with RA[89]. In methotrexate-inadequate responders, both tofacitinib and baricitinib provided enhanced therapeutic responses in patients with RA when compared with placebo[90]. In a phase 2 trial involving patients with psoriasis, the response rate to deucravacitinib (BMS-986165), a Tyk2 selective inhibitor[91], was significantly higher than that to placebo after 12 wk of administration. Treatment with BMS-986165 did not affect the blood cell counts or the serum levels of liver enzymes, lipids, and creatinine. However, BMS-986165 was associated with some severe adverse effects, such as malignant melanoma. Theoretically, therapeutic strategies targeting the immune system may increase the risk of infections from various pathogens, such as herpes zoster virus, cytomegalovirus, and Epstein–Barr virus. Therefore, further studies are needed to determine the long-term efficacy and safety of Tyk2 inhibitors. Additionally, clinical trials on Tyk2 inhibitors will aid in devising better therapeutic strategies for immune/inflammatory diseases than the currently marketed therapeutics.

CONCLUSION

This review summarized the involvement of Tyk2 in the immune system and its possible potential roles in the onset and development of immune and inflammatory diseases (Figure 4).

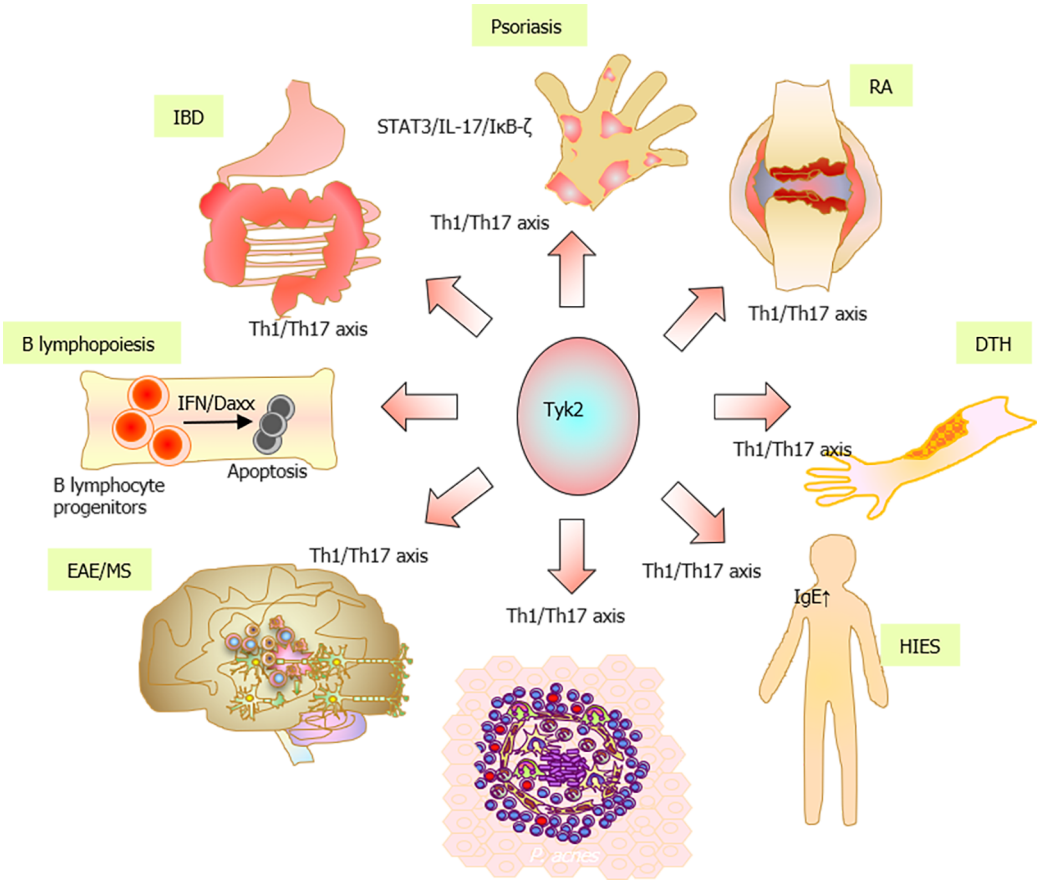

Figure 4 Schematic representation of the involvement of tyrosine kinase 2 in immune and inflammatory responses and its pathological significance. IBD: Inflammatory bowel diseases; RA: Rheumatoid arthritis; DTH: Delayed-type hypersensitivity; HIES: Hyper IgE syndrome; EAE: Experimental autoimmune encephalomyelitis; MS: Multiple sclerosis.

Studies on the *Tyk2*-deficient cells have revealed the involvement of the IFN system and IL-12/IL-23 axis. Constitutive production of a small amount of type I IFNs elicits a pro-inflammatory response against the invading pathogens and mitigates aberrant inflammation by promoting the expression of IL-10, a potent anti-inflammatory cytokine. Tyk2 is critical for maintaining the basal levels of IFNs. The IFN-α-induced decreased CFUs of bone marrow cells in the presence of IL-7 were also dependent on Tyk2. Tyk2 contributes to IFN-α signaling by promoting the nuclear translocation of Daxx and the formation of the Daxx/PML complex, which leads to growth inhibition. Additionally, Tyk2 interacts with the receptors for type I IFN, IL-6, IL-10, IL-12, and IL-23 (Figure 1). Moreover, Tyk2 is essential for IL-12-induced differentiation into Th1 cells, as well as IL-23-induced proliferation, survival, and functional maturation of Th17 cells. Additionally, Tyk2 mediates the production of nitric oxide in macrophages and IL-12 and IL-23 in dendritic cells after the invasion of pathogens.

Studies using *Tyk2*-deficient mice have revealed the potential involvement of Tyk2 in the onset and development of various immune and/or inflammatory disorders, such as RA, MS, IBD, psoriasis, sarcoidosis, and DTH. The development of most phenotypes in these models was mediated by Th1 and Th17 cells, whose differentiation and functions are highly dependent on Tyk2. Additionally, Tyk2 contributes to IL-17-induced IκB-ζ expression in IMQ-induced skin inflammation.

The experimental data summarized in this review along with the known clinical success of the novel Jak inhibitors indicate the therapeutic potential of Tyk2 inhibitors in the clinical setting. Further clinical trials are needed to examine the safety and efficacy profiles of Tyk2 inhibitors for treating psoriasis. Additionally, Tyk2 inhibitors are likely to be widely approved for various Th1/Th17-related immune/inflammatory diseases.

REFERENCES

1 **O'Shea JJ**, Ma A, Lipsky P. Cytokines and autoimmunity. *Nat Rev Immunol* 2002; **2**: 37-45 [PMID: 11905836 DOI: 10.1038/nri702]

2 **Ihle JN**. Cytokine receptor signalling. *Nature* 1995; **377**: 591-594 [PMID: 7566171 DOI: 10.1038/377591a0]

3 **Darnell JE**. STATs and gene regulation. *Science* 1997; **277**: 1630-1635 [PMID: 9287210 DOI: 10.1126/science.277.5332.1630]

4 **Stark GR**, Darnell JE Jr. The JAK-STAT pathway at twenty. *Immunity* 2012; **36**: 503-514 [PMID: 22520844 DOI: 10.1016/j.immuni.2012.03.013]

5 **Rodig SJ**, Meraz MA, White JM, Lampe PA, Riley JK, Arthur CD, King KL, Sheehan KC, Yin L, Pennica D, Johnson EM Jr, Schreiber RD. Disruption of the Jak1 gene demonstrates obligatory and nonredundant roles of the Jaks in cytokine-induced biologic responses. *Cell* 1998; **93**: 373-383 [PMID: 9590172 DOI: 10.1016/s0092-8674(00)81166-6]

6 **Parganas E**, Wang D, Stravopodis D, Topham DJ, Marine JC, Teglund S, Vanin EF, Bodner S, Colamonici OR, van Deursen JM, Grosveld G, Ihle JN. Jak2 is essential for signaling through a variety of cytokine receptors. *Cell* 1998; **93**: 385-395 [PMID: 9590173 DOI: 10.1016/s0092-8674(00)81167-8]

7 **Nosaka T**, van Deursen JM, Tripp RA, Thierfelder WE, Witthuhn BA, McMickle AP, Doherty PC, Grosveld GC, Ihle JN. Defective lymphoid development in mice lacking Jak3. *Science* 1995; **270**: 800-802 [PMID: 7481769 DOI: 10.1126/science.270.5237.800]

8 **Macchi P**, Villa A, Giliani S, Sacco MG, Frattini A, Porta F, Ugazio AG, Johnston JA, Candotti F, O'Shea JJ. Mutations of Jak-3 gene in patients with autosomal severe combined immune deficiency (SCID). *Nature* 1995; **377**: 65-68 [PMID: 7659163 DOI: 10.1038/377065a0]

9 **Shimoda K**, Kato K, Aoki K, Matsuda T, Miyamoto A, Shibamori M, Yamashita M, Numata A, Takase K, Kobayashi S, Shibata S, Asano Y, Gondo H, Sekiguchi K, Nakayama K, Nakayama T, Okamura T, Okamura S, Niho Y. Tyk2 plays a restricted role in IFN alpha signaling, although it is required for IL-12-mediated T cell function. *Immunity* 2000; **13**: 561-571 [PMID: 11070174 DOI: 10.1016/s1074-7613(00)00055-8]

10 **Karaghiosoff M**, Neubauer H, Lassnig C, Kovarik P, Schindler H, Pircher H, McCoy B, Bogdan C, Decker T, Brem G, Pfeffer K, Müller M. Partial impairment of cytokine responses in Tyk2-deficient mice. *Immunity* 2000; **13**: 549-560 [PMID: 11070173 DOI: 10.1016/s1074-7613(00)00054-6]

11 **Minegishi Y**, Saito M, Morio T, Watanabe K, Agematsu K, Tsuchiya S, Takada H, Hara T, Kawamura N, Ariga T, Kaneko H, Kondo N, Tsuge I, Yachie A, Sakiyama Y, Iwata T, Bessho F, Ohishi T, Joh K, Imai K, Kogawa K, Shinohara M, Fujieda M, Wakiguchi H, Pasic S, Abinun M, Ochs HD, Renner ED, Jansson A, Belohradsky BH, Metin A, Shimizu N, Mizutani S, Miyawaki T, Nonoyama S, Karasuyama H. Human tyrosine kinase 2 deficiency reveals its requisite roles in multiple cytokine signals involved in innate and acquired immunity. *Immunity* 2006; **25**: 745-755 [PMID: 17088085 DOI: 10.1016/j.immuni.2006.09.009]

12 **Velazquez L**, Fellous M, Stark GR, Pellegrini S. A protein tyrosine kinase in the interferon alpha/beta signaling pathway. *Cell* 1992; **70**: 313-322 [PMID: 1386289 DOI: 10.1016/0092-8674(92)90105-l]

13 **Darnell JE Jr**, Kerr IM, Stark GR. Jak-STAT pathways and transcriptional activation in response to IFNs and other extracellular signaling proteins. *Science* 1994; **264**: 1415-1421 [PMID: 8197455 DOI: 10.1126/science.8197455]

14 **Gough DJ**, Messina NL, Clarke CJ, Johnstone RW, Levy DE. Constitutive type I interferon modulates homeostatic balance through tonic signaling. *Immunity* 2012; **36**: 166-174 [PMID: 22365663 DOI: 10.1016/j.immuni.2012.01.011]

15 **Taniguchi T**, Takaoka A. A weak signal for strong responses: interferon-alpha/beta revisited. *Nat Rev Mol Cell Biol* 2001; **2**: 378-386 [PMID: 11331912 DOI: 10.1038/35073080]

16 **Karaghiosoff M**, Steinborn R, Kovarik P, Kriegshäuser G, Baccarini M, Donabauer B, Reichart U, Kolbe T, Bogdan C, Leanderson T, Levy D, Decker T, Müller M. Central role for type I interferons and Tyk2 in lipopolysaccharide-induced endotoxin shock. *Nat Immunol* 2003; **4**: 471-477 [PMID: 12679810 DOI: 10.1038/ni910]

17 **Kamezaki K**, Shimoda K, Numata A, Matsuda T, Nakayama K, Harada M. The role of Tyk2, Stat1 and Stat4 in LPS-induced endotoxin signals. *Int Immunol* 2004; **16**: 1173-1179 [PMID: 15226272 DOI: 10.1093/intimm/dxh118]

18 **Vogl C**, Flatt T, Fuhrmann B, Hofmann E, Wallner B, Stiefvater R, Kovarik P, Strobl B, Müller M. Transcriptome analysis reveals a major impact of JAK protein tyrosine kinase 2 (Tyk2) on the expression of interferon-responsive and metabolic genes. *BMC Genomics* 2010; **11**: 199 [PMID: 20338026 DOI: 10.1186/1471-2164-11-199]

19 **Mosmann TR**, Coffman RL. TH1 and TH2 cells: different patterns of lymphokine secretion lead to different functional properties. *Annu Rev Immunol* 1989; **7**: 145-173 [PMID: 2523712 DOI: 10.1146/annurev.iy.07.040189.001045]

20 **Oppmann B**, Lesley R, Blom B, Timans JC, Xu Y, Hunte B, Vega F, Yu N, Wang J, Singh K, Zonin F, Vaisberg E, Churakova T, Liu M, Gorman D, Wagner J, Zurawski S, Liu Y, Abrams JS, Moore KW, Rennick D, de Waal-Malefyt R, Hannum C, Bazan JF, Kastelein RA. Novel p19 protein engages IL-12p40 to form a cytokine, IL-23, with biological activities similar as well as distinct from IL-12. *Immunity* 2000; **13**: 715-725 [PMID: 11114383 DOI: 10.1016/s1074-7613(00)00070-4]

21 **Bettelli E**, Korn T, Oukka M, Kuchroo VK. Induction and effector functions of T(H)17 cells. *Nature*

2008; **453**: 1051-1057 [PMID: 18563156 DOI: 10.1038/nature07036]
22 **Korn T**, Bettelli E, Oukka M, Kuchroo VK. IL-17 and Th17 Cells. *Annu Rev Immunol* 2009; **27**: 485-517 [PMID: 19132915 DOI: 10.1146/annurev.immunol.021908.132710]
23 **Bacon CM**, Petricoin EF 3rd, Ortaldo JR, Rees RC, Larner AC, Johnston JA, O'Shea JJ. Interleukin 12 induces tyrosine phosphorylation and activation of STAT4 in human lymphocytes. *Proc Natl Acad Sci U S A* 1995; **92**: 7307-7311 [PMID: 7638186 DOI: 10.1073/pnas.92.16.7307]
24 **Bacon CM**, McVicar DW, Ortaldo JR, Rees RC, O'Shea JJ, Johnston JA. Interleukin 12 (IL-12) induces tyrosine phosphorylation of JAK2 and TYK2: differential use of Janus family tyrosine kinases by IL-2 and IL-12. *J Exp Med* 1995; **181**: 399-404 [PMID: 7528775 DOI: 10.1084/jem.181.1.399]
25 **Robinson DS**, O'Garra A. Further checkpoints in Th1 development. *Immunity* 2002; **16**: 755-758 [PMID: 12121657 DOI: 10.1016/s1074-7613(02)00331-x]
26 **Parham C**, Chirica M, Timans J, Vaisberg E, Travis M, Cheung J, Pflanz S, Zhang R, Singh KP, Vega F, To W, Wagner J, O'Farrell AM, McClanahan T, Zurawski S, Hannum C, Gorman D, Rennick DM, Kastelein RA, de Waal Malefyt R, Moore KW. A receptor for the heterodimeric cytokine IL-23 is composed of IL-12Rbeta1 and a novel cytokine receptor subunit, IL-23R. *J Immunol* 2002; **168**: 5699-5708 [PMID: 12023369 DOI: 10.4049/jimmunol.168.11.5699]
27 **Harris TJ**, Grosso JF, Yen HR, Xin H, Kortylewski M, Albesiano E, Hipkiss EL, Getnet D, Goldberg MV, Maris CH, Housseau F, Yu H, Pardoll DM, Drake CG. Cutting edge: An in vivo requirement for STAT3 signaling in TH17 development and TH17-dependent autoimmunity. *J Immunol* 2007; **179**: 4313-4317 [PMID: 17878325 DOI: 10.4049/jimmunol.179.7.4313]
28 **Wilson CB**, Rowell E, Sekimata M. Epigenetic control of T-helper-cell differentiation. *Nat Rev Immunol* 2009; **9**: 91-105 [PMID: 19151746 DOI: 10.1038/nri2487]
29 **Tokumasa N**, Suto A, Kagami S, Furuta S, Hirose K, Watanabe N, Saito Y, Shimoda K, Iwamoto I, Nakajima H. Expression of Tyk2 in dendritic cells is required for IL-12, IL-23, and IFN-gamma production and the induction of Th1 cell differentiation. *Blood* 2007; **110**: 553-560 [PMID: 17395783 DOI: 10.1182/blood-2006-11-059246]
30 **Müller M**, Briscoe J, Laxton C, Guschin D, Ziemiecki A, Silvennoinen O, Harpur AG, Barbieri G, Witthuhn BA, Schindler C. The protein tyrosine kinase JAK1 complements defects in interferon-alpha/beta and -gamma signal transduction. *Nature* 1993; **366**: 129-135 [PMID: 8232552 DOI: 10.1038/366129a0]
31 **Shimoda K**, Kamesaki K, Numata A, Aoki K, Matsuda T, Oritani K, Tamiya S, Kato K, Takase K, Imamura R, Yamamoto T, Miyamoto T, Nagafuji K, Gondo H, Nagafuchi S, Nakayama K, Harada M. Cutting edge: tyk2 is required for the induction and nuclear translocation of Daxx which regulates IFN-alpha-induced suppression of B lymphocyte formation. *J Immunol* 2002; **169**: 4707-4711 [PMID: 12391177 DOI: 10.4049/jimmunol.169.9.4707]
32 **Meraz MA**, White JM, Sheehan KC, Bach EA, Rodig SJ, Dighe AS, Kaplan DH, Riley JK, Greenlund AC, Campbell D, Carver-Moore K, DuBois RN, Clark R, Aguet M, Schreiber RD. Targeted disruption of the Stat1 gene in mice reveals unexpected physiologic specificity in the JAK-STAT signaling pathway. *Cell* 1996; **84**: 431-442 [PMID: 8608597 DOI: 10.1016/s0092-8674(00)81288-x]
33 **Durbin JE**, Hackenmiller R, Simon MC, Levy DE. Targeted disruption of the mouse Stat1 gene results in compromised innate immunity to viral disease. *Cell* 1996; **84**: 443-450 [PMID: 8608598 DOI: 10.1016/s0092-8674(00)81289-1]
34 **Park C**, Li S, Cha E, Schindler C. Immune response in Stat2 knockout mice. *Immunity* 2000; **13**: 795-804 [PMID: 11163195 DOI: 10.1016/s1074-7613(00)00077-7]
35 **Namen AE**, Lupton S, Hjerrild K, Wignall J, Mochizuki DY, Schmierer A, Mosley B, March CJ, Urdal D, Gillis S. Stimulation of B-cell progenitors by cloned murine interleukin-7. *Nature* 1988; **333**: 571-573 [PMID: 3259677 DOI: 10.1038/333571a0]
36 **Lin Q**, Dong C, Cooper MD. Impairment of T and B cell development by treatment with a type I interferon. *J Exp Med* 1998; **187**: 79-87 [PMID: 9419213 DOI: 10.1084/jem.187.1.79]
37 **Yang X**, Khosravi-Far R, Chang HY, Baltimore D. Daxx, a novel Fas-binding protein that activates JNK and apoptosis. *Cell* 1997; **89**: 1067-1076 [PMID: 9215629 DOI: 10.1016/s0092-8674(00)80294-9]
38 **Gongora R**, Stephan RP, Zhang Z, Cooper MD. An essential role for Daxx in the inhibition of B lymphopoiesis by type I interferons. *Immunity* 2001; **14**: 727-737 [PMID: 11420043 DOI: 10.1016/s1074-7613(01)00152-2]
39 **Muromoto R**, Ishida M, Sugiyama K, Sekine Y, Oritani K, Shimoda K, Matsuda T. Sumoylation of Daxx regulates IFN-induced growth suppression of B lymphocytes and the hormone receptor-mediated transactivation. *J Immunol* 2006; **177**: 1160-1170 [PMID: 16818774 DOI: 10.4049/jimmunol.177.2.1160]
40 **Gay S**. Rheumatoid arthritis. *Curr Opin Rheumatol* 2001; **13**: 191-192 [PMID: 11333347 DOI: 10.1097/00002281-200105000-00007]
41 **Courtenay JS**, Dallman MJ, Dayan AD, Martin A, Mosedale B. Immunisation against heterologous type II collagen induces arthritis in mice. *Nature* 1980; **283**: 666-668 [PMID: 6153460 DOI: 10.1038/283666a0]
42 **Ortmann R**, Smeltz R, Yap G, Sher A, Shevach EM. A heritable defect in IL-12 signaling in B10.Q/J mice. I. In vitro analysis. *J Immunol* 2001; **166**: 5712-5719 [PMID: 11313413 DOI: 10.4049/jimmunol.166.9.5712]

43 **Yap GS**, Ortmann R, Shevach E, Sher A. A heritable defect in IL-12 signaling in B10.Q/J mice. II. Effect on acute resistance to Toxoplasma gondii and rescue by IL-18 treatment. *J Immunol* 2001; **166**: 5720-5725 [PMID: 11313414 DOI: 10.4049/jimmunol.166.9.5720]

44 **Khachigian LM**. Collagen antibody-induced arthritis. *Nat Protoc* 2006; **1**: 2512-2516 [PMID: 17406499 DOI: 10.1038/nprot.2006.393]

45 **Muromoto R**, Oritani K, Matsuda T. Tyk2-mediated homeostatic control by regulating the PGE2-PKA-IL-10 axis. *AIMS Allergy Immunol* 2021; **5**: 175-183 [DOI: 10.3934/Allergy.2021013]

46 **Itoh T**, Matsuda H, Tanioka M, Kuwabara K, Itohara S, Suzuki R. The role of matrix metalloproteinase-2 and matrix metalloproteinase-9 in antibody-induced arthritis. *J Immunol* 2002; **169**: 2643-2647 [PMID: 12193736 DOI: 10.4049/jimmunol.169.5.2643]

47 **Paniagua RT**, Chang A, Mariano MM, Stein EA, Wang Q, Lindstrom TM, Sharpe O, Roscow C, Ho PP, Lee DM, Robinson WH. c-Fms-mediated differentiation and priming of monocyte lineage cells play a central role in autoimmune arthritis. *Arthritis Res Ther* 2010; **12**: R32 [PMID: 20181277 DOI: 10.1186/ar2940]

48 **Owens B**. Multiple sclerosis. *Nature* 2016; **540**: S1 [PMID: 27902684 DOI: 10.1038/540S1a]

49 **Zamvil SS**, Steinman L. The T lymphocyte in experimental allergic encephalomyelitis. *Annu Rev Immunol* 1990; **8**: 579-621 [PMID: 2188675 DOI: 10.1146/annurev.iy.08.040190.003051]

50 **Oyamada A**, Ikebe H, Itsumi M, Saiwai H, Okada S, Shimoda K, Iwakura Y, Nakayama KI, Iwamoto Y, Yoshikai Y, Yamada H. Tyrosine kinase 2 plays critical roles in the pathogenic CD4 T cell responses for the development of experimental autoimmune encephalomyelitis. *J Immunol* 2009; **183**: 7539-7546 [PMID: 19917699 DOI: 10.4049/jimmunol.0902740]

51 **Spach KM**, Noubade R, McElvany B, Hickey WF, Blankenhorn EP, Teuscher C. A single nucleotide polymorphism in Tyk2 controls susceptibility to experimental allergic encephalomyelitis. *J Immunol* 2009; **182**: 7776-7783 [PMID: 19494301 DOI: 10.4049/jimmunol.0900142]

52 **Roda G**, Chien Ng S, Kotze PG, Argollo M, Panaccione R, Spinelli A, Kaser A, Peyrin-Biroulet L, Danese S. Crohn's disease. *Nat Rev Dis Primers* 2020; **6**: 22 [PMID: 32242028 DOI: 10.1038/s41572-020-0156-2]

53 **Wirtz S**, Neurath MF. Mouse models of inflammatory bowel disease. *Adv Drug Deliv Rev* 2007; **59**: 1073-1083 [PMID: 17825455 DOI: 10.1016/j.addr.2007.07.003]

54 **Ellinghaus D**, Ellinghaus E, Nair RP, Stuart PE, Esko T, Metspalu A, Debrus S, Raelson JV, Tejasvi T, Belouchi M, West SL, Barker JN, Kõks S, Kingo K, Balschun T, Palmieri O, Annese V, Gieger C, Wichmann HE, Kabesch M, Trembath RC, Mathew CG, Abecasis GR, Weidinger S, Nikolaus S, Schreiber S, Elder JT, Weichenthal M, Nothnagel M, Franke A. Combined analysis of genome-wide association studies for Crohn disease and psoriasis identifies seven shared susceptibility loci. *Am J Hum Genet* 2012; **90**: 636-647 [PMID: 22482804 DOI: 10.1016/j.ajhg.2012.02.020]

55 **Kobayashi T**, Siegmund B, Le Berre C, Wei SC, Ferrante M, Shen B, Bernstein CN, Danese S, Peyrin-Biroulet L, Hibi T. Ulcerative colitis. *Nat Rev Dis Primers* 2020; **6**: 74 [PMID: 32913180 DOI: 10.1038/s41572-020-0205-x]

56 **Lowes MA**, Bowcock AM, Krueger JG. Pathogenesis and therapy of psoriasis. *Nature* 2007; **445**: 866-873 [PMID: 17314973 DOI: 10.1038/nature05663]

57 **van der Fits L**, Mourits S, Voerman JS, Kant M, Boon L, Laman JD, Cornelissen F, Mus AM, Florencia E, Prens EP, Lubberts E. Imiquimod-induced psoriasis-like skin inflammation in mice is mediated *via* the IL-23/IL-17 axis. *J Immunol* 2009; **182**: 5836-5845 [PMID: 19380832 DOI: 10.4049/jimmunol.0802999]

58 **Zheng Y**, Danilenko DM, Valdez P, Kasman I, Eastham-Anderson J, Wu J, Ouyang W. Interleukin-22, a T(H)17 cytokine, mediates IL-23-induced dermal inflammation and acanthosis. *Nature* 2007; **445**: 648-651 [PMID: 17187052 DOI: 10.1038/nature05505]

59 **Rizzo HL**, Kagami S, Phillips KG, Kurtz SE, Jacques SL, Blauvelt A. IL-23-mediated psoriasis-like epidermal hyperplasia is dependent on IL-17A. *J Immunol* 2011; **186**: 1495-1502 [PMID: 21172868 DOI: 10.4049/jimmunol.1001001]

60 **Muromoto R**, Hirao T, Tawa K, Hirashima K, Kon S, Kitai Y, Matsuda T. IL-17A plays a central role in the expression of psoriasis signature genes through the induction of IκB-ζ in keratinocytes. *Int Immunol* 2016; **28**: 443-452 [PMID: 26944069 DOI: 10.1093/intimm/dxw011]

61 **Johansen C**, Mose M, Ommen P, Bertelsen T, Vinter H, Hailfinger S, Lorscheid S, Schulze-Osthoff K, Iversen L. IκBζ is a key driver in the development of psoriasis. *Proc Natl Acad Sci U S A* 2015; **112**: E5825-E5833 [PMID: 26460049 DOI: 10.1073/pnas.1509971112]

62 **Tsoi LC**, Spain SL, Ellinghaus E, Stuart PE, Capon F, Knight J, Tejasvi T, Kang HM, Allen MH, Lambert S, Stoll SW, Weidinger S, Gudjonsson JE, Koks S, Kingo K, Esko T, Das S, Metspalu A, Weichenthal M, Enerback C, Krueger GG, Voorhees JJ, Chandran V, Rosen CF, Rahman P, Gladman DD, Reis A, Nair RP, Franke A, Barker JNWN, Abecasis GR, Trembath RC, Elder JT. Enhanced meta-analysis and replication studies identify five new psoriasis susceptibility loci. *Nat Commun* 2015; **6**: 7001 [PMID: 25939698 DOI: 10.1038/ncomms8001]

63 **Müller A**, Hennig A, Lorscheid S, Grondona P, Schulze-Osthoff K, Hailfinger S, Kramer D. IκBζ is a key transcriptional regulator of IL-36-driven psoriasis-related gene expression in keratinocytes. *Proc Natl Acad Sci U S A* 2018; **115**: 10088-10093 [PMID: 30224457 DOI: 10.1073/pnas.1801377115]

64 **Yamazaki S**, Muta T, Matsuo S, Takeshige K. Stimulus-specific induction of a novel nuclear factor-kappaB regulator, IkappaB-zeta, *via* Toll/Interleukin-1 receptor is mediated by mRNA stabilization. *J Biol Chem* 2005; **280**: 1678-1687 [PMID: 15522867 DOI: 10.1074/jbc.M409983200]

65 **Okuma A**, Hoshino K, Ohba T, Fukushi S, Aiba S, Akira S, Ono M, Kaisho T, Muta T. Enhanced

apoptosis by disruption of the STAT3-IκB-ζ signaling pathway in epithelial cells induces Sjögren's syndrome-like autoimmune disease. *Immunity* 2013; **38**: 450-460 [PMID: 23453632 DOI: 10.1016/j.immuni.2012.11.016]

66 **Muromoto R**, Tawa K, Ohgakiuchi Y, Sato A, Saino Y, Hirashima K, Minoguchi H, Kitai Y, Kashiwakura JI, Shimoda K, Oritani K, Matsuda T. IκB-ζ Expression Requires Both TYK2/STAT3 Activity and IL-17-Regulated mRNA Stabilization. *Immunohorizons* 2019; **3**: 172-185 [PMID: 31356171 DOI: 10.4049/immunohorizons.1900023]

67 **Hartupee J**, Liu C, Novotny M, Li X, Hamilton T. IL-17 enhances chemokine gene expression through mRNA stabilization. *J Immunol* 2007; **179**: 4135-4141 [PMID: 17785852 DOI: 10.4049/jimmunol.179.6.4135]

68 **Herjan T**, Hong L, Bubenik J, Bulek K, Qian W, Liu C, Li X, Chen X, Yang H, Ouyang S, Zhou H, Zhao J, Vasu K, Cockman E, Aronica M, Asosingh K, Licatalosi DD, Qin J, Fox PL, Hamilton TA, Driscoll D. IL-17-receptor-associated adaptor Act1 directly stabilizes mRNAs to mediate IL-17 inflammatory signaling. *Nat Immunol* 2018; **19**: 354-365 [PMID: 29563620 DOI: 10.1038/s41590-018-0071-9]

69 **Amatya N**, Childs EE, Cruz JA, Aggor FEY, Garg AV, Berman AJ, Gudjonsson JE, Atasoy U, Gaffen SL. IL-17 integrates multiple self-reinforcing, feed-forward mechanisms through the RNA binding protein Arid5a. *Sci Signal* 2018; **11** [PMID: 30301788 DOI: 10.1126/scisignal.aat4617]

70 **Dhamija S**, Winzen R, Doerrie A, Behrens G, Kuehne N, Schauerte C, Neumann E, Dittrich-Breiholz O, Kracht M, Holtmann H. Interleukin-17 (IL-17) and IL-1 activate translation of overlapping sets of mRNAs, including that of the negative regulator of inflammation, MCPIP1. *J Biol Chem* 2013; **288**: 19250-19259 [PMID: 23658019 DOI: 10.1074/jbc.M113.452649]

71 **Matsushita K**, Takeuchi O, Standley DM, Kumagai Y, Kawagoe T, Miyake T, Satoh T, Kato H, Tsujimura T, Nakamura H, Akira S. Zc3h12a is an RNase essential for controlling immune responses by regulating mRNA decay. *Nature* 2009; **458**: 1185-1190 [PMID: 19322177 DOI: 10.1038/nature07924]

72 **Iwasaki H**, Takeuchi O, Teraguchi S, Matsushita K, Uehata T, Kuniyoshi K, Satoh T, Saitoh T, Matsushita M, Standley DM, Akira S. The IκB kinase complex regulates the stability of cytokine-encoding mRNA induced by TLR-IL-1R by controlling degradation of regnase-1. *Nat Immunol* 2011; **12**: 1167-1175 [PMID: 22037600 DOI: 10.1038/ni.2137]

73 **Monin L**, Gudjonsson JE, Childs EE, Amatya N, Xing X, Verma AH, Coleman BM, Garg AV, Killeen M, Mathers A, Ward NL, Gaffen SL. MCPIP1/Regnase-1 Restricts IL-17A- and IL-17C-Dependent Skin Inflammation. *J Immunol* 2017; **198**: 767-775 [PMID: 27920272 DOI: 10.4049/jimmunol.1601551]

74 **Takaishi M**, Satoh T, Akira S, Sano S. Regnase-1, an Immunomodulator, Limits the IL-36/IL-36R Autostimulatory Loop in Keratinocytes to Suppress Skin Inflammation. *J Invest Dermatol* 2018; **138**: 1439-1442 [PMID: 29339122 DOI: 10.1016/j.jid.2017.12.033]

75 **Grunewald J**, Grutters JC, Arkema EV, Saketkoo LA, Moller DR, Müller-Quernheim J. Sarcoidosis. *Nat Rev Dis Primers* 2019; **5**: 45 [PMID: 31273209 DOI: 10.1038/s41572-019-0096-x]

76 **Tsutsui H**, Imamura M, Fujimoto J, Nakanishi K. The TLR4/TRIF-Mediated Activation of NLRP3 Inflammasome Underlies Endotoxin-Induced Liver Injury in Mice. *Gastroenterol Res Pract* 2010; **2010**: 641865 [PMID: 20634907 DOI: 10.1155/2010/641865]

77 **Black CA**. Delayed type hypersensitivity: current theories with an historic perspective. *Dermatol Online J* 1999; **5**: 7 [PMID: 10673450]

78 **Ghilardi N**, Kljavin N, Chen Q, Lucas S, Gurney AL, De Sauvage FJ. Compromised humoral and delayed-type hypersensitivity responses in IL-23-deficient mice. *J Immunol* 2004; **172**: 2827-2833 [PMID: 14978083 DOI: 10.4049/jimmunol.172.5.2827]

79 **Minegishi Y**. Hyper-IgE syndrome. *Curr Opin Immunol* 2009; **21**: 487-492 [PMID: 19717292 DOI: 10.1016/j.coi.2009.07.013]

80 **Russell SM**, Tayebi N, Nakajima H, Riedy MC, Roberts JL, Aman MJ, Migone TS, Noguchi M, Markert ML, Buckley RH, O'Shea JJ, Leonard WJ. Mutation of Jak3 in a patient with SCID: essential role of Jak3 in lymphoid development. *Science* 1995; **270**: 797-800 [PMID: 7481768 DOI: 10.1126/science.270.5237.797]

81 **Leonard WJ**, Lin JX, O'Shea JJ. The γ_c Family of Cytokines: Basic Biology to Therapeutic Ramifications. *Immunity* 2019; **50**: 832-850 [PMID: 30995502 DOI: 10.1016/j.immuni.2019.03.028]

82 **James C**, Ugo V, Le Couédic JP, Staerk J, Delhommeau F, Lacout C, Garçon L, Raslova H, Berger R, Bennaceur-Griscelli A, Villeval JL, Constantinescu SN, Casadevall N, Vainchenker W. A unique clonal JAK2 mutation leading to constitutive signalling causes polycythaemia vera. *Nature* 2005; **434**: 1144-1148 [PMID: 15793561 DOI: 10.1038/nature03546]

83 **Flex E**, Petrangeli V, Stella L, Chiaretti S, Hornakova T, Knoops L, Ariola C, Fodale V, Clappier E, Paoloni F, Martinelli S, Fragale A, Sanchez M, Tavolaro S, Messina M, Cazzaniga G, Camera A, Pizzolo G, Tornesello A, Vignetti M, Battistini A, Cavé H, Gelb BD, Renauld JC, Biondi A, Constantinescu SN, Foà R, Tartaglia M. Somatically acquired JAK1 mutations in adult acute lymphoblastic leukemia. *J Exp Med* 2008; **205**: 751-758 [PMID: 18362173 DOI: 10.1084/jem.20072182]

84 **Druker BJ**, Tamura S, Buchdunger E, Ohno S, Segal GM, Fanning S, Zimmermann J, Lydon NB. Effects of a selective inhibitor of the Abl tyrosine kinase on the growth of Bcr-Abl positive cells. *Nat Med* 1996; **2**: 561-566 [PMID: 8616716 DOI: 10.1038/nm0596-561]

85 **Ferguson FM**, Gray NS. Kinase inhibitors: the road ahead. *Nat Rev Drug Discov* 2018; **17**: 353-377

[PMID: 29545548 DOI: 10.1038/nrd.2018.21]

86 **Schwartz DM**, Kanno Y, Villarino A, Ward M, Gadina M, O'Shea JJ. JAK inhibition as a therapeutic strategy for immune and inflammatory diseases. *Nat Rev Drug Discov* 2017; **17**: 78 [PMID: 29282366 DOI: 10.1038/nrd.2017.267]

87 **Sonbol MB**, Firwana B, Zarzour A, Morad M, Rana V, Tiu RV. Comprehensive review of JAK inhibitors in myeloproliferative neoplasms. *Ther Adv Hematol* 2013; **4**: 15-35 [PMID: 23610611 DOI: 10.1177/2040620712461047]

88 **Dhillon S**. Tofacitinib: A Review in Rheumatoid Arthritis. *Drugs* 2017; **77**: 1987-2001 [PMID: 29139090 DOI: 10.1007/s40265-017-0835-9]

89 **Al-Salama ZT**, Scott LJ. Baricitinib: A Review in Rheumatoid Arthritis. *Drugs* 2018; **78**: 761-772 [PMID: 29687421 DOI: 10.1007/s40265-018-0908-4]

90 **Taylor PC**. Clinical efficacy of launched JAK inhibitors in rheumatoid arthritis. *Rheumatology (Oxford)* 2019; **58**: i17-i26 [PMID: 30806707 DOI: 10.1093/rheumatology/key225]

91 **Papp K**, Gordon K, Thaçi D, Morita A, Gooderham M, Foley P, Girgis IG, Kundu S, Banerjee S. Phase 2 Trial of Selective Tyrosine Kinase 2 Inhibition in Psoriasis. *N Engl J Med* 2018; **379**: 1313-1321 [PMID: 30205746 DOI: 10.1056/NEJMoa1806382]

World Journal of Biological Chemistry

Submit a Manuscript: https://www.f6publishing.com

World J Biol Chem 2022 January 27; 13(1): 15-34

DOI: 10.4331/wjbc.v13.i1.15

ISSN 1949-8454 (online)

ORIGINAL ARTICLE

Basic Study

Increased monoamine oxidase activity and imidazoline binding sites in insulin-resistant adipocytes from obese Zucker rats

Christian Carpéné, Luc Marti, Nathalie Morin

ORCID number: Christian Carpéné 0000-0001-7765-6647; Luc Marti 0000-0002-8238-1147; Nathalie Morin 0000-0001-9793-371X.

Author contributions: Carpéné C designed the studies, performed hexose uptake assays and literature review, and wrote the manuscript; Marti L performed binding studies, rat experiments, and data analysis, and contributed to the literature review; Morin N performed immunoblots and data analysis, and revised the manuscript.

Institutional review board statement: The study was reviewed and approved by the Institutional Review Board of Institut des Maladies Métaboliques et Cardiovasculaires, Toulouse, France.

Institutional animal care and use committee statement: Rats were housed and manipulated according to the INSERM guidelines and European Directive 2010/63/UE by competent and expert technicians or researchers in animal care facilities with agreements number A 31 555 04 to C 31 555 011. The experimental protocol was approved by the local ethical committee CEEA nb122.

Conflict-of-interest statement: All

Christian Carpéné, Luc Marti, Nathalie Morin, Institut des Maladies Métaboliques et Cardiovasculaires, INSERM, Toulouse 31342, France

Nathalie Morin, Faculté de Pharmacie de Paris, Paris University, Paris 75270, France

Corresponding author: Christian Carpéné, PhD, Senior Researcher, Institut des Maladies Métaboliques et Cardiovasculaires, INSERM, CHU Rangueil, Bat. L4, BP 84225, Toulouse 31342, France. christian.carpene@inserm.fr

Abstract

BACKGROUND

Despite overt insulin resistance, adipocytes of genetically obese Zucker rats accumulate the excess of calorie intake in the form of lipids.

AIM

To investigate whether factors can replace or reinforce insulin lipogenic action by exploring glucose uptake activation by hydrogen peroxide, since it is produced by monoamine oxidase (MAO) and semicarbazide-sensitive amine oxidase (SSAO) in adipocytes.

METHODS

^{3}H-2-deoxyglucose uptake (2-DG) was determined in adipocytes from obese and lean rats in response to insulin or MAO and SSAO substrates such as tyramine and benzylamine. ^{14}C-tyramine oxidation and binding of imidazolinic radioligands [^{3}H-Idazoxan, ^{3}H-(2-benzofuranyl)-2-imidazoline] were studied in adipocytes, the liver, and muscle. The influence of *in vivo* administration of tyramine + vanadium on glucose handling was assessed in lean and obese rats.

RESULTS

2-DG uptake and lipogenesis stimulation by insulin were dampened in adipocytes from obese rats, when compared to their lean littermates. Tyramine and benzylamine activation of hexose uptake was vanadate-dependent and was also limited, while MAO was increased and SSAO decreased. These changes were adipocyte-specific and accompanied by a greater number of imidazoline I_2 binding sites in the obese rat, when compared to the lean. *In vitro*, tyramine precluded the binding to I_2 sites, while *in vivo*, its administration together with vanadium lowered fasting plasma levels of glucose and triacylglycerols in obese rats.

authors declare no competing financial interests for this article.

Data sharing statement: No additional data are available.

ARRIVE guidelines statement: The authors have read the ARRIVE guidelines, and the manuscript was prepared and revised according to the ARRIVE guidelines.

Supported by Recurrent Grants from Institut National de la Santé et de la Recherche Médicale to the INSERM U1048.

Country/Territory of origin: France

Specialty type: Endocrinology and metabolism

Provenance and peer review: Invited article; Externally peer reviewed.

Peer-review model: Single blind

Peer-review report's scientific quality classification

Grade A (Excellent): 0
Grade B (Very good): 0
Grade C (Good): C
Grade D (Fair): 0
Grade E (Poor): 0

Received: March 26, 2021
Peer-review started: March 26, 2021
First decision: July 8, 2021
Revised: July 9, 2021
Accepted: January 13, 2022
Article in press: January 13, 2022
Published online: January 27, 2022

CONCLUSION

The adipocytes from obese Zucker rats exhibit increased MAO activity and imidazoline binding site number. However, probably as a consequence of SSAO down-regulation, the glucose transport stimulation by tyramine is decreased as much as that of insulin in these insulin-resistant adipocytes. The adipocyte amine oxidases deserve more studies with respect to their putative contribution to the management of glucose and lipid handling.

Key Words: Obesity; Adipocyte; Amine oxidases; Imidazoline binding sites; Creatine kinase B; Idazoxan; Lipogenesis; Hydrogen peroxide; Glucose uptake

Core Tip: The substrates of monoamine oxidase (MAO) and semicarbazide-sensitive amine oxidase (SSAO) partly reproduce the stimulatory effect of insulin on sugar entry in rat fat cells. Especially when combined with vanadium, tyramine and benzylamine mimic more than 70% of the insulin stimulation of glucose uptake. Unfortunately, such insulin activation of glucose utilization is strongly diminished in the genetically obese Zucker rat, an animal model of the metabolic syndrome. In this insulin-resistant and obese rat, the stimulation of glucose transport by tyramine is decreased as much as that of insulin, while the effect of benzylamine is even more altered. SSAO, responsible for benzylamine oxidation, is down-regulated in adipocytes from obese Zucker rats. In contrast, MAO, which predominantly supports the oxidation of tyramine, is increased, apparently not in a sufficient manner to reach the same hexose uptake activation seen in fat cells from lean rats. However, this greater ability to oxidize tyramine was found only in white adipocytes from obese rats since no change was found in the liver or skeletal muscle when compared to lean controls. Moreover, increased MAO activity in the large adipocytes of obese rats was accompanied by an enlarged number of imidazoline binding sites, previously described to be located on MAO. Since the repeated subcutaneous administration of tyramine plus vanadate is somewhat capable of reducing plasma glucose and triglycerides in obese rats, SSAO, MAO, and its associated imidazoline I_2 sites deserve further studies with respect to their mimicking insulin action on glucose and lipid metabolism in fat cells.

Citation: Carpéné C, Marti L, Morin N. Increased monoamine oxidase activity and imidazoline binding sites in insulin-resistant adipocytes from obese Zucker rats. *World J Biol Chem* 2022; 13(1): 15-34
URL: https://www.wjgnet.com/1949-8454/full/v13/i1/15.htm
DOI: https://dx.doi.org/10.4331/wjbc.v13.i1.15

INTRODUCTION

Alongside the numerous models of transgenic mice exhibiting an overt obese phenotype, the Zucker fatty rat remains since decades one of the most widely studied animal models of genetic obesity. Obesity in these rats is inherited as an autosomal recessive trait, as initially reported in 1961 by Zucker and Zucker[1]. It was in 1996 that independent studies demonstrated the molecular basis of such obesity, which does not need any challenge with hypercaloric diet to develop spontaneously[2-4]. Affected rats have a missense mutation in the leptin receptor and show hyperphagia together with various endocrine and metabolic alterations similar to those that appear in the human metabolic syndrome. Leptin is an adipokine produced by adipose tissue and it plays an important role in the central regulation of energy balance[5], together with other functions (*e.g.*, in reproduction). Leptin activates its own receptors in the brain, thereby decreasing energy intake and increasing energy expenditure. Thus, the obese Zucker rats (previously called recessive homozygous fa/fa fatty rats) spontaneously exhibit bulimia and obesity and rapidly become hyperinsulinemic. Consequently, they have been considered as a useful model of insulin resistance and of dyslipidemia with related kidney diseases[6]. Nevertheless, the usefulness of Zucker fatty rats as a model of type 2 diabetes is questionable, since these hyperphagic animals have only mild

P-Reviewer: Yi X
S-Editor: Zhang H
L-Editor: Wang TQ
P-Editor: Zhang H

glucose intolerance, at the expense of dramatically increased insulin release by endocrine pancreas. Indeed, it has been reported that, during the early onset of obesity, the Zucker fatty rats are hypersensitive to insulin[7] and more capable to store lipids than their lean littermates[8]. One assumes that, once adult and obese, these rats develop alternative pathways allowing a still efficient storage of ingested energy in the form of triacylglycerols in the large lipid droplets of their adipocytes[9]. The impressive adipogenic and lipogenic activities maintained throughout the growth of fatty rats, boosted by an excessive energy intake, explains how 40% of body weight is composed of lipids when the Zucker rats reach 14 wk of age[9]. As in obese patients, the adipose depots of mature obese rats are hypertrophied despite established insulin resistance, which results in a lowered sensitivity of the adipocytes to anabolic actions of insulin such as lipogenesis stimulation[10]. The obese Zucker rat is, by definition, also resistant to leptin, and the obese animals present higher circulating levels of this adipokine compared to their lean littermate[11]. Our primary objective was to detect what type of adaptation might occur in adipocytes to circumvent such insulin/leptin resistance in order to maintain a still efficient fat deposition.

It has been reported that pharmacological adrenergic intervention on obese Zucker rats, such as treatment with the β-adrenergic agents celiprolol or clenbuterol[12,13], mitigates their insulin resistance, probably by improving insulin-stimulated glucose uptake in skeletal muscles and adipose tissues. The improvements were not accompanied with a notable body weight loss but were related to a tendency to normalize the repartition of energy fluxes between fat and muscular tissues[14]. To support such beneficial effect of reinforcing adrenergic inputs in the obese Zucker rat, was the demonstration that, in the adipose tissue of young suckling littermates, there was already, at 2 wk of age, a difference in the β-adrenergic signaling pathway in white adipocytes between the future obese and the future lean[15]. It is therefore admitted that impairment of the responsiveness to catecholamines plays a role in worsening the obesity syndrome triggered by leptinergic system invalidation. This led us to further study the alterations of biogenic amine pathways in obese Zucker rats, since these metabolites have a potential role as biomarkers of the metabolic syndrome [16].

It has been already reported that the basal lipolytic activity is higher in adipocytes from obese rats, and that resistance to the lipolytic action of catecholamines appears to counteract such elevated baseline lipolysis[17]. This decrease of β-adrenergic responsiveness seems therefore to be an adaptive mechanism aiming at moderating *in vivo* increase in plasma free fatty acids (FFA). In fact, any excessive increase in circulating FFA is deleterious as it contributes to the complications of insulin-resistant states, such as hepatic steatosis. In addition to their important role in lipid mobilization, the catecholamines also activate glucose utilization in muscles[18] and in brown adipose tissue (BAT)[19]. In a recent study, we observed that high doses of catecholamines mimic the stimulatory effects of insulin on glucose transport, at least *in vitro* in rodent isolated adipocytes[20]. All these observations indicated that amines might constitute factors other than insulin capable of affecting directly glucose utilization in fat cells. More precisely, the insulin-like effect of high doses of catecholamines was independent from adrenoceptor stimulation and was rather depending on the presence of the tyrosine phosphatase inhibitor vanadium[20]. In this complex situation, we focused our comparison between lean and obese Zucker rats on the still elusive influence of amines on adipose cell biology.

Alongside their activation of receptors on pre- and post-synaptic cell types, catecholamines are exquisitely regulating various adipocyte functions, *via* their rapid release from presynaptic vesicles or other supposed stores[21,22] and their prompt turn-off mechanisms, involving reuptake, degradation, and desensitization to avoid overstimulation. One of the major catabolic steps of catecholamine degradation is catalyzed by monoamine oxidase (MAO). When oxidating any given substrate, MAO does not only terminate its neurotransmitter function, it also releases the corresponding aldehyde and hydrogen peroxide. The MAO activity has been reported to be lower in the liver of the obese than in the lean rat[23], but to our knowledge, no report has described so far a change of this mitochondrial enzyme in adipose depots.

The following results will compare in obese and lean Zucker littermates, the metabolic effects of a MAO substrate, tyramine, as well as its oxidation by MAO and another amine oxidase highly expressed in fat cells, the semicarbazide-sensitive amine oxidase (SSAO). The data presented thereafter will also indicate that the imidazoline binding sites (I_2-sites) that have been documented to be present on MAO[24-27] are more numerous in the white adipose tissue (WAT) of the obese than in the lean rat.

MATERIALS AND METHODS

Chemicals

2-1, 2-^{3}H-deoxy-D-glucose (2-DG; 10 Ci/mmol), 3-^{3}H-D-glucose (10 Ci/mmol), and ^{14}C-tyramine were from PerkinElmer (Shelton, United States). ^{3}H-2-(2-benzofuranyl)-2-imidazoline (^{3}H-BFI; 50 Ci/mmol) and ^{3}H-Idazoxan (42 Ci/mmol) were purchased from Amersham Bioscience/GE Healthcare in 2004 (Buckinghamshire, England), then isotopically diluted in ethanol and stored at -12 °C, and yearly verified since by high performance liquid chromatography (> 90% pure) before being used as radioligands for binding experiments until 2010. Electrophoresis products and devices were from Bio-Rad (Ivry/Seine, France). Rabbit polyclonal antibodies against MAO and SSAO were kindly given by Pr. A. Parini (Toulouse, France), and by Pr. M. Unzeta (Barcelona, Spain), respectively. Rauwolscine was kindly given by Dr. A. Remaury (Sanofi, Chilly-Mazarin, France). All remaining chemicals and drugs, such as cirazoline, sodium orthovanadate, and bovine insulin, were purchased from Merck (Darmstadt, Germany) or its affiliate Sigma-Aldrich (Paris, France).

Animals

Three sets of experiments were successively performed to explore the imidazoline binding sites and the MAO/SSAO activities in various tissues from Zucker rats, and the functional response of adipocytes. All the comparisons between lean and obese Zucker rats were made between littermates. Such comparative approach between littermates was performed on a number of male and female rats that was not always the same for each genotype in each successive experiment. This was due to the fact that the number of pups of a given litter is not always distributed equally according to the gender and to the obese phenotype (which were stated after weaning only). Consequently, the number and gender of analyzed animals are given thereafter for each subset of experiments. All the rats (Charles River Laboratories, L'Arbresle, France) were housed in hanging wire cages with free access to food and water on a 12 h light/dark cycle (lights on 6 a.m.) at a temperature of 20 °C. They were euthanized after overnight fasting between 9 and 10 wk of age in accordance with the ARRIVE guidelines (Animal Research: Reporting of *In Vivo* Experiments)[28].

Adipocyte glucose uptake and lipogenic activity

WAT was removed from intra-abdominal (perigonadic, retroperitoneal, and perirenal; thereafter named visceral WAT) and from subcutaneous (inguinal) locations. It was immediately digested by collagenase in Krebs-Ringer buffer containing 15 mmol/L bicarbonate, 10 mmol/L HEPES, 2 mmol/L pyruvate, and 3.5% bovine serum albumin. Separation, washing, and dilution of the buoyant adipocytes were performed in the immediate continuity at 37 °C with fresh buffer prior to the functional assays, which were performed as previously described[20].

The radiolabeled non-metabolizable analog of glucose, ^{3}H-2-DG, was used at 0.1 mmol/L for hexose uptake assays as described previously[20], save that the assays lasted 5 min instead of 10 min for human fat cells, which are less metabolically active.

Lipogenic activity was determined by measuring the radioactivity incorporated into cellular lipids after 120-min incubation with the indicated agents and 0.5 mmol/L ^{3}H-glucose. This very simple bioassay, primarily designed by Moody and coworkers[29], was performed with slight adaptations[30] in the same plastic vial, which was used for incubation, extraction, and scintillation counting, since the ^{3}H-glucose that was not metabolized by the fat cells remained in the lower phase and could not excite the non-water-miscible liquid scintillation cocktail (InstaFluor-Plus, PerkinElmer, Waltham, United States) of the upper phase, containing the neosynthesized lipids, as already demonstrated[31].

Immunoblots

Homogenates were prepared in RIPA buffer, and proteins were solubilized in loading buffer (60 mmol/L Tris-HCl with 2% SDS, 10% glycerol, 1% β-mercaptoethanol, pH 6.8) at 100 °C for 5 min prior to sodium dodecyl sulfate-polyacrylamide gel electrophoresis. After migration, proteins were transferred to polyvinylidene difluoride membranes with a semidry electroblotter (Trans-blot, Bio-Rad). The blots were blocked in wash buffer (50 mmol/L Tris, 200 mmol/L NaCl, 0.1% Tween 20, pH 7.5) with 5% nonfat dried milk for 1 h at room temperature. Then they were incubated overnight at 4 °C with rabbit polyclonal antisera (1:1000) obtained from rabbits immunized against an epitope of MAO-A and MAO-B as described previously[32]. After washing, the blots were incubated with peroxidase-labeled anti-rabbit IgG

(1:7000) in wash buffer for 60 min. The immunoreactive proteins were detected using enhanced chemiluminescence (Pharmacia Biotech, Piscataway, NJ). Similar procedure was followed when using an anti-SSAO polyclonal antibody developed and tested previously[33]. β-actin amount was determined in stripped membranes, and as no change was observed between preparations from lean and obese animals (not shown), no normalization to β-actin was performed.

Amine oxidase assay

Amine oxidase activity was measured on homogenates of thawed tissues with ^{14}C-tyramine in 200 mM phosphate buffer in the presence of an antiprotease cocktail from Sigma as previously described[30]. MAO activity was defined as oxidation inhibited by pargyline 0.1 mmol/L, while SSAO activity was sensitive to semicarbazide 1 mmol/L. BAT was removed from the core of the interscapular fat depot, and the soleus muscle was chosen as representative of skeletal muscles. Like liver samples, these tissues were snap-frozen without buffer and homogenates were prepared on thawed samples as already described[34]. Protein content was measured with DC-protein assay from Bio-Rad. In the case of amine oxidation by intact fat cells, 1 mM of an isotopic dilution of ^{14}C-tyramine was incubated for 30 min with adipocyte suspension (~10 mg of cell lipids) in 400 µl of KRBH medium instead of phosphate buffer, and treated as above stated for homogenates.

Radioligand binding

For saturation-binding isotherms, membranes were incubated with increasing concentrations of ^{3}H-idazoxan at room temperature for 45 min in Tris-HCl buffer, pH 7.4. The presence of 10 µmol/L rauwolscine was used to mask α_2-adrenoceptors as already demonstrated[32]. For ^{3}H-BFI, it was not necessary to preclude binding to adrenergic receptors since this imidazolinic radioligand has been shown to be selective for the I_2-sites[30,35,36]. In both cases, incubation was stopped by vacuum filtration through Whatman GF/C microfilters with extensive washes with the same buffer at 4 °C. Nonspecific binding was defined in the presence of 100 µmol/L cirazoline and represented 30% to 50% of the total binding depending on the radioligand nature, its concentration, and the biological material tested. Radioactivity bound on the filters was counted in a liquid scintillation spectrometer (Packard, model Tri-Carb 4000) with 4 mL of Packard Emulsifier-Safe scintillation fluid per scintillation microvial.

Statistical analysis

Results are presented as the mean ± SEM of (*n*) observations. Statistical analyses for comparisons between parameters were performed using ANOVA followed by post-hoc Dunnett's multiple comparisons test, and were performed with Prism 6 for Mac OS X (from GraphPad software, San Diego, CA).

RESULTS

Hyperinsulinemia and insulin resistance of adipocytes are characteristic traits of the obese Zucker rat

Some characteristic features of the obese Zucker rats were first verified. At the age of 9-10 wk, the obese rats exhibited larger body weight and adiposity, with elevated insulin and triacylglycerol plasma levels, when compared to their lean littermates of the same age (Table 1). Fasting plasma glucose levels were slightly higher in the obese group, but with a less pronounced difference with respect to the other circulating parameters influenced by genotype. Blood glucose was 1.12 times higher in obese rats, while insulin was four to five times higher and triacylglycerol two times higher than in lean controls. As expected, the males bearing the two alleles with the mutated leptin receptor (fa/fa) were hyperphagic since their daily food consumption was increased by 1.3 times, *i.e.*, similarly to their increased body weight, while the sum of their dissected fat depots was five-to-six-fold heavier than in lean littermates (Table 1).

Our descriptive approach readily confirmed in white adipocytes the insulin-resistant state of the obese rats, which accompanies their clear-cut hyperinsulinemia. The hexose uptake assays showed that the maximal effect of insulin (obtained at 0.1 µmol/L-1 µmol/L) was one-half lower in obese than in lean rats (Figure 1A). The white adipocytes of obese rats also exhibited a reduced sensitivity to insulin: Their response to 10 nmol/L insulin represented less than 60% of the maximal effect of the pancreatic hormone in obese rats while it reached 80% in lean controls (Figure 1A). A

Table 1 Biological parameters of the lean and obese rats used in this study

Littermate phenotype	Lean (8)	Obese (9)
Final body weight (g at 9-10 wk)	230 ± 21	312 ± 16[b]
Visceral WAT weight (g)	1.8 ± 0.3	8.9 ± 1.4[c]
Subcutaneous WAT weight (g)	2.5 ± 0.3	13.4 ± 1.6[c]
Plasma levels		
Insulin (UI/mL)	37 ± 2	178 ± 46[b]
Glucose (mmol/L)	7.7 ± 0.2	8.6 ± 0.2[a]
Triacylglycerols (mmol/L)	0.7 ± 0.2	1.5 ± 0.1[b]

Significantly different from each corresponding value in lean at:
[a]$P < 0.05$.
[b]$P < 0.01$.
[c]$P < 0.001$.
mean ± SEM of the number of rats indicated in parentheses.

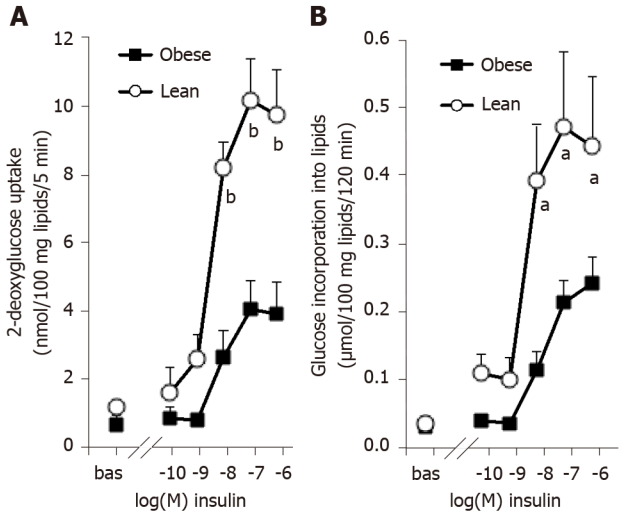

Figure 1 Influence of obesity on the dose-dependent responses of rat adipocytes to insulin activation of hexose uptake and of lipogenesis. A: ^{3}H-2-deoxyglucose (2-DG) transport was assayed for 5 min after 45-min incubation of rat fat cells without (bas) or with increasing doses of insulin. 2-DG uptake is expressed as nmoles of intracellular radiolabeled 2-DG/100 mg lipids/5 min; B: ^{3}H-glucose incorporation into lipids was measured after 120-min incubation with the indicated doses of insulin and is expressed as µmoles tritiated glucose incorporated/100 mg lipids. Adipocytes from lean (open circles) or obese rats (black squares) were incubated at a cell suspension averaging 11.5 and 11.7 mg lipids/assay tube, respectively. A significant influence of genotype on the three higher doses of insulin was found at [b]$P < 0.001$ for 2-DG uptake (n = 10 lean and 10 obese male rats, with male/female = 1) and at [a]$P < 0.05$ for lipogenesis (n = 8 lean and 6 obese male rats). Each point is the mean ± SEM of n animals, with error bars lying within the caption in several occurrences.

similar pattern was obtained when lipogenic activity of the adipocytes was assessed by the incorporation of radioactivity into cell lipids after 120-min incubation with 3-^{3}H-D-glucose (Figure 1B). The insulin resistance was not totally complete in these young obese rats, since the baseline incorporation was increased by a six-fold factor in response to 100 nmol/L insulin. Nevertheless, this maximal activation reached a 12-fold factor in adipocytes from lean rats (Figure 1B). As for hexose transport, the lipogenic effect of 10 nmol/L insulin reached 42% ± 8% and 86% ± 7% of maximal response in obese and lean rats, respectively (n = 8 and 6, respectively, $P < 0.002$).

In order to bring evidence that other factors other than insulin may help the adipocytes in accumulating large amounts of lipids during the growth of the insulin-resistant obese rat, vanadium was tested alone and with hydrogen peroxide, either when directly added at 1 mmol/L, or when generated endogenously by the adipocytes *via* the oxidation of the MAO and SSAO substrates tyramine and benzylamine at 1 mmol/L (Figure 2). Sodium orthovanadate was inefficient at 100 µmol/L, either on basal or on insulin-stimulated 2-DG uptake. However, vanadium potentiated the insulin-mimicking action of 1 mmol/L hydrogen peroxide. The combination of these

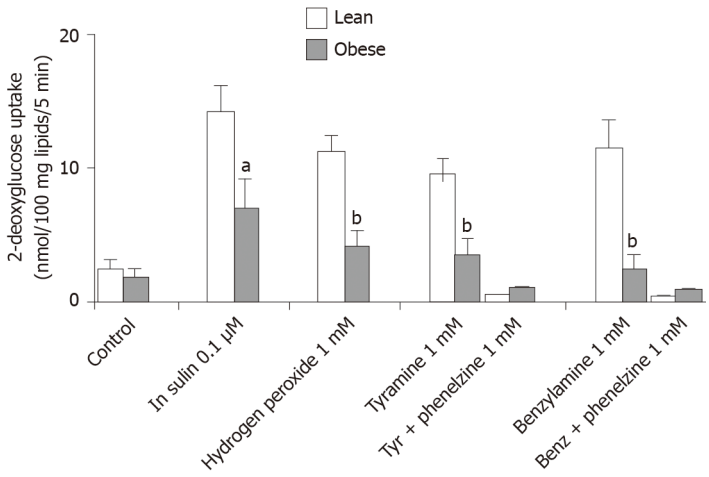

Figure 2 Insulin-like effects of vanadium combined with hydrogen peroxide or with amine oxidase substrates on hexose uptake into rat adipocytes. Sodium orthovanadate was present at 100 µmol/L in all the conditions: Alone (control) or combined with 100 nmol/L insulin, or with 1 mmol/L hydrogen peroxide, tyramine, and benzylamine. The amines were tested without and with 1 mmol/L phenelzine. 2-deoxyglucose (2-DG) uptake is expressed as nmoles of intracellular 2-DG/100 mg lipids/5 min. Mean ± SEM of five lean (open columns) and five obese male rats (shaded columns). Significantly different from corresponding condition in lean at: $^{a}P < 0.05$; $^{b}P < 0.01$. Blockade of tyramine (tyr) or benzylamine (benz) effect by phenelzine was significant at $P < 0.001$ in both genotypes.

two agents is known to generate peroxovanadate, a powerful protein tyrosine phosphatase inhibitor[37,38]. It led to a stimulation of glucose uptake equivalent to 70%-80% of the response to insulin in lean rats (Figure 2). Tyramine, a substrate of both MAO and SSAO in rodents[34], was also able, when combined with vanadium, to reproduce 60%-70% of insulin maximal response in the lean rats. This insulin mimicry was also obtained with 1 mmol/L benzylamine, but it represented 84% ± 16% of insulin + vanadate effect in lean and only 38% ± 7% in obese rats ($n = 5$, $P < 0.03$). As expected, the MAO and SSAO inhibitor phenelzine abolished the effects of tyramine or benzylamine plus vanadium in both genotypes (Figure 2).

These first observations indicated that the MAO- or SSAO-mediated effects of tyramine on glucose handling by fat cells were limited similarly as those of insulin in obese Zucker rats. However, since the effect of benzylamine plus vanadate seemed to decrease even more with obesity, we further studied the protein expression of the amine oxidases in WAT.

Western blot analysis of amine oxidases in adipose tissues of lean and obese Zucker rats

When the expression of MAO and SSAO was determined by Western blot in subcutaneous WAT, opposite changes were observed for these membrane proteins. WAT expressed less SSAO in obese than in lean rats, at least in the subcutaneous depots of 10-wk-old animals (Figure 3). This lower abundancy was agreeing with the above reported lower insulin-like effects of benzyamine regarding glucose uptake in adipocytes. More puzzling was the obesity-related increase in MAO-A protein, while MAO-B was poorly affected in obese rats. As a consequence of these opposite regulations, the resulting effect on glucose transport of the MAO and SSAO substrate tyramine did not exhibit a dramatic change in adipocytes from obese rats, at least when normalized to the maximal insulin response. To state whether tyramine catabolism is really greater in WAT from obese rats, it was decided to investigate its oxidation in various tissues.

Amine oxidase activities in several tissues of lean and obese Zucker rats

The oxidation of 0.5 mmol/L ^{14}C-tyramine by crude membranes of different tissues is shown in Figure 4, in which 'total oxidation' means spontaneous oxidation of the amine in the presence of biological material, without any added inhibitor or catalyst. Since the liver is known for being rich in MAO activity, it was tested here as a positive control. As expected, the liver was the richest of the tested tissues regarding MAO activity, which entirely supported total tyramine oxidation, and which did not exhibit difference between genotypes. No SSAO activity was detectable in liver homogenates regardless of the genotype.

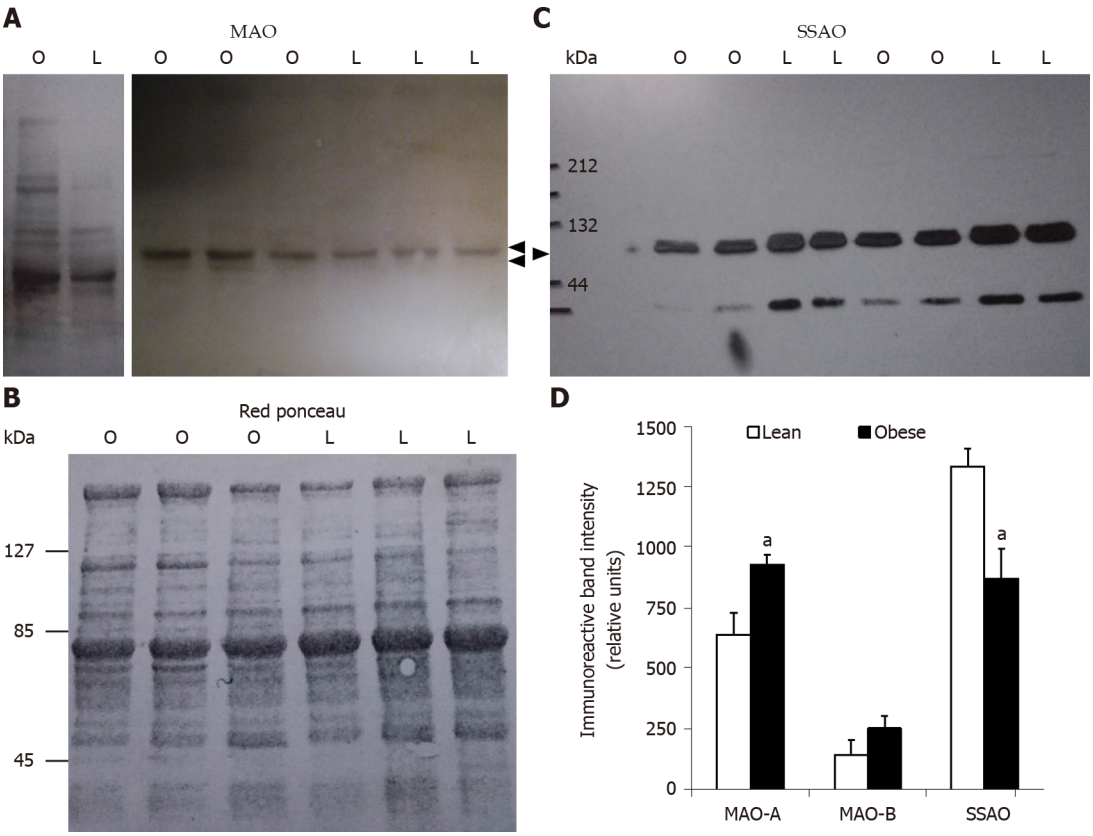

Figure 3 Increased monoamine oxidase and decreased semicarbazide-sensitive amine oxidase protein expression in subcutaneous adipose tissue from obese rats when compared to lean littermates. Proteins solubilized from white adipose tissue homogenates were separated by sodium dodecyl sulfate-polyacrylamide gel electrophoresis and blotted proteins detected using primary antibodies directed against monoamine oxidase (MAO) or semicarbazide-sensitive amine oxidase (SSAO). 50 μg and 5 μg proteins per lane were deposed for MAO and SSAO immunoblots, respectively. A: Immunoblots showing immunoreactive MAO-A and MAO-B at approximately 61 and 55 kDa (arrows) for obese (O) and lean (L) rats; B: Red ponceau control of protein loading for a representative membrane shown in panel A; C: Representative immunoblot of SSAO showing a major band at approximately 85 kDa (arrow); D: Densitometry analysis of the major bands is shown for 7-8 rats per genotype. Different from lean (open columns) at: $^{a}P < 0.05$.

Tyramine oxidation in crude membranes of adipose cells from visceral fat depots was greater in obese than in lean rats (Figure 4). This was largely due to an increased MAO activity, which was prominent in white adipocytes when considering the large proportion of total tyramine oxidation that was inhibited by pargyline (therefore MAO-dependent). The smaller fraction of tyramine oxidation that was sensitive to semicarbazide (therefore SSAO-dependent) was not clearly reduced in visceral adipocytes from obese rats (Figure 4). Altogether, these changes were similar to those observed in immunoblots of subcutaneous WAT.

In the interscapular adipose tissue, which contains brown adipocytes, thereby considered as BAT, increased tyramine oxidation was also found in obese rats (Figure 4). Although both MAO and SSAO activities were higher in BAT from obese than from lean rats, none of them reached the levels found in WAT. Lastly, in skeletal muscle crude membranes, tyramine oxidation was weak regardless of the genotype.

The fact that an increase in tyramine oxidation only occurred in WAT and BAT raised a concern about possible yield variations during membrane preparation between obese and lean rats. In fact, only the adipose depots were impressively much fatter in the obese than in the lean rat, while this was less evident for the liver and skeletal muscles. To circumvent a possible bias generated by an excess of fat in the different centrifugation steps necessary for membrane preparation, we studied the genotype influence on the capacity to oxidize tyramine in undamaged, functional adipocytes freshly isolated from visceral WAT. Again, adipocytes from obese rats possessed a higher capacity to oxidize tyramine when compared to lean ones (Figure 5). Even being of larger cell size, the adipocytes of obese Zucker rats definitely exhibited a larger MAO activity than lean controls. Figure 5 also shows that the same SSAO activity was found in adipocytes from obese rats and lean controls. Finally, MAO and SSAO activities were complementary to account for the total tyramine oxidation performed by adipocytes, ruling out a notable contribution of other amine oxidases.

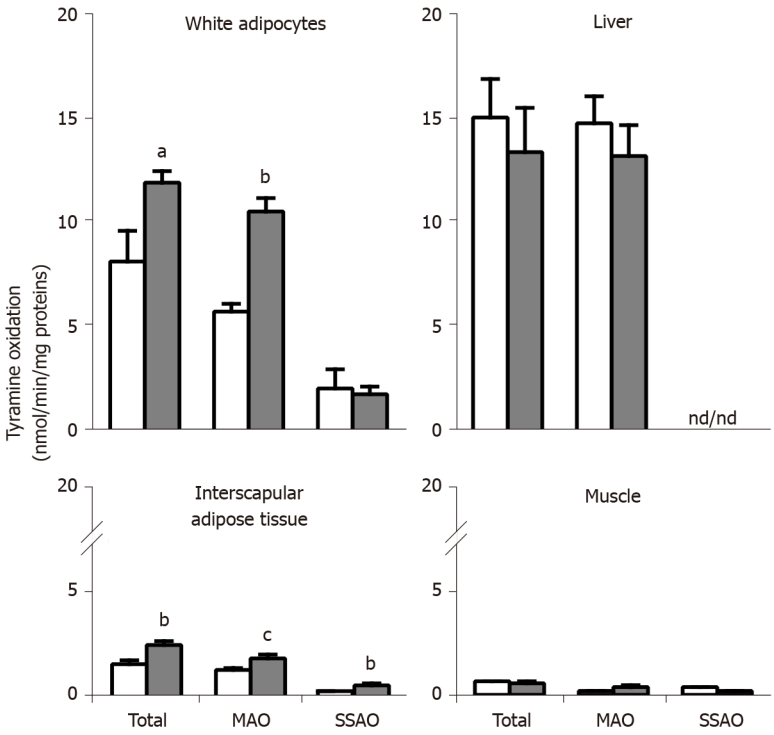

Figure 4 Oxidation of tyramine by membrane preparations from different tissues of obese and lean Zucker rats. Crude membranes prepared by centrifugation from adipocytes isolated from visceral white adipose tissue, or from the liver, brown adipose tissue, and soleus muscle, were incubated for 20 min at 37 °C with 0.5 mmol/L ^{14}C-tyramine in phosphate buffer (200 mmol/L) without (total oxidation), with 1 mmol/L semicarbazide (monoamine oxidase, MAO), or with 1 mmol/L pargyline (semicarbazide-sensitive amine oxidase, SSAO). The minor oxidation remaining in the presence of both inhibitors (semicarbazide + pargyline), therefore non-SSAO and non-MAO, was subtracted in all cases. Mean ± SEM from four determinations for lean (open columns) and five for obese male rats (dark columns); ND: Non-detectable. Significantly different from lean at: $^{a}P < 0.05$; $^{b}P < 0.01$; $^{c}P < 0.001$.

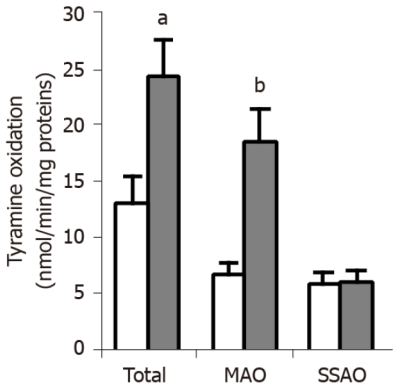

Figure 5 Tyramine oxidation in adipocytes from obese and lean Zucker rats. Undamaged adipocytes isolated from visceral white adipose tissue of lean (open columns) and obese (dark columns) rats were incubated in the presence of 1 mmol/L ^{14}C-tyramine for 45 min at 37 °C. Total oxidation was measured without any inhibitor, while the oxidation that resisted to 1 mmol/L semicarbazide was due to monoamine oxidase, and the oxidation resistant to 1 mmol/L pargyline was semicarbazide-sensitive amine oxidase-dependent. The velocities of oxidation are expressed as as nmoles of radiolabeled tyramine oxidation products generated per min and per mg of proteins. Each column is the mean ± SEM of eight determinations for lean and nine determinations for obese male rats. Significantly different from lean at: $^{a}P < 0.05$; $^{b}P < 0.01$.

In view of the enlarged MAO activity that appeared specific for WAT and BAT, we reanalyzed in various tissues from obese and lean rats an unpublished comparison of the population of I_2 imidazoline binding sites, previously described to be present on MAO enzymes[24,26,27] and distinct from the I_1 sites, essentially labeled by clonidine or moxonidine[39,40].

Pharmacological analysis of imidazoline binding sites in tissues of lean and obese Zucker rats

By using a saturating concentration of ^{3}H-BFI (20 nmol/L), we quantified the I_2

imidazoline binding sites in crude membranes from the same anatomical locations as above. A difference in the amount of ^{3}H-BFI bound was evident between obese and lean rats in visceral adipocytes only. The obese rats exhibited the same ^{3}H-BFI binding as the lean controls in the liver, interscapular BAT, and skeletal muscle (Figure 6).

This comparison was completed by saturation binding experiments in adipocyte membranes from visceral and subcutaneous WAT with ^{3}H-BFI and ^{3}H-idazoxan. Increasing concentrations of ^{3}H-BFI (from 0.2 to 26 nmol/L) resulted in saturation curves for total binding, with a clearly lower non-specific binding that was defined in the presence of 100 µmol/L cirazoline (Figure 7). Scatchard plots of the resulting specific binding gave an almost linear relationship between the bound/free ratio and the quantity of bound radioligand (Figure 7). The estimates of the affinity constant (K_D) and of the population density (B_{max}) of the corresponding single class of binding sites are reported in Table 2. A significant increase of the number of I_2 imidazoline binding sites was found in WAT of the obese Zucker rats when compared to lean controls. The nature of these binding sites was not modified by the obesity status since the K_D values were not different between obese and lean rats (Figure 7 and Table 2).

Similar saturation binding parameters were observed when using ^{3}H-idazoxan (from 0.7 to 45 nmol/L) as radioligand in the presence of 10 µmol/L rauwolscine to preclude its binding to α_2-adrenoceptors. Again, higher B_{max} values were found in the WAT of obese rats without notable change in K_D values when compared to lean controls (Figure 7 and Table 2). ^{3}H-idazoxan exhibited a lower affinity for the I_2 sites than ^{3}H-BFI, and it exhibited also a less selectivity towards imidazoline sites since, at 14 nmol/L, non-specific binding reached 50% of total binding in lean while it represented 10% of total binding in obese rats (not shown).

Nevertheless, the B_{max} values obtained with ^{3}H-idazoxan were of the same order of magnitude as the values observed with ^{3}H-BFI, suggesting that both imidazolinic radioligands recognized the same binding sites. Moreover, the observed increase in the density of I_2 sites in obese rat could not be associated to changes in the protein amounts used in binding experiments since we used similar protein levels regardless of the genotype, at least for visceral WAT (Table 2).

Thus, the larger density of I_2 sites specifically found in the WAT of obese rats was related to an increased MAO activity. Binding data were also in agreement with the previously reported capacity of BFI to inhibit MAO activity present in human and rodent adipose tissues[30]. To further explore the functional link between I_2 sites, MAO activity, and tyramine insulin-like effect, we performed two distinct approaches, one consisting in a short-term *in vitro* experiment on the interplay between I_2 binding sites and MAO activity, and the other based on repeated *in vivo* administration of tyramine plus vanadate to Zucker rats.

Since MAO activity and I_2 binding sites appeared to be linked with respect to their higher levels in WAT from obese rats when compared to lean controls, we took advantage of their abundancy in the liver to verify whether the one can influence the other. Figure 8 shows the total and the non-specific binding of increasing doses of ^{3}H-idazoxan to liver crude membranes from lean Zucker rats. The former followed a curve reaching saturation while the latter was linearly increasing with radioligand concentration. Addition of a large dose of tyramine (5 mmol/L) to saturate the active sites of hepatic MAO abolished the total idazoxan binding without altering the non-specific one. This confirmed the functional interaction between MAO activity and I_2 binding sites.

In vivo treatment of lean and obese rats with tyramine plus vanadate

A repeated treatment with 'tyramine + vanadate' was performed on 9-wk-old lean and obese rats to investigate whether the *in vitro* insulin-mimicking effects of this combination could have any *in vivo* relevance. The subcutaneous administration of tyramine at 3 mg/kg/d combined with sodium orthovanadate at 0.3 mg/kg/d for 1 wk was well tolerated, and did not modify significantly the body weight gain in obese rats when compared to controls receiving the vehicle (daily s.c. bolus of 0.3 mL NaCl 0.9%): 47 + 8 *vs* 46 ± 8 g (n = 3-4, NS). Body weight gain was also unaltered in treated lean rats (33 ± 3 *vs* 32 ± 3 g; n = 3-4, NS). Daily food intake was also unchanged since it remained around 23 g/rat in the treated and control lean groups, and was comprised between 29 and 40 g/rat in the obese groups (not shown). Obviously, the clear-cut difference between obese and lean rats regarding fat deposition could not be modified by this relatively short-term treatment. Only a non-significant tendency to enhance the mass of dissected adipose depots was seen in obese treated rats, while one of the dissected fat depots was heavier in lean rats receiving tyramine (Figure 9). Interestingly, tyramine + vanadate treatment reduced moderately but significantly the fasting plasma levels of glucose and triacylglycerols in the obese treated group (Figure 9).

Table 2 Imidazoline binding sites labeled by ^{3}H-2-(2-benzofuranyl)-2-imidazoline or ^{3}H-idazoxan: Comparison between visceral and subcutaneous white adipose tissues of lean and obese rats

Radioligand genotype	^{3}H-BFI		^{3}H-idazoxan + rauwolscine 10 μmol/L	
	Lean	Obese	Lean	Obese
	Visceral WAT			
Bmax (fmol/mg protein)	608 ± 39	1467 ± 208[c]	232 ± 42	1268 ± 108[c]
K_D (nmol/L)	8.9 ± 2.0	6.5 ± 0.5	16.9 ± 2.2	17.6 ± 2.6
proteins (μg/assay)	45 ± 6	49 ± 2	34 ± 7	46 ± 2
	Subcutaneous WAT			
Bmax (fmol/mg protein)	309 ± 25	1046 ± 12[c]	212 ± 39	914 ± 53[c]
K_D (nmol/L)	9.3 ± 0.8	5.7 ± 1.2	22.5 ± 2.3	16.5 ± 3.1
proteins (μg/assay)	51 ± 7	83 ± 12[a]	51 ± 7	83 ± 12[a]

Significantly different from each corresponding value in lean at:
[a]$P < 0.05$.
[c]$P < 0.001$.
The maximal binding value, B_{max} expressed as fmol/mg proteins, and affinity constant, K_D expressed as nmol/L, were calculated from three independent Scatchard plots built for each radioligand. The mean quantity of membrane proteins used per assay tube is also reported for each white adipose tissue anatomical location and radioligand.

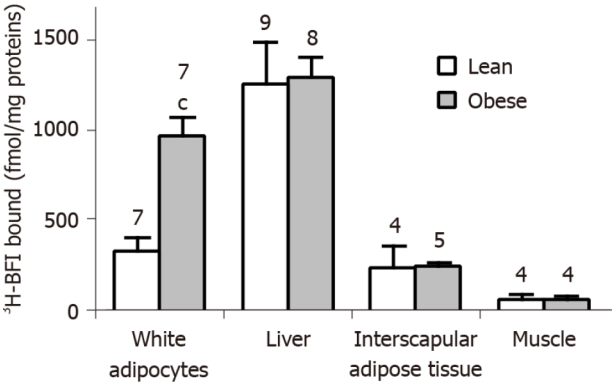

Figure 6 Tissue-selective larger imidazoline binding site density in the white adipocytes from obese rats when compared to lean littermates. Crude membranes were prepared from adipocytes isolated from white subcutaneous fat depots, the liver, interscapular brown adipose tissue, and soleus muscle, and incubated for 45 min with 20 nmol/L ^{3}H-2-(2-benzofuranyl)-2-imidazoline (^{3}H-BFI), before separation by vacuum filtration as indicated in Methods. Only the specific binding of ^{3}H-BFI, *i.e.*, displaceable by 100 μmol/L cirazoline, is shown. For each tissue, there was one determination of specific binding per rat, calculated by the difference between total and non-specific binding. Results are the mean ± SEM of the number of rats indicated above each column (open for lean, shaded for obese rats). Significantly different from corresponding value in lean at: [c]$P < 0.001$.

Regarding glucose uptake, the tyramine + vanadate treatment was not sufficient to mitigate the clear insulin-resistant state of the adipocytes of obese Zucker rats (Figure 9). However, it was investigated whether the insulin-effect of peroxovanadate on glucose transport in adipocytes (generated by *in vitro* addition of 1 mmol/L hydrogen peroxide + 0.1 mmol/L vanadate) was modified by the tyramine + vanadate treatment, especially in the obese rats, in view of their higher MAO content. The hexose uptake stimulated by hydrogen peroxide plus vanadate was similar in control and treated obese rats: 4.19 ± 1.30 and 3.29 ± 1.55 nmol 2-DG/100 mg lipids/5 min, respectively (n = 5, NS). Again, this peroxovanadate-dependent stimulation of hexose uptake was higher in lean rats, regardless of treatment: 11.32 ± 1.26 and 10.46 ± 2.61 nmol 2-DG/100 mg lipids/5 min (n = 5, NS). Nevertheless, it is worth noting that these values were, in each genotype, close to the maximal stimulation of hexose uptake triggered by high doses of insulin (see Figure 9). At least, the tyramine + vanadate treatment did not induce any desensitization of the insulin mimicking action of hydrogen peroxide plus vanadate.

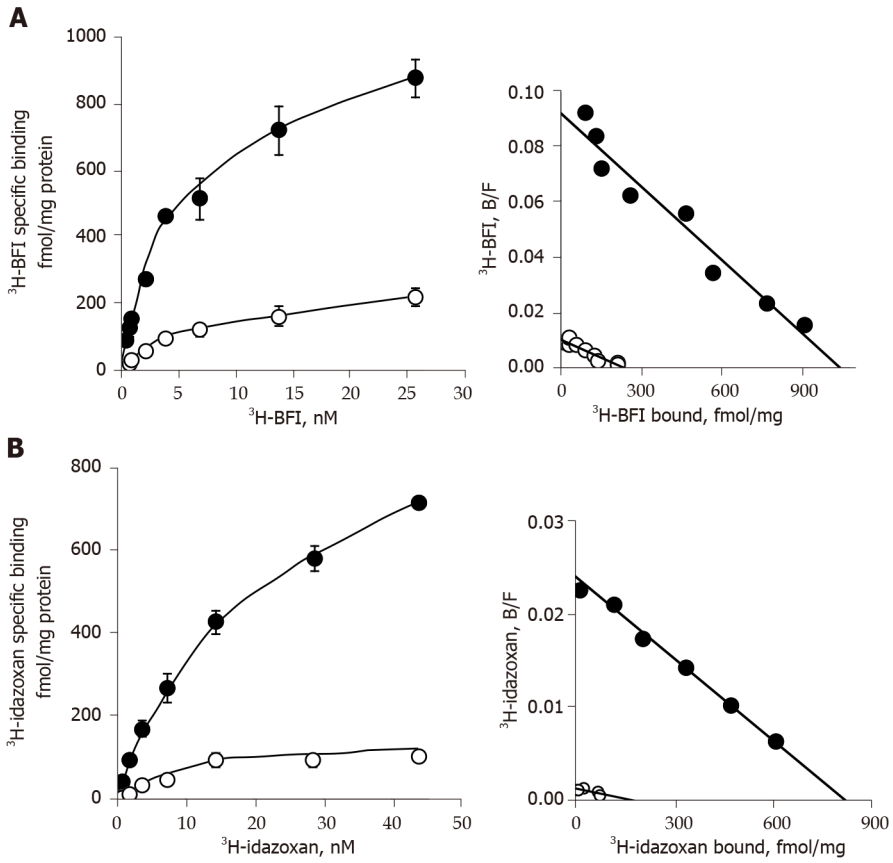

Figure 7 Saturation binding analysis with ^{3}H-2-(2-benzofuranyl)-2-imidazoline and ^{3}H-idazoxan in adipocyte membranes from white subcutaneous adipose tissue of lean and obese rats. A and B: Adipocyte membranes from subcutaneous white adipose tissue of lean (open circles) or obese (dark circles) littermates were incubated for 45 min with increasing concentrations of ^{3}H-2-(2-benzofuranyl)-2-imidazoline alone (A) or ^{3}H-idazoxan plus 10 μmol/L rauwolscine (B). For each tested concentration, total binding was measured in the absence of any competitor while non-specific binding was determined in the presence of 100 μmol/L cirazoline. Left panels show the saturation curves of specific binding, with each point corresponding to the mean ± SEM of three separate saturation experiments. Right panels show the Scatchard plot (bound/free *vs* bound) of the saturation experiment for each radioligand. Calculated parameters of saturation experiments are reported in Table 2.

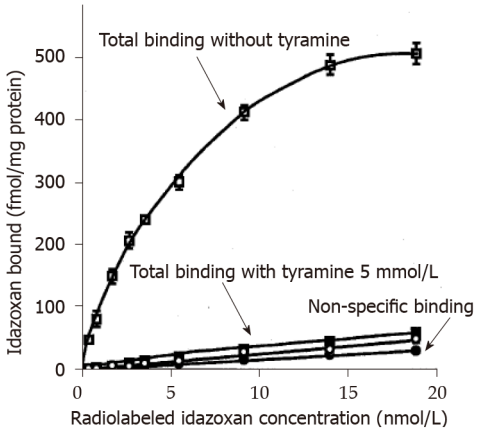

Figure 8 Influence of tyramine on idazoxan binding to liver crude membranes. Total and non-specific binding of ^{3}H-idazoxan to liver crude membranes from lean Zucker rats is shown without (open symbols) and with 5 mmol/L tyramine (closed symbols) added prior to 45-min incubation at room temperature. Without tyramine, the resulting specific binding was characterized by a B_{max} of 622 ± 15 fmol/mg protein and a K_D of 5.1 ± 0.4 nmol/L. Each point is the mean ± SEM of three liver preparations containing 617 ± 120 μg protein/assay. Inhibitory influence of tyramine on total binding was significant at $P < 0.001$.

Thus, the effects of *in vivo* tyramine + vanadate treatment could not reveal relevant antidiabetic or anti-obesity properties, at least at the dose and duration tested. However, the limited - but encouraging - beneficial influence of this treatment on hyperglycemia and hypertriglyceridemia leaves opens the possibility to improve metabolic control by providing MAO substrates, which might enhance glucose

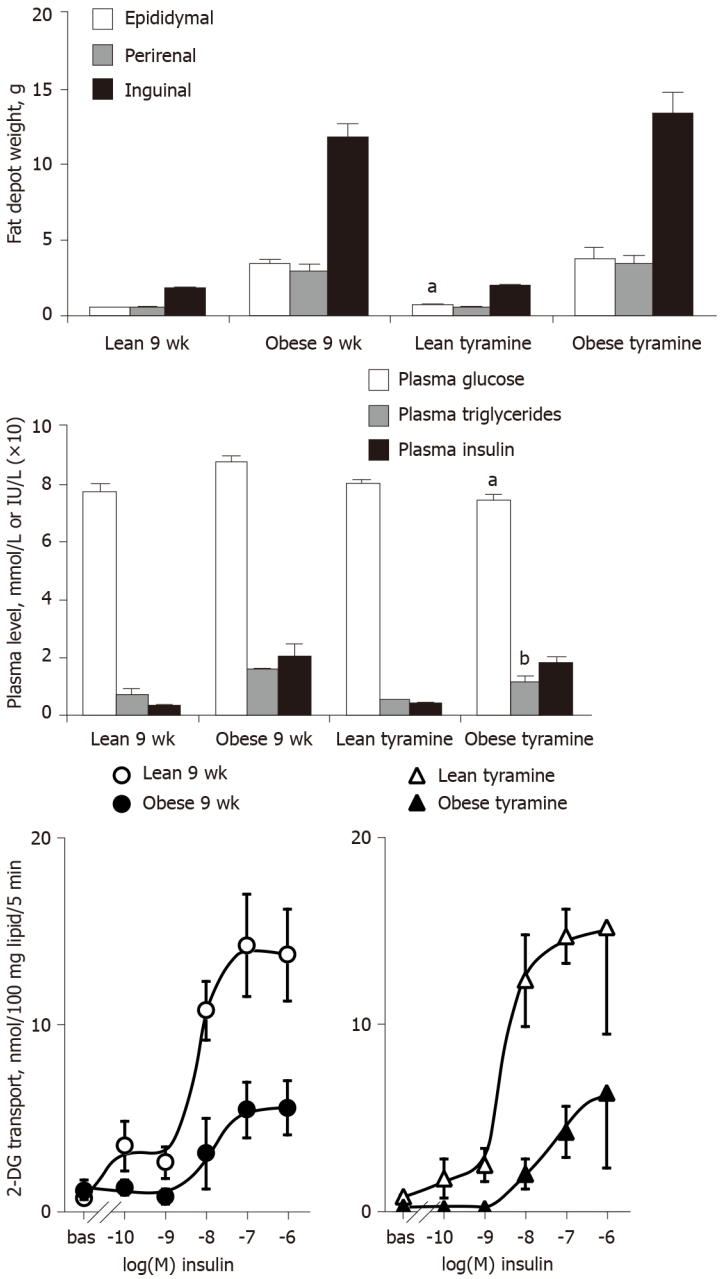

Figure 9 Influence of 'tyramine + vanadate' treatment on adiposity, glucose and lipid handling, and insulin responsiveness of adipocytes in lean and obese rats. Upper part: Weight of three white adipose tissues from 9-wk old Zucker male rats, either from the lean and obese control groups (left) or from the groups receiving daily s.c. administration of 3 mg/kg tyramine + 0.3 mg/kg vanadate (tyramine, right) for 7 d. Middle part: Glucose, triacylglycerol, and insulin fasting plasma levels in the same control and treated groups. Lower part: Hexose transport in adipocytes from lean (open symbols) or obese (closed symbols) rats, in the absence (bas = basal) or presence of the indicated doses of insulin in control (circles) or treated (triangles) groups. Each column or point is the mean ± SEM of three treated or four control rats per genotype. The influence of genotype on all parameters was identical to that specified in previous figures and not indicated for the sake of clarity. Significant difference between tyramine-treated and corresponding control at: $^{a}P < 0.05$; $^{b}P < 0.01$.

utilization in fat depots and facilitate glucose handling at the expense of a slightly larger fattening.

DISCUSSION

The first unexpected observation of this comparison between obese and lean Zucker rats was that the stimulatory effect of millimolar dose of tyramine + vanadate on glucose uptake in adipocytes was altered as much as that of insulin in the obese rat.

Obviously, insulin resistance of adipocytes from obese Zucker rat was expected, and fully confirmed here, but it could be supposed that agents that act independently from insulin receptor activation were less hampered with obesity.

Indeed, many factors could be involved in the decreased insulin-like effect of the combination tyramine + vanadate or benzylamine + vanadate on adipocytes from obese rats, such as altered glucose transporter equipment and recruitment[41]. Anyhow, our initial working hypothesis was based on a putative reduction in the amount of adipose amine oxidases since we recently reported that mice bearing genetic invalidations of SSAO are obese[31].

The second major finding was that, contrarily to our assumptions, MAO activity was higher in the WAT of obese rats than in lean ones. In other words, the MAO substrate tyramine was not more efficient in activating glucose utilization while its degradation was increased in adipocytes from obese animals. This could have a sense if tyramine effect was mediated by a receptor-dependent mechanism, thereby considering that its increased degradation hampered receptor activation. But, in the case of tyramine, the insulin-like effect on glucose utilization by rat adipocytes is mediated by amine oxidation and subsequent hydrogen peroxide release[34]. This is also the case for various other amine oxidase substrates, such as benzylamine or methylamine, which are also active in rodent[42] and human adipocytes[43].

Although the insulin-mimicking action of tyramine is tremendously potentiated by vanadium[34], it was amazing to observe a decrease of such MAO-mediated response together with an increase of MAO activity in the adipocytes from obese rats. We confirmed the latter increase with regard to the level of enzyme activity, protein immunoreactivity, and an increased number of I_2 imidazoline binding sites, located on this mitochondrial enzyme[24,25,32]. Unfortunately, we encountered some technical difficulties with the quantification of rat MAO mRNA despite our know-how developed on MAO expression in the mouse WAT[31]. Consequently, we cannot add to the above converging data that the expression of the genes *Maoa* and *Maob* is increased in the WAT of obese Zucker rats. Despite such limitation, our study clearly indicates that the obesity-related increase of MAO activity was selective of WAT and of BAT, since no change was detected in the liver or in skeletal muscle. Moreover, MAO up-regulation was not paralleled by similar changes of SSAO in WAT. This will be discussed below after summarizing other major metabolic and endocrine defects of the obese Zucker rats that have been confirmed in the present study.

The overweight of the obese rats used for this comparative approach, and the stabilization of their fasting blood glucose close to the normal range at the expense of dramatically increased insulin levels are characteristic traits of this obesity model, which were highly similar to those primarily described for over half a century in the Zucker fatty rat[44]. While the original pioneering findings demonstrated the insulin resistance of skeletal muscles from obese Zucker rats, we confirm here the insulin resistance of white adipocytes at the level of glucose transport and lipogenic activities. More importantly, such insulin resistance was associated in WAT to dysregulations not described so far.

Thus, MAO activity, MAO immunoreactive protein amount, and imidazoline I_2-binding site population were increased in adipocytes from the obese Zucker rats. In muscles of the same animals, the low expression of MAO and SSAO, already documented by diverse techniques[45,46], was unmodified in spite of similar insulin resistance regarding glucose utilization[44]. Facing to such tissue-specific difference, it was therefore difficult to establish a mere link between MAO expression and insulin sensitivity. Although the mechanisms underlying the overexpression of MAO activity specifically in WAT and BAT could not be deciphered here, it must be reminded that MAO is regulated in various organs by numerous factors, including aging, and in different directions for A and B forms[27]. This complexity of regulations may explain why the decreased hepatic MAO previously found in obese rats[23] was not confirmed here. Other possible explanation of this discrepancy can be that in the previous study, it was the decreased mitochondrial content per mass of fatty liver that was the drive for the observed reduction, while in the present study MAO activity was expressed per mass unit of crude membrane proteins. In WAT and BAT, whether adipose MAO was up-regulated by an excess of its substrates as a consequence of the hyperphagia driving obesity remains speculative, and has no rationale to be different from the contradictory changes found in the liver.

Closely related to the MAO increase found in the adipose tissue of obese rats was the increase in imidazoline I_2 binding sites. It occurred only in WAT and was readily visualized by a larger B_{max} for either ^{3}H-BFI or ^{3}H-idazoxan regardless of fat depot anatomical location. The link between I_2 sites and MAO was further supported in the liver by two observations. First, a lack of change between lean and obese rats was found for both parameters: Neither MAO V_{max} nor ^{3}H-BFI B_{max} was altered with obesity in the liver. Second, the ^{3}H-idazoxan binding to hepatic I_2 sites was completely prevented by a high dose of tyramine. These observations complete our previous

report about the capacity of BFI to inhibit MAO-A and MAO-B activities[30]. The obesity-related changes in imidazoline I_2 binding sites seemed to be specific of adipose cells, since no change was evidenced in several other peripheral tissues (this study), and in the brain of obese rats when compared to lean controls[47].

Also of interest was that a lower SSAO activity was concomitant to a larger MAO richness in the adipose cells from obese rats. It can be hypothesized that the small reduction in SSAO activity was involved in the resulting weak insulin-like effect of tyramine, since tyramine is a substrate of both enzymes, at least in rats[34]. Thus, according to our working assumptions, SSAO was reduced in WAT from obese rats, and accordingly the activation of glucose uptake by the SSAO substrate benzylamine (plus vanadate) was diminished.

Indeed, reduced expression of SSAO has been already reported at the level of mRNA abundance and of benzylamine oxidation in the WAT of obese rats as compared with their lean littermates[48]. In this study, the SSAO activity found in the WAT of obese rats was one-half lower than that found in lean controls. Although this reduction is apparently greater than that reported here for immunoreactive SSAO, both observations remain in good agreement. Since benzylamine oxidation was measured *via* a fluorometric method quantifying the hydrogen peroxide production in the previous study[48], it can be supposed *a posteriori* that this had generated underestimates of SSAO activity in obese rats, in view of the increased catalase activity found in their WAT[49]. Such increased catalase might also impair the hydrogen peroxide-dependent activation of glucose uptake that we report here in the obese adipocytes. Whether the decreased SSAO activity in obese WAT is related to a previously reported increase in the spermine and spermidine content of the adipocytes of obese Zucker rats [50] remains to be established, but it must be noted that, alongside their role of regulator of triacylglycerol synthetic enzymes, polyamines are also SSAO substrates. More surely, it can be asserted that the SSAO decrease appeared to be tissue-specific for WAT, as no change in SSAO activity has been found in other anatomical locations (this study), as well as in the aorta of obese Zucker rats[51]. Anyhow, a similar diminution of SSAO has not been found in other animal models of obesity, since modest increases in SSAO activity have been observed in the adipose tissue from db/db mice and dogs fed a high-fat diet when compared to respective control (reviewed in[43]).

It becomes evident that it is not only overweight and WAT hypertrophy that can be related to SSAO expression, but also the overall alteration of glucose and lipid handling of obese states. Of course, SSAO is one of the most abundant proteins present on the cell surface of the adipocytes[52]. SSAO-mediated oxidation of exogenous substrates induces glucose uptake in adipocytes isolated from WAT or obtained by *in vitro* differentiation of preadipose cell lines (reviewed in[43]) and in several other models[53]. SSAO-mediated deamination reactions generate hydrogen peroxide, which also induces antilipolytic and lipogenic effects[54], especially in the presence of vanadate, by forming pervanadate, a potent insulin-like agent[38,55]. More recently, it has been proposed that SSAO interplays with Zinc-α2-glycoprotein[56] and with lipid metabolism in adipocytes[57]. In addition, SSAO is identical to vascular adhesion protein-1 (VAP-1), which supports leukocyte extravasation[58]. These multifunctional facets of SSAO are therefore rendering highly probable the occurrence of various apparently contrasting regulations according to the pathological states of adipose tissues.

Two very recent findings are dealing with our observations of a parallel increase of MAO and I_2 sites in the WAT of obese Zucker rats.

On the one hand, untargeted metabolomics analysis performed in the blood of Zucker diabetic rats indicates that the tryptophan and tyrosine metabolisms are the most dysregulated pathways in this model[59]. This is somewhat dealing with our description of changes in MAO activity occurring in the insulin-resistant adipocytes from obese rats. First, tryptophan is linked with kynurenine and serotonin, which is readily oxidized by MAO and generates 5-hydroxyindoleacetic acid. Second, tyrosine is the precursor of biosynthetic pathways for catecholamines and trace amines and therefore an important source of MAO substrates. By associating these two independent findings, it can be assumed that both biosynthesis and degradation of catecholamines are altered in the obese Zucker rat. Although poorly described, catecholamine catabolism occurs in adipose tissues, especially in visceral WAT, and has been shown to influence both glucose metabolism[60] and adrenergic contraction of mesenteric arteries[61].

On the other hand, it has been proposed during the completion of this work that creatine kinase B controls futile creatine cycling, and is powerfully induced by thermogenic stimuli in both mouse and human adipocytes[62]. Intriguingly, creatine

kinase B has also been proposed to be an imidazoline binding protein in rodents[36]. Indeed, "non-MAO" imidazoline binding sites have been evidenced in diverse mammalian tissues, such as those related to brain creatine kinase B[63]. At the present time, one limitation of our study is that we cannot attest that the reported ^{3}H-idazoxan and ^{3}H-BFI B_{max} values are overestimating or not the MAO quantity in the studied peripheral tissues.

Although we have already documented that I_2 site ligands inhibit MAO[24] and in spite of confirming this link in the present study, it is necessary to remind that we have serendipitously described the antilipolytic properties of 0.1-1 mmol/L BFI in human fat cells without bringing clear demonstration of the underlying mechanisms[30]. Whether the "non-MAO" imidazoline binding sites such as creatine kinase B are involved in this effect as well as the obesity-related changes of I_2 sites in WAT remains to be established.

CONCLUSION

This work is reporting for the first time an adipocyte-specific increase of both MAO and I_2 sites in obese Zucker rats when compared to their lean controls. In spite of this higher capacity of catabolizing endogenous or exogenous amines, the insulin-like effects of tyramine and benzylamine, decreased as much as the insulin activation of glucose transport in the large fat cells of the obese rat. It remains to establish whether the activation of glucose uptake by MAO and SSAO substrates, which can be readily observed *in vitro* in the presence of vanadate, really occurs *in vivo* and might help the insulin-resistant fat cells in storing energy under the form of lipids.

ARTICLE HIGHLIGHTS

Research background

The genetically obese Zucker rat is hyperphagic and accumulates the excess of calorie intake in the form of lipids in spite of the insulin-resistant state of its adipocytes.

Research motivation

To investigate what biological events or natural biochemical processes drive the glucose utilization in fat cells of obese Zucker rats, which are not fully responsive to the lipogenic action of insulin.

Research objectives

Hydrogen peroxide is a biological chemical that can mimic several insulin actions on adipocytes, such as stimulating glucose entry and lipogenesis, and inhibiting lipolysis. Since it is a product of various enzymes in adipocytes, we focused our objective in searching whether the expression activity and biological effect of two types of them, namely, the monoamine oxidase (MAO) and semicarbazide sensitive amine oxidase (SSAO), abundant in adipocytes, were modified in obesity states.

Research methods

Experimental methods included Zucker rat husbandry, with obese and lean littermates (the former bearing homozygotous recessive mutation of fa/fa gene), preparations of freshly isolated adipocytes, functional exploration of hexose transport using uptake assays with appropriate pharmacological agents, and determination of lipogenic activity, immunobloting, measurement of amine oxidase activities, and saturation binding analyses.

Research results

There is a good relationship between the increased binding capacity of tritiated-idazoxan and tritiated-(2-benzofuranyl)-2-imidazoline to imidazoline binding sites and the increased MAO-dependent tyramine oxidation in adipose tissue of obese rats. Stimulation of MAO or SSAO by their substrates in the presence of vanadate reproduced approximately two-thirds of the insulin stimulation of glucose uptake in fat cells. However, this insulin-like effect decreased as the insulin responsiveness of adipocytes decreased with obesity.

Research conclusions

It cannot be stated whether the changes in MAO and SSAO expression are a cause or a consequence of the altered glucose handling in the fat cells of obese Zucker rats. At least, the increased tyramine oxidation is found in adipose tissues of the obese rats, not in the liver or in skeletal muscles, and can be associated with the dysregulation of the catecholaminergic system and of the energy balance found in that animal model of genetic obesity.

Research perspectives

The increase of MAO activity in adipose tissue from obese rats has never been reported, at least to our knowledge. Among the limitations of our first description of an increased MAO activity in the adipose tissue of this animal model of obesity, is that we did not decipher the mechanisms supporting such up-regulation, and that it remains unclear whether elevated MAO is a cause or a consequence of the dysmetabolic profile of the Zucker obese rats. This issue deserves further investigations.

ACKNOWLEDGEMENTS

We thank the staff of animal unit CREFRE, headed by Dr. Collet X (Toulouse, France) and Dr. Guerre-Millo M (Paris, France), for their knowledge about Zucker rat physiology. The authors are also indebted for the invaluable technical assistance of Pré vot D & Jousseaume M, and for the hierarchical benevolence of Bouloumié A.

REFERENCES

1 **Zucker LM**, Zucker TF. Fatty, a new mutation in the rat. *J Heredity* 1961; **52**: 275-278
2 **Chua SC Jr**, Chung WK, Wu-Peng XS, Zhang Y, Liu SM, Tartaglia L, Leibel RL. Phenotypes of mouse diabetes and rat fatty due to mutations in the OB (leptin) receptor. *Science* 1996; **271**: 994-996 [PMID: 8584938 DOI: 10.1126/science.271.5251.994]
3 **Phillips MS**, Liu Q, Hammond HA, Dugan V, Hey PJ, Caskey CJ, Hess JF. Leptin receptor missense mutation in the fatty Zucker rat. *Nat Genet* 1996; **13**: 18-19 [PMID: 8673096 DOI: 10.1038/ng0596-18]
4 **Takaya K**, Ogawa Y, Isse N, Okazaki T, Satoh N, Masuzaki H, Mori K, Tamura N, Hosoda K, Nakao K. Molecular cloning of rat leptin receptor isoform complementary DNAs--identification of a missense mutation in Zucker fatty (fa/fa) rats. *Biochem Biophys Res Commun* 1996; **225**: 75-83 [PMID: 8769097 DOI: 10.1006/bbrc.1996.1133]
5 **Himms-Hagen J**. Physiological roles of the leptin endocrine system: differences between mice and humans. *Crit Rev Clin Lab Sci* 1999; **36**: 575-655 [PMID: 10656540 DOI: 10.1080/10408369991239259]
6 **Michel O**, Heudes D, Lamarre I, Masurier C, Lavau M, Bariety J, Chevalier J. Reduction of insulin and triglycerides delays glomerulosclerosis in obese Zucker rats. *Kidney Int* 1997; **52**: 1532-1542 [PMID: 9407498 DOI: 10.1038/ki.1997.483]
7 **Debant A**, Guerre-Millo M, Le Marchand-Brustel Y, Freychet P, Lavau M, Van Obberghen E. Insulin receptor kinase is hyperresponsive in adipocytes of young obese Zucker rats. *Am J Physiol* 1987; **252**: E273-E278 [PMID: 3548422 DOI: 10.1152/ajpendo.1987.252.2.E273]
8 **Bazin R**, Lavau M. Development of hepatic and adipose tissue lipogenic enzymes and insulinemia during suckling and weaning on to a high-fat diet in Zucker rats. *J Lipid Res* 1982; **23**: 839-849 [PMID: 6752318]
9 **Johnson PR**, Zucker LM, Cruce JA, Hirsch J. Cellularity of adipose depots in the genetically obese Zucker rat. *J Lipid Res* 1971; **12**: 706-714 [PMID: 5124535]
10 **Stern JS**, Johnson PR, Batchelor BR, Zucker LM, Hirsch J. Pancreatic insulin release and peripheral tissue resistance in Zucker obese rats fed high- and low-carbohydrate diets. *Am J Physiol* 1975; **228**: 543-548 [PMID: 1091158 DOI: 10.1152/ajplegacy.1975.228.2.543]
11 **Hardie LJ**, Rayner DV, Holmes S, Trayhurn P. Circulating leptin levels are modulated by fasting, cold exposure and insulin administration in lean but not Zucker (fa/fa) rats as measured by ELISA. *Biochem Biophys Res Commun* 1996; **223**: 660-665 [PMID: 8687452 DOI: 10.1006/bbrc.1996.0951]
12 **Jacob S**, Fogt DL, Dietze GJ, Henriksen EJ. The beta2-adrenergic modulator celiprolol reduces insulin resistance in obese Zucker rats. *Life Sci* 1999; **64**: 2071-2079 [PMID: 10374932 DOI: 10.1016/s0024-3205(99)00154-x]
13 **Pan SJ**, Hancock J, Ding Z, Fogt D, Lee M, Ivy JL. Effects of clenbuterol on insulin resistance in conscious obese Zucker rats. *Am J Physiol Endocrinol Metab* 2001; **280**: E554-E561 [PMID: 11254461 DOI: 10.1152/ajpendo.2001.280.4.E554]
14 **Rothwell NJ**, Stock MJ. Influence of clenbuterol on energy balance, thermogenesis and body composition in lean and genetically obese Zucker rats. *Int J Obes* 1987; **11**: 641-647 [PMID:

3440683]
15 **Mory G**, Wiel M, Adli H, Diot-Dupuy F, Ferré P, Bazin R. Impaired beta-adrenergic signaling pathway in white adipocytes of suckling fa/fa Zucker rats: a defect in receptor coupling. *Int J Obes Relat Metab Disord* 2001; **25**: 1592-1598 [PMID: 11753576 DOI: 10.1038/sj.ijo.0801811]
16 **Lent-Schochet D**, McLaughlin M, Ramakrishnan N, Jialal I. Exploratory metabolomics of metabolic syndrome: A status report. *World J Diabetes* 2019; **10**: 23-36 [PMID: 30697368 DOI: 10.4239/wjd.v10.i1.23]
17 **Bairras C**, Mauriege P, Bukowiecki L, Atgie C. Regulation of lypolysis in white adipose tissues of lean and obese Zucker rats. *J Physiol Biochem* 2007; **63**: 287-296 [PMID: 18457004 DOI: 10.1007/bf03165760]
18 **Mukaida S**, Evans BA, Bengtsson T, Hutchinson DS, Sato M. Adrenoceptors promote glucose uptake into adipocytes and muscle by an insulin-independent signaling pathway involving mechanistic target of rapamycin complex 2. *Pharmacol Res* 2017; **116**: 87-92 [PMID: 28025104 DOI: 10.1016/j.phrs.2016.12.022]
19 **Chernogubova E**, Cannon B, Bengtsson T. Norepinephrine increases glucose transport in brown adipocytes *via* beta3-adrenoceptors through a cAMP, PKA, and PI3-kinase-dependent pathway stimulating conventional and novel PKCs. *Endocrinology* 2004; **145**: 269-280 [PMID: 14551227 DOI: 10.1210/en.2003-0857]
20 **Fontaine J**, Tavernier G, Morin N, Carpéné C. Vanadium-dependent activation of glucose transport in adipocytes by catecholamines is not mediated *via* adrenoceptor stimulation or monoamine oxidase activity. *World J Diabetes* 2020; **11**: 622-643 [PMID: 33384769 DOI: 10.4239/wjd.v11.i12.622]
21 **Nguyen KD**, Qiu Y, Cui X, Goh YP, Mwangi J, David T, Mukundan L, Brombacher F, Locksley RM, Chawla A. Alternatively activated macrophages produce catecholamines to sustain adaptive thermogenesis. *Nature* 2011; **480**: 104-108 [PMID: 22101429 DOI: 10.1038/nature10653]
22 **Fischer K**, Ruiz HH, Jhun K, Finan B, Oberlin DJ, van der Heide V, Kalinovich AV, Petrovic N, Wolf Y, Clemmensen C, Shin AC, Divanovic S, Brombacher F, Glasmacher E, Keipert S, Jastroch M, Nagler J, Schramm KW, Medrikova D, Collden G, Woods SC, Herzig S, Homann D, Jung S, Nedergaard J, Cannon B, Tschöp MH, Müller TD, Buettner C. Alternatively activated macrophages do not synthesize catecholamines or contribute to adipose tissue adaptive thermogenesis. *Nat Med* 2017; **23**: 623-630 [PMID: 28414329 DOI: 10.1038/nm.4316]
23 **Clouet P**, Henninger C, Bézard J. Study of some factors controlling fatty acid oxidation in liver mitochondria of obese Zucker rats. *Biochem J* 1986; **239**: 103-108 [PMID: 3800970 DOI: 10.1042/bj2390103]
24 **Carpéné C**, Collon P, Remaury A, Cordi A, Hudson A, Nutt D, Lafontan M. Inhibition of amine oxidase activity by derivatives that recognize imidazoline I2 sites. *J Pharmacol Exp Ther* 1995; **272**: 681-688 [PMID: 7853182]
25 **Limon-Boulez I**, Tesson F, Gargalidis-Moudanos C, Parini A. I2-imidazoline binding sites: relationship with different monoamine oxidase domains and identification of histidine residues mediating ligand binding regulation by H+1. *J Pharmacol Exp Ther* 1996; **276**: 359-364 [PMID: 8632297]
26 **Basile L**, Pappalardo M, Guccione S, Milardi D, Ramsay RR. Computational comparison of imidazoline association with the I2 binding site in human monoamine oxidases. *J Chem Inf Model* 2014; **54**: 1200-1207 [PMID: 24601544 DOI: 10.1021/ci400346k]
27 **Tipton KF**. 90 years of monoamine oxidase: some progress and some confusion. *J Neural Transm (Vienna)* 2018; **125**: 1519-1551 [PMID: 29637260 DOI: 10.1007/s00702-018-1881-5]
28 **Kilkenny C**, Browne W, Cuthill IC, Emerson M, Altman DG; NC3Rs Reporting Guidelines Working Group. Animal research: reporting in vivo experiments: the ARRIVE guidelines. *Br J Pharmacol* 2010; **160**: 1577-1579 [PMID: 20649561 DOI: 10.1111/j.1476-5381.2010.00872.x.]
29 **Moody AJ**, Stan MA, Stan M, Gliemann J. A simple free fat cell bioassay for insulin. *Horm Metab Res* 1974; **6**: 12-16 [PMID: 4819286 DOI: 10.1055/s-0028-1093895]
30 **Bour S**, Iglesias-Osma MC, Marti L, Duro P, Garcia-Barrado MJ, Pastor MF, Prévot D, Visentin V, Valet P, Moratinos J, Carpéné C. The imidazoline I2-site ligands BU 224 and 2-BFI inhibit MAO-A and MAO-B activities, hydrogen peroxide production, and lipolysis in rodent and human adipocytes. *Eur J Pharmacol* 2006; **552**: 20-30 [PMID: 17056035 DOI: 10.1016/j.ejphar.2006.09.021]
31 **Jargaud V**, Bour S, Tercé F, Collet X, Valet P, Bouloumié A, Guillemot JC, Mauriège P, Jalkanen S, Stolen C, Salmi M, Smith DJ, Carpéné C. Obesity of mice lacking VAP-1/SSAO by Aoc3 gene deletion is reproduced in mice expressing a mutated vascular adhesion protein-1 (VAP-1) devoid of amine oxidase activity. *J Physiol Biochem* 2021; 77: 141-154 [PMID: 32712883 DOI: 10.1007/s13105-020-00756-y]
32 **Remaury A**, Raddatz R, Ordener C, Savic S, Shih JC, Chen K, Seif I, De Maeyer E, Lanier SM, Parini A. Analysis of the pharmacological and molecular heterogeneity of I(2)-imidazoline-binding proteins using monoamine oxidase-deficient mouse models. *Mol Pharmacol* 2000; **58**: 1085-1090 [PMID: 11040057 DOI: 10.1124/mol.58.5.1085]
33 **Ramonet D**, Rodríguez M, Saura J, Lizcano JM, Romera M, Unzeta M, Finch C, Billett E, Mahy N. Localization of monoamine oxidase A and B and semicarbazide-sensitive amine oxidase in human peripheral tissues. *Inflammopharmacology* 2003; **11**: 111-117 [PMID: 15035812 DOI: 10.1163/156856003765764272]
34 **Marti L**, Morin N, Enrique-Tarancon G, Prevot D, Lafontan M, Testar X, Zorzano A, Carpéné C. Tyramine and vanadate synergistically stimulate glucose transport in rat adipocytes by amine oxidase-

dependent generation of hydrogen peroxide. *J Pharmacol Exp Ther* 1998; **285**: 342-349 [PMID: 9536030]

35 **Miralles A**, Esteban S, Sastre-Coll A, Moranta D, Asensio VJ, García-Sevilla JA. High-affinity binding of beta-carbolines to imidazoline I2B receptors and MAO-A in rat tissues: norharman blocks the effect of morphine withdrawal on DOPA/noradrenaline synthesis in the brain. *Eur J Pharmacol* 2005; **518**: 234-242 [PMID: 16061219 DOI: 10.1016/j.ejphar.2005.06.023]

36 **Kimura A**, Tyacke RJ, Robinson JJ, Husbands SM, Minchin MC, Nutt DJ, Hudson AL. Identification of an imidazoline binding protein: creatine kinase and an imidazoline-2 binding site. *Brain Res* 2009; **1279**: 21-28 [PMID: 19410564 DOI: 10.1016/j.brainres.2009.04.044]

37 **Lönnroth P**, Eriksson JW, Posner BI, Smith U. Peroxovanadate but not vanadate exerts insulin-like effects in human adipocytes. *Diabetologia* 1993; **36**: 113-116 [PMID: 8458524 DOI: 10.1007/bf00400690]

38 **Aureliano M**. Recent perspectives into biochemistry of decavanadate. *World J Biol Chem* 2011; **2**: 215-225 [PMID: 22031844 DOI: 10.4331/wjbc.v2.i10.215]

39 **Velliquette RA**, Kossover R, Previs SF, Ernsberger P. Lipid-lowering actions of imidazoline antihypertensive agents in metabolic syndrome X. *Naunyn Schmiedebergs Arch Pharmacol* 2006; **372**: 300-312 [PMID: 16416266 DOI: 10.1007/s00210-005-0024-3]

40 **Aubertin G**, Weiss M, Traversi F, Benameur D, Choquet P, Dali-Youcef N, Pons F, Sigrist S, Greney H, Monassier L, Bousquet P, Niederhoffer N. Effects of imidazoline-like drugs on liver and adipose tissues, and their role in preventing obesity and associated cardio-metabolic disorders. *Int J Obes (Lond)* 2019; **43**: 2163-2175 [PMID: 30926950 DOI: 10.1038/s41366-019-0342-z]

41 **Wang T**, Wang J, Hu X, Huang XJ, Chen GX. Current understanding of glucose transporter 4 expression and functional mechanisms. *World J Biol Chem* 2020; **11**: 76-98 [PMID: 33274014 DOI: 10.4331/wjbc.v11.i3.76]

42 **Yu PH**, Wang M, Fan H, Deng Y, Gubisne-Haberle D. Involvement of SSAO-mediated deamination in adipose glucose transport and weight gain in obese diabetic KKAy mice. *Am J Physiol Endocrinol Metab* 2004; **286**: E634-E641 [PMID: 14656718 DOI: 10.1152/ajpendo.00272.2003]

43 **Carpéné C**, Boulet N, Chaplin A, Mercader J. Past, Present and Future Anti-Obesity Effects of Flavin-Containing and/or Copper-Containing Amine Oxidase Inhibitors. *Medicines (Basel)* 2019; **6** [PMID: 30650583 DOI: 10.3390/medicines6010009]

44 **Crettaz M**, Prentki M, Zaninetti D, Jeanrenaud B. Insulin resistance in soleus muscle from obese Zucker rats. Involvement of several defective sites. *Biochem J* 1980; **186**: 525-534 [PMID: 6990920 DOI: 10.1042/bj1860525]

45 **Saura J**, Kettler R, Da Prada M, Richards JG. Quantitative enzyme radioautography with 3H-Ro 41-1049 and 3H-Ro 19-6327 in vitro: localization and abundance of MAO-A and MAO-B in rat CNS, peripheral organs, and human brain. *J Neurosci* 1992; **12**: 1977-1999 [PMID: 1578281 DOI: 10.1523/jneurosci.12-05-01977.1992]

46 **Lewinsohn R**, Böhm K, Glover V, Sandler M. A benzylamine oxidase distinct from monoamine oxidase B--widespread distribution in man and rat. *Biochem Pharmacol* 1978; **27**: 1857-1863 [PMID: 708467 DOI: 10.1016/0006-2952(78)90033-3]

47 **Miralles A**, Ribas C, Olmos G, García-Sevilla JA. No effect of genetic obesity and mazindol on imidazoline I2 binding sites in the brain of Zucker rats. *Eur J Pharmacol* 1993; **243**: 305-308 [PMID: 8276084 DOI: 10.1016/0014-2999(93)90191-j]

48 **Moldes M**, Fève B, Pairault J. Molecular cloning of a major mRNA species in murine 3T3 adipocyte lineage. differentiation-dependent expression, regulation, and identification as semicarbazide-sensitive amine oxidase. *J Biol Chem* 1999; **274**: 9515-9523 [PMID: 10092636 DOI: 10.1074/jbc.274.14.9515]

49 **Galinier A**, Carrière A, Fernandez Y, Carpéné C, André M, Caspar-Bauguil S, Thouvenot JP, Périquet B, Pénicaud L, Casteilla L. Adipose tissue proadipogenic redox changes in obesity. *J Biol Chem* 2006; **281**: 12682-12687 [PMID: 16377639 DOI: 10.1074/jbc.M506949200]

50 **Jamdar SC**, Cao WF, Samaniego E. Relationship between adipose polyamine concentrations and triacylglycerol synthetic enzymes in lean and obese Zucker rats. *Enzyme Protein* 1996; **49**: 222-230 [PMID: 9030889 DOI: 10.1159/000468632]

51 **Liu J**, Wang R, Desai K, Wu L. Upregulation of aldolase B and overproduction of methylglyoxal in vascular tissues from rats with metabolic syndrome. *Cardiovasc Res* 2011; **92**: 494-503 [PMID: 21890532 DOI: 10.1093/cvr/cvr239]

52 **Morris NJ**, Ducret A, Aebersold R, Ross SA, Keller SR, Lienhard GE. Membrane amine oxidase cloning and identification as a major protein in the adipocyte plasma membrane. *J Biol Chem* 1997; **272**: 9388-9392 [PMID: 9083076 DOI: 10.1074/jbc.272.14.9388]

53 **El Hadri K**, Moldes M, Mercier N, Andreani M, Pairault J, Feve B. Semicarbazide-sensitive amine oxidase in vascular smooth muscle cells: differentiation-dependent expression and role in glucose uptake. *Arterioscler Thromb Vasc Biol* 2002; **22**: 89-94 [PMID: 11788466 DOI: 10.1161/hq0102.101550]

54 **Mukherjee SP**. Mediation of the antilipolytic and lipogenic effects of insulin in adipocytes by intracellular accumulation of hydrogen peroxide. *Biochem Pharmacol* 1980; **29**: 1239-1246 [PMID: 6249328 DOI: 10.1016/0006-2952(80)90280-4]

55 **Shisheva A**, Shechter Y. Mechanism of pervanadate stimulation and potentiation of insulin-activated glucose transport in rat adipocytes: dissociation from vanadate effect. *Endocrinology* 1993; **133**: 1562-1568 [PMID: 8404595 DOI: 10.1210/endo.133.4.8404595]

56 **Romauch M**. Zinc-α2-glycoprotein as an inhibitor of amine oxidase copper-containing 3. *Open Biol* 2020; **10**: 190035 [PMID: 32315567 DOI: 10.1098/rsob.190035]

57 **Yang H**, Ralle M, Wolfgang MJ, Dhawan N, Burkhead JL, Rodriguez S, Kaplan JH, Wong GW, Haughey N, Lutsenko S. Copper-dependent amino oxidase 3 governs selection of metabolic fuels in adipocytes. *PLoS Biol* 2018; **16**: e2006519 [PMID: 30199530 DOI: 10.1371/journal.pbio.2006519]

58 **Salmi M**, Jalkanen S. Vascular Adhesion Protein-1: A Cell Surface Amine Oxidase in Translation. *Antioxid Redox Signal* 2019; **30**: 314-332 [PMID: 29065711 DOI: 10.1089/ars.2017.7418]

59 **Liu Q**, Quach SY. Untargeted metabolomics analysis of serum metabolites in Zucker diabetic fatty rats. *E3S Web of Conferences* 2021; **233**: 02017 [DOI: 10.1051/e3sconf/202123302017]

60 **Walton RG**, Zhu X, Tian L, Heywood EB, Liu J, Hill HS, Bruemmer D, Yang Q, Fu Y, Garvey WT. AP2-NR4A3 transgenic mice display reduced serum epinephrine because of increased catecholamine catabolism in adipose tissue. *Am J Physiol Endocrinol Metab* 2016; **311**: E69-E81 [PMID: 27166283 DOI: 10.1152/ajpendo.00330.2015]

61 **Ayala-Lopez N**, Thompson JM, Watts SW. Perivascular Adipose Tissue's Impact on Norepinephrine-Induced Contraction of Mesenteric Resistance Arteries. *Front Physiol* 2017; **8**: 37 [PMID: 28228728 DOI: 10.3389/fphys.2017.00037]

62 **Rahbani JF**, Roesler A, Hussain MF, Samborska B, Dykstra CB, Tsai L, Jedrychowski MP, Vergnes L, Reue K, Spiegelman BM, Kazak L. Creatine kinase B controls futile creatine cycling in thermogenic fat. *Nature* 2021; **590**: 480-485 [PMID: 33597756 DOI: 10.1038/s41586-021-03221-y]

63 **Li JX**. Imidazoline I_2 receptors: An update. *Pharmacol Ther* 2017; **178**: 48-56 [PMID: 28322973 DOI: 10.1016/j.pharmthera.2017.03.009]

Published by **Baishideng Publishing Group Inc**
7041 Koll Center Parkway, Suite 160, Pleasanton, CA 94566, USA
Telephone: +1-925-3991568
E-mail: bpgoffice@wjgnet.com
Help Desk: https://www.f6publishing.com/helpdesk
https://www.wjgnet.com

ISSN 1949-8454 (online)

World Journal of *Biological Chemistry*

World J Biol Chem 2022 March 27; 13(2): 35-65

Published by Baishideng Publishing Group Inc

WJBC

World Journal of Biological Chemistry

Contents

Bimonthly Volume 13 Number 2 March 27, 2022

MINIREVIEWS

ORIGINAL ARTICLE

Basic Study

World Journal of Biological Chemistry

Bimonthly Volume 13 Number 2 March 27, 2022

Contents

ABOUT COVER

Editorial Board Member of *World Journal of Biological Chemistry*, Dr. Manoj Kumar Gupta, PhD, Postdoctoral Fellow, Department of Computational Biology for Individualised Infection Medicine, Centre for Individualised Infection Medicine (CiiM) & TWINCORE, joint ventures between the Helmholtz-Centre for Infection Research (HZI) and the Hannover Medical School (MHH), Feodor-Lynen-Str. 7, 30625 Hannover, Germany. mkg21@helmholtz-hzi.de

AIMS AND SCOPE

The primary aim of the *World Journal of Biological Chemistry* (*WJBC*, *World J Biol Chem*) is to provide scholars and readers from various fields of biological chemistry a platform to publish high-quality basic and clinical research articles and communicate their research findings online.

WJBC mainly publishes articles reporting research results and findings obtained in the field of biological chemistry and covering a wide range of topics including bioenergetics, cell biology, chromosomes, developmental biology, DNA, enzymology, extracellular matrices, gene regulation, genomics, glycobiology, immunology, lipids, membrane biology, metabolism, molecular bases of disease, molecular biophysics, neurobiology, plant biology, protein structure and folding, protein synthesis and degradation, proteomics, and signal transduction.

INDEXING/ABSTRACTING

The *WJBC* is now abstracted and indexed in PubMed, PubMed Central, Reference Citation Analysis, China National Knowledge Infrastructure, China Science and Technology Journal Database, and Superstar Journals Database.

RESPONSIBLE EDITORS FOR THIS ISSUE

NAME OF JOURNAL
World Journal of Biological Chemistry

ISSN
ISSN 1949-8454 (online)

LAUNCH DATE
July 26, 2010

FREQUENCY
Bimonthly

PUBLICATION DATE
March 27, 2022

World Journal of Biological Chemistry

Submit a Manuscript: https://www.f6publishing.com

World J Biol Chem 2022 March 27; 13(2): 35-46

DOI: 10.4331/wjbc.v13.i2.35

ISSN 1949-8454 (online)

MINIREVIEWS

LIN28A: A multifunctional versatile molecule with future therapeutic potential

Kenneth Wu, Tauseef Ahmad, Rajaraman Eri

Specialty type: Biochemistry and molecular biology

Provenance and peer review: Invited article; Externally peer reviewed.

Peer-review model: Single blind

Peer-review report's scientific quality classification

Grade A (Excellent): 0
Grade B (Very good): 0
Grade C (Good): C
Grade D (Fair): 0
Grade E (Poor): 0

P-Reviewer: Yang YZ, China

Received: March 27, 2021
Peer-review started: March 27, 2021
First decision: July 27, 2021
Revised: September 6, 2021
Accepted: March 4, 2022
Article in press: March 4, 2022
Published online: March 27, 2022

Kenneth Wu, Tauseef Ahmad, Rajaraman Eri, Department of Laboratory Medicine, School of Health Sciences, College of Health and Medicine, University of Tasmania, Launceston, Tasmania 7250, Australia

Corresponding author: Rajaraman Eri, DVM, PhD, Associate Professor, Department of Laboratory Medicine, School of Health Sciences, College of Health and Medicine, University of Tasmania, Health Sciences Building (Newnham-C), 2nd Level, Room M216, Launceston, Tasmania 7250, Australia. rajaraman.eri@utas.edu.au

Abstract

An RNA-binding protein, LIN28A was initially discovered in nematodes *Caenorhabditis elegans* and regulated stem cell differentiation and proliferation. With the aid of mouse models and cancer stem cells models, LIN28A demonstrated a similar role in mammalian stem cells. Subsequent studies revealed LIN28A's roles in regulating cell cycle and growth, tissue repair, and metabolism, especially glucose metabolism. Through regulation by pluripotency and neurotrophic factors, LIN28A performs these roles through *let-7* dependent (binding to *let-7*) or independent (binding directly to mature mRNA) pathways. Elevated LIN28A levels are associated with cancers such as breast, colon, and ovarian cancers. Overexpressed LIN28A has been implicated in liver diseases and Rett syndrome whereas loss of LIN28A was linked to Parkinson's disease. LIN28A inhibitors, LIN28A-specific nanobodies, and deubiquitinases targeting LIN28A could be feasible options for cancer treatments while drugs upregulating LIN28A could be used in regenerative therapy for neuropathies. We will review the upstream and downstream signalling pathways of LIN28A and its physiological functions. Then, we will examine current research and gaps in research regarding its mechanisms in conditions such as cancers, liver diseases, and neurological diseases. We will also look at the therapeutic potential of LIN28A in RNA-targeted therapies including small interfering RNAs and RNA-protein interactions.

Key Words: *Let-7*; Differentiation; Proliferation; Cancer; Inflammation

Core Tip: The overexpression of LIN28A has been correlated with a number of tumours and a higher risk of relapse in cancer patients. Therefore, LIN28A could be developed as a prognostic indicator. With an increasing understanding of its roles in the pathological context, LIN28A has also become a promising therapeutic target for cancer treatment and regenerative therapy for neuropathies.

Citation: Wu K, Ahmad T, Eri R. LIN28A: A multifunctional versatile molecule with future therapeutic potential. *World J Biol Chem* 2022; 13(2): 35-46
URL: https://www.wjgnet.com/1949-8454/full/v13/i2/35.htm
DOI: https://dx.doi.org/10.4331/wjbc.v13.i2.35

INTRODUCTION

First discovered in nematodes *Caenorhabditis elegans* (*C. elegans*) in 1997, the LIN28A (commonly referred to as LIN28 in some literature) protein is predominantly localised in the cytoplasm but can travel back and forth between the nucleus and cytoplasm. It was noted to be highly expressed during embryogenesis but gradually diminished to absent expression in adulthood in nematodes[1]. In humans, the absent expression was found to be only true in lung epithelium but it remains expressed during adulthood in certain cell or tissue types such as erythrocytes, renal epithelia of the loop of Henle and collecting ducts, cardiac muscle, and skeletal muscle[2]. Nonetheless, examination of LIN28 homologues in humans, mice, and *Drosophila* demonstrated its typical expression in undifferentiated and pluripotent cells, especially in embryonic stems cells (ESCs), then it is downregulated in response to development and differentiation. These findings suggested that LIN28A was involved in cellular development and differentiation. In fact, increased LIN28 expression has been associated with less differentiated and more aggressive tumours[2].

Invertebrates such as *C. elegans* and *D. melanogaster* possess a single *LIN28* gene whereas all vertebrates possess two LIN28 paralogs. LIN28's structure includes two RNA-binding domains, a N-terminal cold-shock domains (CSD), and a cysteine cysteine histidine cysteine (CCHC) zinc knuckle domains (ZKD) (Figure 1). LIN28 is regarded as the sole animal protein to possess the unique combination of a CSD and a C-terminal ZKD and has been implicated in promoting self-renewal and delaying differentiation, that resulted in proliferation of stem cells. Contrarily, its loss-of-function resulted in increased stem cell differentiation[2]. Its role in mammalian stem cells was elucidated in the early 2000s through studies such as human LIN28 being used to reprogram somatic fibroblasts into pluripotent stem cells[1]. These studies eventually demonstrated that LIN28A could bind to *let-7* gene to repress its expression in regulating translation. This binding was observed in a similar mechanism in *C. elegans*[1]. Thus, the findings had validated LIN28A's conserved role in stem cell self-renewal and differentiation.

In recent years, other roles of LIN28A have been linked to wound healing and tissue repair, cell growth and metabolism, and carcinogenesis while the signalling pathways have become more complex. In this review, we will elaborate on recent findings regarding the mechanisms and roles of the LIN28A protein in physiological functions and pathological processes. Subsequently, we will examine how these findings have translated into RNA-targeted therapies and drugs targeting protein interactions involving LIN28A in the treatment of cancer and other diseases.

SIGNALLING AND LET-7 PATHWAYS OF LIN28A

Regulatory signals

In vertebrates, an important intrinsic signal in downregulating LIN28A would be the microRNA-*125a* (miRNA-*125a*)[3]. In contrast, pluripotency factors such as Sox2, Nanog, and Tcf3 can promote *LIN28A* expression. Among these factors, Sox2 is regarded the most essential in this promotion of expression based on a Bayesian probabilistic network modelling of single-cell gene expression[3]. In addition, inhibition of Dot1L H3K79 histone methyltransferase indirectly upregulates LIN28A[3]. Extrinsic signalling has been demonstrated in *C. elegans*: Nuclear receptor *daf-12* transmits signals from steroid hormones to LIN28A, and *in vitro*: Homologous retinoic acid and oestrogen receptors downregulate LIN28A[3]. However, it is unclear if similar extrinsic signalling occurs in mammals.

Another signalling pathway involves brain-derived neurotrophic factor (BDNF) that initially activates extracellular signal-regulated protein kinase (Erk), which in turn mediates mitogen-activated protein kinase (MAPK) phosphorylation of transactivation response element RNA-binding protein (TRBP), an RNA-binding cofactor of the Dicer enzyme[4]. The act of phosphorylation decreased Merlin binding, which impedes polyubiquitination and proteasomal degradation of TRBP. Subsequently, BDNF can

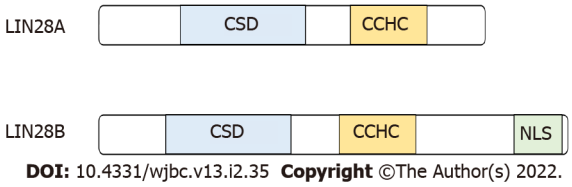

DOI: 10.4331/wjbc.v13.i2.35

Figure 1 Structure of LIN28 protein. LIN28 paralogs in vertebrates contain relatively conserved cold-shock domains and cysteine cysteine histidine cysteine. LIN28B contains a nuclear localisation signal at the end and is slightly longer than LIN28A. CSD: Cold-shock domains; NLS: Nuclear localisation signal; CCHC: Cysteine cysteine histidine cysteine.

stabilise and elevate levels of LIN28A *via* co-association with TRBP. An interesting finding was this MAPK-mediated TRBP phosphorylation and induction only targeted LIN28A but not its paralog, LIN28B. Hence, the BDNF-MAPK pathway induces LIN28A for physiological functions connected to dendritic spine growth and peritoneal macrophage survival as part of the trophic responses[4].

LIN28A has been found to be involved in several feedback loops. Firstly, it has been ascertained that LIN28A inhibits *let-7* expression while *let-7* itself binds to mRNA of LIN28A to downregulate LIN28A expression, which establishes a double negative feedback loop[3]. Secondly, LIN28A can derepress c-Myc *via let-7* inhibition, then c-Myc can upregulate LIN28A expression, which establishes a positive feedback loop. Thirdly, an initial inflammatory signal activates nuclear factor kappa-light-chain-enhancer (NF-κB) that elevates interleukin-6 (IL-6) levels that is also elevated by LIN28A's inhibition of *let-7*. The increased IL-6 levels activate NF-κB, which completes the positive feedback loop[1].

Let-7 pathways

In *C. elegans*, the mechanisms in regulating its four developmental stages can be divided into *let-7* dependent and *let-7* independent pathways[2]. The former involves LIN28 promoting the expression of *lin-41* by repressing *let-7*, which in turn reduces binding of *let-7* to LIN28A mRNA. Therefore, either LIIN28A or *let-7* can suppress one another in forming a bistable switch. The latter involves *lin-4* targeting LIN28 which upregulates hunchback-like protein-1 (hbl-1) that inhibits *let-7*[2]. Interestingly, the latter may be utilised in mammalian systems which would further corroborate the conserved role of LIN28 but there does not appear to be any concrete findings.

In this review, these two divisions are adapted to elaborate on LIN28A mechanisms in humans.

Let-7 dependent pathways: In the nucleus, LIN28A binds primary *lethal-7* (pri-*let-7*) synergistically with RNA-binding protein musashi 1 (MSI1) to block *let-7* processing *via* a miRNA-processing enzyme Drosha (Figure 1)[2]. In the cytoplasm, LIN28A binds precursor *lethal-7* (pre-*let-7*) to competitively block the Dicer processing (another microRNA-processing enzyme) to prevent the formation of mature *let-7*. Then, LIN28A recruits terminal uridylyl transferase 4 (TUT4) for the oligo-uridylation of pre-*let-7*; this process prevents the cleavage of pre-*let-7* by Dicer and acts as a signal for exonuclease DIS3L12 for its degradation (Figure 2)[2].

In terms of structural significance of LIN28, the pri-*let-7* pathway appears not be as expounded as much as the pre-*let-7* pathway. In the nucleus, it is hypothesised that the LIN28A's CSDs bind with increased affinity to pri-*let-7*[5] to block cleavage by Drosha which prevents Drosha-mediated processing[6]. In a related study, LIN28 has demonstrated another mechanism similar to that of its counterpart, LIN28B: The histone H3K4 methyltransferase can mono-methylate LIN28A; which appears to enable its localisation in the nucleus and especially nucleolus, and increases its binding affinity to pri-*let-7*[7].

In the cytosol, LIN28's ZKDs can recognise and bind to GGAG or GGAG-like motifs in pre-*let-7*'s terminal loop to compete with Dicer in inhibiting Dicer-mediated processing and TUTase would then be recruited[6]. Furthermore, TUT4 and TUT7 also possess CCHC Zn knuckles that are required in pre-*let-7* oligouridylation[1]. While initial research only involved mechanisms surrounding binding of LIN28A to *let-7* (*let-7* dependent), subsequent research examined binding of LIN28A to specific mRNAs (*let-7* independent).

Let-7 independent pathways: Several small-scale studies have isolated a number of potential LIN28 mRNA targets and most of them are mature mRNA and involved in cell cycle regulation, metabolism, or formation of ribonucleoprotein complexes (Table 1)[2,8]. In first understanding how LIN28 recognises these targets, three genome-wide studies determined rather divergent consensus sequences amongst the targets despite such large data sets[2].

Furthermore, Cho *et al*[9] located their consensus sequence within the terminal loop of small hairpins [2]. Wilbert *et al*[10] noted their targets' consensus sequences of interest were enriched in single-stranded RNA (ssRNA) within the hairpin and other loop structures whereas Qiu *et al*[11] found that their targets were enriched in LIN28-containing polysome fractions[2]. Then, Hafner *et al*[8] discovered LIN28 preferentially binds to ssRNA containing a uridine-rich element and guanosines when embedded in secondary structure[8]. However, the presence of this secondary structure may not be significant due

Table 1 Classes of mRNA targets[2]

Cell cycle regulation	RNA-binding proteins	Histone components	Glucose metabolism	Early embryogenic genes
Cyclin A	hnRNP F	Histone H2A	IGF receptor	*Sox2*
CDK4	TDP-43	Histone H4H	Insulin receptor	*Sall4*
CCNB1	TIA-1	Linker histone H1FX	HMGA2	*Oct4*

IGF: Insulin-like growth factor 1. Citation: Tsialikas J, Romer-Seibert J. LIN28: roles and regulation in development and beyond. *Development* 2015; **142**: 2397-2404. Copyright© The Authors 2015. Published by The Company of Biologists Ltd.

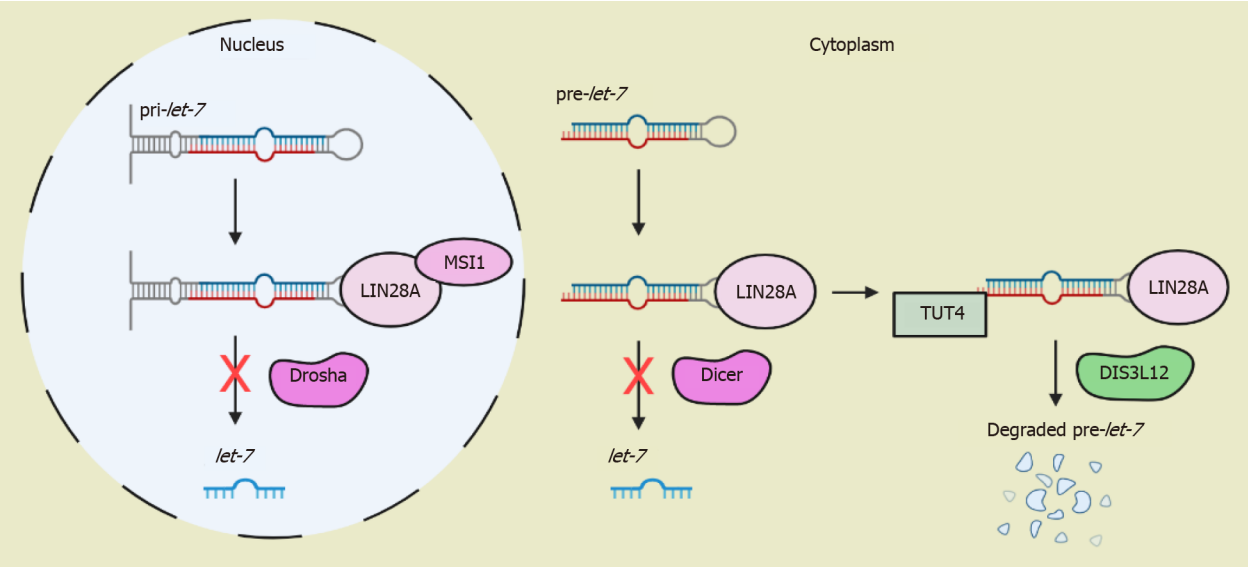

DOI: 10.4331/wjbc.v13.i2.35

Figure 2 Molecular pathways of LIN28A/*let-7* axis. LIN28A binds to pri-*let-7* in the nucleus to prevent its processing by Drosha and to pre-*let-7* in the cytoplasm to prevent Dicer processing as well as facilitate its degradation.

to variation in stem length and loop size and lack of formal statistical analysis.

Despite the divergent consensus sequences, similarities such as the ssRNAs and loop structures indicate that the recognition mechanisms for LIN28 to these RNAs is gradually being uncovered. With an improved understanding of how LIN28 binds to its targets, researchers also looked at the significance of its pathways in humans.

PHYSIOLOGICAL FUNCTIONS

Cell differentiation and cell cycle

LIN28A is most prominently known as a regulator of cell renewal and differentiation. Multiple studies highlight this evolutionarily conserved role in ESCs and trophoblast stem cells. In fact, Li *et al*[12] reported that *PpCSP1* (a homologue of LIN28) can revert differentiated leaf cells to stem cells in moss *Physcomitrella patens*; indicating that LIN28's role involving cell differentiation extends beyond the animal kingdom[12]. In the classical *let-7* dependent pathway, LIN28 can suppress *let-7* biogenesis to promote ESC differentiation[13]. In the *let-7* independent pathway, LIN28 can impede translation of mRNAs such as high mobility group AT-Hook 2 (HMGA2) to either prevent its disruption of ESC differentiation or its effect of uncontrolled cell proliferation and apoptosis when HMGA2 is allowed to accumulate[13].

Similarly, LIN28A utilises the classical pathway to regulate trophoblast differentiation and neural precursor cells (NPCs) proliferation. To retain pluripotency in trophoblast progenitors, LIN28A increases; suppressing *let-7* whereas to initiate their differentiation, LIN28 decreases; enabling *let-7* to mature[14]. Proliferation of NPCs and increase in brain size is promoted by Sox2 through LIN28A. Notably, LIN28 has been suggested to be sufficient in rescuing NPC proliferation and neurogenic deficits in the absence of Sox2[15]. In facilitating cell cycle progression, LIN28A can promote expression of cyclin D1 (CCND1) and cell division cycle 25 homolog A (CDC25A) by inhibiting miRNA biogenesis (

let-7 dependent) and bind to cell cycle regulatory mRNAs such as cyclin-dependent kinase 2 (CDK2) to promote their translation (*let-7* independent)[16].

Cell and tissue repair

Overexpression of LIN28A improves tissue repair such as digit repair, pinnal tissue repair, epidermal hair regrowth, and axon regeneration in both peripheral nervous system and central nervous system (CNS)[17,18]. The LIN28A/*let-7* axis was implicated in these various tissues. Firstly, LIN28A enhances proliferation of connective tissue and bone for digit repair and mesenchymal tissue for pinnal tissue repair[17]. Secondly, it prolongs anagen phases (the active phase of the hair growth cycle) in hair follicles to promote hair regrowth[17]. Lastly, it represses glial *let-7* miRNAs which can inhibit axon regeneration by targeting nerve growth factor in Schwann cells; the inhibitory effects of neuronal *let-7* miRNAs on axon regeneration are uncertain[18].

In addition, LIN28 manipulates reprogramming factors such as Klf4, c-Myc, and Sox11 to enable mature CNS neurons to regain their ability to support axon regeneration, with the possible involvement of Akt-mTOR and GSK3β pathways[18]. Corroborating studies indicate that LIN28 can also functionally replace c-Myc, one of the Yamanaka factors responsible in reprogramming mature cells into induced pluripotent stem cells, and recruit Tet1 to regulate DNA methylation and gene expression. These properties enable LIN28 to influence epigenetic remodelling in facilitating axon regeneration.

On the other hand, the LIN28-mediated metabolic enhancements such as enhanced glycolysis could meet the higher energetic demands of anabolic biosynthesis and cell migration in accelerating tissue repair. However, it was observed that *let-7* repression alone is insufficient to replicate this facet of LIN28's role; indicating that the *let-7*independent pathway is imperative in tissue repair[17].

Growth and metabolism

LIN28A is one of the elements affecting organismal mortality and growth including the onset of puberty. Constitutive loss or embryonic deficiency of *LIN28A* has been associated with perinatal lethality and dwarfism. While diminished organogenesis contributed to dwarfism, the exact cause of the LIN28-deficient perinatal lethality is currently unknown[19]. An interesting finding is *LIN28A* acts earlier on organismal growth compared to its paralog *LIN28B*, such that the impacts by the former's deletion are primarily restricted to foetal or early postnatal tissues and already manifest in utero[19]. However, the prenatal impacts can have life-long consequences, as described in Barker hypothesis, which states that epigenetic memory of poor foetal or infantile environment can become an important determinant of risk for major chronic diseases such as cardiovascular disease and type 2 diabetes[19].

In terms of skeletal muscle development, overexpression of *let-7* (due to decreased LIN28A) in skeletal muscle is capable of causing growth retardation[20]. Studies demonstrate that *let-7* can impede cell proliferation by downregulating insulin-like growth factor 1, an essential hormone in growth and development, and initiate cell cycle arrest by downregulating cell cycle factors such as CKD6 and CDC34. As a result, the activation, proliferation, and maturation of myosatellite cells (precursors to skeletal myocytes) are hindered[20]. Conversely, overexpression of LIN28A is associated with increased body size and delayed onset of puberty. It is hypothesised that the LIN28A/*let-7* axis influences the hypothalamic-pituitary gland axis through secretion of hormones such as growth hormone and gonadotropin releasing hormone, which are required for growth and initiating the puberty onset[21].

In both *in vitro* and *in vivo* models, LIN28A overexpression demonstrates elevated glucose uptake and glycolysis. This is achieved by LIN28 increasing the levels of hexokinase 2, the enzyme considered as the rate-limiting step and the first step in glycolysis[22]. Concurrently, LIN28 overexpression also increased PTEN-induced kinase 1 and mitofusin 2, which mediates mitochondrial recycling and thus, reduce oxygen consumption in these LIN28-overexpressed cells such as Hep3B cells[22]. However, LIN28-overexpressed MEF isolated from mice presented an increased oxygen consumption; intimating that LIN28A's effect on oxygen consumption may depend on cell type. Nonetheless, LIN28 catalyses a shift from oxidative metabolism towards glycolytic metabolism. Now that LIN28A has been established as a regulator of glucose metabolism; increased LIN28A expression and thus, decreased expression of *let-7* led to normal glucose tolerance and an insulin-sensitised state, which lowered the risk of obesity and diabetes[23].

PATHOLOGICAL IMPLICATIONS

LIN28A's various physiological roles have linked it to various pathological processes. Its relevance in cancers, especially of breast, ovarian, and colon tissue are covered extensively in comparison to diseases such as Friedrich's ataxia and Parkinson's disease.

Cancer

Being a regulator of cell proliferation and differentiation, LIN28 overexpression and reduced *let-7* expression is often correlated with certain cancers. It has been proven that downregulation of *let-7* miRNAs catalyses the derepression of oncogenes such as Ras and c-MYC, contributing to tumorigenesis

or metastasis (Table 2)[24,25]. Notably, these oncogenes play a role in cell differentiation and proliferation; the former resulting in activation of the RAS-mitogen-activated protein kinases (RAS-MAPK) pathway which leads to uncontrolled cell proliferation while the latter influences a multitude of pathways involved in cell cycle progression, cell proliferation and differentiation, cell adhesion, and metabolism[26]. Alternatively, LIN28A was involved in oncogenesis through other pathways such as the direct interaction with mRNA.

For example, LIN28A can bind to mRNA of bone morphogenetic proteins 4 (BMP4) to induce BMP4 overexpression, which stimulates cell proliferation and tumour growth in ovarian cancer[24]. Another example is LIN28 enhancing mRNA translation of human epidermal growth factor receptor 2 (HER2) and HMGA1, which promotes cell proliferation in breast cancer[24]. Therefore, LIN28A overexpression is typically associated with poor prognosis and a higher risk of relapse (Table 2)[25].

From a metabolic perspective, LIN28A promotes aerobic glycolysis in cancer cells by upregulating glycolysis-associated genes. Previously, it was thought that the insulin-Akt-mTor pathway was the primary cause but the pathway was not significantly impacted by LIN28A levels[27]. Further studies demonstrated LIN28A overexpression resulting in elevation of an important glycolytic enzyme, pyruvate dehydrogenase kinase 1 (PDK1). PDK1 inactivates pyruvate dehydrogenase, the enzyme that converts pyruvate to acetyl-coenzyme A in the Krebs cycle. This inhibits oxidative phosphorylation activity.

Consequently, cancer cells would undergo a metabolic switch from oxidative phosphorylation to aerobic glycolysis in normoxic conditions, *i.e.* Warburg effect, as part of cancer progression[27]. In addition, LIN28A has been demonstrated to bind with the mRNAs of sterol regulatory element-binding protein 1 (SREBP-1) and SREBP cleavage-activating protein (SCAP) to augment translation and maturation of SREBP-1. This promotes fatty acid synthesis, which in turn protects cancel cells from fatty acid-induced endoplasmic reticulum stress[28].

In understanding the pathophysiology of carcinogenesis, cancer stem cells (CSCs) in certain cancers such as breast, colon/colorectal, and ovarian cancers are examined. In colon cancer, LIN28A overexpression promotes proliferation of colon cancer cells by promoting the transition of cell cycle from S to G2/M phase[29] through upregulation of cell cycle factors such as cyclin A2[30]. In breast and ovarian cancer, LIN28A promoted the G0 or G1 transition instead through the *let-7* suppression and increase in expression of cell cycle factors such as CCND1 and CDK34 for breast cancer or CDK2 for ovarian cancer [16,31]. These findings suggest that LIN28A's regulatory control in the cell cycle differs from tissue to tissue.

There are a few studies stating that LIN28A stabilises RNA FBXL19-AS1 which sponges anti-oncogenic proteins such as miRNA-203 (in colorectal cancer) and WD Repeat Domain 66 (in breast cancer)[32,33]. Consequently, cell migration and invasion are no longer inhibited. Interestingly, a number of articles point towards its paralog LIN28B for being responsible in cell migration and invasion by decreasing *let-7* expression and activating the Wingless Integration 1 (Wnt)/ β-catenin pathway; leading to a significant reduction of E-cadherin levels but an elevation of vimentin levels; causing disruption of the epithelium which enables the migration of cancer cells from the primary site[34,35]. Furthermore, abnormal β-catenin-E-cadherin complexes could diminish cellular adhesion and epithelial cell interstitialisation, which are required in limiting cell growth and cell migration primarily through contact inhibition[35]. Consequently, cell migration and invasion are facilitated.

For ovarian cancer, its malignancy is exacerbated by LIN28A hindering the activity of cleaved caspase-3, caspase-7, and caspase-9. Thus, the DNA damage repair enzyme, poly adenosine diphosphate-ribose polymerase (PARP) cannot be cleaved, which inhibits cell apoptosis of these cancer cells[36]. A unique mechanism in LIN28-expressing ovarian cancer cells is their secretion of exosomes, which contain miRNAs such as miRNA-200 and miRNA-17-92 that are taken up by non-tumour cells [37]. Subsequently, they induce EMT with miRNA-200 inhibiting zinc finger E-box binding homeobox 1 (ZEB1) to derepress E-cadherin as well as miRNA-17-92 regulating CYP7B1 and E-cadherin expression to ultimately promote migration and invasion[38].

In contrast with the previous three cancers, overexpression of LIN28A and hence, downregulation of *let-7* expression impeded cell proliferation, migration, and cell cycle progression in gastric cancer cells [39]. In fact, LIN28A overexpression induced apoptosis of these cells. Neither the related study or current literature explain this inverse relationship and its mechanisms.

Liver diseases

In hepatitis, LIN28A plays an active role in the balancing of EMT for fibrosis with mesenchymal-to-epithelial transition (MET) for liver regeneration; both processes are vital for liver repair[40]. Firstly, one of LIN28A targets include miRNA-200c which decreases expression of Fas-associated phosphatase 1 in order to increase expression of a proto-oncogene, tyrosine-protein kinase Src kinase (Src) and stimulate liver fibrosis[40]. In addition, another target, miRNA-107 can modulate components of the IL-6 receptor (IL-6R) complex in order to downregulate expression of chemokine (C-C motif) ligand 2 (CCL2), that is an inflammatory chemokine elevated in chronic liver diseases such as hepatitis C. Therefore, miRNA-107 can inhibit IL-6 signalling in regulating the inflammatory response and to an extent, fibrosis[40]. Secondly, LIN28A's repression of *let-7* removes the latter's inhibitory effect on IL-6 so activation of SRC can now elevate IL-6 Levels to induce inflammation[40]. Consequently, LIN28A and its targets disrupt

Table 2 Clinical relevance of LIN28A in certain cancers[25]

Tissue	Primary tumour	Clinical Relevance of LIN28A
Breast	HER2 + tumour	Overexpression correlated with HER2 + tumours
Colon	Primary adenocarcinoma	Expressed in approximately 30% tumours
Kidney	Primary Wilms' tumour	Overexpressed in late stage
Lung	Small cell lung cancer	Loss increases *let-7* levels; inhibits cell cycle
Oesophagus	Primary human tumour	Expression linked to metastasis and poor prognosis
Ovary	Primary ovarian tumour	Knockdown increases *let-7* expression

Citation: Thornton JE, Gregory RI. How does Lin28 Let-7 control development and disease? *Trends Cell Biol* 2012; **22**: 474-482. Copyright© The Authors 2012. Published by Elsevier Ltd. All rights reserved.

the balance of the inflammatory response and prolong fibrosis, which can have detrimental effects such as cirrhosis, portal hypertension, and liver failure.

Chronic cirrhosis can lead to oncogenic transformation into hepatocellular carcinoma (HCC), considered the most common primary liver tumour and leading cause of cancer death in the world[41]. As with most LIN28-linked cancers, increased LIN28 and decreased *let-7* are involved in the unregulated cellular proliferation and enhanced metastatic ability[40,41].

Biliary diseases can refer to primary biliary cholangitis, an autoimmune destruction of small to medium-sized bile ducts are destroyed and primary sclerosing cholangitis, inflammation of bile ducts coupled with structuring and sclerosis[40]. Both conditions contribute to cholestasis but more importantly, both involve inflammation. Therefore, LIN28A is suggested to play a critical role in tissue repair and inflammation or progression to cholangiocarcinoma. This is supported by *in vitro* studies showing that *let-7* can regulate inflammatory processes by modulating expression of lipopolysaccharide (LPS) toll-like receptor of cholangiocytes[40], and mice with cholangiocarcinoma presenting with decreased *let-7* and increased LIN28B instead[42].

Other liver diseases include non-alcoholic fatty liver disease (NAFLD), which is characterised by steatosis due to excessive consumption of sugar and fats or certain medications; and polycystic liver disease (PCLD), which encompasses autosomal dominant or recessive disorders occurring in association with polycystic kidney diseases[40]. In NAFLD, a primary inflammatory regulator is the NF-κB which has been correlated with an elevation of LIN28 Levels, which would decrease *let-7* levels[43]. In PCLD, LIN28's influence is hypothesised through two findings: The cholangiocytes in PCLD possessing the ability to undergo EMT and majority of miRNAs that were part of the *let-7* family exhibited reduced expression in cystic cholangiocytes[40]. However, current literature does not elucidate LIN28's roles and mechanisms in PCLD.

Neurological diseases

Parkinson's disease is characterised by degeneration of the dopamine neurons in the midbrain's substantia nigra that results in tremors and stiffness. *In vitro*, loss of LIN28A yielded neural stem cells with absent dopamine neurogenic potential and diminished repair capacity as well as more vulnerable dopamine neurons when exposed to toxic environments. This indicates loss of LIN28A affected development of healthy and properly functional dopamine neurons[44]. Hence, this loss is correlated with the pathogenesis involving degeneration of neurons. Next, Rett syndrome is characterised by loss-of-function mutations in *MECP2* that results in intellectual and motor impairments. Proteomic analyses revealed that LIN28 overexpression repressed astrocyte differentiation and decreased synapse formation. This leads to defects in glial differentiation and neuronal maturation, which in turn impairs neurodevelopment and hence, creates a dysfunctional nervous system[45].

THERAPEUTIC APPROACHES

Considering LIN28A's various physiological functions and pathological roles, therapeutic approaches have been developed involving its pathways and pharmaceutical drugs. This review will focus on drugs or proteins that directly target LIN28A or those that target essential or related components in the LIN28/*let-7* axis.

Cancer

With regard to LIN28A inhibitors, studies have investigated compounds such as 1632, TPEN, and L171. Firstly, 1632 prevented LIN28 from interacting with *let-7*, which in turn enables *let-7* levels to rise to

avoid the occurrence of stem-like phenotype in cancer cells and it was found to diminish clonogenic activity, indicating decreased capacity for proliferation by tumour cells[46]. *In vitro* studies demonstrate 1632's ability to reduce tumour sphere formation, which correlates with reduced *in vivo* tumour formation and metastasis. Most importantly, 1632 does not appear to have instantaneous cytotoxic effects but rather selectively inhibit tumour-specific characteristics of cells[46].

Secondly, tristetraprolin (TTP) binds to the three prime untranslated region (3' UTR) of LIN28A mRNA that stimulates its decay. As a result, the increased mature *let-7* levels lead to suppression of *CDC34* expression, which prevents unregulated cell cycle progression to curb the growth of cancer cells. Furthermore, expression of TTP has an inverse correlation with LIN28A levels in ovarian adenocarcinoma and human cancer cell lines including breast adenocarcinoma, erythroleukaemia, HCC, and neuron-committed teratocarcinoma[47].

Thirdly, compounds such as TPEN inhibits LIN28A's ZKDs by chelating zinc ions to catalyse apoptosis in LIN28A-expressing stem cells while L171 directly binds to LIN28A's CSDs to disrupt RNA binding and LIN28A-mediated oligouridylation of let-7[48]. Studies demonstrated that TPEN targeted LIN28-expressing mouse ESCs but non-LIN28-expressing HeLa cells as well while L171 was effective in LIN28-dependent human leukaemia cells and ESCs. However, TPEN's zinc chelation is not specific to LIN28A so it could cause apoptosis in cells that do not express LIN28A and L171 has a low potency for its inhibitory effects so both compounds require improvements. Moreover, there have been other potential LIN28A inhibitors such as 5-(methylamino) nicotinic acid that could block LIN28-mediated oligouridylation and gossypol that is hypothesised to hinder growth of LIN28-expressing tumours by suppressing oncoproteins such as Bcl-1 and MSI1, but further research would need to be conducted into their mechanisms and efficacy[48].

LIN28A inhibitors such as C1632 can restore *let-7*–mediated downregulation of programmed death ligand-1 (PD-L1). PD-L1 is frequently overexpressed in cancer cells and is a mechanism through which these cells evade T-cell recognition of tumour-specific and enhance tumour progression. Furthermore, high expression levels of PD-L1 are associated with more malignant tumour subtypes and poor prognosis in patients. By restoring *let-7* levels, C1632 can hamper tumour growth by hindering proliferation of cancer cells and improve the immune surveillance[49]. Currently, C1632 treatment can suppress PD-L1 in antigen-presenting cells such as THP-1 macrophages, and elevate secretion of interferon gamma and tumour necrosis factor alpha to enhance their T-cell mediated anti-tumour activity[49].

In vitro studies involving treatment with C1632 did not seem to exhibit cytotoxic effects as significant increase in apoptosis was not observed. However, this does not necessarily translate to a therapeutically effective dose against cancer in humans. Interestingly, metformin and C1632 produce synergistic anti-tumour effects in oral squamous cell carcinoma (OSCC). Studies suggest that metformin activates Dicer *via* the AMP-activated protein kinase pathway to enable maturation of *let-7*. Consequently, a decline in proliferative and migratory capacity of human OSCC cells *in vitro* (reduced closure of wound) and decline in tumour growth *in vivo* (reduced weight), without obvious signs of toxicity were observed [50]. While this combined treatment is promising for a non-invasive treatment of OSCC, the side effects and immunoreactivity in humans are unclear so further testing is needed.

In addition, LIN28 expression has been positively correlated with aldehyde dehydrogenase (ALDH) levels, a marker of CSCs and particularly with a subpopulation of tumour cells that are ALDH 1 positive ($ALDH1^+$)[51]. ALDHs could affect mechanisms in DNA repair and radioresistance and thus, contribute to carcinogenesis. Since LIN28 regulates and maintains the $ALDH1^+$ cell population through the *let-7* pathway or a *let-7* independent pathway through reprogramming factors such as OCT4, inhibiting LIN28 would diminish the tumour cell population. This could be carried out by either manipulating TUTase to increase let-7 or using nanoparticle-delivered LIN28 small interfering RNA or let-7.

In fact, research has explored nanobodies that can directly interact with a functional region on the TUT4 known as 106-reside LIN28: Let-7 interaction (LLI) fragment. These nanobodies can bind to the LLI fragments to interfere with the recruitment of TUTase and impeding LIN28-dependent (*i.e.* involving TUT4) oligouridylation of pre-let-7 microRNAs and LIN28-independent monouridylation of group II pre-let-7 microRNAs[51]. Hence, inhibition of TUT4 activity leads to elevated levels of mature *let-7*; countering the potential oncogenic implications of the LIN28/*let-7* pathway.

Lastly, ubiquitin-specific protease 28 (USP28) is a deubiquitinase that removes polyubiquitin from proteins such as LIN28A to stop the proteasomal degradation, thereby stabilising and extending its half-life. Studies indicate that USP28 augments LIN28A's inhibitory and oncogenic function. The former function involves enhanced inhibition of let-7 while the latter function involves enhanced colony formation, cell migration and invasion, and cell anchorage-independent proliferation[52]. Moreover, USP28 is overexpressed in cancers such as colorectal cancer and non-small cell lung cancer. This can be attributed to USP28 stabilising proto-oncogenic factors such as MYC. Considering MYC can facilitate cancer cell proliferation, it is hypothesised that USP28 can influence the LIN28-mediated cancer cell proliferation as well[52]. Therefore, disrupting USP28 itself or targeting other proteins that regulate it could become a viable option for cancer therapy.

Neuropathies

In optical neuropathies, retinal ischaemia-reperfusion (RIR) injury is characterised by expedited neuronal cell death due to lack of nutrients and oxygen as well as reactive oxygen species (ROS). Treatment with rasagiline and idebenone can utilise LIN28A's inhibitory effects on caspase-3 to mitigate oxidative damage by ROS and apoptosis[53]. Next, these drugs can upregulate Dicer expression through the LIN28A/*let-7* pathway, which enables cleavage of pre-miRNA into mature miRNA for optic neuroprotection and retinal development. Therefore, this combined treatment can alleviate RIR injury[53].

In auditory neuropathies, sensorineural hearing loss can be due to loss of auditory neurons. *In vitro* studies demonstrated that LIN28 overexpression activates basic helix-loop-helix (bHLH) transcription factors *via let-7* inhibition and upregulates Sox2 and HMGA2, which leads to increased proliferation and reprogramming of inner ear glial cells into neurons[54]. Therefore, neuronal dedifferentiation and proliferation could possibly restore auditory function. These findings indicate the potential of LIN28A in cell replacement therapy.

CONCLUSION

Since its discovery, LIN28A has been found to regulate several physiological processes such as stem cell renewal and differentiation, tissue repair, and glucose metabolism through *let-7* dependent and independent pathways. While downstream signalling pathways such as the insulin-Akt-mTor pathway and certain mRNA targets such as HMGA2 have been identified, the exact mechanisms have not been completely understood. Next, it remains unclear how these pathways eventuate in different and sometimes, contrasting effects in cell types. Pathologically, overexpression of LIN28A is generally correlated with poor prognosis in certain cancers, and negative outcomes in some biliary diseases and neuropathies. Consequently, therapeutic approaches have been developed, which either target LIN28A or other proteins which interact with LIN28A. By inhibiting LIN28A expression or function and manipulating its pathways, cellular proliferation and differentiation, and tissue repair can be regulated, which would especially be imperative in cancer therapy and tissue regeneration. However, further research is required before the efficacy of these approaches can be verified.

ACKNOWLEDGEMENTS

I would like to thank Dr. Rajaraman Eri for his guidance in writing this review. I would also like to thank him and Tauseef Ahmad for providing constructive feedback.

FOOTNOTES

Author contributions: Wu K wrote the review; all authors have read and approved the final version of the review.

Conflict-of-interest statement: The authors declare no conflict of interest.

Country/Territory of origin: Australia

ORCID number: Kenneth Wu 0000-0002-1666-6152; Tauseef Ahmad 0000-0001-5322-9413; Rajaraman Eri 0000-0003-1688-8043.

S-Editor: Fan JR
L-Editor: A
P-Editor: Fan JR

REFERENCES

1 **Mayr F**, Heinemann U. Mechanisms of Lin28-mediated miRNA and mRNA regulation--a structural and functional perspective. *Int J Mol Sci* 2013; **14**: 16532-16553 [PMID: 23939427 DOI: 10.3390/ijms140816532]

2 **Tsialikas J**, Romer-Seibert J. LIN28: roles and regulation in development and beyond. *Development* 2015; **142**: 2397-2404 [PMID: 26199409 DOI: 10.1242/dev.117580]
3 **Shyh-Chang N**, Daley GQ. Lin28: primal regulator of growth and metabolism in stem cells. *Cell Stem Cell* 2013; **12**: 395-406 [PMID: 23561442 DOI: 10.1016/j.stem.2013.03.005]
4 **Amen AM**, Ruiz-Garzon CR, Shi J, Subramanian M, Pham DL, Meffert MK. A Rapid Induction Mechanism for Lin28a in Trophic Responses. *Mol Cell* 2017; **65**: 490-503.e7 [PMID: 28132840 DOI: 10.1016/j.molcel.2016.12.025]
5 **Ustianenko D**, Chiu HS, Treiber T, Weyn-Vanhentenryck SM, Treiber N, Meister G, Sumazin P, Zhang C. LIN28 Selectively Modulates a Subclass of Let-7 MicroRNAs. *Mol Cell* 2018; **71**: 271-283.e5 [PMID: 30029005 DOI: 10.1016/j.molcel.2018.06.029]
6 **Lee H**, Han S, Kwon CS, Lee D. Biogenesis and regulation of the let-7 miRNAs and their functional implications. *Protein Cell* 2016; **7**: 100-113 [PMID: 26399619 DOI: 10.1007/s13238-015-0212-y]
7 **Kim SK**, Lee H, Han K, Kim SC, Choi Y, Park SW, Bak G, Lee Y, Choi JK, Kim TK, Han YM, Lee D. SET7/9 methylation of the pluripotency factor LIN28A is a nucleolar localization mechanism that blocks let-7 biogenesis in human ESCs. *Cell Stem Cell* 2014; **15**: 735-749 [PMID: 25479749 DOI: 10.1016/j.stem.2014.10.016]
8 **Hafner M**, Max KE, Bandaru P, Morozov P, Gerstberger S, Brown M, Molina H, Tuschl T. Identification of mRNAs bound and regulated by human LIN28 proteins and molecular requirements for RNA recognition. *RNA* 2013; **19**: 613-626 [PMID: 23481595 DOI: 10.1261/rna.036491.112]
9 **Cho J**, Chang H, Kwon SC, Kim B, Kim Y, Choe J, Ha M, Kim YK, Kim VN. LIN28A is a suppressor of ER-associated translation in embryonic stem cells. *Cell* 2012; **151**: 765-777 [PMID: 23102813 DOI: 10.1016/j.cell.2012.10.019]
10 **Wilbert ML**, Huelga SC, Kapeli K, Stark TJ, Liang TY, Chen SX, Yan BY, Nathanson JL, Hutt KR, Lovci MT, Kazan H, Vu AQ, Massirer KB, Morris Q, Hoon S, Yeo GW. LIN28 binds messenger RNAs at GGAGA motifs and regulates splicing factor abundance. *Mol Cell* 2012; **48**: 195-206 [PMID: 22959275 DOI: 10.1016/j.molcel.2012.08.004]
11 **Qiu C**, Ma Y, Wang J, Peng S, Huang Y. Lin28-mediated post-transcriptional regulation of Oct4 expression in human embryonic stem cells. *Nucleic Acids Res* 2010; **38**: 1240-1248 [PMID: 19966271 DOI: 10.1093/nar/gkp1071]
12 **Li C**, Sako Y, Imai A, Nishiyama T, Thompson K, Kubo M, Hiwatashi Y, Kabeya Y, Karlson D, Wu SH, Ishikawa M, Murata T, Benfey PN, Sato Y, Tamada Y, Hasebe M. A Lin28 homologue reprograms differentiated cells to stem cells in the moss Physcomitrella patens. *Nat Commun* 2017; **8**: 14242 [PMID: 28128346 DOI: 10.1038/ncomms14242]
13 **Parisi S**, Passaro F, Russo L, Musto A, Navarra A, Romano S, Petrosino G, Russo T. Lin28 is induced in primed embryonic stem cells and regulates let-7-independent events. *FASEB J* 2017; **31**: 1046-1058 [PMID: 27920151 DOI: 10.1096/fj.201600848R]
14 **Seabrook JL**, Cantlon JD, Cooney AJ, McWhorter EE, Fromme BA, Bouma GJ, Anthony RV, Winger QA. Role of LIN28A in mouse and human trophoblast cell differentiation. *Biol Reprod* 2013; **89**: 95 [PMID: 24006280 DOI: 10.1095/biolreprod.113.109868]
15 **Yang M**, Yang SL, Herrlinger S, Liang C, Dzieciatkowska M, Hansen KC, Desai R, Nagy A, Niswander L, Moss EG, Chen JF. Lin28 promotes the proliferative capacity of neural progenitor cells in brain development. *Development* 2015; **142**: 1616-1627 [PMID: 25922525 DOI: 10.1242/dev.120543]
16 **Li N**, Zhong X, Lin X, Guo J, Zou L, Tanyi JL, Shao Z, Liang S, Wang LP, Hwang WT, Katsaros D, Montone K, Zhao X, Zhang L. Lin-28 homologue A (LIN28A) promotes cell cycle progression *via* regulation of cyclin-dependent kinase 2 (CDK2), cyclin D1 (CCND1), and cell division cycle 25 homolog A (CDC25A) expression in cancer. *J Biol Chem* 2012; **287**: 17386-17397 [PMID: 22467868 DOI: 10.1074/jbc.M111.321158]
17 **Shyh-Chang N**, Zhu H, Yvanka de Soysa T, Shinoda G, Seligson MT, Tsanov KM, Nguyen L, Asara JM, Cantley LC, Daley GQ. Lin28 enhances tissue repair by reprogramming cellular metabolism. *Cell* 2013; **155**: 778-792 [PMID: 24209617 DOI: 10.1016/j.cell.2013.09.059]
18 **Wang XW**, Li Q, Liu CM, Hall PA, Jiang JJ, Katchis CD, Kang S, Dong BC, Li S, Zhou FQ. Lin28 Signaling Supports Mammalian PNS and CNS Axon Regeneration. *Cell Rep* 2018; **24**: 2540-2552.e6 [PMID: 30184489 DOI: 10.1016/j.celrep.2018.07.105]
19 **Shinoda G**, Shyh-Chang N, Soysa TY, Zhu H, Seligson MT, Shah SP, Abo-Sido N, Yabuuchi A, Hagan JP, Gregory RI, Asara JM, Cantley LC, Moss EG, Daley GQ. Fetal deficiency of lin28 programs life-long aberrations in growth and glucose metabolism. *Stem Cells* 2013; **31**: 1563-1573 [PMID: 23666760 DOI: 10.1002/stem.1423]
20 **Zacharewicz E**, Lamon S, Russell AP. MicroRNAs in skeletal muscle and their regulation with exercise, ageing, and disease. *Front Physiol* 2013; **4**: 266 [PMID: 24137130 DOI: 10.3389/fphys.2013.00266]
21 **Corre C**, Shinoda G, Zhu H, Cousminer DL, Crossman C, Bellissimo C, Goldenberg A, Daley GQ, Palmert MR. Sex-specific regulation of weight and puberty by the Lin28/let-7 axis. *J Endocrinol* 2016; **228**: 179-191 [PMID: 26698568 DOI: 10.1530/JOE-15-0360]
22 **Docherty CK**, Salt IP, Mercer JR. Lin28A induces energetic switching to glycolytic metabolism in human embryonic kidney cells. *Stem Cell Res Ther* 2016; **7**: 78 [PMID: 27230676 DOI: 10.1186/s13287-016-0323-2]
23 **Kim JD**, Toda C, Ramírez CM, Fernández-Hernando C, Diano S. Hypothalamic Ventromedial Lin28a Enhances Glucose Metabolism in Diet-Induced Obesity. *Diabetes* 2017; **66**: 2102-2111 [PMID: 28550108 DOI: 10.2337/db16-1558]
24 **Balzeau J**, Menezes MR, Cao S, Hagan JP. The LIN28/let-7 Pathway in Cancer. *Front Genet* 2017; **8**: 31 [PMID: 28400788 DOI: 10.3389/fgene.2017.00031]
25 **Thornton JE**, Gregory RI. How does Lin28 let-7 control development and disease? *Trends Cell Biol* 2012; **22**: 474-482 [PMID: 22784697 DOI: 10.1016/j.tcb.2012.06.001]
26 **Roncarati R**, Lupini L, Shankaraiah RC, Negrini M. The Importance of microRNAs in RAS Oncogenic Activation in Human Cancer. *Front Oncol* 2019; **9**: 988 [PMID: 31612113 DOI: 10.3389/fonc.2019.00988]
27 **Ma X**, Li C, Sun L, Huang D, Li T, He X, Wu G, Yang Z, Zhong X, Song L, Gao P, Zhang H. Lin28/let-7 axis regulates aerobic glycolysis and cancer progression *via* PDK1. *Nat Commun* 2014; **5**: 5212 [PMID: 25301052 DOI: 10.1038/ncomms6212]
28 **Zhang Y**, Li C, Hu C, Wu Q, Cai Y, Xing S, Lu H, Wang L, Huang, Sun L, Li T, He X, Zhong X, Wang J, Gao P, Smith ZJ, Jia W, Zhang H. Lin28 enhances de novo fatty acid synthesis to promote cancer progression *via* SREBP-1. *EMBO Rep*

2019; **20**: e48115 [PMID: 31379107 DOI: 10.15252/embr.201948115]
29 **Wang T**, He Y, Zhu Y, Chen M, Weng M, Yang C, Zhang Y, Ning N, Zhao R, Yang W, Jin Y, Li J, Redpath RJ, Zhang L, Jin X, Zhong Z, Zhang F, Wei Y, Shen G, Wang D, Liu Y, Wang G, Li X. Comparison of the expression and function of Lin28A and Lin28B in colon cancer. *Oncotarget* 2016; **7**: 79605-79616 [PMID: 27793004 DOI: 10.18632/oncotarget.12869]
30 **Mizuno R**, Kawada K, Sakai Y. The Molecular Basis and Therapeutic Potential of *Let-7* MicroRNAs against Colorectal Cancer. *Can J Gastroenterol Hepatol* 2018; **2018**: 5769591 [PMID: 30018946 DOI: 10.1155/2018/5769591]
31 **Xiong H**, Zhao W, Wang J, Seifer BJ, Ye C, Chen Y, Jia Y, Chen C, Shen J, Wang L, Sui X, Zhou J. Oncogenic mechanisms of Lin28 in breast cancer: new functions and therapeutic opportunities. *Oncotarget* 2017; **8**: 25721-25735 [PMID: 28147339 DOI: 10.18632/oncotarget.14891]
32 **Shen B**, Yuan Y, Zhang Y, Yu S, Peng W, Huang X, Feng J. Long non-coding RNA FBXL19-AS1 plays oncogenic role in colorectal cancer by sponging miR-203. *Biochem Biophys Res Commun* 2017; **488**: 67-73 [PMID: 28479250 DOI: 10.1016/j.bbrc.2017.05.008]
33 **Zhang Y**, Xiao X, Zhou W, Hu J, Zhou D. LIN28A-stabilized FBXL19-AS1 promotes breast cancer migration, invasion and EMT by regulating WDR66. *In Vitro Cell Dev Biol Anim* 2019; **55**: 426-435 [PMID: 31140103 DOI: 10.1007/s11626-019-00361-4]
34 **King CE**, Wang L, Winograd R, Madison BB, Mongroo PS, Johnstone CN, Rustgi AK. LIN28B fosters colon cancer migration, invasion and transformation through let-7-dependent and -independent mechanisms. *Oncogene* 2011; **30**: 4185-4193 [PMID: 21625210 DOI: 10.1038/onc.2011.131]
35 **Liu Y**, Li H, Feng J, Cui X, Huang W, Li Y, Su F, Liu Q, Zhu J, Lv X, Chen J, Huang D, Yu F. Lin28 induces epithelial-to-mesenchymal transition and stemness *via* downregulation of let-7a in breast cancer cells. *PLoS One* 2013; **8**: e83083 [PMID: 24349438 DOI: 10.1371/journal.pone.0083083]
36 **Zhong Y**, Yang S, Wang W, Wei P, He S, Ma H, Yang J, Wang Q, Cao L, Xiong W, Zhou M, Li G, Shuai C, Peng S. The interaction of Lin28A/Rho associated coiled-coil containing protein kinase2 accelerates the malignancy of ovarian cancer. *Oncogene* 2019; **38**: 1381-1397 [PMID: 30266988 DOI: 10.1038/s41388-018-0512-9]
37 **Enriquez VA**, Cleys ER, Da Silveira JC, Spillman MA, Winger QA, Bouma GJ. High LIN28A Expressing Ovarian Cancer Cells Secrete Exosomes That Induce Invasion and Migration in HEK293 Cells. *Biomed Res Int* 2015; **2015**: 701390 [PMID: 26583126 DOI: 10.1155/2015/701390]
38 **Fang LL**, Wang XH, Sun BF, Zhang XD, Zhu XH, Yu ZJ, Luo H. Expression, regulation and mechanism of action of the miR-17-92 cluster in tumor cells (Review). *Int J Mol Med* 2017; **40**: 1624-1630 [PMID: 29039606 DOI: 10.3892/ijmm.2017.3164]
39 **Song H**, Xu W, Song J, Liang Y, Fu W, Zhu XC, Li C, Peng JS, Zheng JN. Overexpression of Lin28 inhibits the proliferation, migration and cell cycle progression and induces apoptosis of BGC-823 gastric cancer cells. *Oncol Rep* 2015; **33**: 997-1003 [PMID: 25515921 DOI: 10.3892/or.2014.3674]
40 **McDaniel K**, Hall C, Sato K, Lairmore T, Marzioni M, Glaser S, Meng F, Alpini G. Lin28 and let-7: roles and regulation in liver diseases. *Am J Physiol Gastrointest Liver Physiol* 2016; **310**: G757-G765 [PMID: 27012771 DOI: 10.1152/ajpgi.00080.2016]
41 **Nguyen LH**, Robinton DA, Seligson MT, Wu L, Li L, Rakheja D, Comerford SA, Ramezani S, Sun X, Parikh MS, Yang EH, Powers JT, Shinoda G, Shah SP, Hammer RE, Daley GQ, Zhu H. Lin28b is sufficient to drive liver cancer and necessary for its maintenance in murine models. *Cancer Cell* 2014; **26**: 248-261 [PMID: 25117712 DOI: 10.1016/j.ccr.2014.06.018]
42 **Yang H**, Li TW, Peng J, Tang X, Ko KS, Xia M, Aller MA. A mouse model of cholestasis-associated cholangiocarcinoma and transcription factors involved in progression. *Gastroenterology* 2011; **141**: 378-388, 388.e1 [PMID: 21440549 DOI: 10.1053/j.gastro.2011.03.044]
43 **Gori M**, Arciello M, Balsano C. MicroRNAs in nonalcoholic fatty liver disease: novel biomarkers and prognostic tools during the transition from steatosis to hepatocarcinoma. *Biomed Res Int* 2014; **2014**: 741465 [PMID: 24745023 DOI: 10.1155/2014/741465]
44 **Chang MY**, Oh B, Choi JE, Sulistio YA, Woo HJ, Jo A, Kim J, Kim EH, Kim SW, Hwang J, Park J, Song JJ, Kwon OC, Henry Kim H, Kim YH, Ko JY, Heo JY, Lee MJ, Lee M, Choi M, Chung SJ, Lee HS, Lee SH. LIN28A loss of function is associated with Parkinson's disease pathogenesis. *EMBO J* 2019; **38**: e101196 [PMID: 31750563 DOI: 10.15252/embj.2018101196]
45 **Kim JJ**, Savas JN, Miller MT, Hu X, Carromeu C, Lavallée-Adam M, Freitas BCG, Muotri AR, Yates JR 3rd, Ghosh A. Proteomic analyses reveal misregulation of LIN28 expression and delayed timing of glial differentiation in human iPS cells with MECP2 loss-of-function. *PLoS One* 2019; **14**: e0212553 [PMID: 30789962 DOI: 10.1371/journal.pone.0212553]
46 **Roos M**, Pradère U, Ngondo RP, Behera A, Allegrini S, Civenni G, Zagalak JA, Marchand JR, Menzi M, Towbin H, Scheuermann J, Neri D, Caflisch A, Catapano CV, Ciaudo C, Hall J. A Small-Molecule Inhibitor of Lin28. *ACS Chem Biol* 2016; **11**: 2773-2781 [PMID: 27548809 DOI: 10.1021/acschembio.6b00232]
47 **Kim CW**, Vo MT, Kim HK, Lee HH, Yoon NA, Lee BJ, Min YJ, Joo WD, Cha HJ, Park JW, Cho WJ. Ectopic over-expression of tristetraprolin in human cancer cells promotes biogenesis of let-7 by down-regulation of Lin28. *Nucleic Acids Res* 2012; **40**: 3856-3869 [PMID: 22210895 DOI: 10.1093/nar/gkr1302]
48 **Wang L**, Rowe RG, Jaimes A, Yu C, Nam Y, Pearson DS, Zhang J, Xie X, Marion W, Heffron GJ, Daley GQ, Sliz P. Small-Molecule Inhibitors Disrupt let-7 Oligouridylation and Release the Selective Blockade of let-7 Processing by LIN28. *Cell Rep* 2018; **23**: 3091-3101 [PMID: 29874593 DOI: 10.1016/j.celrep.2018.04.116]
49 **Yang X**, Lin X, Zhong X, Kaur S, Li N, Liang S, Lassus H, Wang L, Katsaros D, Montone K, Zhao X, Zhang Y, Bützow R, Coukos G, Zhang L. Double-negative feedback loop between reprogramming factor LIN28 and microRNA let-7 regulates aldehyde dehydrogenase 1-positive cancer stem cells. *Cancer Res* 2010; **70**: 9463-9472 [PMID: 21045151 DOI: 10.1158/0008-5472.CAN-10-2388]
50 **Yu C**, Wang L, Rowe RG, Han A, Ji W, McMahon C, Baier AS, Huang YC, Marion W, Pearson DS, Kruse AC, Daley GQ, Wu H, Sliz P. A nanobody targeting the LIN28:let-7 interaction fragment of TUT4 blocks uridylation of let-7. *Proc*

Natl Acad Sci U S A 2020; **117**: 4653-4663 [PMID: 32060122 DOI: 10.1073/pnas.1919409117]

51 **Chen Y**, Xie C, Zheng X, Nie X, Wang Z, Liu H, Zhao Y. LIN28/*let-7*/PD-L1 Pathway as a Target for Cancer Immunotherapy. *Cancer Immunol Res* 2019; **7**: 487-497 [PMID: 30651289 DOI: 10.1158/2326-6066.CIR-18-0331]

52 **Haq S**, Das S, Kim DH, Chandrasekaran AP, Hong SH, Kim KS, Ramakrishna S. The stability and oncogenic function of LIN28A are regulated by USP28. *Biochim Biophys Acta Mol Basis Dis* 2019; **1865**: 599-610 [PMID: 30543854 DOI: 10.1016/j.bbadis.2018.12.006]

53 **Lei D**, Shao Z, Zhou X, Yuan H. Synergistic neuroprotective effect of rasagiline and idebenone against retinal ischemia-reperfusion injury *via* the Lin28-let-7-Dicer pathway. *Oncotarget* 2018; **9**: 12137-12153 [PMID: 29552298 DOI: 10.18632/oncotarget.24343]

54 **Kempfle JS**, Luu NC, Petrillo M, Al-Asad R, Zhang A, Edge ASB. Lin28 reprograms inner ear glia to a neuronal fate. *Stem Cells* 2020; **38**: 890-903 [PMID: 32246510 DOI: 10.1002/stem.3181]

World Journal of Biological Chemistry

Submit a Manuscript: https://www.f6publishing.com

World J Biol Chem 2022 March 27; 13(2): 47-65

DOI: 10.4331/wjbc.v13.i2.47

ISSN 1949-8454 (online)

ORIGINAL ARTICLE

Basic Study

Mesenchymal stromal cell delivery as a potential therapeutic strategy against COVID-19: Promising evidence from *in vitro* results

Panagiotis Mallis, Theofanis Chatzistamatiou, Zetta Dimou, Eirini-Faidra Sarri, Eleni Georgiou, Maria Salagianni, Vasiliki Triantafyllia, Evangelos Andreakos, Catherine Stavropoulos-Giokas, Efstathios Michalopoulos

Specialty type: Cell biology

Provenance and peer review: Invited article; Externally peer reviewed.

Peer-review model: Single blind

Peer-review report's scientific quality classification

Grade A (Excellent): A
Grade B (Very good): B
Grade C (Good): 0
Grade D (Fair): D
Grade E (Poor): 0

P-Reviewer: Alberca RW, Brazil; Munteanu C, Romania; Zhang Z, China

Received: November 6, 2021
Peer-review started: November 6, 2021
First decision: December 27, 2021
Revised: December 28, 2021
Accepted: March 6, 2022
Article in press: March 6, 2022
Published online: March 27, 2022

Panagiotis Mallis, Theofanis Chatzistamatiou, Zetta Dimou, Eirini-Faidra Sarri, Eleni Georgiou, Catherine Stavropoulos-Giokas, Efstathios Michalopoulos, Hellenic Cord Blood Bank, Biomedical Research Foundation Academy of Athens, Athens 11527, Greece

Maria Salagianni, Vasiliki Triantafyllia, Evangelos Andreakos, Laboratory of Immunobiology, Center for Clinical, Experimental Surgery and Translational Research, Biomedical Research Foundation Academy of Athens, Athens 11527, Greece

Corresponding author: Panagiotis Mallis, MSc, PhD, Associate Research Scientist, Teaching Assistant, Hellenic Cord Blood Bank, Biomedical Research Foundation Academy of Athens, No. 4 Soranou Ephessiou Street, Athens 11527, Greece. pmallis@bioacademy.gr

Abstract

BACKGROUND

Severe acute respiratory syndrome coronavirus 2 (SARS-CoV-2) is responsible for the coronavirus disease 2019 (COVID-19) pandemic, which was initiated in December 2019. COVID-19 is characterized by a low mortality rate (< 6%); however, this percentage is higher in elderly people and patients with underlying disorders. COVID-19 is characterized by mild to severe outcomes. Currently, several therapeutic strategies are evaluated, such as the use of anti-viral drugs, prophylactic treatment, monoclonal antibodies, and vaccination. Advanced cellular therapies are also investigated, thus representing an additional therapeutic tool for clinicians. Mesenchymal stromal cells (MSCs), which are known for their immunoregulatory properties, may halt the induced cytokine release syndrome mediated by SARS-CoV-2, and can be considered as a potential stem cell therapy.

AIM

To evaluate the immunoregulatory properties of MSCs, upon stimulation with COVID-19 patient serum.

METHODS

MSCs derived from the human Wharton's Jelly (WJ) tissue and bone marrow (BM) were isolated, cryopreserved, expanded, and defined according to the criteria outlined by the International Society for Cellular Therapies. Then, WJ and

BM-MSCs were stimulated with a culture medium containing 15% COVID-19 patient serum, 1% penicillin-streptomycin, and 1% L-glutamine for 48 h. The quantification of interleukin (IL)-1 receptor a (Ra), IL-6, IL-10, IL-13, transforming growth factor (TGF)-β1, vascular endothelial growth factor (VEGF)-a, fibroblast growth factor (FGF), platelet-derived growth factor (PDGF), and indoleamine-2,3-dioxygenase (IDO) was performed using commercial ELISA kits. The expression of HLA-G1, G5, and G7 was evaluated in unstimulated and stimulated WJ and BM-MSCs. Finally, the interactions between MSCs and patients' macrophages were established using co-culture experiments.

RESULTS

Thawed WJ and BM-MSCs exhibited a spindle-shaped morphology, successfully differentiated to "osteocytes", "adipocytes", and "chondrocytes", and in flow cytometric analysis were characterized by positivity for CD73, CD90, and CD105 (> 95%) and negativity for CD34, CD45, and HLA-DR (< 2%). Moreover, stimulated WJ and BM-MSCs were characterized by increased cytoplasmic granulation, in comparison to unstimulated cells. The HLA-G isoforms (G1, G5, and G7) were successfully expressed by the unstimulated and stimulated WJ-MSCs. On the other hand, only weak expression of HLA-G1 was identified in BM-MSCs. Stimulated MSCs secreted high levels of IL-1Ra, IL-6, IL-10, IL-13, TGF-β1, FGF, VEGF, PDGF, and IDO in comparison to unstimulated cells ($P < 0.05$) after 12 and 24 h. Finally, macrophages derived from COVID-19 patients successfully adapted the M2 phenotype after co-culturing with stimulated WJ and BM-MSCs.

CONCLUSION

WJ and BM-MSCs successfully produced high levels of immunoregulatory agents, which may efficiently modulate the over-activated immune responses of critically ill COVID-19 patients.

Key Words: SARS-CoV-2; COVID-19; MSCs; Stem cell therapy; Cytokine storm; Immunomodulation

Core Tip: Coronavirus disease 2019 (COVID-19) is responsible for the acute respiratory distress syndrome occurrence, a disorder that might prove life-threatening for a great number of hospitalized patients. As an alternative to the already evaluated therapeutic protocols, mesenchymal stromal cells (MSCs) can be evaluated as a potential stem cell therapy. MSCs exert key immunoregulatory properties, either through direct or indirect contact. In the current study, stimulated Wharton's Jelly and bone marrow-MSCs produced high levels of anti-inflammatory cytokines and growth factors and also efficiently performed the M2 phenotype switch of macrophages. Considering this data, MSCs could be considered as a valuable stem cell therapy for better COVID-19 management.

Citation: Mallis P, Chatzistamatiou T, Dimou Z, Sarri EF, Georgiou E, Salagianni M, Triantafyllia V, Andreakos E, Stavropoulos-Giokas C, Michalopoulos E. Mesenchymal stromal cell delivery as a potential therapeutic strategy against COVID-19: Promising evidence from *in vitro* results. *World J Biol Chem* 2022; 13(2): 47-65
URL: https://www.wjgnet.com/1949-8454/full/v13/i2/47.htm
DOI: https://dx.doi.org/10.4331/wjbc.v13.i2.47

INTRODUCTION

Coronavirus disease 2019 (COVID-19), which is caused by severe acute respiratory syndrome coronavirus 2 (SARS-CoV-2), was initially reported in Wuhan, China in 2019[1-3]. Currently, it is believed that the zoonotic transmission of SARS-CoV-2 initiated from a local wild animal market in Wuhan. Due to the fast global transmission of SARS-CoV-2, the World Health Organization (WHO) declared on January 2020 the COVID-19 as a Public Health Emergency of International Concern (PHEIC), followed by an upgrade to pandemic status on March 11 of the same year[4,5].

Now, COVID-19 represents a major global issue, counting more than 281484620 total cases and more than 5409113 fatalities, since the initial outbreak[6]. Indeed, the COVID-19 pandemic has spread in more than 220 countries[6,7]. Accurate date regarding the worldwide spread of COVID-19 can be provided by global monitoring platforms such as Johns Hopkins University Coronavirus Research Center[6].

SARS-CoV-2 affects primarily the respiratory system (upper and lower respiratory tract), followed by infection of multiple organs (*e.g.*, the liver, kidney, intestine, and heart)[8]. The clinical manifestations of SARS-CoV-2 include: (1) Initial mild symptoms, such as cough, fever, fatigue, and general malaise; (2)

moderate symptoms, such as pneumonia and low oxygen levels; and (3) severe symptoms, including the acute respiratory distress syndrome, cytokine release syndrome, and multiorgan failure[8,9]. COVID-19 is currently characterized by an average mortality rate of less than 6% globally; however, in patients aged above 65 years old or patients with significant underlying disorders, the mortality rate is increasing dramatically[6,10,11]. Currently, it has been reported that the transmission of SARS-CoV-2 between healthy individuals can be performed through three main ways: (1) Contact transmission with SARS-CoV-2 positive subjects; (2) droplet; and (3) aerosol transmission. The latter might explain the fast transmission of SARS-CoV-2 globally[12].

The entry of SARS-CoV-2 to the host cells is mediated through the connection between the spike (S) protein and the angiotensin-converting enzyme (ACE) II receptor[8-12]. A second receptor named transmembrane protease serine 2 (TMPRSS2) favors the priming of the S protein and is implicated in the viral entry process[8-12]. After its entrance, SARS-CoV-2 is starting to multiply its virion to infect more cells. In this case, the host's immune system may recognize the SARS-CoV-2[8-12]. This can result in the local release of interferons, activation of immune cells (such as macrophages, dendritic cells [DCs], natural killer [NK] cells, and T and B lymphocytes), and finally virus clearance[8-12]. However, in case of escaping from the immune surveillance and recognition mechanisms, SARS-CoV-2 can induce severe pneumonia[13]. SARS-CoV-2 pathophysiology is related to the alveolar epithelial cell damage, which could result in ground-glass opacity of the lungs[14]. The latter is mediated mainly by the stimulated T helper (Th) 1, 2, and Th17 cells[13]. Critically ill patients are characterized by increased levels of several cytokines including IL-2, IL-6, IL-7, G-CSF, IP10, MCP1, MIP1A, and TNF-α, a situation which is also known as "cytokine storm"[13,15]. These patients are characterized by lymphopenia, thrombocytopenia, NK cell reduction, respiratory failure, and multi-organ injury (*e.g.*, cardiac and lung fibrosis)[16].

To date, several therapeutic strategies, which can ameliorate the above manifestations, have been proposed and used in the clinical setting[17]. Among them, antimalarial drugs such as hydroxychloroquine or chloroquine, doxycycline, corticosteroids, monoclonal antibodies against IL-6, and convalescent plasma antibodies have been applied in COVID-19 patients with different effectiveness results[17,18]. In this way, the prevention of SARS-CoV-2 transmission through the vaccination program may represent the best option against this pandemic. However, there are still a great number of patients that are hospitalized or require the intensive care unit, accompanied by connection to extracorporeal membrane oxygenation.

Considering the great prevalence of COVID-19, more therapeutic strategies targeting the aberrant host immune responses must be evaluated. One such therapeutic intervention with potential benefit for critically ill patients may be the utilization of mesenchymal stromal cells (MSCs)[19,20].

MSCs are non-hematopoietic stem cells with great immunoregulatory/immunosuppressive abilities. MSCs represent a mesodermal multipotent stem cell population, which initially was discovered in bone marrow (BM) aspirate samples by Bianco *et al*[21]. Currently, MSCs can be obtained from various sources of the human body, including the liver, lungs, adipose tissue (AT), umbilical cord blood, placenta, and umbilical cord tissue (Wharton's Jelly [WJ] tissue)[22]. Based on the proposed guidelines of the MSC Committee of the International Society for Cell and Gene Therapy (ISCT), MSCs must fulfill specific criteria[23,24]. Briefly, MSCs must exhibit: (1) Plastic-adhesion ability (spindle-shaped cells); (2) tri-lineage differentiation towards "osteocytes", "chondrocytes", and "adipocytes" under defined conditions; and (3) specific immunophenotype[23,24]. Interestingly, MSCs are characterized by positive and negative expression of specific cell surface markers (clusters of differentiation [CDs]). More than 95% of MSCs express CD73 (5'-nucleotidase), CD90 (Thy-1 antigen), and CD105 (endoglin), and < 2% express CD34 (hemopoietic stem cell marker), CD45 (pan-lymphocyte antigen), HLA-DR (HLA class II molecules), CD11b (macrophage marker), and CD19 (B-lymphocyte marker)[23,24].

Also, MSCs are considered as immune-evasive stem cells and thus cannot be recognized by the immune cells, *e.g.*, macrophages and T and B cells[25,26]. Intriguingly, the immune evasion of MSCs is elicited mainly by the lack of HLA class II molecules and costimulatory molecules such as CD80, CD86, CD40, and CD40 ligand[25,26].

Besides, according to the proposed guidelines by the ISCT, MSCs from different sources are characterized by variable functional properties. Indeed, fetal MSCs (*e.g.*, derived from amniotic fluid, placenta, and WJ tissue) may have significant differences in terms of proliferation and differentiation efficiency, telomere length, and telomerase activity, compared to adult MSCs (*e.g.*, adipose tissue and bone marrow)[22,27-29]. Also, it has been shown that fetal MSCs are characterized by better immunoregulatory/immunosuppressive properties and have acquired less mutagenic or epigenetic changes to their genome, in comparison to MSCs derived from adult sources[22,27-29].

MSCs are known for their immunoregulatory properties, mediated either through the cell-cell contact mechanisms or through the secretion of bioactive molecules[30]. MSCs have broad effects on the cells of innate and adaptive immunity. Specifically, MSCs can orchestrate the phenotype switching from proinflammatory M1 to anti-inflammatory M2 macrophages, promote the production of tolerogenic DCs, and induce T and B cell inhibition[31]. These functions can be mediated either through direct contact of MSCs with the immune cells and activation of cell signaling pathways (promoted after cell contact interactions) such as Fas/Fas ligand, TNF-α/TNF-R, PD-L1/PD-1, and HLA-G, or through the release of specific molecules, *e.g.*, indoleamine-2.3-dioxygenase (IDO), nitric oxide (NO), galectins, and the soluble forms of HLA-G (HLA-G5-G7)[31]. Currently, MSCs have been utilized in over 80 clinical

trials for COVID-19, registered to the international database clinicaltrials.gov (www. clinicaltrials.gov) [32,33]. In the majority of the studies, the safety and efficiency of the infused MSCs have been well evaluated[32-37]. However, in those studies, the exact interplay between MSCs and hyper-stimulated immune cells in COVID-19 patients has not been satisfactorily explained.

Furthermore, due to the mesodermal lineage differentiation capacity of MSCs, these cells may exert beneficial tissue regeneration of the damaged tissue. The pathogenesis of COVID-19 involves the injury of the alveolar epithelium, which further may induce lung fibrosis, a state which is known as ground glass opacity. MSCs can either be differentiated to endothelial and epithelial cells or can direct the differentiation of epithelial and endothelial progenitor cells, through a paracrine manner. MSCs can exert both immunoregulatory properties and tissue regeneration abilities, and therefore, their use as an alternative therapeutic strategy in critically-ill COVID-19 patients must be strongly considered by the physicians.

Therefore, the aim of the current study was focused on the *in vitro* evaluation of the immunoregulatory properties of MSCs, upon stimulation with serum obtained from critically ill COVID-19 patients. COVID-19 patient serum is characterized by high levels of pro-inflammatory cytokines, which can stimulate efficiently the MSCs under *in vitro* conditions. This assessment was performed in cryopreserved MSCs derived from WJ and BM samples. In this way, the discrepancy in the key immunoregulatory properties between WJ and BM-MSCs may be revealed. The obtained data may give fundamental insights into the beneficial effects of MSCs in tolerating the overactivated immune responses. Furthermore, the MSCs from both sources may be proven to be a satisfactory cell therapy, ameliorating the manifestations of COVID-19.

MATERIALS AND METHODS

Isolation, expansion, and cryopreservation of WJ-MSCs

WJ-MSCs were isolated from the human umbilical cords (hUCs) that were delivered to Hellenic Cord Blood Bank (HCBB). In the current study, hUCs (n = 10) derived from full-term (gestational ages 38-40 wk) normal and caesarian deliveries, were used for the isolation of the WJ-MSCs. All hUCs were accompanied by informed consent, which was in accordance with the declaration of Helsinki and conformed with the ethical standards of the Greek National Ethical Committee. The informed consent was provided by the mothers, few days before the delivery. The overall study has received approval from the Institution's ethical board (Reference No. 1754, January 21, 2021). After the delivery of the hUCs to the HCBB, the samples were processed immediately for MSCs isolation. Initially, the hUCs were rinsed in excess 1 × phosphate buffer saline (PBS, Sigma-Aldrich, Darmstadt, Germany), to remove any blood clots. Then, isolation of WJ tissue was performed with the use of sterile instruments. The isolated WJ tissue was dissected into small pieces (0.3 cm × 0.3 cm) and placed in a 6-well culture plate (Costar, Corning Life, Canton, MA, United States). Finally, 1 mL of complete culture medium was added to each well, and the cultures were transferred to an incubator at 37 °C in an atmosphere containing 5% CO_2, for a time period of 18 d. After 18 d of cultivation, the cultures were microscopically checked and in case of cell confluency near to 80% (in each well), the MSCs were trypsinized (Trypsin-EDTA solution 0.25% w/v, Gibco, Thermo Fisher Scientific, Waltham, United States) and placed to a 75 cm^2 tissue culture flask. The WJ-MSCs were grown in the cell cultures until reaching passage (P) 3. Then, WJ-MSCs at P3 were detached from the flasks and centrifuged at 500 g for 6 min, and the cell pellet was cryopreserved using the Bambanker solution (Nippon Genetics, Duren, Germany) into 1.8 mL cryotubes. Finally, the cryotubes were placed into a Mr. Frosty freezing container (Thermo Fisher Scientific), ensuring the control rate freezing (1 °C/min) of the cells. The cryotubes were transferred to a liquid nitrogen tank at -196 °C for a time period of 6 mo.

The complete culture medium used in the whole study consisted of α-minimum essentials medium (α -MEM, Sigma-Aldrich) supplemented with 15% fetal bovine serum (FBS, Sigma-Aldrich), 1% v/v penicillin-streptomycin (P-S, Sigma Aldrich), and 1% v/v L-glutamine (L-Glu, Sigma Aldrich).

Isolation, expansion and cryopreservation of BM-MSCs

BM-MSCs (n = 10) were isolated from donor samples, after obtaining the signed informed consent for the current study. BM-MSCs were isolated accordingly. Ten milliliters of BM was transferred to 75 cm^2 tissue cultured flasks supplemented with the complete culture medium. The BM cell cultures were placed in an incubator at 37 °C in an atmosphere containing 5% CO_2 for a time period of 10 d. BM-MSCs were microscopically checked for their morphology and confluency, followed by passaging to 175 cm^2 tissue culture flasks. The BM-MSCs were grown in the cell cultures until reaching P3. Then cryopreservation of BM-MSCs was performed (in the same way as mentioned above). Finally, the cryotubes remained in the liquid nitrogen tank for a time period of 6 mo.

Thawing procedure of WJ and BM-MSCs

The thawing procedure of MSCs from both sources involved their quick transfer from -196 °C to a water bath at 37 °C (Memmert, Germany). Then, thawed MSCs of each cryotube were transferred to 50 mL

conical falcon tubes (Costar, Corning Life) with the addition of 30 mL 1 × PBS (Sigma-Aldrich), followed by centrifugation at 500 g for 6 min. Finally, the MSCs were placed to 75 cm^2 cell culture flasks (Costar, Corning Life) with 14 mL of complete culture medium, and remained until further processing.

Characterization of WJ and BM-MSCs

Following the criteria of the ISCT, the WJ and BM-MSCs were evaluated for their quality characteristics. The quality check of the WJ and BM-MSCs at P3 involved: (1) Microscopic examination; (2) evaluation of differentiation capacity into "osteocytes", "adipocytes", and "chondrocytes"; and (3) flow cytometry analysis for the evaluation of specific CDs expression.

Morphological assessment of WJ and BM-MSCs was performed using an inverted light microscope (Leica DM L2, Leica, Microsystems, Weltzar, Germany) and images were acquired with IC Imaging Control (The ImagineSource, Bremen, Germany) and processed with Image J (v1.533, National Institute of Health, United States).

The ability of MSCs from both sources to differentiate to "osteocytes", "adipocytes", and "chondrocytes" was evaluated. For this purpose, the StemPro Osteogenesis, Adipogenesis, and Chondrogenesis kits (Thermo Fischer Scientific) were used, according to the manufacturer's instructions. To validate their successful differentiation, histological analysis with the use of specific stains was performed. Alizarin Red S, Oil Red O, and Alcian Blue (Sigma-Aldrich) were applied for the evaluation of calcium deposition, lipid droplet, and glycosaminoglycans (sGAGs) production, respectively.

Determination of the MSCs' immunophenotype was performed using a panel of 15 monoclonal antibodies, using the FACS Calibur (BD Biosciences, Franklin Lakes, NJ, United States). Specifically, fluorescein (FITC) labeled antibodies against CD90, CD45, CD29, CD31, and HLA-ABC, phycoerythrin (PE) labeled antibodies against CD44, CD3, CD11b, and CD34, peridinin-chlorophyll-protein (PerCP) labeled antibodies against CD105 and HLA-DR, and allophycocyanin (APC) labeled antibodies against CD73, CD10, and CD340 were used. All monoclonal antibodies were purchased from Becton Dickinson (BD biosciences). For each tube, on average 10000 total events were acquired. Complete flow cytometric analysis was performed with FlowJo v10 (BD biosciences).

Stimulation of WJ and BM-MSCs with COVID-19 patient serum

Stimulation of WJ-MSCs (n = 10) and BM-MSCs (n = 10) was achieved using a culture medium supplemented with COVID-19 patient serum (COVID-19 culture medium) obtained from five critically ill patients. These critically ill patients (n = 5) exhibited moderate to severe symptoms and had pneumonia which was confirmed by radiological findings. The COVID-19 patients fulfilled the following criteria: (1) Respiratory distress (≥ 30 breaths/min); (2) low oxygen levels (≤ 93% at rest); and (3) arterial partial pressure of oxygen (PaO_2)/fraction of inspired oxygen (FiO_2) ≤ 300 mmHg with no other organ failure. All patients were acquired from the 2nd Respiratory Clinic of "Sotiria" General Chest Diseases Hospital, Athens, Greece. All patients were informed and provided informed consent for the current study.

Thawed WJ and BM-MSCs at a density of 150 × 10^3 cells/well were placed in 6-well plates with 1 mL of COVID-19 culture medium and incubated for a time period of 48 h. Then, removal of the culture medium was performed, followed by extensive washes with 1 × PBS. Finally, α-MEM (Sigma-Aldrich) supplemented with 1% v/v P-S (Sigma-Aldrich) was added and remained until cytokine and growth factor quantification analysis was performed. COVID-19 medium consisted of α-MEM (Sigma-Aldrich) supplemented with 15% v/v COVID-19 patient serum and 1% v/v P-S (Sigma-Aldrich).

Characterization of stimulated MSCs

Stimulated MSCs from both sources were evaluated for their morphological features. For this purpose, stimulated MSCs were observed using an inverted light microscope (Leica DM L2, Microsystems), and images were acquired with IC Imaging Control (The Imagine Source) and processed with Image J (v1.533, National Institute of Health, United States). Furthermore, cell viability and number were measured in unstimulated and stimulated MSCs. To perform this evaluation, cell counting and viability estimation were performed using trypan blue dye. The measurement was performed in the automated Cell Countess system (Thermo Fischer Scientific).

Immunophenotype evaluation was also performed in MSCs before and after the stimulation with COVID-19 patient serum. Immunophenotype analysis was performed using an antibody panel consisting of antibodies against CD73, CD90, CD105, CD29, CD340, CD45, and HLA-DR. The whole process was performed as described in the previous section (Characterization of WJ and BM-MSCs).

Cytokine and growth factor quantification analysis

The cytokine and growth factor profile of stimulated WJ and BM MSCs was performed using ELISA. Specifically, IL-1 receptor antagonist (RA), IL-6, IL-10, and IL-13 and transforming growth factor (TGF)-β1, vascular endothelial growth factor (VEGF), fibroblast growth factor (FGF)-1, platelet-derived growth factor (PDGF), and IDO were evaluated in unstimulated and stimulated MSCs. The quantification of cytokines and growth factors was performed after 12 and 24 h (after the addition of α-MEM with 1% v/v P-S, Sigma-Aldrich). All assays were performed according to the manufacturer's instructions and

the final concentration was estimated through interpolation to the standard curve.

Evaluation of HLA-G mRNA expression in stimulated MSCs

Evaluation of the HLA-G expression was performed in unstimulated (n = 3) and stimulated MSCs derived either from the WJ (n = 3) or BM (n = 3). Briefly, the mRNA from the aforementioned MSCs was isolated using the TRI reagent (Sigma-Aldrich) following the manufacturer's instructions. Then, the mRNA was quantified and 800 ng was used for the performance of reverse transcription (RT)-polymerase chain reaction (PCR). Complementary DNA (cDNA) was used as a template and amplified using the primers listed in Table 1. The PCR was performed on Eppendorf Master Cycler (Eppendorf, Hamburg, Germany), involving the following steps: (1) Initial denaturation at 95 °C for 15 s; (2) denaturation at 94 °C for 30 s; (3) annealing at 60–61 °C for 90s; and (4) extension at 72 °C for 3 min. The current program involved a total of 35 cycles. The PCR products were analyzed by 1% v/v agarose gel electrophoresis (Biorad, California, United States). Glyceraldehyde 3-phosphate dehydrogenase (GAPDH) was used as an internal housekeeping gene for the evaluation of the results.

Evaluation of HLA-G protein expression

Evaluation of HLA-G expression was performed using the flow cytometric and immunofluorescence assays. The indirect immunofluorescence assay was performed in unstimulated MSCs (n = 3/from each source) and stimulated WJ (n = 3) and BM-MSCs (n = 3). MSCs were placed at a density of 2 × 10^4 on culture slides (Costar, Corning Life). When confluency was observed, the cells were exposed to 10% v/v neutral formalin (Sigma-Aldrich) for 20 min and fixed. Initially, antigen epitope retrieval was applied in all samples, followed by blocking and addition of primary monoclonal antibody against human HLA-G (1:1000, Catalog MA1-10359, Thermo Fisher Scientific). Extensive washes were performed and the secondary FITC-conjugated mouse IgG antibody (1:100, Sigma-Aldrich) was added. DAPI (Thermo Fisher Scientific) was used to stain nuclei. The slides were mounted and observed under a fluorescence microscope. Images were acquired with LEICA SP5 II microscope equipped with LAS Suite v2 software (Leica, Microsystems).

Isolation of peripheral blood mononuclear cells and macrophage differentiation

The isolation of human peripheral blood mononuclear cells (PBMCs) was performed from critically ill COVID-19 patients (n = 5). Specifically, 10 mL of peripheral blood was diluted (1:1) with 1 × PBS (Sigma-Aldrich) and placed carefully on the top of Ficoll (Sigma-Aldrich). Then, centrifugation was performed at 450 g for 30 min. PBMCs layer was isolated and placed in a different conical tube, where 10 mL of 1 × PBS (Sigma-Aldrich) was added. Then, centrifugation at 350 g for 5 min was performed. Finally, the CD14+ cells were separated with negative selection using the human CD14+ cell enrichment (Stem Cell Technologies) according to the manufacturer's instructions.

The isolated monocytes were submitted to macrophage differentiation. Monocytes at a density of 1 × 10^5/well were added to 24-transwell (bottom) plates with 1 mL of α-MEM supplemented with 1% v/v L-Glu, 1% v/v P-S, and 100 ng/ ml granulocyte-macrophage colony-stimulating factor (GM-CSF). The differentiation process lasted 9 d, and the medium was changed twice a week.

Co-culture of stimulated MSCs with macrophages

After macrophage differentiation from the patient's PBMCs, co-culturing experiments with the stimulated WJ (n = 5) and BM-MSCs (n = 5) were performed. This set of experiments was performed using 24 trans-well plates (Costar, Corning Life) coupled with 3 μm pores. Unstimulated (n = 5) and stimulated WJ (n = 5) or BM-MSCs (n = 5) at a density of 5 × 10^4/well were placed on the top, while patient's macrophages were placed on the bottom of the trans-well plates. Finally, 1 mL of regular culture medium was added to each well, and the trans-wells placed were transferred to an incubator at 37 °C in an atmosphere containing 5% CO_2 for 10 d. The change of the medium was performed once a week. The cultures were observed under an inverted light microscope (Leica DM L2, Microsystems). The images were acquired with IC Imaging Control (The ImagineSource) and processed with Image J (v1.533, National Institute of Health, United States). Also, flow cytometry analysis, to determine the macrophage phenotype switch from M1 to M2, was performed using the markers CD14-PE, CD45-FITC, CD11b-PE, CD29-FITC, and CD163-PerCP. All monoclonal antibodies were purchased from Becton Dickinson (BD biosciences). For each tube, on average 10000 total events were acquired. Complete flow cytometric analysis was performed with FlowJo v10 (BD biosciences).

Statistical analysis

Statistical analyses were performed using the statistical software GraphPad Prism v 6.01 (GraphPad Software, San Diego, CA, United States). All comparisons in the current study were performed by the unpaired non-parametric Kruskal–Wallis test. Statistically significant difference between group values was considered when the P value was less than 0.05. Values are presented as the mean ± SD.

Table 1 Primer sequences used in the current study

Gene	Forward	Reverse	Size
HLA-G1	AGGAGACACGGAACACCAAG	CCAGCAACGATACCCATGAT	685
HLA-G5	AACCCTCTTCCTGCTGCTCT	GCCTCCATCTCCCTCCTTAC	895
HLA-G7	AACCCTCTTCCTGCTGCTCT	TTACTCACTGGCCTCGCTCT	331
GAPDH	AAGGGCCCTGACAACTCTTT	CTCCCCTCTTCAAGGGGTCT	244

RESULTS

Evaluation of WJ and BM-MSCs characteristics

Prior to stimulation of cells with the culture medium containing COVID-19 patient serum, thawed WJ and BM-MSCs were comprehensively evaluated for their characteristics. MSCs from both sources were characterized as plastic adherent spindle-shaped cells with a few cytoplasmic vacuoles (Figure 1A and Supplementary Figure 1). Successful differentiation of MSCs to "osteocytes", "adipocytes", and "chondrocytes" was confirmed using specific histological stains. Specifically, Alizarin red S and oil red O stained positively the calcium deposits and oil-droplets, produced from WJ and BM-MSCs, respectively. Further characterization of MSCs involved the immunophenotypic evaluation, using the flow cytometry analysis. WJ and BM-MSCs shared similar size features (Figure 1B and C). On the other hand, BM-MSCs were characterized by increased cytoplasmic granulation and therefore greater forward to side scatter ratio, compared to WJ-MSCs (Figure 1B). Over 95% of both WJ and BM-MSCs expressed the CD73, CD90, CD105, CD10, CD29, and CD340, while less than 2% expressed CD34, CD45, HLA-DR, CD11b, and CD31(Figure 1C and Supplementary Table 1). The only discrepancy in CDs expression between WJ and BM-MSCs was found in HLA-ABC. Specifically, over 75% of WJ-MSCs expressed the HLA-ABC, while over 90%of BM-MSCs expressed the same marker (Figure 1C and Supplementary Table 1). Thawed MSCs from both sources retained successfully their morphological and immunophenotypic characteristics until reaching P4, and hence can be considered as well-defined MSCs, which can efficiently be used in the current study.

Evaluation of stimulated WJ and BM-MSCs characteristics

After the initial evaluation of WJ and BM-MSCs characteristics, stimulation with patient-derived COVID-19 serum was performed. WJ and BM-MSCs were exposed to culture medium containing COVID-19 patient serum for 48 h, followed by morphological, immunophenotypic, and molecular evaluations (Figure 2A). Morphological analysis using an inverted light microscope showed the preservation of the fibroblastic-like morphology of stimulated MSCs from both sources. Moreover, stimulated WJ and BM-MSCs exhibited increased cytoplasmic granulation, compared to unstimulated MSCs (Figure 2B). After 48 h of incubation with COVID-19 culture medium, the total cell number of stimulated WJ and BM-MSCs was $4.8 \pm 0.4 \times 10^5$ and $3.5 \pm 0.2 \times 10^5$, respectively (Supplementary Table 2). The initial cell number of WJ and BM-MSCs was $3.1 \pm 0.1 \times 10^5$ (for both cell sources). A statistically significant difference was found in cell numbers between unstimulated and stimulated WJ and BM-MSCs ($P < 0.001$, Supplementary Table 2). The viability rate of unstimulated WJ and BM-MSCs was 94 ± 1% and 93 ± 2%, respectively, while stimulated MSCs presented similar viability rates (Figure 2C). Further characterization of stimulated MSCs involved the immunophenotypic analysis. Stimulated WJ and BM-MSCs exhibited increased cytoplasmic granulation, thus confirming further the initial morphological evaluation (Figure 2D). No statistically significant alteration in CD expression was observed between stimulated and unstimulated WJ and BM-MSCs. Specifically, in unstimulated and stimulated MSCs obtained from both sources, > 95% of the cells expressed CD73, CD90, CD105, CD29, and CD340, while < 2% expressed CD45 and HLA-DR (Figure 2D). A detailed description of the CD marker expression in unstimulated and stimulated WJ and BM MSCs is provided as supplementary data (Supplementary Table 3).

Additional analysis involved the evaluation of the HLA-G expression in stimulated MSCs. For this purpose, RNA was isolated from unstimulated and stimulated MSCs, followed by the performance of RT-PCR and PCR. Finally, the PCR products were analyzed by agarose gel electrophoresis. In this study, the HLA-G1, G5, and G7 isoforms were determined. WJ-MSCs successfully expressed the HLA-G isoforms. Specifically, unstimulated WJ MSCs expressed the cytoplasmic HLA-G1 and the soluble forms of HLA-G5 and HLA-G7 (Figure 2E). Stimulated WJ-MSCs were characterized by elevated expression of the above HLA-G isoforms. On the contrary, BM-MSCs (unstimulated and stimulated) expressed only the HLA-G1 (Figure 2E). These results were further confirmed by indirect immunofluorescence. Stimulated WJ-MSCs exhibited higher expression of the HLA-G1 compared to the unstimulated cells (Figure 2F). On the other hand, BM-MSCs exhibited a weak fluorescence signal regarding the HLA-G1 (Figure 3F).

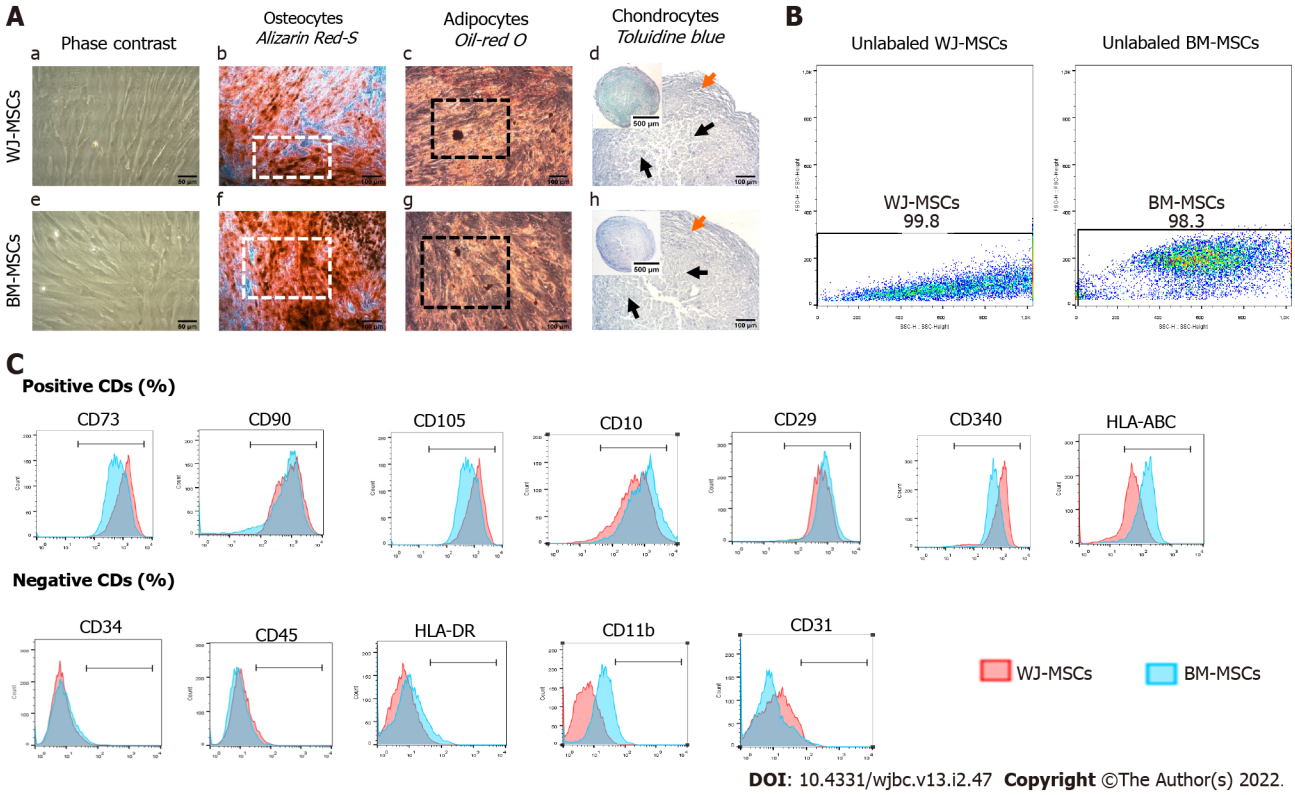

DOI: 10.4331/wjbc.v13.i2.47

Figure 1 Evaluation of characteristics of Wharton's Jelly and bone marrow-mesenchymal stromal cells. A: Morphological characteristics of mesenchymal stromal cells (MSCs) derived from Wharton's Jelly (WJ) tissue and bone marrow (BM). MSCs from both sources were characterized as spindle-shaped cells with a few internal vacuoles. Both WJ and BM-MSCs were successfully differentiated to "osteocytes", "adipocytes", and "chondrocytes". White squares and black squares indicate the presence of calcium deposits and oil droplets, respectively. Black and orange arrows indicate the differentiated and undifferentiated state, respectively. a and e: Original magnification 20 ×, scale bars = 50 μm; b-d and f-h: Original magnification 10 ×, scale bars = 100 μm; B: Unlabeled WJ and BM-MSCs; C: Evaluation of CD marker expression by WJ and BM-MSCs. BM: Bone marrow; MSCs: Mesenchymal stromal cells; WJ: Wharton's Jelly.

Quantification of cytokines and growth factors

The next step of the current study involved the examination of the effect of inflammatory stimuli on the release of the immunosuppressive cytokines and growth factors by the WJ and BM-MSCs. Stimulated MSCs from both sources were evaluated for the cytokine secretion including IL-1Ra, IL-6, IL-10, and IL-13, growth factor production including TGF-b1, FGF, VEGF, and PDGF, and the release of the immunosuppressive agent IDO. The secretion of the aforementioned factors was evaluated after 12 and 24 h, from the initial activation of MSCs with COVID-19 culture medium. The results of this study indicated an increase in the release of the immunoregulatory agents compared to the unstimulated cells after 12 and 24 h (Figure 3). Specifically, after 8 h from the initial activation, the levels of IL-1RA, IL-6, IL-10, and IL-13 were 924 ± 100, 66 ± 11, 195 ± 51, and 174 ± 23 pg/mL for the stimulated WJ-MSCs, respectively, and 432 ± 162, 33 ± 16, 88 ± 24, and 132 ± 24 pg/mL for the stimulated BM-MSCs, respectively (Figure 3A-D, Supplementary Table 4). After 24 h, the levels of the same cytokines were 407 ± 57, 44 ± 7, 103 ± 14, and 114 ± 5 pg/mL for the stimulated WJ-MSCs, respectively, and 235 ± 50, 21 ± 4, 71 ± 8, and 79 ± 14 pg/mL for the stimulated BM-MSCs, respectively (Figure 4A-D, Supplementary Table 5). Statistically significant differences were found in cytokine release after 12 and 24 h between stimulated and unstimulated MSCs ($P < 0.05$) and also between stimulated WJ and BM-MSCs ($P < 0.05$). In the same way, the levels of TGF-b1, FGF, VEGFA, and PDGF after 8h of activation for the stimulated WJ-MSCs were 955 ± 210, 1048 ± 82, 801 ± 143 and 941 ± 107 pg/mL, respectively, and for stimulated BM-MSCs were 840 ± 43, 995 ± 88, 790 ± 108, and 826 ± 145 pg/mL, respectively (Figure 3E-H, Supplementary Table 4). After 24 h, the levels of the above growth factors for the stimulated WJ-MSCs were 813 ± 140, 669 ± 84, 646 ± 102, and 754 ± 74 pg/mL, respectively, and for the stimulated BM-MSCs were 653 ± 182, 627± 107, 585 ± 55, and 672 ± 108 pg/mL, respectively (Figure 4E-H, Supplementary Table 5). Finally, the levels of the immunosuppressive agent IDO after 12 and 24 h from the initial activation for the activated WJ-MSCs were 1228 ± 92 and 835 ± 77 pg/mL and for stimulated BM-MSCs were 1152 ± 80 and 674 ± 100 pg/mL, respectively (Figures 3I and 4I, Supplementary Tables 4 and 5). A detailed description regarding the levels of all immunomodulatory agents derived from unstimulated and stimulated WJ and BM-MSCs is provided in Table S4.

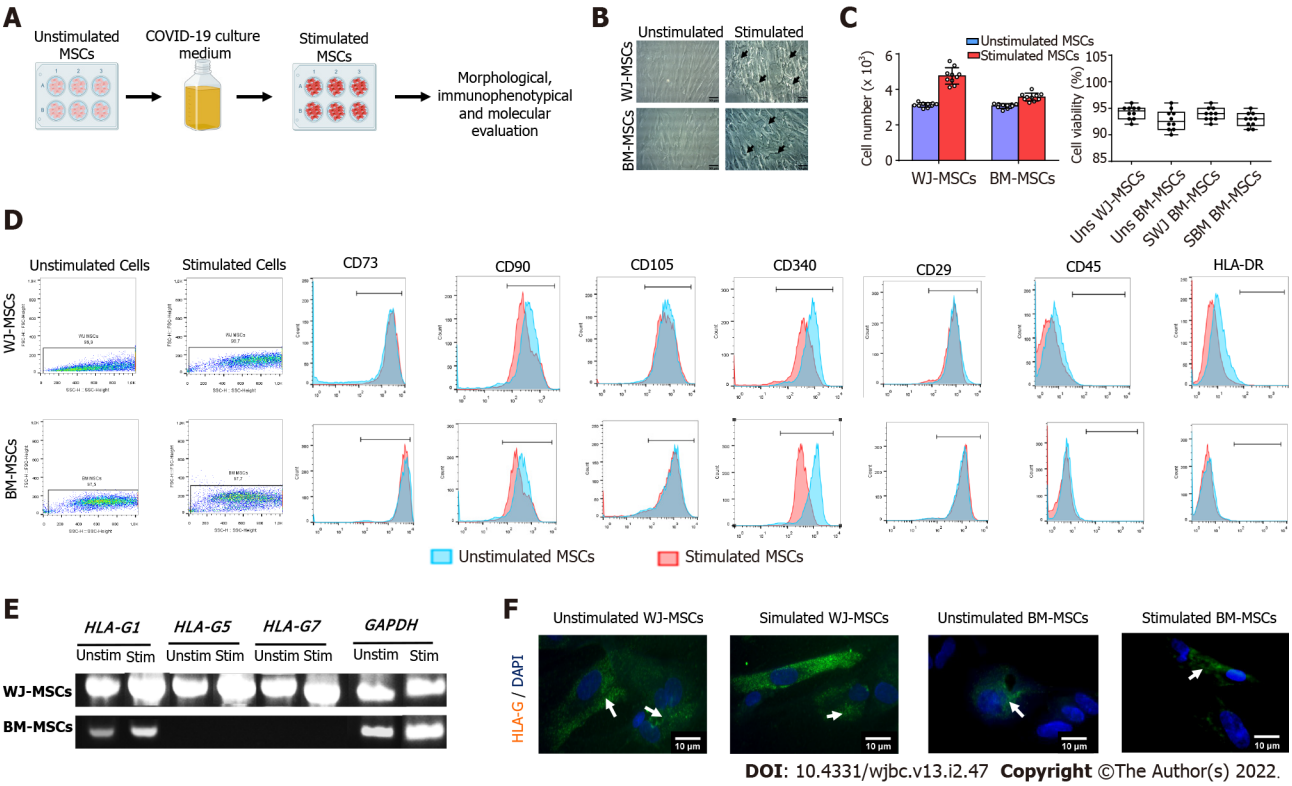

DOI: 10.4331/wjbc.v13.i2.47

Figure 2 Comprehensive characterization of characteristics of stimulated Wharton's Jelly and bone marrow mesenchymal stromal cells.
A: Experimental workflow; B: Morphological analysis of characteristics of unstimulated and stimulated Wharton's Jelly (WJ) and bone marrow-mesenchymal stromal cells (BM-MSCs). Original magnification 20 ×, scale bars = 50 μm; C: Determination of cell proliferation and viability. Statistically significant differences were observed in cell proliferation between stimulated and unstimulated WJ-MSCs ($P < 0.05$) and stimulated and unstimulated BM-MSCs ($P < 0.05$). No statistically significant difference was observed in cell viability either in an unstimulated or stimulated state ($P = 0.873$); D: Immunophenotypic analysis of stimulated and unstimulated WJ and BM-MSCs. Over 95% of WJ and BM-MSCs in both states expressed CD73, CD90, CD105, CD29, and CD340, and less than 2% expressed CD34 and CD45; E: Determination of HLA-G isoforms (HLA-G1, G5, and G7) in unstimulated and stimulated MSCs from both sources; F: Indirect immunofluorescence against HLA-G1 in combination with DAPI stain was performed on unstimulated and stimulated WJ and BM-MSCs. Original magnification 63 ×, scale bars = 10 μm. BM: Bone marrow; MSCs: Mesenchymal stromal cells; WJ: Wharton's Jelly.

Evaluation of macrophage polarization

To investigate the ability of WJ and BM-MSCs in inducing an anti-inflammatory phenotype in macrophages obtained from COVID-19 patients, co-culturing experiments were performed. Briefly, the isolated CD14+ monocytes from PBMCs were induced to differentiate into M1 macrophages in the presence of GM-CSF. Over 90% of differentiated cells expressed CD11b in flow cytometry analysis, a typical macrophage marker. Then, stimulated WJ and BM-MSCs were added to the top of the transwell plates, while the differentiated macrophages were placed in the bottom of the plate. Initially, macrophages were characterized by a round-shape morphology, which is a typical feature of the M1 phenotype. After 9 d of co-culturing, shapeshift of macrophages was observed with the use of an inverted light microscope (Figure 5). Specifically, macrophages exhibited a spindle-shaped morphology, a common characteristic of the M2 phenotype. In addition, flow cytometry analysis showed an increase in the integrin b1 subunit (CD29) and the scavenger receptor (CD163) expression in macrophages after 9 d of co-culturing either with WJ or BM-MSCs (Supplementary Table 6). Statistically significant differences regarding the CD29 and CD163 were observed in macrophages before and after the co-culturing with the MSCs ($P < 0.001$). The above data indicated the positive effect of stimulated MSCs in macrophage polarization into the anti-inflammatory M2 phenotype.

DISCUSSION

The pandemic COVID-19, which was initiated at the end of 2019, has been considered a severe life-threatening condition[1-5]. COVID-19 now is a global public and economic burden for most countries[1-5]. SARS-CoV-2 is responsible for the severe acute respiratory distress syndrome occurrence, which may further cause lung fibrosis, multiorgan failure, and eventually life loss. The pathophysiologic mechanisms of SARS-CoV-2 include also the induction of CRS, which is associated with increased levels of IL-2, IL-6, IL-7, G-CSF, IP10, MCP1, MIP1A, and TNF-α[13-15]. CRS is also related to altered host

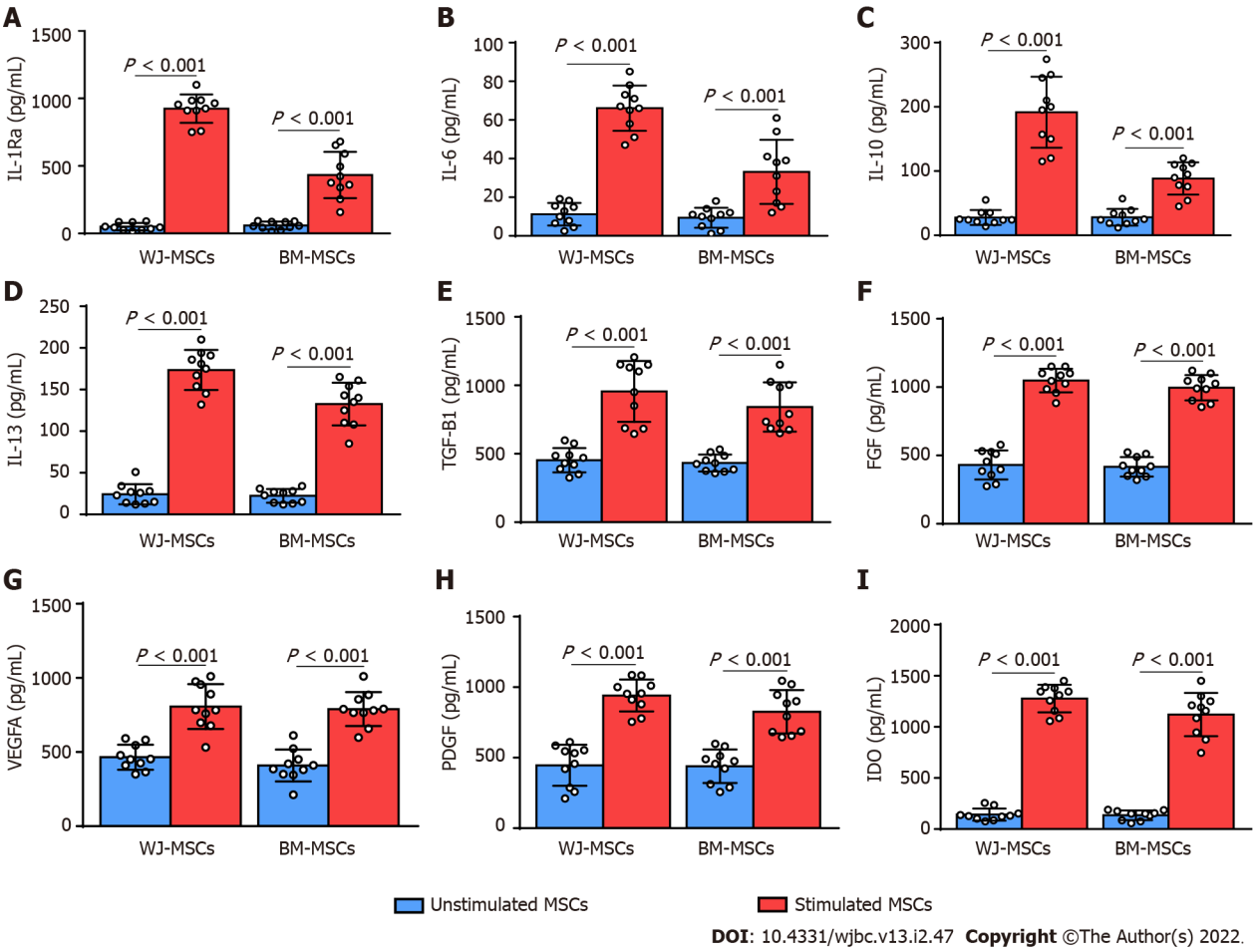

Figure 3 Quantification of immunosuppressive agents after 12 h from the initial activation with coronavirus disease 2019 patient serum.
A-D: Quantification of cytokines including IL-1Ra, IL-6, IL-10, and IL-13 in unstimulated and stimulated Wharton's Jelly (WJ) and bone marrow-mesenchymal stromal cells (BM-MSCs); E-H: Quantification of growth factors including TGF-b1, FGF, VEGFA, and PDGF in unstimulated and stimulated WJ and BM-MSCs; I: Quantification of indoleamine-2,3-dioxygenase in unstimulated and stimulated WJ and BM-MSCs. BM: Bone marrow; MSCs: Mesenchymal stromal cells; WJ: Wharton's Jelly.

immune responses, and activation mostly of M1 macrophages, Th1, and Th17 cells. Until now, several therapeutic protocols have been evaluated, including the administration of antivirals drugs (such as remdesivir and favipiravir), corticosteroids, and monoclonal antibodies against IL-6, with the vaccination to emerge as the most promising solution[17,18]. However, besides the vaccination, modern cell therapies are now evaluated and considered as promising strategies for critically ill COVID-19 patients. In this way, MSCs, which are sharing key immunoregulatory properties, may serve as a potential stem cell therapy[25-32]. Currently, a great number of clinical trials (where the MSCs are used) are being performed, with very encouraging results[33-37]. However, until now, the studies focusing on the molecular mechanisms by which MSCs may exert their beneficial properties against COVID-19 are limited. Therefore, in the current study, we evaluated the immunoregulatory properties of stimulated WJ and BM-MSCs as a result stimulation with COVID-19 patient serum.

Initially, the characterization of the thawed WJ and BM-MSCs was performed, and no discrepancies were observed according to the already published literature[22-24]. Both thawed WJ and BM-MSCs fulfilled the criteria outlined by the ISCT and hence were considered as well-defined cells[23,24]. Then, stimulation of MSCs from both sources using COVID-19 patient serum was performed. Stimulated MSCs retained their initial morphology; however, increased cytoplasmic granulation was observed in the stimulated cells. Besides that, no alteration was observed in MSCs markers. Importantly, no variability in CD340 expression was observed between unstimulated and stimulated MSCs (from both sources). CD340 is a stem cell marker, and its preservation after the stimulation indicated no alteration in the stemness properties of MSCs[38]. Indeed, Kim *et al*[39] showed that increased levels of CD340 were associated with MSCs that can exert high stem cell characteristics and therapeutic benefits. Moreover, in the study of Kim *et al*[39], CD340+ MSCs highly expressed OCT4 and NANOG, accompanied by elevated growth ability and differentiation potential. Specifically, CD340+ MSCs exhibited increased differentiation capacity towards the "osteogenic" lineage, as it was also confirmed by the increased alkaline phosphatase signal intensity[39]. Moreover, in our study, it was shown that CD340+ WJ and BM-MSCs, besides the differentiation potential, were efficiently stimulated and

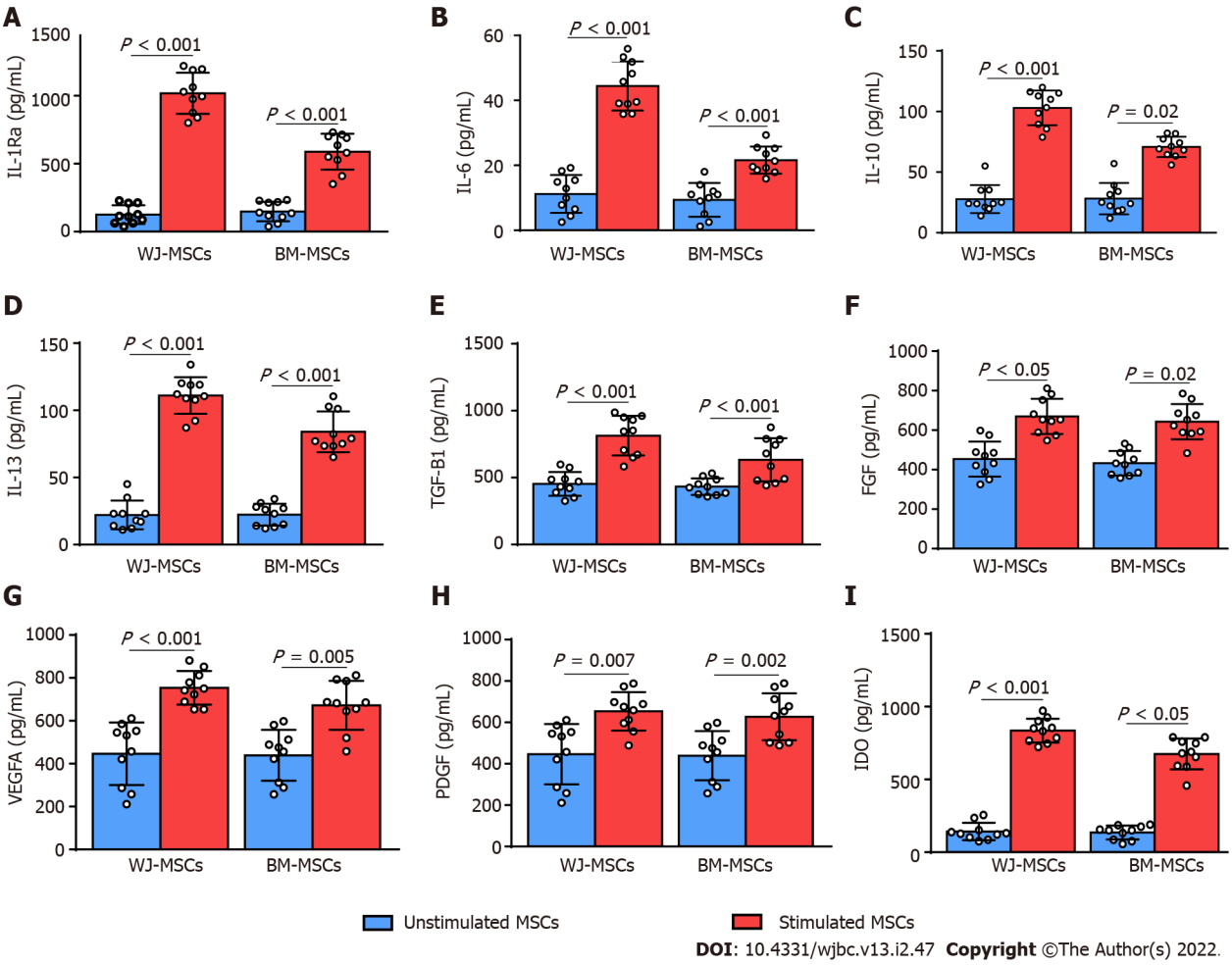

DOI: 10.4331/wjbc.v13.i2.47

Figure 4 Quantification of immunosuppressive agents after 24 h from the initial activation with coronavirus disease 2019 patient serum.
A-D: Quantification of cytokines including IL-1Ra, IL-6, IL-10, and IL-13 in unstimulated and stimulated Wharton's Jelly (WJ) and bone marrow mesenchymal stromal cells (BM-MSCs); E-H: Quantification of growth factors including TGF-b1, FGF, VEGFA, and PDGF in unstimulated and stimulated WJ and BM-MSCs; I: Quantification of IDO in unstimulated and stimulated WJ and BM-MSCs. BM: Bone marrow; MSCs: Mesenchymal stromal cells; WJ: Wharton's Jelly.

secreted a high amount of immunomodulatory agents.

Initially, the expression of the immunomodulatory molecule HLA-G was evaluated. Specifically, unstimulated and stimulated WJ-MSCs expressed the HLA-G1, HLA-G5, and HLA-G7 whereas only weak expression of HLA-G1 was found in BM-MSCs. HLA-G shares a close relationship with the extraembryonic tissues, where can induce the mother's tolerance against the semi-allogeneic fetus[40]. Considering this, it may explain the elevated levels of HLA-G expression in WJ-MSCs compared to BM-MSCs. WJ-MSCs are derived from the umbilical cord, an extraembryonic tissue, which is characterized by high HLA-G expression levels. Moreover, Yen *et al*[41] showed that adult MSCs (such as BM-MSCs) are characterized by different methylation patterns in the promoter region of the *HLA-G*, compared to MSCs from fetal tissues. Importantly, it was shown that different methylation patterns were also evident within the *HLA-G* gene between different MSCs sources[41]. Accordingly, the difference in methylation patterns might also explain the variability of HLA-G expression between the WJ and BM-MSCs. In the literature, controversial data regarding the expression of the HLA-G between MSCs from fetal and adult sources have also been reported[42-46]. It is well known that HLA-G shares important immunomodulatory properties, which can efficiently modulate the immune responses exerted by stimulated immune cells such as macrophages, DCs, NK cells, and T and B cells[31]. In this way, HLA-G might have a significant role in tolerating the CRS in critically ill COVID-19 patients.

Furthermore, priming of MSCs with COVID-19 patient serum enhanced both the secreted immunoregulatory and regenerative agents in response to the inflammatory stimuli. In the current study, it was observed that the COVID-19 inflammatory stimuli were able to increase the production of IL-1Ra, IL-6, IL-10, and IL-13 by WJ and BM-MSCs. It has been shown in the past that the secreted anti-inflammatory cytokines may act positively in the inflamed microenvironment, tolerating the over-activated immune responses[47-49]. Specifically, IL-1Ra which binds selectively to the secreted IL-1 can efficiently block the immune cell activation through downregulation of signaling pathways such as the nuclear factor kappa-light-chain-enhancer (NF-κB) of the stimulated B cells[50,51]. Importantly, several studies have shown that IL-1Ra and IL-10 have a synergistic effect in modulating the immune responses[52]. IL-10

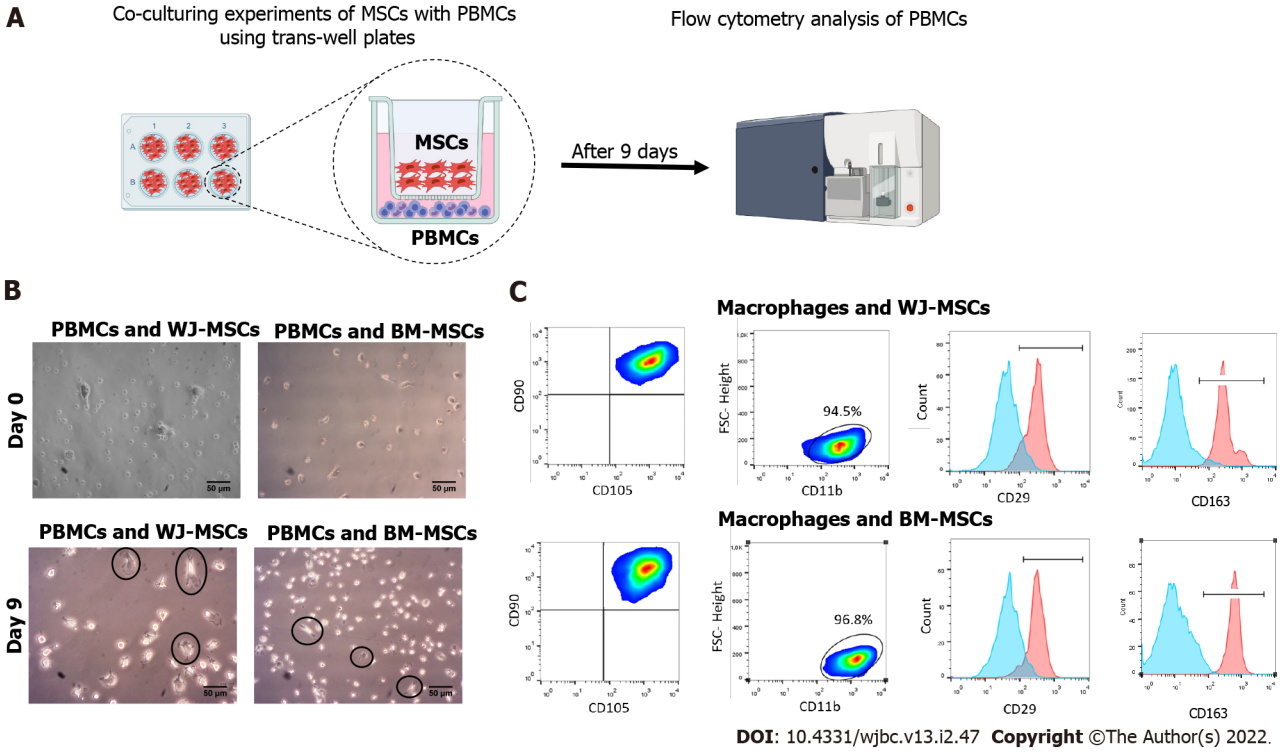

Figure 5 Co-culturing experiments of M1 macrophages with stimulated Wharton's Jelly and bone marrow-mesenchymal stromal cells. A: Schematic representation of the experimental workflow; B: Macrophage morphology was changed 9 d after co-culture either with Wharton's Jelly or bone marrow-mesenchymal stromal cells. After 9 d, macrophages exhibited a more elongated shape and plastic adherence. Black arrows indicate the presence of elongated plastic adherent cells; C: Flow cytometry analysis showed the positive expression of CD45, CD14, and CD11b by the differentiated macrophages. After 9 d, the macrophages exhibited an increase in the CD29 and CD163 expression, compared to the cells at day 0. Statistically significant differences regarding the CD29 and CD163 were observed in M2 compared to M1 macrophages ($P < 0.001$). BM: Bone marrow; MSCs: Mesenchymal stromal cells; WJ: Wharton's Jelly; PBMCs: Peripheral blood mononuclear cells.

can suppress the stimulated cellular population of innate and adaptive immunity such as the activated macrophages, inhibit the Th1 and promote the Th2 response, and also can act as an antagonist of IL-1 and TNF-a[52,53]. In the same way, IL-13 can cause a shift towards the Th2 response. Indeed, upon IL-13 binding to its receptor, activation of JAK-STAT1/STAT6 and IRS-1/IRS-2 pathways is induced, which further leads to the adaptation of Th2 response[54,55]. IL-13 is a known anti-inflammatory cytokine, which is also implicated in M2 phenotype switch and acts as an antagonist of IL-1β, IL-3, IL-12, and TNF-α[56-58]. In addition, COVID-19 stimulated MSCs secreted high levels of IL-6. IL-6 is a pleiotropic cytokine produced in the initial stages of inflammation, and exerts key functions in immune cells[58,59]. Critically ill COVID-19 patients have increased IL-6 levels, which is considered as the main mediator for the orchestration of the pro-inflammatory cytokines to the infected region[60]. However, there are several studies indicating that IL-6 can serve as a regulator between pro- and anti-inflammatory responses[61,62]. IL-6 can stimulate IL-10 production, which synergistically can act on activated immune cells[61-63]. Specifically, both cytokines can suppress the antigen presentation function of the activated DCs, thus resulting in the formation of the tolerogenic DCs[61-63]. Recently, Dorronsoro *et al* [64] showed that silencing of IL-6 with shRNA significantly induced impaired immunoregulatory functions by human MSCs. Therefore, IL-6 seems to play a significant role in the immunomodulation mediated by the activated MSCs[64]. The anti-inflammatory actions of the aforementioned cytokines can be enhanced by other immunosuppressive agents such as the secreted IDO. IDO is a strong immunoregulatory molecule that is implicated in the T cell cycle, by inhibiting the tryptophan catabolism to kynurenine[65]. In this way, T cells can be poised to G1 arrest state, thus their proliferation is stopped [66,67]. Besides T cells, IDO can exhibit an immunosuppressive action on B and NK cells, while its production is elevated by IFN-γ stimulated MSCs[31].

In addition, several growth factors are produced by the MSCs in response to the COVID-19 inflammatory stimuli. Among them, TGF-β, FGF, VEGF, and PDGF play a crucial role in the regulation of various fundamental immune functions, such as cell stimulation, migration, proliferation, and apoptosis [31]. Notably, the suppression of CD4+ and CD8+ T cell proliferation is induced through the upregulation of cyclin-dependent kinase (CDK) inhibitors p15, p21, and p27 and downregulation of c-Myc, cyclin D2, and E, a process which can be regulated by the secreted growth factors[68]. T cell suppression is mediated through the TGF-β/SMAD3-dependent downregulation of CDK4, as has been proposed by several research teams[69,70]. Secreted growth factors in combination with the anti-inflammatory

cytokines besides the described immunomodulation, can induce the proliferation of progenitor cells, favoring the tissue regeneration of the damaged tissue[71,72].

The immunoregulatory properties of the stimulated MSCs were further verified by the co-culture experiments. Differentiated macrophages derived from COVID-19 patients successfully adapted the anti-inflammatory M2 phenotype after their interaction with the stimulated MSCs. It has been proposed in the past that MSCs can educate and tolerate the inflammatory macrophages[73,74]. In the current study, we noticed the elevated expression of CD29 and CD163. Of note, CD163 represents a specific marker of the M2 phenotype[75,76]. CD29 represents the β1 integrin subunit, which is also related to the fibroblastic shape of the M2 macrophages[77,78]. M2 macrophage phenotype is closely related to the expression of anti-inflammatory properties, thus contributing both to immunomodulation and tissue regeneration. The results of this study were in agreement with the study of Domenis *et al*[79], showing the successful M2 phenotype switch after exosome (derived from MSCs) mediated crosstalk. In addition, de Witte *et al*[80] and Weiss *et al*[81] have shown that infused MSCs may follow the apoptotic or necroptotic program, thus undergoing phagocytosis by the alveolar macrophages. Through this process, the macrophages shift to the M2 phenotype efficiently.

MSCs currently are considered as Advanced Therapeutic Medicinal Products (ATMPs), hence clinical trials establishing the safe and tolerability of these cells must be conducted[20,32-37]. In the majority of the clinical trials, allogeneic or autologous MSCs are intravenously (IV) administrated in COVID-19 patients. Possible adverse events (AEs) that are associated with the IV administration include fever risk, toxicity, infection, pulmonary embolism, and possible malignancy formation. However, in the currently conducted clinical trials utilizing the MSCs as a possible COVID-19 treatment strategy, only an increased risk of fever was reported. Furthermore, after IV administration of MSCs, the AEs are considered mild to moderate. Besides the aforementioned AEs, other incidences also have been reported and evaluated for the possible relation with MSCs administration. The study of Shi *et al*[82] reported an increase in lactic acid dehydrogenase, serum alanine aminotransferase, creatine phosphatase, aspartate aminotransferase, and uric acid, and reported hypokalemia during the 1-year follow-up. However, all these AEs were on-site judged and considered as unrelated to the MSCs administration[82]. Considering these data, MSCs are a safe and tolerable therapy, therefore more clinical trials (phases I, II, and III) have been registered (www.clinicaltrials.gov) and are currently performed to further evaluate the potential application of these cells in critically ill COVID-19 patients.

At this point, it is worthy to mention the limitations of the current study. This study involved an initial evaluation of immunomodulatory agent release in a small sample size of WJ and BM-MSCs. Further evaluation of the immunomodulatory agents in a greater number of samples must be performed to verify better our initial results. Future experiments should also involve the evaluation of the direct interaction between MSCs and immune cells. Also, further assessment of the beneficial properties of MSCs may include their utilization in humanized ACE2 transgenic mouse models.

The results of this study represent only preliminary evidence; however, in this study, significant data which may decipher the molecular mechanisms associated with the immunomodulatory activity of MSCs have been presented. Besides the immunomodulatory properties, MSCs possess key differentiation capabilities, committed mostly to mesodermal lineage cell types. In this way, MSCs can act in both the immune regulation of the overactivated immune responses and alveolar epithelium regeneration. The latter may be related with the rapid reversal of ground-glass opacity in the lung, which consists of a major underlying disorder in critically ill COVID-19 patients. Additionally, in this study, it was shown that MSC therapy can be quickly administrated to COVID-19 patients, upon demand. Therefore, allogeneic MSCs can be isolated, expanded at great numbers, and cryopreserved over a long time. Upon IV administration to patients, MSCs can be activated by the microenvironment stimuli, therefore no need for initial *in vitro* priming is required.

MSCs should be considered as a safe alternative therapeutic option, which may improve the COVID-19 patients' condition and result in less loss of life.

CONCLUSION

In conclusion, MSCs derived either from the WJ or BM, can exert key immunoregulatory functions towards inflammation. SARS-CoV-2 have a broad effect in patients' body, orchestrating the production of the pro-inflammatory cytokines and also inducing extensive damage to alveolar epithelial cells[83]. MSCs are currently used in a great number of clinical trials, ameliorating efficiently the immune system dysregulation[32-37]. Importantly, MSCs from the BM are characterized by lower production of the studied immunoregulatory agents compared to WJ-MSCs. However, more research is required to characterize better the immunoregulation mediated by MSCs from various tissue sources. WJ-MSCs possess more naïve cells compared to MSCs derived from adult sources. Moreover, it has been shown that MSCs derived from fetal tissues are characterized by fewer mutations and epigenetic modifications, greater proliferation, and differentiation capacity, compared to adult MSCs[22] In addition, MSCs from fetal tissues can be isolated noninvasively (compared to adult MSCs)[22]. Allogeneic MSCs are considered immune-evasive cells, as they are not expressing either the HLA-DR or stimulatory (CD40)

and co-stimulatory molecules (CD80 and CD86)[22,26]. Therefore, their infusion in human subjects should be considered safe. Furthermore, Avanzini *et al*[84] showed that MSCs are negative for ACE2 and TMPRSS2, and thus can evade the intrabody SARS-CoV-2infection. This may represent an additional benefit for the application of MSC therapy in critically ill COVID-19 patients, reversing in this way the manifestation of the current disease.

MSCs may also be utilized efficiently in the recovery phase of COVID-19 patients. COVID-19 patients are suffering from extensive lung fibrosis and multiorgan damage of variable severity. Importantly, MSCs after their IV infusion: (1) Are initially distributed widespread in the body through the systemic circulation; (2) accumulate early in the lungs and then in the spleen and liver; (3) migrate to the injury or inflamed sites; and (4) finally persist to the migrated tissue for a short time before their clearance[32]. In such a way, and due to accumulation in the lung capillary network, MSCs can give rise to differentiated cells such as endothelial and epithelial cells, which can replace the damaged tissue[32]. The latter may be translated to less required recovery time for COVID-19 patients.

Considering the results of this study, MSCs may represent an important therapeutic tool for clinicians, as they can exert drastic key immunoregulatory and tissue regenerative properties. Alongside the modern therapeutic strategies, MSCs can be considered as an advanced cellular therapy, which can be applied, besides COVID-19, to other immune-related disorders such as autoimmune diseases.

ARTICLE HIGHLIGHTS

Research background

Severe acute respiratory syndrome coronavirus 2 (SARS-CoV-2) is responsible for the coronavirus disease 2019 (COVID-19) pandemic, which was initiated in December 2019. COVID-19 is characterized by a low mortality rate (< 6%); however, this percentage is higher in elderly people and patients with underlying disorders. COVID-19 is characterized by mild to severe outcomes. Currently, several therapeutic strategies have been evaluated, such as the use of anti-viral drugs, prophylactic treatment, monoclonal antibodies, and vaccination. Advanced cellular therapies are also investigated, thus representing an additional therapeutic tool for clinicians. Mesenchymal stromal cells (MSCs), which are known for their immunoregulatory properties, may halt the induced cytokine release syndrome mediated by SARS-CoV-2, and can be considered as a potential stem cell therapy.

Research motivation

Currently, a great number of clinical trials, which include the intravenous infusion of MSCs in COVID-19 patients, are performed worldwide. Preliminary data of those studies are providing encouraging results regarding the application of MSCs for better management of COVID-19. However, the exact mechanisms by which MSCs exert their beneficial properties is not fully understand. Moreover, the majority of the currently performed studies are focusing primarily to the final outcome. In this study, an initial evaluation of the immunoregulatory properties of MSCs stimulated by COVID-19 patient serum was performed. The results of this study will provide significant insights into the role of MSCs as novel immunoregulatory players.

Research objectives

The main objective of this study was to evaluate the immunoregulatory properties of WJ and BM-MSCs, which may be used as a potential advanced cellular therapy against COVID-19. The secondary objectives were to determine any discrepancies between WJ- and BM-MSCs regarding the secretion of the immunoregulatory agents (such as cytokines and growth factors) and their ability to perform M2 phenotype switch of macrophages derived from COVID-19 patients.

Research methods

Initially, WJ and BM-MSCs were isolated, expanded, and characterized according to the criteria provided by the ISCT. Then, stimulation of MSCs with a culture medium containing COVID-19 patient serum was performed. After 48 h, the COVID-19 culture medium was removed, and extensive washes of MSCs cultures were performed. Finally, new culture medium (without FBS) was added for another 48 h. Cytokine levels (IL-1Ra, IL-6, IL-10, and IL-13), growth factor levels (TGF-β1, FGF, VEGF, and PDGF), and the immunoregulatory molecule (IDO) were measured in the conditioned medium of stimulated MSCs. Also, using molecular and protein assays, the HLA-G isoforms (HLA-G1, G5, and G7) were determined. Finally, the ability of stimulated WJ and BM-MSCs to modulate the M2 macrophage phenotype was also investigated.

Research results

WJ and BM-MSCs were successfully expanded and characterized, before the performance of the stimulation experiments. MSCs from both sources exhibited a spindle-shaped morphology and successfully expressed CD73, CD90, CD105, CD29, and CD340, but did not express CD34 or CD45.

Furthermore, MSCS were successfully differentiated to "osteocytes", "chondrocytes", and "adipocytes", and therefore fulfilled the minimum criteria as defined by the ISCT. Then, the well-defined MSCs were stimulated with culture medium containing COVID-19 patient serum. Stimulated WJ and B-MSCs expressed increased levels of IL-1Ra, IL-6, IL-10, and IL-13 ($P < 0.05$) compared to unstimulated MSCs. Also, increased levels of TGF-β1, FGF, VEGF, and PDGF were observed in stimulated MSCs (from both sources) in comparison to the control group ($P < 0.05$). Co-culturing experiments of stimulated MSCs with macrophages obtained from COVID-19 patients showed the successful switch towards the M2 phenotype. Interestingly, M2 macrophages were characterized by high levels of CD206 and CD29 and low level of CD80, while CD11b was stable expressed.

Research conclusions

MSCs were successfully activated by COVID-19 patient serum and secreted anti-inflammatory cytokines and growth factors, in response towards to the initial stimuli. It has been shown that this specific set of anti-inflammatory cytokines and growth factors can efficiently modulate the overactivated immune responses in a paracrine manner. In this way, the "cytokine storm" may be halted in critically ill COVID-19 patients. Besides that, MSCs can exert key regenerative properties and thus can reverse the lung alveolar damage. This study provided evidence regarding the beneficial application of MSCs in immune-related disorders such as COVID-19.

Research perspectives

The next step of this study will be focused on performing more experiments under both *in vitro* and *in vivo* conditions. Specifically, the RNA-seq and proteomic analysis in unstimulated and stimulated WJ and BM-MSCs will provide further evidence regarding the differentially expressed proteins. Furthermore, the infusion of stimulated MSCs in animal models exhibiting acute respiratory distress syndrome will provide significant data for their immunoregulatory properties. To this direction, well-defined MSCs may represent an additional therapeutic tool for critically ill COVID-19 patients.

FOOTNOTES

Author contributions: Mallis P designed the study, performed the experimental procedures and statistical analysis, and prepared the whole manuscript; Sarri EF, Dimou Z, and Georgiou E contributed to performing the experimental procedures; Salagianni M and Triantafyllia V contributed to performing the experimental procedures and data analysis; Michalopoulos E, Chatzistamatiou T, and Andreakos E made critical revisions related to the content of the manuscript; Stavropoulos-Giokas C and Michalopoulos E performed the final approval of the manuscript.

Institutional review board statement: The overall study has received approval from the Institution's ethical board (Reference No. 1754, January 21, 2021).

Informed consent statement: The patient's legal guardian provided informed written consent prior to study enrollment.

Conflict-of-interest statement: All authors declare no conflict of interest for the current study.

Data sharing statement: No additional data are available.

Country/Territory of origin: Greece

ORCID number: Panagiotis Mallis 0000-0001-9429-190X; Theofanis Chatzistamatiou 0000-0003-4895-0155; Zetta Dimou 0000-0003-2721-0780; Eirini-Faidra Sarri 0000-0002-5185-0879; Eleni Georgiou 0000-0001-6446-2069; Maria Salagianni 0000-0001-9821-1559; Vasiliki Triantafyllia 0000-0001-5832-4014; Evangelos Andreakos 0000-0001-5536-1661; Catherine Stavropoulos-Giokas 0000-0003-0698-6061; Efstathios Michalopoulos 0000-0002-1901-6294.

Corresponding Author's Membership in Professional Societies: European Federation of Immunogenetics, No. 2527; EFIS Young Immunologist Task Force (yEFIS); Hellenic Society of Immunology; Hellenic Society of Biochemistry and Molecular Biology.

S-Editor: Xing YX
L-Editor: Wang TQ
P-Editor: Xing YX

REFERENCES

1 **Lu H**, Stratton CW, Tang YW. Outbreak of pneumonia of unknown etiology in Wuhan, China: The mystery and the miracle. *J Med Virol* 2020; **92**: 401-402 [PMID: 31950516 DOI: 10.1002/jmv.25678]

2 **Coronaviridae Study Group of the International Committee on Taxonomy of Viruses**. The species Severe acute respiratory syndrome-related coronavirus: classifying 2019-nCoV and naming it SARS-CoV-2. *Nat Microbiol* 2020; **5**: 536-544 [PMID: 32123347 DOI: 10.1038/s41564-020-0695-z]

3 **Lai CC**, Shih TP, Ko WC, Tang HJ, Hsueh PR. Severe acute respiratory syndrome coronavirus 2 (SARS-CoV-2) and coronavirus disease-2019 (COVID-19): The epidemic and the challenges. *Int J Antimicrob Agents* 2020; **55**: 105924 [PMID: 32081636 DOI: 10.1016/j.ijantimicag.2020.105924]

4 **Nature**. Why did the world's pandemic warning system fail when COVID hit? [cited 19 October 2021]. Available from: https://www.nature.com/articles/d41586-021-00162-4

5 **Jee Y**. WHO International Health Regulations Emergency Committee for the COVID-19 outbreak. *Epidemiol Health* 2020; **42**: e2020013 [PMID: 32192278 DOI: 10.4178/epih.e2020013]

6 **Johns Hopkins University of Medicine**. COVID-19 Map. 2020 [cited 7 May 2020]. Available from: https://coronavirus.jhu.edu/map.html

7 **Gebru AA**, Birhanu T, Wendimu E, Ayalew AF, Mulat S, Abasimel HZ, Kazemi A, Tadesse BA, Gebru BA, Deriba BS, Zeleke NS, Girma AG, Munkhbat B, Yusuf QK, Luke AO, Hailu D. Global burden of COVID-19: Situational analyis and review. *Hum Antibodies* 2021; **29**: 139-148 [PMID: 32804122 DOI: 10.3233/HAB-200420]

8 **Naqvi AAT**, Fatima K, Mohammad T, Fatima U, Singh IK, Singh A, Atif SM, Hariprasad G, Hasan GM, Hassan MI. Insights into SARS-CoV-2 genome, structure, evolution, pathogenesis and therapies: Structural genomics approach. *Biochim Biophys Acta Mol Basis Dis* 2020; **1866**: 165878 [PMID: 32544429 DOI: 10.1016/j.bbadis.2020.165878]

9 **Lotfi M**, Rezaei N. SARS-CoV-2: A comprehensive review from pathogenicity of the virus to clinical consequences. *J Med Virol* 2020; **92**: 1864-1874 [PMID: 32492197 DOI: 10.1002/jmv.26123]

10 **Parasher A**. COVID-19: Current understanding of its Pathophysiology, Clinical presentation and Treatment. *Postgrad Med J* 2021; **97**: 312-320 [PMID: 32978337 DOI: 10.1136/postgradmedj-2020-138577]

11 **Lotfi M**, Hamblin MR, Rezaei N. COVID-19: Transmission, prevention, and potential therapeutic opportunities. *Clin Chim Acta* 2020; **508**: 254-266 [PMID: 32474009 DOI: 10.1016/j.cca.2020.05.044]

12 **Yesudhas D**, Srivastava A, Gromiha MM. COVID-19 outbreak: history, mechanism, transmission, structural studies and therapeutics. *Infection* 2021; **49**: 199-213 [PMID: 32886331 DOI: 10.1007/s15010-020-01516-2]

13 **Paces J**, Strizova Z, Smrz D, Cerny J. COVID-19 and the immune system. *Physiol Res* 2020; **69**: 379-388 [PMID: 32469225 DOI: 10.33549/physiolres.934492]

14 **Schmitt W**, Marchiori E. Covid-19: Round and oval areas of ground-glass opacity. *Pulmonology* 2020; **26**: 246-247 [PMID: 32411942 DOI: 10.1016/j.pulmoe.2020.04.011]

15 **Hu B**, Huang S, Yin L. The cytokine storm and COVID-19. *J Med Virol* 2021; **93**: 250-256 [PMID: 32592501 DOI: 10.1002/jmv.26232]

16 **Leng Z**, Zhu R, Hou W, Feng Y, Yang Y, Han Q, Shan G, Meng F, Du D, Wang S, Fan J, Wang W, Deng L, Shi H, Li H, Hu Z, Zhang F, Gao J, Liu H, Li X, Zhao Y, Yin K, He X, Gao Z, Wang Y, Yang B, Jin R, Stambler I, Lim LW, Su H, Moskalev A, Cano A, Chakrabarti S, Min KJ, Ellison-Hughes G, Caruso C, Jin K, Zhao RC. Transplantation of ACE2^{-} Mesenchymal Stem Cells Improves the Outcome of Patients with COVID-19 Pneumonia. *Aging Dis* 2020; **11**: 216-228 [PMID: 32257537 DOI: 10.14336/AD.2020.0228]

17 **Gavriatopoulou M**, Ntanasis-Stathopoulos I, Korompoki E, Fotiou D, Migkou M, Tzanninis IG, Psaltopoulou T, Kastritis E, Terpos E, Dimopoulos MA. Emerging treatment strategies for COVID-19 infection. *Clin Exp Med* 2021; **21**: 167-179 [PMID: 33128197 DOI: 10.1007/s10238-020-00671-y]

18 **Trivedi N**, Verma A, Kumar D. Possible treatment and strategies for COVID-19: review and assessment. *Eur Rev Med Pharmacol Sci* 2020; **24**: 12593-12608 [PMID: 33336780 DOI: 10.26355/eurrev_202012_24057]

19 **Li Z**, Niu S, Guo B, Gao T, Wang L, Wang Y, Tan Y, Wu J, Hao J. Stem cell therapy for COVID-19, ARDS and pulmonary fibrosis. *Cell Prolif* 2020; **53**: e12939 [PMID: 33098357 DOI: 10.1111/cpr.12939]

20 **Shi L**, Wang L, Xu R, Zhang C, Xie Y, Liu K, Li T, Hu W, Zhen C, Wang FS. Mesenchymal stem cell therapy for severe COVID-19. *Signal Transduct Target Ther* 2021; **6**: 339 [PMID: 34497264 DOI: 10.1038/s41392-021-00754-6]

21 **Bianco P**, Robey PG, Simmons PJ. Mesenchymal stem cells: revisiting history, concepts, and assays. *Cell Stem Cell* 2008; **2**: 313-319 [PMID: 18397751 DOI: 10.1016/j.stem.2008.03.002]

22 **Mallis P**, Michalopoulos E, Chatzistamatiou T, Giokas CS. Interplay between mesenchymal stromal cells and immune system: clinical applications in immune-related diseases. *Explor Immunol* 2021; **1**: 112-139 [DOI: 10.37349/ei.2021.00010]

23 **Dominici M**, Le Blanc K, Mueller I, Slaper-Cortenbach I, Marini F, Krause D, Deans R, Keating A, Prockop Dj, Horwitz E. Minimal criteria for defining multipotent mesenchymal stromal cells. The International Society for Cellular Therapy position statement. *Cytotherapy* 2006; **8**: 315-317 [PMID: 16923606 DOI: 10.1080/14653240600855905]

24 **Viswanathan S**, Shi Y, Galipeau J, Krampera M, Leblanc K, Martin I, Nolta J, Phinney DG, Sensebe L. Mesenchymal stem *vs* stromal cells: International Society for Cell & Gene Therapy (ISCT®) Mesenchymal Stromal Cell committee position statement on nomenclature. *Cytotherapy* 2019; **21**: 1019-1024 [PMID: 31526643 DOI: 10.1016/j.jcyt.2019.08.002]

25 **Griffin MD**, Ritter T, Mahon BP. Immunological aspects of allogeneic mesenchymal stem cell therapies. *Hum Gene Ther* 2010; **21**: 1641-1655 [PMID: 20718666 DOI: 10.1089/hum.2010.156]

26 **Machado Cde V**, Telles PD, Nascimento IL. Immunological characteristics of mesenchymal stem cells. *Rev Bras Hematol Hemoter* 2013; **35**: 62-67 [PMID: 23580887 DOI: 10.5581/1516-8484.20130017]

27 **Via AG**, Frizziero A, Oliva F. Biological properties of mesenchymal Stem Cells from different sources. *Muscles Ligaments Tendons J* 2012; **2**: 154-162 [PMID: 23738292]

28 **Chen JY**, Mou XZ, Du XC, Xiang C. Comparative analysis of biological characteristics of adult mesenchymal stem cells with different tissue origins. *Asian Pac J Trop Med* 2015; **8**: 739-746 [PMID: 26433660 DOI: 10.1016/j.apjtm.2015.07.022]

29 **Stewart MC**, Stewart AA. Mesenchymal stem cells: characteristics, sources, and mechanisms of action. *Vet Clin North Am Equine Pract* 2011; **27**: 243-261 [PMID: 21872757 DOI: 10.1016/j.cveq.2011.06.004]

30 **Yi T**, Song SU. Immunomodulatory properties of mesenchymal stem cells and their therapeutic applications. *Arch Pharm Res* 2012; **35**: 213-221 [PMID: 22370776 DOI: 10.1007/s12272-012-0202-z]

31 **Mallis P**, Michalopoulos E, Chatzistamatiou T, Stavropoulos-Giokas C. Mesenchymal stromal cells as potential immunomodulatory players in severe acute respiratory distress syndrome induced by SARS-CoV-2 infection. *World J Stem Cells* 2020; **12**: 731-751 [PMID: 32952855 DOI: 10.4252/wjsc.v12.i8.731]

32 **da Silva KN**, Gobatto ALN, Costa-Ferro ZSM, Cavalcante BRR, Caria ACI, de Aragão França LS, Nonaka CKV, de Macêdo Lima F, Lopes-Pacheco M, Rocco PRM, de Freitas Souza BS. Is there a place for mesenchymal stromal cell-based therapies in the therapeutic armamentarium against COVID-19? *Stem Cell Res Ther* 2021; **12**: 425 [PMID: 34315546 DOI: 10.1186/s13287-021-02502-7]

33 **Meng F**, Xu R, Wang S, Xu Z, Zhang C, Li Y, Yang T, Shi L, Fu J, Jiang T, Huang L, Zhao P, Yuan X, Fan X, Zhang JY, Song J, Zhang D, Jiao Y, Liu L, Zhou C, Maeurer M, Zumla A, Shi M, Wang FS. Human umbilical cord-derived mesenchymal stem cell therapy in patients with COVID-19: a phase 1 clinical trial. *Signal Transduct Target Ther*. 2020; **5**: 172 [PMID: 32855385 DOI: 10.1038/s41392-020-00286-5]

34 **Saleh M**, Vaezi AA, Aliannejad R, Sohrabpour AA, Kiaei SZF, Shadnoush M, Siavashi V, Aghaghazvini L, Khoundabi B, Abdoli S, Chahardouli B, Seyhoun I, Alijani N, Verdi J. Cell therapy in patients with COVID-19 using Wharton's jelly mesenchymal stem cells: a phase 1 clinical trial. *Stem Cell Res Ther* 2021; **12**: 410 [PMID: 34271988 DOI: 10.1186/s13287-021-02483-7]

35 **Sharma D**, Zhao F. Updates on clinical trials evaluating the regenerative potential of allogenic mesenchymal stem cells in COVID-19. *NPJ Regen Med* 2021; **6**: 37 [PMID: 34193864 DOI: 10.1038/s41536-021-00147-x]

36 **Payares-Herrera C**, Martínez-Muñoz ME, Vallhonrat IL, de Molina RM, Torres MP, Trisan A, de Diego IS, Alonso R, Zafra R, Donaire T, Sánchez R, Rubio JJ, Duarte Palomino RF, Solá CA. Double-blind, randomized, controlled, trial to assess the efficacy of allogenic mesenchymal stromal cells in patients with acute respiratory distress syndrome due to COVID-19 (COVID-AT): A structured summary of a study protocol for a randomised controlled trial. *Trials* 2021; **22**: 9 [PMID: 33407777 DOI: 10.1186/s13063-020-04964-1]

37 **Shetty AK**, Shetty PA, Zanirati G, Jin K. Further validation of the efficacy of mesenchymal stem cell infusions for reducing mortality in COVID-19 patients with ARDS. *NPJ Regen Med* 2021; **6**: 53 [PMID: 34504110 DOI: 10.1038/s41536-021-00161-z]

38 **Bühring HJ**, Battula VL, Treml S, Schewe B, Kanz L, Vogel W. Novel markers for the prospective isolation of human MSC. *Ann N Y Acad Sci* 2007; **1106**: 262-271 [PMID: 17395729 DOI: 10.1196/annals.1392.000]

39 **Kim M**, Bae YK, Um S, Kwon JH, Kim GH, Choi SJ, Oh W, Jin HJ. A Small-Sized Population of Human Umbilical Cord Blood-Derived Mesenchymal Stem Cells Shows High Stemness Properties and Therapeutic Benefit. *Stem Cells Int* 2020; **2020**: 5924983 [PMID: 32399043 DOI: 10.1155/2020/5924983]

40 **Hunt JS**, Petroff MG, McIntire RH, Ober C. HLA-G and immune tolerance in pregnancy. *FASEB J* 2005; **19**: 681-693 [PMID: 15857883 DOI: 10.1096/fj.04-2078rev]

41 **Yen BL**, Hwa HL, Hsu PJ, Chen PM, Wang LT, Jiang SS, Liu KJ, Sytwu HK, Yen ML. HLA-G Expression in Human Mesenchymal Stem Cells (MSCs) Is Related to Unique Methylation Pattern in the Proximal Promoter as well as Gene Body DNA. *Int J Mol Sci* 2020; **21** [PMID: 32708387 DOI: 10.3390/ijms21145075]

42 **Rizzo R**, Lanzoni G, Stignani M, Campioni D, Alviano F, Ricci F, Tazzari PL, Melchiorri L, Scalinci SZ, Cuneo A, Bonsi L, Lanza F, Bagnara GP, Baricordi OR. A simple method for identifying bone marrow mesenchymal stromal cells with a high immunosuppressive potential. *Cytotherapy* 2011; **13**: 523-527 [PMID: 21171826 DOI: 10.3109/14653249.2010.542460]

43 **Rizzo R**, Campioni D, Stignani M, Melchiorri L, Bagnara GP, Bonsi L, Alviano F, Lanzoni G, Moretti S, Cuneo A, Lanza F, Baricordi OR. A functional role for soluble HLA-G antigens in immune modulation mediated by mesenchymal stromal cells. Cytotherapy. 2008;10 :364-75. [PMID: 18574769 DOI: 10.1080/14653240802105299]

44 **Montespan F**, Deschaseaux F, Sensébé L, Carosella ED, Rouas-Freiss N. Osteodifferentiated mesenchymal stem cells from bone marrow and adipose tissue express HLA-G and display immunomodulatory properties in HLA-mismatched settings: implications in bone repair therapy. *J Immunol Res* 2014; **2014**: 230346 [PMID: 24877156 DOI: 10.1155/2014/230346]

45 **Mallis P**, Boulari D, Michalopoulos E, Dinou A, Spyropoulou-Vlachou M, Stavropoulos-Giokas C. Evaluation of HLA-G Expression in Multipotent Mesenchymal Stromal Cells Derived from Vitrified Wharton's Jelly Tissue. *Bioengineering (Basel)* 2018; **5** [PMID: 30388848 DOI: 10.3390/bioengineering5040095]

46 **Ding DC**, Chou HL, Chang YH, Hung WT, Liu HW, Chu TY. Characterization of HLA-G and Related Immunosuppressive Effects in Human Umbilical Cord Stroma-Derived Stem Cells. *Cell Transplant* 2016; **25**: 217-228 [PMID: 26044082 DOI: 10.3727/096368915X688182]

47 **Venkatesha SH**, Dudics S, Acharya B, Moudgil KD. Cytokine-modulating strategies and newer cytokine targets for arthritis therapy. *Int J Mol Sci* 2014; **16**: 887-906 [PMID: 25561237 DOI: 10.3390/ijms16010887]

48 **Koorts AM**, Levay PF, Becker PJ, Viljoen M. Pro- and anti-inflammatory cytokines during immune stimulation: modulation of iron status and red blood cell profile. *Mediators Inflamm* 2011; **2011**: 716301 [PMID: 21547258 DOI: 10.1155/2011/716301]

49 **Sanjabi S**, Zenewicz LA, Kamanaka M, Flavell RA. Anti-inflammatory and pro-inflammatory roles of TGF-beta, IL-10, and IL-22 in immunity and autoimmunity. *Curr Opin Pharmacol* 2009; **9**: 447-453 [PMID: 19481975 DOI: 10.1016/j.coph.2009.04.008]

50 **Arend WP**, Malyak M, Guthridge CJ, Gabay C. Interleukin-1 receptor antagonist: role in biology. *Annu Rev Immunol* 1998; **16**: 27-55 [PMID: 9597123 DOI: 10.1146/annurev.immunol.16.1.27]

51 **Dayer JM**. [Biological modulation of IL-1 activity: role and development of its natural inhibitor IL-1Ra]. *Reumatismo* 2004; **56**: 3-8 [PMID: 15201935]

52 **Bustos ML**, Huleihel L, Meyer EM, Donnenberg AD, Donnenberg VS, Sciurba JD, Mroz L, McVerry BJ, Ellis BM, Kaminski N, Rojas M. Activation of human mesenchymal stem cells impacts their therapeutic abilities in lung injury by increasing interleukin (IL)-10 and IL-1RN levels. *Stem Cells Transl Med* 2013; **2**: 884-895 [PMID: 24089414 DOI: 10.5966/sctm.2013-0033]

53 **Couper KN**, Blount DG, Riley EM. IL-10: the master regulator of immunity to infection. *J Immunol* 2008; **180**: 5771-5777 [PMID: 18424693 DOI: 10.4049/jimmunol.180.9.5771]

54 **Hershey GK**. IL-13 receptors and signaling pathways: an evolving web. *J Allergy Clin Immunol* 2003; **111**: 677-90; quiz 691 [PMID: 12704343 DOI: 10.1067/mai.2003.1333]

55 **Bhattacharjee A**, Shukla M, Yakubenko VP, Mulya A, Kundu S, Cathcart MK. IL-4 and IL-13 employ discrete signaling pathways for target gene expression in alternatively activated monocytes/macrophages. *Free Radic Biol Med* 2013; **54**: 1-16 [PMID: 23124025 DOI: 10.1016/j.freeradbiomed.2012.10.553]

56 **Martinez-Nunez RT**, Louafi F, Sanchez-Elsner T. The interleukin 13 (IL-13) pathway in human macrophages is modulated by microRNA-155 *via* direct targeting of interleukin 13 receptor alpha1 (IL13Ralpha1). *J Biol Chem* 2011; **286**: 1786-1794 [PMID: 21097505 DOI: 10.1074/jbc.M110.169367]

57 **Huang XL**, Wang YJ, Yan JW, Wan YN, Chen B, Li BZ, Yang GJ, Wang J. Role of anti-inflammatory cytokines IL-4 and IL-13 in systemic sclerosis. *Inflamm Res* 2015; **64**: 151-159 [PMID: 25725697 DOI: 10.1007/s00011-015-0806-0]

58 **Tanaka T**, Narazaki M, Kishimoto T. IL-6 in inflammation, immunity, and disease. *Cold Spring Harb Perspect Biol* 2014; **6**: a016295 [PMID: 25190079 DOI: 10.1101/cshperspect.a016295]

59 **Gabay C**. Interleukin-6 and chronic inflammation. *Arthritis Res Ther* 2006; **8** Suppl 2: S3 [PMID: 16899107 DOI: 10.1186/ar1917]

60 **Galani IE**, Rovina N, Lampropoulou V, Triantafyllia V, Manioudaki M, Pavlos E, Koukaki E, Fragkou PC, Panou V, Rapti V, Koltsida O, Mentis A, Koulouris N, Tsiodras S, Koutsoukou A, Andreakos E. Untuned antiviral immunity in COVID-19 revealed by temporal type I/III interferon patterns and flu comparison. *Nat Immunol* 2021; **22**: 32-40 [PMID: 33277638 DOI: 10.1038/s41590-020-00840-x]

61 **Xing Z**, Gauldie J, Cox G, Baumann H, Jordana M, Lei XF, Achong MK. IL-6 is an antiinflammatory cytokine required for controlling local or systemic acute inflammatory responses. *J Clin Invest* 1998; **101**: 311-320 [PMID: 9435302 DOI: 10.1172/JCI1368]

62 **Jones SA**. Directing transition from innate to acquired immunity: defining a role for IL-6. *J Immunol* 2005; **175**: 3463-3468 [PMID: 16148087 DOI: 10.4049/jimmunol.175.6.3463]

63 **Steensberg A**, Fischer CP, Keller C, Møller K, Pedersen BK. IL-6 enhances plasma IL-1ra, IL-10, and cortisol in humans. *Am J Physiol Endocrinol Metab* 2003; **285**: E433-E437 [PMID: 12857678 DOI: 10.1152/ajpendo.00074.2003]

64 **Dorronsoro A**, Lang V, Ferrin I, Fernández-Rueda J, Zabaleta L, Pérez-Ruiz E, Sepúlveda P, Trigueros C. Intracellular role of IL-6 in mesenchymal stromal cell immunosuppression and proliferation. *Sci Rep* 2020; **10**: 21853 [PMID: 33318571 DOI: 10.1038/s41598-020-78864-4]

65 **Wang G**, Cao K, Liu K, Xue Y, Roberts AI, Li F, Han Y, Rabson AB, Wang Y, Shi Y. Kynurenic acid, an IDO metabolite, controls TSG-6-mediated immunosuppression of human mesenchymal stem cells. *Cell Death Differ* 2018; **25**: 1209-1223 [PMID: 29238069 DOI: 10.1038/s41418-017-0006-2]

66 **Mellor AL**, Keskin DB, Johnson T, Chandler P, Munn DH. Cells expressing indoleamine 2,3-dioxygenase inhibit T cell responses. *J Immunol* 2002; **168**: 3771-3776 [PMID: 11937528 DOI: 10.4049/jimmunol.168.8.3771]

67 **Munn DH**, Shafizadeh E, Attwood JT, Bondarev I, Pashine A, Mellor AL. Inhibition of T cell proliferation by macrophage tryptophan catabolism. *J Exp Med* 1999; **189**: 1363-1372 [PMID: 10224276 DOI: 10.1084/jem.189.9.1363]

68 **Black AR**, Black JD. Protein kinase C signaling and cell cycle regulation. *Front Immunol* 2012; **3**: 423 [PMID: 23335926 DOI: 10.3389/fimmu.2012.00423]

69 **Jones SM**, Kazlauskas A. Connecting signaling and cell cycle progression in growth factor-stimulated cells. *Oncogene* 2000; **19**: 5558-5567 [PMID: 11114735 DOI: 10.1038/sj.onc.1203858]

70 **Jones SM**, Kazlauskas A. Growth factor-dependent signaling and cell cycle progression. *FEBS Lett* 2001; **490**: 110-116 [PMID: 11223025 DOI: 10.1016/s0014-5793(01)02113-5]

71 **Tabata Y**. Tissue regeneration based on growth factor release. *Tissue Eng* 2003; **9** Suppl 1: S5-15 [PMID: 14511467 DOI: 10.1089/10763270360696941]

72 **Kulebyakin KY**, Nimiritsky PP, Makarevich PI. Growth Factors in Regeneration and Regenerative Medicine: "the Cure and the Cause". *Front Endocrinol (Lausanne)* 2020; **11**: 384 [PMID: 32733378 DOI: 10.3389/fendo.2020.00384]

73 **Vasandan AB**, Jahnavi S, Shashank C, Prasad P, Kumar A, Prasanna SJ. Human Mesenchymal stem cells program macrophage plasticity by altering their metabolic status *via* a PGE_2-dependent mechanism. *Sci Rep* 2016; **6**: 38308 [PMID: 27910911 DOI: 10.1038/srep38308]

74 **Jin L**, Deng Z, Zhang J, Yang C, Liu J, Han W, Ye P, Si Y, Chen G. Mesenchymal stem cells promote type 2 macrophage polarization to ameliorate the myocardial injury caused by diabetic cardiomyopathy. *J Transl Med* 2019; **17**: 251 [PMID: 31382970 DOI: 10.1186/s12967-019-1999-8]

75 **Barros MH**, Hauck F, Dreyer JH, Kempkes B, Niedobitek G. Macrophage polarisation: an immunohistochemical approach for identifying M1 and M2 macrophages. *PLoS One* 2013; **8**: e80908 [PMID: 24260507 DOI: 10.1371/journal.pone.0080908]

76 **Hu JM**, Liu K, Liu JH, Jiang XL, Wang XL, Chen YZ, Li SG, Zou H, Pang LJ, Liu CX, Cui XB, Yang L, Zhao J, Shen XH, Jiang JF, Liang WH, Yuan XL, Li F. CD163 as a marker of M2 macrophage, contribute to predicte aggressiveness and prognosis of Kazakh esophageal squamous cell carcinoma. *Oncotarget* 2017; **8**: 21526-21538 [PMID: 28423526 DOI: 10.18632/oncotarget.15630]

77 **Cao X**, Yakala GK, van den Hil FE, Cochrane A, Mummery CL, Orlova VV. Differentiation and Functional Comparison of Monocytes and Macrophages from hiPSCs with Peripheral Blood Derivatives. *Stem Cell Reports* 2019; **12**: 1282-1297 [PMID: 31189095 DOI: 10.1016/j.stemcr.2019.05.003]

78 **Ammon C**, Meyer SP, Schwarzfischer L, Krause SW, Andreesen R, Kreutz M. Comparative analysis of integrin expression on monocyte-derived macrophages and monocyte-derived dendritic cells. *Immunology* 2000; **100**: 364-369 [PMID: 10929059 DOI: 10.1046/j.1365-2567.2000.00056.x]

79 **Domenis R**, Cifù A, Quaglia S, Pistis C, Moretti M, Vicario A, Parodi PC, Fabris M, Niazi KR, Soon-Shiong P, Curcio F. Pro inflammatory stimuli enhance the immunosuppressive functions of adipose mesenchymal stem cells-derived exosomes. *Sci Rep* 2018; **8**: 13325 [PMID: 30190615 DOI: 10.1038/s41598-018-31707-9]

80 **de Witte SFH**, Luk F, Sierra Parraga JM, Gargesha M, Merino A, Korevaar SS, Shankar AS, O'Flynn L, Elliman SJ, Roy D, Betjes MGH, Newsome PN, Baan CC, Hoogduijn MJ. Immunomodulation By Therapeutic Mesenchymal Stromal Cells (MSC) Is Triggered Through Phagocytosis of MSC By Monocytic Cells. *Stem Cells* 2018; **36**: 602-615 [PMID: 29341339 DOI: 10.1002/stem.2779]

81 **Weiss ARR**, Dahlke MH. Immunomodulation by Mesenchymal Stem Cells (MSCs): Mechanisms of Action of Living, Apoptotic, and Dead MSCs. *Front Immunol* 2019; **10**: 1191 [PMID: 31214172 DOI: 10.3389/fimmu.2019.01191]

82 **Shi L**, Yuan W, Wang S, Zhang C, Zhang B, Song J, Huang L, Xu Z, Fu JL, Li Y, Xu R, Li TT, Dong J, Cai J, Li G, Xie Y, Shi M, Zhang Y, Xie WF, Wang FS. Human Mesenchymal Stem Cells Treatment for severe COVID-19: 1-year follow-up results of a randomized, double blind, placebo control trial. EBioMedicine 2022; 75: 103789 [PMID: 34963099 DOI: 10.1016/j.ebiom.2021.103789]

83 **Gallelli L**, Zhang L, Wang T, Fu F. Severe Acute Lung Injury Related to COVID-19 Infection: A Review and the Possible Role for Escin. *J Clin Pharmacol* 2020; **60**: 815-825 [PMID: 32441805 DOI: 10.1002/jcph.1644]

84 **Avanzini MA**, Mura M, Percivalle E, Bastaroli F, Croce S, Valsecchi C, Lenta E, Nykjaer G, Cassaniti I, Bagnarino J, Baldanti F, Zecca M, Comoli P, Gnecchi M. Human mesenchymal stromal cells do not express ACE2 and TMPRSS2 and are not permissive to SARS-CoV-2 infection. *Stem Cells Transl Med* 2021; **10**: 636-642 [PMID: 33188579 DOI: 10.1002/sctm.20-0385]

Published by **Baishideng Publishing Group Inc**
7041 Koll Center Parkway, Suite 160, Pleasanton, CA 94566, USA
Telephone: +1-925-3991568
E-mail: bpgoffice@wjgnet.com
Help Desk: https://www.f6publishing.com/helpdesk
https://www.wjgnet.com

ISSN 1949-8454 (online)

World Journal of *Biological Chemistry*

World J Biol Chem 2022 May 27; 13(3): 66-71

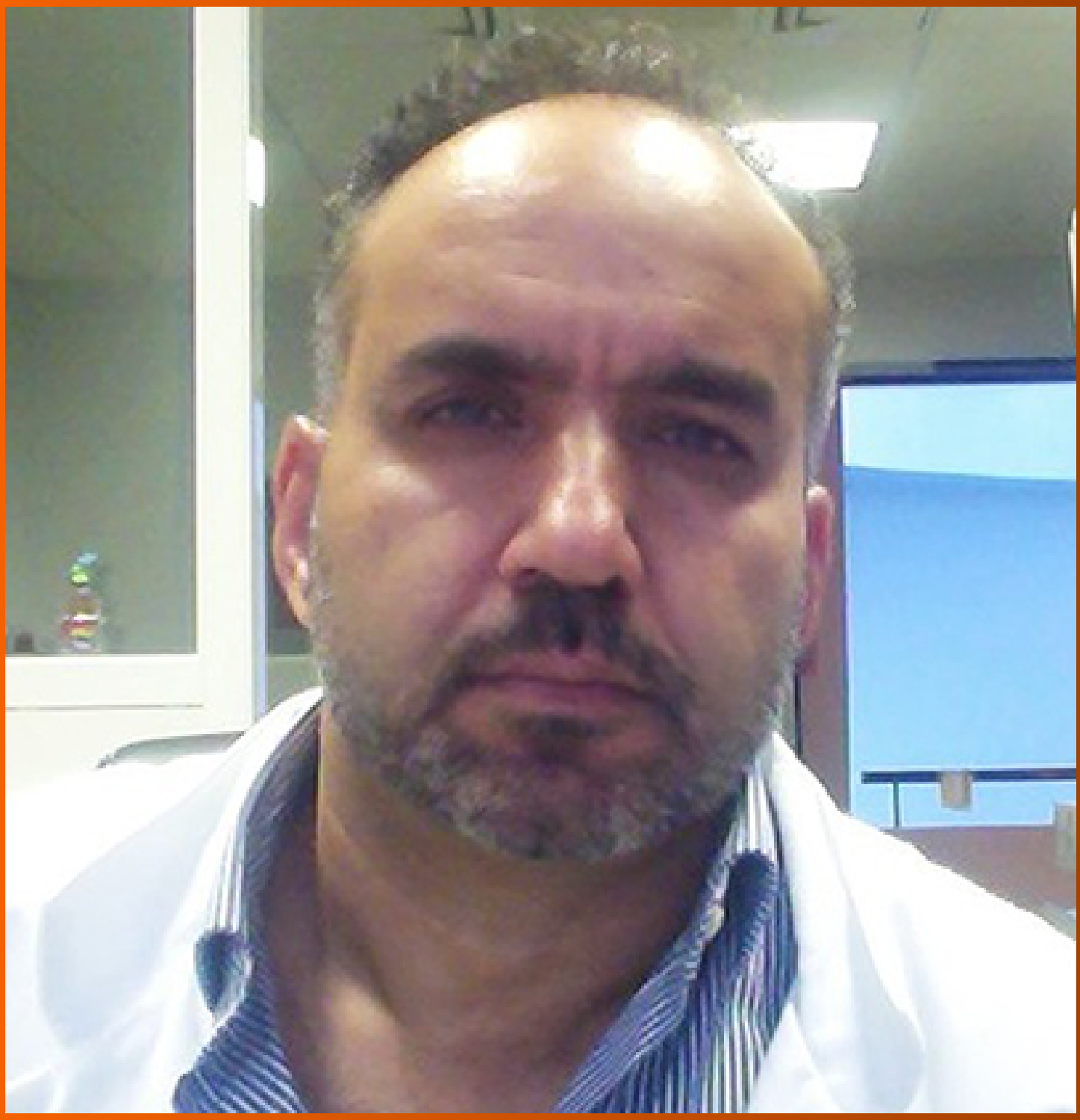

Published by Baishideng Publishing Group Inc

WJBC

World Journal of Biological Chemistry

Contents

Bimonthly Volume 13 Number 3 May 27, 2022

MINIREVIEWS

World Journal of Biological Chemistry

Bimonthly Volume 13 Number 3 May 27, 2022

Contents

ABOUT COVER

Editorial Board Member of *World Journal of Biological Chemistry*, Kamel Laghmani, PhD, Associate Professor, Research Scientist, Metabolism and Renal Physiology, Cordeliers Research Center, Paris 75006, France. Kamel.Laghmani@crc.jussieu.fr

AIMS AND SCOPE

The primary aim of the *World Journal of Biological Chemistry* (*WJBC*, *World J Biol Chem*) is to provide scholars and readers from various fields of biological chemistry a platform to publish high-quality basic and clinical research articles and communicate their research findings online.

WJBC mainly publishes articles reporting research results and findings obtained in the field of biological chemistry and covering a wide range of topics including bioenergetics, cell biology, chromosomes, developmental biology, DNA, enzymology, extracellular matrices, gene regulation, genomics, glycobiology, immunology, lipids, membrane biology, metabolism, molecular bases of disease, molecular biophysics, neurobiology, plant biology, protein structure and folding, protein synthesis and degradation, proteomics, and signal transduction.

INDEXING/ABSTRACTING

The *WJBC* is now abstracted and indexed in PubMed, PubMed Central, Reference Citation Analysis, China National Knowledge Infrastructure, China Science and Technology Journal Database, and Superstar Journals Database.

RESPONSIBLE EDITORS FOR THIS ISSUE

NAME OF JOURNAL
World Journal of Biological Chemistry

ISSN
ISSN 1949-8454 (online)

LAUNCH DATE
July 26, 2010

FREQUENCY
Bimonthly

EDITORS-IN-CHIEF
Vsevolod Gurevich, Jean-Marie Exbrayat, Chunpeng Craig Wan

EDITORIAL BOARD MEMBERS
https://www.wjgnet.com/1949-8454/editorialboard.htm

PUBLICATION DATE
May 27, 2022

INSTRUCTIONS TO AUTHORS
https://www.wjgnet.com/bpg/gerinfo/204

GUIDELINES FOR ETHICS DOCUMENTS
https://www.wjgnet.com/bpg/GerInfo/287

GUIDELINES FOR NON-NATIVE SPEAKERS OF ENGLISH
https://www.wjgnet.com/bpg/gerinfo/240

PUBLICATION ETHICS
https://www.wjgnet.com/bpg/GerInfo/288

PUBLICATION MISCONDUCT
https://www.wjgnet.com/bpg/gerinfo/208

ARTICLE PROCESSING CHARGE
https://www.wjgnet.com/bpg/gerinfo/242

STEPS FOR SUBMITTING MANUSCRIPTS
https://www.wjgnet.com/bpg/GerInfo/239

ONLINE SUBMISSION
https://www.f6publishing.com

World Journal of Biological Chemistry

Submit a Manuscript: https://www.f6publishing.com

World J Biol Chem 2022 May 27; 13(3): 66-71

DOI: 10.4331/wjbc.v13.i3.66

ISSN 1949-8454 (online)

MINIREVIEWS

Progesterone in gender-affirming therapy of trans women

Charalampos Milionis, Ioannis Ilias, Eftychia Koukkou

Specialty type: Endocrinology and metabolism

Provenance and peer review: Invited article; Externally peer reviewed.

Peer-review model: Single blind

Peer-review report's scientific quality classification

Grade A (Excellent): 0
Grade B (Very good): B
Grade C (Good): 0
Grade D (Fair): D
Grade E (Poor): 0

P-Reviewer: Bansal C, India; Cazzato G, Italy

Received: December 20, 2021
Peer-review started: December 20, 2021
First decision: February 21, 2022
Revised: February 28, 2022
Accepted: April 22, 2022
Article in press: April 22, 2022
Published online: May 27, 2022

Charalampos Milionis, Ioannis Ilias, Eftychia Koukkou, Department of Endocrinology, Diabetes and Metabolism, Elena Venizelou Hospital, Athens GR-11521, Greece

Corresponding author: Ioannis Ilias, MD, PhD, Consultant Physician-Scientist, Department of Endocrinology, Diabetes and Metabolism, Elena Venizelou Hospital, 2, Elena Venizelou Square, Athens GR-11521, Greece. iiliasmd@yahoo.com

Abstract

Progesterone is an endogenous steroid hormone with an important role for the physiology of the female reproductive system and the mammary gland. It has additional significant actions in other tissues, such as the cardiovascular system, the central nervous system, and bones. The present article explores potential clinical implications from the addition of bioidentical progesterone to gender-affirming treatment of trans women. For this purpose, it provides an overview of the physiological action of progesterone in target tissues and speculates on possible benefits for gender transitioning. Progesterone is expected to exert moderate anti-androgen action through suppression of the hypothalamic-pituitary-gonadal axis and inhibition of the conversion of testosterone to dihydrotestosterone. It may also contribute to breast maturation. In the long-term, progesterone could prevent bone loss and protect cardiovascular health. The potential benefits are mainly inferred by extrapolating evidence from biological actions in cisgender women and medical assumptions and hence, clinicians need to be cautious when applying these data into practice. Further research is needed to ascertain the efficacy and safety of progesterone in current hormonal regimens.

Key Words: Progesterone; Transgender persons; Breast; Human; Gender dysphoria

Core Tip: The addition of bioidentical progesterone to the gender-affirming treatment of trans women may be beneficial in many ways. However, since relevant studies are lacking, further research is needed.

Citation: Milionis C, Ilias I, Koukkou E. Progesterone in gender-affirming therapy of trans women. *World J Biol Chem* 2022; 13(3): 66-71
URL: https://www.wjgnet.com/1949-8454/full/v13/i3/66.htm
DOI: https://dx.doi.org/10.4331/wjbc.v13.i3.66

INTRODUCTION

Physiology of progesterone

Progesterone (P4) is an endogenous hormone with an important role for the physiology of the reproductive system of cisgender females. It is the major member of a class of steroid hormones (progestogens) that bind to and activate the progesterone receptor (PR). All steroid hormones consist of a common structure of a polycyclic (four-ring) complex which derives from the cholesterol molecule. The biosynthesis of steroid hormones follows the same pathways in all steroidogenic organs (the ovary, testis, adrenal cortex, and placenta), but the type and amount of the produced hormones vary depending on the presence and expression of specific enzymes in each tissue[1].

Like all steroid hormones in mammals, P4 is synthesised from pregnenolone. The conversion of pregnenolone to P4 is catalysed by the type 2 3β-hydroxysteroid dehydrogenase/ Δ 5- Δ 4 isomerase through modification of the 3β-hydroxyl group to a ketone and isomerisation of the C-5 to C-4 double bond[2]. P4 is a potent agonist of the nuclear PR. Ligand binding induces a signalling pathway which results in activation of genes containing P4 response elements. However, P4 also acts through non-classical signalling pathways, often mediated by non-genomic processes[3].

P4 is mainly secreted by the ovary after ovulation and by the placenta during pregnancy. Before ovulation, ovarian granulosa cells in the follicle synthesise and secrete oestrogens. After the rupture of the follicle and the release of the ovum, these granulosa cells mature to form the corpus luteum. The latter produces P4 (and oestrogens) in the luteal (secretory) phase of the cycle. If fertilisation does not occur, the corpus luteum will further enlarge for the next 10-12 days and then it will regress and discontinue the release of P4 (and oestrogens). In case of fertilisation, the corpus luteum will continue to grow and function for the first 2-3 months of pregnancy. Afterwards, it will gradually regress as the placenta assumes the role of hormonal biosynthesis. The release of P4 from the corpus luteum is influenced by a number of hormones. Luteinising hormone (LH) exerts the primary action, whilst follicle stimulation hormone (FSH), prolactin, prostaglandins, activin, follistatin, and beta-adrenergic agents play a secondary role in the control of P4 production[4].

Reproductive function is inextricably related to P4. The latter is involved in the endometrial transition from the proliferative to the secretory phase during the menstrual cycle, the facilitation of the implantation of the blastocyst, and the maintenance of pregnancy. However, P4 has additional significant actions in other tissues, besides the reproductive system, including the mammary gland, the cardiovascular system, the central nervous system, and bones[5]. The actions of oestradiol (E2) and P4 are well balanced and coordinated in order to result in a healthy physiology[6]. Table 1 presents the main roles of P4.

P4 is the only natural progestogen that is used therapeutically. Micronised crystals of P4 allow for a better gastrointestinal absorption. Progestins are a variety of synthetic progestogens with a different potency and pharmacokinetics from P4. Although these compounds mimic some of the effects of P4, they may have different actions on PR at the same target tissues[7]. The present article explores the effects of bioidentical P4 on gender-affirming therapy of transgender females. Nevertheless, hypotheses about progestins can be drawn according to their degree of P4-like effects.

Gender-affirming hormonal therapy

Transgender individuals are persons whose gender identity is compatible with the opposite sex or with a variance that falls outside the classical binary definition of male/female. In particular, transgender females (also called trans women) are individuals who self-identify as females but were assigned male gender at birth. Gender-affirming therapy in trans women aims at inducing physical changes towards feminine biologic characteristics[8]. Treatment with E2 (mainly oral or transdermal) and anti-androgens (usually cyproterone acetate and less frequently spironolactone) or gonadotrophin-releasing hormone (GnRH) agonist is expected to result in redistribution of body fat and decrease in muscle mass, softening of the skin, breast development, and decreased terminal hair growth accompanied by decreased sexual desire and erections, testicular atrophy, and reduced sperm production. These changes evolve over a period starting from the first months of the administration until more than three years later. The relevant possible risks include thromboembolic disease, enlargement of an underlying prolactinoma, breast cancer, coronary artery and cerebrovascular disease, cholelithiasis, and hypertriglyceridaemia[9].

P4 AS A COMPONENT OF FEMINISING TREATMENT

Hormonal treatment in transgender persons aims at suppressing the secretion of the endogenous sex hormones and replacing them with the hormones of the desired gender. The therapeutic interventions need to maintain sex hormone blood levels within the respective normal range of the affirmed gender [10]. As P4 constitutes an important hormone in cisgender females, it is hypothesised that a daily or cyclic treatment with oral P4 could be a beneficial component of gender-affirming therapy of trans women, in addition to E2 and anti-androgen regimens. According to this perspective, the importance of P4 for transgender health is expected to be due to metabolic and anti-androgen effects. However, the

Table 1 Known physiological actions of progesterone

Uterine endometrium	Inhibition of proliferation and differentiation of the endometrium into a secretory organ for the potential implantation of a fertilised ovum
Uterine cervix	Inhibition of cervical mucus secretion
Breast tissue	Ductal side branching and lobulo-alveolar development; increase of the areolar size
Skeleton	Bone formation (in conjunction with oestradiol)
Arterial endothelium	Amplification of the actions of endogenous nitric oxide
Brain	Mitigation of central stress hormone responses; induction of deep sleep

relevant potential benefits are mainly inferred by extrapolating evidence from biological actions in cisgender women and thus, clinicians need to be cautious when applying these data into practice[11].

Anti-androgen effects

The direct anti-androgen action of P4 on the androgen receptors (AR) appears to be minimal[12]. Nevertheless, the treatment with exogenous P4 at pharmacological dosages is expected to exert negative feedback on the hypothalamic-pituitary-gonadal axis[13] and hence generate an indirect anti-androgen activity. According to this mechanism, the suppression of LH will eventually lead to a reduction of the synthesis and secretion of gonadal testosterone (Te) by Leydig cells[14]. In addition, exogenous P4 may possibly enhance the impairment of spermatogenesis in Sertoli cells by decreasing intratesticular Te and suppressing FSH[15]. Therefore, the administration of sufficient doses of P4 in daily regimens, rather than cyclically, may enhance the anti-androgen action of gender-affirming therapy in trans women and could be clinically useful until orchiectomy is performed.

The 5-alpha-reductase enzyme family consists of three isoenzymes which catalyse the conversion of Te to 5-alpha-dihydrotestosterone (DHT) by promoting an irreversible break of the double bond between carbons 4 and 5 of the Te molecule with nicotinamide adenine dinucleotide phosphate (NADPH) acting as a cofactor[16]. DHT has a several-fold more potent androgen action in comparison with Te. As 5-alpha-reductase is highly expressed in the skin, hair follicles, and prostate gland, DHT is mainly involved in facial, axillary, pubic, and body hair growth, as well as scalp pattern hair loss and prostate enlargement in males[17]. P4 is an inhibitor of 5-alpha-reductase and as such, it might mitigate masculinising effects of DHT in target tissues. However, the inhibition of 5-alpha-reductase by P4 is rather weak and thus can only be demonstrated at supraphysiological concentrations[18].

Breast maturation and enlargement

P4 is substantially involved in breast tissue development. Indeed, it appears to have a potentiating or accelerating role in oestrogen-mediated mammary ductal development and alveolar expansion during puberty. Moreover, P4 enhances the actions of oestrogens on proliferation of the epithelial and stromal compartments in the adult mammary gland[19]. During pregnancy, P4 acts synergistically with prolactin in order to promote lobulo-alveolar development of the mammary gland. The goal is to prepare the breast for lactation after parturition[20]. Oestrogens enhance the action of P4 on breast tissue[21]. Therefore, treatment of transgender females with exogenous oestrogen and P4 may be beneficial for glandular development. However, it should be noted that although oestrogens are undisputed breast tissue mitogens, the role of P4 action in breast cancer is unclear[22] and any therapeutic intervention should be followed with caution.

Bone health

It is established that the role of oestrogens is critical for skeletal homeostasis as they regulate bone remodelling, partly through the osteoprotegerin/receptor activator of nuclear factor kappa-B ligand (RANKL) system. Furthermore, oestrogen deficiency upregulates bone turnover and causes bone loss [23]. In contrast, the actions of P4 on the promotion of bone health are largely unrecognised. P4 likely acts complementarily with oestrogens in bone formation and hence, it may have an active role in maintaining women's bone health in osteoporosis prevention. *In vitro* studies of human osteoblasts indicate that it enhances osteoblast proliferation and promotes their maturation and differentiation[24]. Therefore, micronised P4 in conjunction with E2 may be effective in prevention of osteoporosis in trans women. However, further research is needed to confirm the contribution of P4 to clinically significant bone formation.

Cardiovascular protection

The protective functions of P4 in the cardiovascular system have not been extensively studied. Existing evidence suggests that P4 decreases vasoconstriction and causes natriuresis. In addition, it promotes endothelial nitric oxide synthase activity and calcium influx in vascular endothelial and smooth muscle

cells, respectively, and hence, it lowers blood pressure[25]. P4 is expected to have a neutral effect on blood lipid levels[26]. The vascular actions of P4 may assist in preventing cardiovascular disease in trans women. However, the cardiovascular benefits of P4 have not been clinically confirmed and thus claims about potential cardiovascular protection are controversial[27]. Moreover, some synthetic progestins may have a negative effect on cardiovascular health with regard to lipid changes, atheroma development, or vasomotion[28].

DISSCUSSION

The number of individuals, with gender dysphoria, who seek cross-sex treatment, has increased over the past years[29]. The administration of oestrogen (combined with GnRH agonist or anti-androgen in case of present testes) is the mainstay of hormonal regimens in transgender females. However, the clinical results of gender transitioning are sometimes less than satisfactory and additional therapy may be required. P4 is a natural endogenous steroid hormone with multiple important physiologic effects, including anti-androgen activity, mammary gland growth, reduction of bone resorption, and anti-mineralocorticoid action[30]. Therefore, pairing bioidentical P4 with oestrogen could be a novel approach to gender-affirming treatment. P4 is not typically recommended in the hormonal treatment of trans women because of a lack of thorough evidence concerning its safety and efficacy[31,32]. The advocacy of the use of bioidentical P4 as part of the feminising treatment is currently anecdotal and is driven by the prospect of mirroring, in trans women, the hormonal status of cisgender females.

The anti-androgen effect of P4 consists of suppression of the hypothalamic-pituitary-gonadal axis and inhibition of the conversion of Te to DHT. As discussed earlier, feminising treatment includes either a GnRH agonist to suppress gonadal Te levels or an anti-androgen to block the AR. Nonetheless, GnRH analogues are expensive pharmaceutical products, whilst maximum AR blockade with anti-androgens (such as cyproterone acetate and spironolactone) has potential serious side effects. The addition of micronised P4 could theoretically lead to a considerable reduction of the needed dosage of GnRH agonist or anti-androgen for gender transitioning until the testes are surgically excised.

Breast development is a major goal of cross-sex hormonal treatment of trans women. However, transgender females most usually do not achieve the same shape and level of breast enlargement compared with their cisgender counterparts[33]. At present, mammoplasty is the only option for constructing a fully developed female breast in trans women[34]. The administration of P4 on top of usual oestrogen treatment could hypothetically promote breast development in transgender females. However, there have been no reliable studies of the role of exogenous P4 in breast development in trans women so far[35].

CONCLUSION

In conclusion, oral micronised P4 is identical to the natural hormone and could be added to E2 in gender-affirming treatment of trans women. Indeed, P4 may aid anti-androgen action through two main pathways: (1) Suppression of the hypothalamic-pituitary-testicular axis; and (2) inhibition of Te conversion to DHT. Furthermore, it may promote physiological feminine breast maturation. In the long-term, P4 could also prevent bone loss and protect cardiovascular function. Nevertheless, the clinical usefulness of P4 in trans women's health is currently based mainly on clinical assumptions emerging from physiologic mechanisms, observational data, and daily experience. Further nonclinical and clinical trials are necessary to investigate the efficacy and safety of the addition of P4 to current hormonal treatment regimens. Then, commissioned systematic review on the available data could provide relevant clinical guidance.

FOOTNOTES

Author contributions: Milionis C and Ilias I performed the majority of the writing and prepared the table; Ilias I and Koukkou E provided input in writing the paper; Koukkou E coordinated the writing of the paper.

Conflict-of-interest statement: The authors state that they have no conflict of interest to report.

Country/Territory of origin: Greece

ORCID number: Charalampos Milionis 0000-0003-2442-3772; Ioannis Ilias 0000-0001-5718-7441; Eftychia Koukkou 0000-0002-1433-3151.

S-Editor: Liu JH
L-Editor: Wang TQ
P-Editor: Liu JH

REFERENCES

1 **Miller WL**, Auchus RJ. The molecular biology, biochemistry, and physiology of human steroidogenesis and its disorders. *Endocr Rev* 2011; **32**: 81-151 [PMID: 21051590 DOI: 10.1210/er.2010-0013]
2 **MacKenzie SM**, van Kralingen JC, Davies E. Regulation of Aldosterone Secretion. *Vitam Horm* 2019; **109**: 241-263 [PMID: 30678858 DOI: 10.1016/bs.vh.2018.07.001]
3 **Garg D**, Ng SSM, Baig KM, Driggers P, Segars J. Progesterone-Mediated Non-Classical Signaling. *Trends Endocrinol Metab* 2017; **28**: 656-668 [PMID: 28651856 DOI: 10.1016/j.tem.2017.05.006]
4 **Graham JD**, Clarke CL. Physiological action of progesterone in target tissues. *Endocr Rev* 1997; **18**: 502-519 [PMID: 9267762 DOI: 10.1210/edrv.18.4.0308]
5 **Taraborrelli S**. Physiology, production and action of progesterone. *Acta Obstet Gynecol Scand* 2015; **94** Suppl 161: 8-16 [PMID: 26358238 DOI: 10.1111/aogs.12771]
6 **Prior JC**. Women's reproductive system as balanced estradiol and progesterone actions—A revolutionary, paradigm-shifting concept in women's health. Drug Discovery Today: Disease Models. 2020; 32: 31-40 [DOI: 10.1016/j.ddmod.2020.11.005]
7 **Asi N**, Mohammed K, Haydour Q, Gionfriddo MR, Vargas OL, Prokop LJ, Faubion SS, Murad MH. Progesterone vs. synthetic progestins and the risk of breast cancer: a systematic review and meta-analysis. *Syst Rev* 2016; **5**: 121 [PMID: 27456847 DOI: 10.1186/s13643-016-0294-5]
8 **Glintborg D**, T'Sjoen G, Ravn P, Andersen MS. MANAGEMENT OF ENDOCRINE DISEASE: Optimal feminizing hormone treatment in transgender people. *Eur J Endocrinol* 2021; **185**: R49-R63 [PMID: 34081614 DOI: 10.1530/EJE-21-0059]
9 **Hembree WC**, Cohen-Kettenis PT, Gooren L, Hannema SE, Meyer WJ, Murad MH, Rosenthal SM, Safer JD, Tangpricha V, T'Sjoen GG. Endocrine Treatment of Gender-Dysphoric/Gender-Incongruent Persons: An Endocrine Society Clinical Practice Guideline. *J Clin Endocrinol Metab* 2017; **102**: 3869-3903 [PMID: 28945902 DOI: 10.1210/jc.2017-01658]
10 **T'Sjoen G**, Arcelus J, Gooren L, Klink DT, Tangpricha V. Endocrinology of Transgender Medicine. *Endocr Rev* 2019; **40**: 97-117 [PMID: 30307546 DOI: 10.1210/er.2018-00011]
11 **Prior JC**. Progesterone Is Important for Transgender Women's Therapy-Applying Evidence for the Benefits of Progesterone in Ciswomen. *J Clin Endocrinol Metab* 2019; **104**: 1181-1186 [PMID: 30608551 DOI: 10.1210/jc.2018-01777]
12 **Yeh YT**, Chang CW, Wei RJ, Wang SN. Progesterone and related compounds in hepatocellular carcinoma: basic and clinical aspects. *Biomed Res Int* 2013; **2013**: 290575 [PMID: 23484104 DOI: 10.1155/2013/290575]
13 **Nieschlag E**, Zitzmann M, Kamischke A. Use of progestins in male contraception. *Steroids* 2003; **68**: 965-972 [PMID: 14667989 DOI: 10.1016/s0039-128x(03)00135-1]
14 **Brady BM**, Anderson RA, Kinniburgh D, Baird DT. Demonstration of progesterone receptor-mediated gonadotrophin suppression in the human male. *Clin Endocrinol (Oxf)* 2003; **58**: 506-512 [PMID: 12641635 DOI: 10.1046/j.1365-2265.2003.01751.x]
15 **McLachlan RI**, Robertson DM, Pruysers E, Ugoni A, Matsumoto AM, Anawalt BD, Bremner WJ, Meriggiola C. Relationship between serum gonadotropins and spermatogenic suppression in men undergoing steroidal contraceptive treatment. *J Clin Endocrinol Metab* 2004; **89**: 142-149 [PMID: 14715841 DOI: 10.1210/jc.2003-030616]
16 **Azzouni F**, Godoy A, Li Y, Mohler J. The 5 alpha-reductase isozyme family: a review of basic biology and their role in human diseases. *Adv Urol* 2012; **2012**: 530121 [PMID: 22235201 DOI: 10.1155/2012/530121]
17 **Marchetti PM**, Barth JH. Clinical biochemistry of dihydrotestosterone. *Ann Clin Biochem* 2013; **50**: 95-107 [PMID: 23431485 DOI: 10.1258/acb.2012.012159]
18 **Cassidenti DL**, Paulson RJ, Serafini P, Stanczyk FZ, Lobo RA. Effects of sex steroids on skin 5 alpha-reductase activity in vitro. *Obstet Gynecol* 1991; **78**: 103-107 [PMID: 1828548]
19 **Diep CH**, Daniel AR, Mauro LJ, Knutson TP, Lange CA. Progesterone action in breast, uterine, and ovarian cancers. *J Mol Endocrinol* 2015; **54**: R31-R53 [PMID: 25587053 DOI: 10.1530/JME-14-0252]
20 **Oakes SR**, Hilton HN, Ormandy CJ. The alveolar switch: coordinating the proliferative cues and cell fate decisions that drive the formation of lobuloalveoli from ductal epithelium. *Breast Cancer Res* 2006; **8**: 207 [PMID: 16677418 DOI: 10.1186/bcr1411]
21 **Brisken C**. Progesterone signalling in breast cancer: a neglected hormone coming into the limelight. *Nat Rev Cancer* 2013; **13**: 385-396 [PMID: 23702927 DOI: 10.1038/nrc3518]
22 **Lange CA**, Yee D. Progesterone and breast cancer. *Womens Health (Lond)* 2008; **4**: 151-162 [PMID: 19072517 DOI: 10.2217/17455057.4.2.151]
23 **Streicher C**, Heyny A, Andrukhova O, Haigl B, Slavic S, Schüler C, Kollmann K, Kantner I, Sexl V, Kleiter M, Hofbauer LC, Kostenuik PJ, Erben RG. Estrogen Regulates Bone Turnover by Targeting RANKL Expression in Bone Lining Cells. *Sci Rep* 2017; **7**: 6460 [PMID: 28744019 DOI: 10.1038/s41598-017-06614-0]

24 **Seifert-Klauss V**, Prior JC. Progesterone and bone: actions promoting bone health in women. *J Osteoporos* 2010; **2010**: 845180 [PMID: 21052538 DOI: 10.4061/2010/845180]

25 **Thomas P**, Pang Y. Protective actions of progesterone in the cardiovascular system: potential role of membrane progesterone receptors (mPRs) in mediating rapid effects. *Steroids* 2013; **78**: 583-588 [PMID: 23357432 DOI: 10.1016/j.steroids.2013.01.003]

26 **Jiang Y**, Tian W. The effects of progesterones on blood lipids in hormone replacement therapy. *Lipids Health Dis* 2017; **16**: 219 [PMID: 29157280 DOI: 10.1186/s12944-017-0612-5]

27 **Medina RA**, Aranda E, Verdugo C, Kato S, Owen GI. The action of ovarian hormones in cardiovascular disease. *Biol Res* 2003; **36**: 325-341 [PMID: 14631866 DOI: 10.4067/s0716-97602003000300005]

28 **Sitruk-Ware R**. Progestins and cardiovascular risk markers. *Steroids* 2000; **65**: 651-658 [PMID: 11108872 DOI: 10.1016/s0039-128x(00)00174-4]

29 **Zucker KJ**. Epidemiology of gender dysphoria and transgender identity. *Sex Health* 2017; **14**: 404-411 [PMID: 28838353 DOI: 10.1071/SH17067]

30 **Fedotcheva TA**. Clinical Use of Progestins and Their Mechanisms of Action: Present and Future (Review). *Sovrem Tekhnologii Med* 2021; **13**: 93-106 [PMID: 34513071 DOI: 10.17691/stm2021.13.1.11]

31 **Abramowitz J**, Tangpricha V. Hormonal Management for Transfeminine Individuals. *Clin Plast Surg* 2018; **45**: 313-317 [PMID: 29908618 DOI: 10.1016/j.cps.2018.03.003]

32 **Tangpricha V**, Hannema SE, Irwig MS, Meyer WJ 3rd, Safer JD, Hembree WC. 2017 american association of clinical endocrinologists/endocrine society update on transgender medicine: Case discussions. *Endocr Pract* 2017; **23**: 1430-1436 [PMID: 29320643 DOI: 10.4158/GL-2017-0115]

33 **de Blok CJM**, Dijkman BAM, Wiepjes CM, Staphorsius AS, Timmermans FW, Smit JM, Dreijerink KMA, den Heijer M. Sustained Breast Development and Breast Anthropometric Changes in 3 Years of Gender-Affirming Hormone Treatment. *J Clin Endocrinol Metab* 2021; **106**: e782-e790 [PMID: 33206172 DOI: 10.1210/clinem/dgaa841]

34 **Fakin RM**, Zimmermann S, Kaye K, Lunger L, Weinforth G, Giovanoli P. Long-Term Outcomes in Breast Augmentation in Trans-Women: A 20-Year Experience. *Aesthet Surg J* 2019; **39**: 381-390 [PMID: 29901707 DOI: 10.1093/asj/sjy143]

35 **Wierckx K**, Gooren L, T'Sjoen G. Clinical review: Breast development in trans women receiving cross-sex hormones. *J Sex Med* 2014; **11**: 1240-1247 [PMID: 24618412 DOI: 10.1111/jsm.12487]

Published by **Baishideng Publishing Group Inc**
7041 Koll Center Parkway, Suite 160, Pleasanton, CA 94566, USA
Telephone: +1-925-3991568
E-mail: bpgoffice@wjgnet.com
Help Desk: https://www.f6publishing.com/helpdesk
https://www.wjgnet.com

ISSN 1949-8454 (online)

World Journal of *Biological Chemistry*

World J Biol Chem 2022 September 27; 13(4): 72-82

Published by Baishideng Publishing Group Inc

World Journal of Biological Chemistry

Contents

Bimonthly Volume 13 Number 4 September 27, 2022

ORIGINAL ARTICLE

Basic Study

World Journal of Biological Chemistry

Bimonthly Volume 13 Number 4 September 27, 2022

Contents

ABOUT COVER

Editorial Board Member of *World Journal of Biological Chemistry*, Saeed Mohammadi, PhD, Assistant Professor, Stem Cell Research Center, Golestan University of Medical Sciences, Gorgan 4916698719, Golestan, Iran. s.mohammadi@goums.ac.ir

AIMS AND SCOPE

The primary aim of the *World Journal of Biological Chemistry* (*WJBC*, *World J Biol Chem*) is to provide scholars and readers from various fields of biological chemistry a platform to publish high-quality basic and clinical research articles and communicate their research findings online.

WJBC mainly publishes articles reporting research results and findings obtained in the field of biological chemistry and covering a wide range of topics including bioenergetics, cell biology, chromosomes, developmental biology, DNA, enzymology, extracellular matrices, gene regulation, genomics, glycobiology, immunology, lipids, membrane biology, metabolism, molecular bases of disease, molecular biophysics, neurobiology, plant biology, protein structure and folding, protein synthesis and degradation, proteomics, and signal transduction.

INDEXING/ABSTRACTING

The *WJBC* is now abstracted and indexed in PubMed, PubMed Central, Reference Citation Analysis, China National Knowledge Infrastructure, China Science and Technology Journal Database, and Superstar Journals Database.

RESPONSIBLE EDITORS FOR THIS ISSUE

NAME OF JOURNAL
World Journal of Biological Chemistry

ISSN
ISSN 1949-8454 (online)

LAUNCH DATE
July 26, 2010

FREQUENCY
Bimonthly

EDITORS-IN-CHIEF
Vsevolod Gurevich, Jean-Marie Exbrayat, Chunpeng Craig Wan

EDITORIAL BOARD MEMBERS
https://www.wjgnet.com/1949-8454/editorialboard.htm

PUBLICATION DATE
September 27, 2022

INSTRUCTIONS TO AUTHORS
https://www.wjgnet.com/bpg/gerinfo/204

GUIDELINES FOR ETHICS DOCUMENTS
https://www.wjgnet.com/bpg/GerInfo/287

GUIDELINES FOR NON-NATIVE SPEAKERS OF ENGLISH
https://www.wjgnet.com/bpg/gerinfo/240

PUBLICATION ETHICS
https://www.wjgnet.com/bpg/GerInfo/288

PUBLICATION MISCONDUCT
https://www.wjgnet.com/bpg/gerinfo/208

ARTICLE PROCESSING CHARGE
https://www.wjgnet.com/bpg/gerinfo/242

STEPS FOR SUBMITTING MANUSCRIPTS
https://www.wjgnet.com/bpg/GerInfo/239

ONLINE SUBMISSION
https://www.f6publishing.com

World Journal of Biological Chemistry

Submit a Manuscript: https://www.f6publishing.com

World J Biol Chem 2022 September 27; 13(4): 72-82

DOI: 10.4331/wjbc.v13.i4.72

ISSN 1949-8454 (online)

ORIGINAL ARTICLE

Basic Study

Profiles of interferon-gamma and interleukin-2 in patients after allogeneic hematopoietic stem cell transplantation

Malwina Rybicka-Ramos, Mirosław Markiewicz, Aleksandra Suszka-Świtek, Ryszard Wiaderkiewicz, Sylwia Mizia, Monika Dzierżak-Mietła, Krzysztof Białas

Specialty type: Hematology

Provenance and peer review: Invited article; Externally peer reviewed.

Peer-review model: Single blind

Peer-review report's scientific quality classification

Grade A (Excellent): 0
Grade B (Very good): 0
Grade C (Good): C
Grade D (Fair): D
Grade E (Poor): E, E

P-Reviewer: Fru PN, South Africa; Jabbarpour Z, Iran

Received: March 8, 2022
Peer-review started: March 8, 2022
First decision: April 25, 2022
Revised: May 11, 2022
Accepted: September 21, 2022
Article in press: September 21, 2022
Published online: September 27, 2022

Malwina Rybicka-Ramos, Department of Hematology, Specialist Hospital No. 1 in Bytom, Bytom 41-902, Poland

Mirosław Markiewicz, Department of Hematology, University of Rzeszow, College of Medical Sciences, Institute of Medical Sciences, Rzeszów 35-315, Poland

Aleksandra Suszka-Świtek, Ryszard Wiaderkiewicz, Department of Histology and Embryology, School of Medicine in Katowice, Medical University of Silesia, Katowice 40-752, Poland

Sylwia Mizia, Department of Population Health, Division of Epidemiology and Health Education, Wroclaw Medical University, Wrocław 51-618, Poland

Monika Dzierżak-Mietła, Department of Bone Marrow Transplantation and Hematooncology, Maria Sklodowska-Curie National Research Institute of Oncology, Gliwice 44-102, Poland

Krzysztof Białas, Department of Hematology and Bone Marrow Transplantation, SPSK-M Hospital, Katowice 40-027, Poland

Corresponding author: Malwina Rybicka-Ramos, MD, PhD, Doctor, Department of Hematology, Specialist Hospital No. 1 in Bytom, 7 Zeromskiego Street, Bytom 41-902, Poland. malwina.rybicka@gmail.com

Abstract

BACKGROUND

Allogeneic hematopoietic stem cell transplantation (allo-HSCT) may be related to the occurrence of complications, including graft-versus-host disease (GvHD) and infections. The pathogenesis of acute GvHD is connected with T lymphocytes, which identify alloantigens on host's antigen-presenting cells, activate production of interferon-gamma (IFN-gamma) and interleukin-2 (IL-2), and act on the immune effector cells and damage tissues and organs.

AIM

The aim of the study was to investigate and distinguish serum concentration profiles of IFN-gamma and IL-2 within a 30-d period after allo-HSCT.

METHODS

We enrolled 62 patients, *i.e.*, 30 (48%) male and 32 (52%) female subjects [median

age 49.5 (19-68) years], after allo-HSCT from siblings (n = 12) or unrelated donors (n = 50) due to acute myeloid leukemia with myeloablative conditioning (n = 26; 42%) and with non-myeloablative conditioning (n = 36; 58%). All patients were given standard immunosuppressive therapy with cyclosporin-A and methotrexate and pre-transplant antithymocyte globulin in the unrelated setting. Blood samples were collected pre-transplant before and after (on day -1) the conditioning therapy and on days +2,+4, +6, +10, +20, and +30 after allo-HSCT. Serum levels of IL-2 and IFN-gamma were determined using ELISA.

RESULTS

Patients were divided into four groups depending on the presence of acute GvHD and clinical manifestations of infection. Group I included patients with neither acute GvHD nor infections [n = 15 (24%)], group II consisted of patients with infections without acute GvHD [n = 17 (27%)], group III was comprised of patients with acute GvHD without infections [n = 9 (15%)], and group IV included patients with both acute GvHD and infections [n = 21 (34%)]. IFN-gamma concentrations were higher in Group II than in other groups on days +20 (P = 0.014) and +30 (P = 0.008). Post-hoc tests showed lower concentrations of IFN-gamma on day +30 in groups I (P = 0.039) and IV (P = 0.017) compared to group II. The levels of IL-2 were mostly undetectable.

CONCLUSION

Serum levels of IFN-gamma following allo-HSCT progressively escalate. High serum levels of IFN-gamma are related to infectious complications rather than acute GvHD. Serum concentrations of IL-2 in most patients are undetectable.

Key Words: Interleukin-2; Interferon-gamma; Cytokine profiles; Acute myeloid leukemia; Allogeneic hematopoietic stem cell transplantation; Acute graft-versus-host disease

Core Tip: This paper presents the profiles of interleukin-2 and interferon-gamma levels depending on the occurrence of acute graft-versus-host disease and infection complications after allogeneic hematopoietic stem cell transplantation (allo-HSCT). In this study, the cytokine levels were assessed in the early period after allo-HSCT (within the first 30 d after transplantation). Before, during, and after blood sampling for cytokine determination, cytokine-producing cells were not stimulated with mitogenic substances (lipopolysaccharide or phytohemagglutinin). Therefore, the obtained cytokine levels and their profiles may be regarded as those which reflect real values in patients who underwent allo-HSCT.

Citation: Rybicka-Ramos M, Markiewicz M, Suszka-Świtek A, Wiaderkiewicz R, Mizia S, Dzierżak-Mietła M, Białas K. Profiles of interferon-gamma and interleukin-2 in patients after allogeneic hematopoietic stem cell transplantation. *World J Biol Chem* 2022; 13(4): 72-82
URL: https://www.wjgnet.com/1949-8454/full/v13/i4/72.htm
DOI: https://dx.doi.org/10.4331/wjbc.v13.i4.72

INTRODUCTION

Allogeneic hematopoietic stem cell transplantation (allo-HSCT) may be related to the occurrence of complications such as graft-versus-host disease (GvHD) and infections. GvHD is a crucial and potentially fatal complication of allo-HSCT. It is observed in the case of transplantation from related or unrelated donors and occurs in two forms, *i.e.*, acute GvHD (aGvHD) and chronic GvHD. GvHD is induced by donor T lymphocytes, which are stimulated by classic human leukocyte antigens (HLA) in the event of transplantation from not fully matched donors, or by weak human leukocyte antigens in the case of transplantation from fully matched donors[1-3]. The concept of aGvHD created by Ferrara *et al* [4] assumes that the pathogenesis of aGvHD involves three consecutive stages. In the first stage, pre-transplantation conditioning treatment involves lesions and stimulation of host tissues with the elicitation of proinflammatory cytokines (TNF-α and interleukin [IL]-1) and induction of antigen-presenting cells. The second stage involves T lymphocytes, which recognize alloantigens on the host cells, initiate the cytokine storm, secrete interferon (IFN)-gamma and IL-2, and act on effector cells of the immune system. In the third stage, the tissues and organs are damaged by the inflammatory process activated by cytokines secreted by their cytotoxic T cells, NK cells, and macrophages. IFN-gamma and IL-2 are core cytokines inducing the graft-versus-host reaction by enhanced activation of the immune

cells in response to alloantigens[5-7].

MATERIAL AND METHODS

This study included 62 subjects diagnosed with acute myeloid leukemia who underwent allo-HSCT at the Department of Hematology and Bone Marrow Transplantation of the Independent Public Clinical Hospital, Medical University of Silesia in Katowice, Poland between 2012 and 2014. The subjects included 30 (48%) males and 32 (52%) females aged 19-68 years (median age 49.5). Time from diagnosis to transplantation ranged from 4 mo to 10 years (median 11 mo). At the moment of transplantation, 54 (87%) patients were in complete remission, three (5%) in partial remission, and others did not reach remission. Conditioning treatment was based on the following regimens: TreoFluATG (n = 26, 42%), BuCyATG (n = 14, 23%), BuCy (n = 6, 10%), TreoFlu (n = 5, 8%), TBICyATG (n = 5, 8%), BuFluATG (n = 3, 5%), and in isolated cases TreoFluThymo, BuFlu, and BuCyThymo. Myeloablative conditioning was given to 42% (n = 26) of the patients, while reduced intensity conditioning (RIC) was administered to 58% (n = 36). Fifty (81%) patients underwent unrelated donor hematopoietic stem cell transplantation, while other patients (n = 12, 19%) underwent sibling hematopoietic stem cell transplantation. All patients underwent standard immunosuppressive therapy. Ninety percent (n = 59) of patients were treated with cyclosporin and methotrexate with antilymphocyte globulin in the case of unrelated donor transplantation. aGvHD was diagnosed based on clinical criteria and was assessed according to the Glucksberg scale. Infection complications were diagnosed based on clinical symptoms and the findings of bacteriological tests. Death during hospitalization was reported in four (6%) patients within +30 d after allo-HSCT. Peripheral blood samples (5 mL) were collected from each patient into clot activator tubes at the following time points: Before conditioning treatment, after its completion (day -1), and after transplantation on days +2 +4, +6, +10, +20, and +30, unless death occurred earlier. The collected blood was immediately centrifuged, and the serum was frozen at -80 °C until analysis. The levels of IFN-gamma and IL-2 were determined using ELISA.

Statistical analysis

Statistical analyses were performed by a biomedical statistician. The study population was characterized by the presentation of the percentage distribution of the qualitative variable variants, while in the case of quantitative variables, the median value and range were used. The cytokine levels were initially analyzed at all checkpoints by estimating the mean, median, standard deviation, and standard error of the mean, and by defining the minimum and maximum values. Due to significant right-skewed cytokine distribution, resulting in rejecting the hypothesis of the normal distribution verified by the Shapiro-Wilk test, further analysis used the median as the measure of central tendency, and the interquartile range was used as the measure of dispersion. Moreover, non-parametric procedures were used to test statistical hypotheses. Due to multiple 0 values of the cytokines, the variables defining their levels at the test time points were categorized not only based on the cut-off point defined by the manufacturer (for IL-2, 7 pg/mL and for IFN-gamma, 5 pg/mL), but also based on the 0 value. A P value less than 0.05 ($P < 0.05$) was considered statistically significant.

RESULTS

Hematological recovery after stem cell transplantation was observed in 61 (98%) patients and median time to recovery was as follows: White blood cells (> 1.0 G/L), day +15 (range 11-25 d); absolute neutrophil count (> 0.5 G/L), day +17 (11-27 d).

The manifestation of aGvHD after allo-HSCT was observed in 30 (48%) patients, and median time to manifestation was day +17 (range 8-29 d). aGvHD was diagnosed with the following grades: I, 26 (42%) patients; II, 3 (5%); III, 1 (2%); IV, not recorded. aGvHD involved the following organs: Skin, 28 (45%) patients; intestines, 3 (5%); liver, not recorded. The remaining 32 (52%) patients did not present with aGvHD symptoms. An infectious complication independent of its etiology occurred in 38 (61%) patients, and median time to the occurrence of the first incident was day +9 (range, 0-27 d). Mucositis was reported in 26 (42%) patients, and median time to the occurrence was day +1 (range, 0-20 d) (Table 1).

Twenty-one (70%) patients with aGvHD also presented with bacterial and/or fungal and/or viral infection, and median time to the first infection was day +10 (range, 1-27 d). Mucositis was reported in 15 (50%) patients, and median time to the occurrence was day +2 (0-8 d). However, it was not significantly different in comparison with the group of patients without aGvHD (Table 1).

The assessment included kinetics of IFN-gamma changes after allo-HSCT in the groups with and without aGvHD at consecutive time points, including the assessment before and after conditioning treatment (Figure 1).

Table 1 Complications after allogeneic hematopoietic stem cell transplantation

Infection, *n* (%)	Yes	38 (61)
	No	24 (39)
Onset of first symptoms of infection (d), median (range)		9 (0-27)
Mucositis, *n* (%)	Yes	26 (42)
	No	36 (58)
Onset of first symptoms of mucositis (d), median (range)		1 (0-20)
aGvHD, *n* (%)	0	32 (52)
	I	26 (42)
	II	3 (5)
	III	1 (2)
	IV	0 (0)
aGvHD, *n* (%)	Skin	28 (45)
	Intestines	3 (5)
	Liver	0 (0)
Time of aGvHD manifestation (d), median (range)		17 (8-29)

aGvHD: Acute graft-versus-host disease.

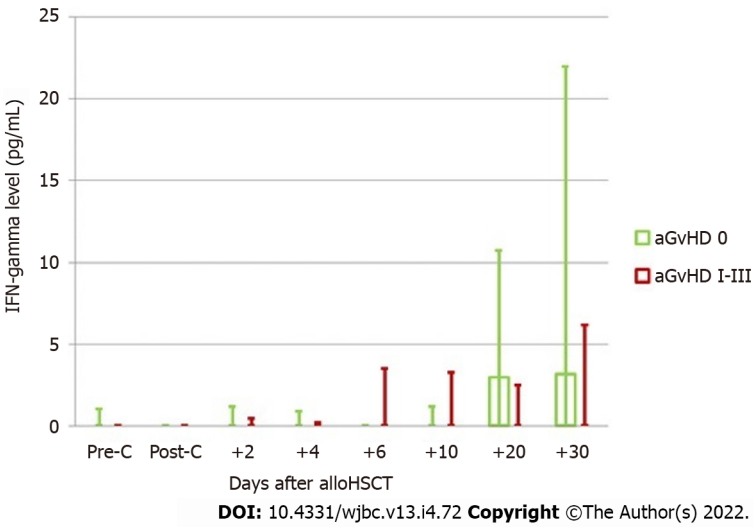

DOI: 10.4331/wjbc.v13.i4.72

Figure 1 Serum levels of interferon-gamma in the groups with and without acute graft-versus-host disease. aGvHD: Acute graft-versus-host disease; allo-HSCT: Allogeneic hematopoietic stem cell transplantation; IFN: Interferon; Pre-C: Before conditioning treatment; Post-C: After conditioning treatment.

No differences regarding the IFN levels assessed before and after conditioning treatment were observed between the subjects with and without aGvHD. In the group of patients without aGvHD, a significant increase in the cytokine level was observed on day +20. The obtained level was similar during the next measurement. In patients with aGvHD, an increase in IFN-gamma levels was observed on day +6 in relation to the levels before conditioning treatment. At this measurement point, higher IFN-gamma levels in the aGvHD group were the most pronounced in relation to the group without aGvHD. This advantage could also be observed on day +10. At the next measurement point, a shift was observed regarding IFN-gamma levels, which were higher in patients without aGvHD. The above finding may be correlated with the disease onset (median on day +17).

The assessment also included the kinetics of IFN-gamma changes after allo-HSCT in the groups of patients with and without infections at consecutive time points, including the assessment before and after conditioning treatment (Figure 2).

No significant difference in IFN-gamma levels before conditioning treatment was observed between the groups with and without infection, although a tendency to higher cytokine levels was found in the

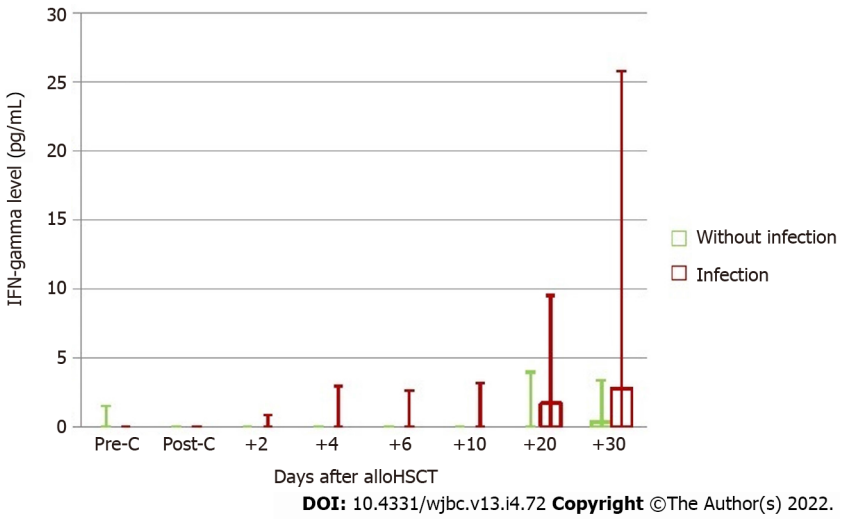

DOI: 10.4331/wjbc.v13.i4.72

Figure 2 Serum levels of interferon-gamma in the groups with and without infection. allo-HSCT: Allogeneic hematopoietic stem cell transplantation; IFN: Interferon; Pre-C: Before conditioning treatment; Post-C: After conditioning treatment.

group without infection. The analysis of the effect of conditioning treatment on the cytokine level showed its decrease only in patients whose post-transplantation period was not complicated by infection, which in turn led to the reversal of proportions in both groups. A tendency to higher IFN-gamma levels in the group of patients with infection after conditioning treatment was maintained during the entire post-transplantation period, and on day +6, the difference in IFN-gamma levels reached significance. In the group of patients with infection, an almost continuous increase in IFN-gamma levels was observed during the entire study period, while on day +20, the concentration was significantly higher compared to baseline, and was also slightly increased at the next measurement point. In other patients, after conditioning treatment, the lowest IFN-gamma levels showed a growing tendency at subsequent measurements. However, this tendency was not as significant as that in the group of patients with infection.

Moreover, the median and maximum values of IFN-gamma levels were measured in each patient in the post-transplantation period (between days +2 and +30). These values were significantly higher in the group of subjects with infection compared with those without (median 0.058 *vs* 0 pg/mL, $P = 0.043$; 19.295 *vs* 2.260 pg/mL, $P = 0.002$, respectively) (Tables 2 and 3).

The presence of IL-2 assessed before conditioning treatment was reported only in one patient who did not develop aGvHD and had no infection due to transplantation. The levels of IL-2 decreased after conditioning treatment to the value below the cut-off level, but were maintained above 0, with no increase in the cytokine levels in other patients.

The levels of IL-2 assessed after allo-HSCT were above 0 at least at one measurement point only in five patients, including three subjects in whom the cut-off point was above 7 pg/mL. None of these patients showed manifestations of aGvHD, but three patients presented with infections independent of their etiology, and two subjects had mucositis. In all patients, the levels of IL-2 were undetectable on the day of infection onset. Figure 3 shows the kinetics of IL-2 changes in serum of patients whose level was above 0 at any time during the post-transplantation period.

In the final analysis, the patients were divided into four groups based on the occurrence of aGvHD and infection: Group I, patients ($n = 15$, 24%) who presented with no signs of acute GvHD or infection; group II, patients ($n = 17$, 27%) who showed complications in the form of infection after allo-HSCT without acute GvHD; group III, patients ($n = 9$, 15%) who showed acute GvHD with no infection; group IV, patients ($n = 21$, 34%) who showed both acute GvHD and infection. The analysis of IFN-gamma levels measured at subsequent measurement points showed the occurrence of differences between the groups on days +20 and +30 after allo-HSCT (Table 4).

Significantly higher levels of this cytokine were observed in group II on days +20 ($P = 0.014$) and +30 ($P = 0.008$) in comparison with other groups of patients. Post-hoc tests revealed significantly lower IFN-gamma levels on day +30 in groups I ($P = 0.039$) and IV ($P = 0.017$) in comparison with group II. The levels of IL-2 were undetectable in most patients at all checkpoints. Figure 4 shows mean IFN-gamma levels before and after allo-HSCT in the four groups of patients.

DISCUSSION

This paper shows the profiles of IL-2 and IFN-gamma levels depending on the occurrence of aGvHD

Table 2 Median and maximum values of serum levels of interferon-gamma (pg/mL) in patients with and without acute graft-versus-host disease in the post-transplantation period (between days +2 and +30)

		Median IFN-gamma after allo-HSCT	Maximum IFN-gamma after allo-HSCT
aGvHD 0	Me	0	12.950
	Q1	0	0.185
	Q3	2.268	32.035
aGvHD I-III	Me	0	6.535
	Q1	0	0
	Q3	1.650	20.870
Mann-Whitney *U* test (*P*)		0.619	0.473

Me: Median; Q1: Quartile 1; Q3: Quartile 3; aGvHD: Acute graft-versus-host disease; allo-HSCT: Allogeneic hematopoietic stem cell transplantation; IFN: Interferon.

Table 3 Median and maximum values of serum levels of interferon-gamma (pg/mL) in patients with and without infection in the post-transplantation period (between days +2 and +30)

		Median IFN-gamma after allo-HSCT	Maximum IFN-gamma after allo-HSCT
Without infection	Me	0	2.260
	Q1	0	0
	Q3	0	10.675
Infection	Me	0.058	19.295
	Q1	0	1.210
	Q3	2.375	37.620
Mann-Whitney U test (*P*)		0.043	0.002

Me: Median; Q1: Quartile 1; Q3: Quartile 3; allo-HSCT: Allogeneic hematopoietic stem cell transplantation; IFN: Interferon.

Table 4 Serum levels of interferon-gamma (pg/mL) in patients divided into groups based on the occurrence of acute graft-versus-host disease and infection

IFN-gamma level (pg/mL)								
Median (Q1-Q3)	Pre-C	Post-C (day -1)	+2	+4	+6	+10	+20	+30
Group I	0 (0-1.50)	0 (0-0)	0 (0-0.50)	0 (0-0.58)	0 (0-0)	0 (0-0.63)	0 (0-3.97)	0 (0-3.00)
Group II	0 (0-0)	0 (0-1.63)	0 (0-1.52)	0 (0-1.25)	0 (0-1.10)	0 (0-1.52)	8.25 (0.28-30.46)	17.58 (3.00-46.12)
Group III	0 (0-0.84)	0 (0-0)	0 (0-0)	0 (0-0)	0 (0-0)	0 (0-0)	0 (0-3.83)	1.05 (0-6.78)
Group IV	0 (0-0)	0 (0-0)	0 (0-0.52)	0 (0-3.45)	0 (0-12.7)	0 (0-4.32)	0.22 (0-2.51)	0 (0-4.30)
Kruskal-Wallis test (*P*)	0.305	0.077	0.714	0.431	0.123	0.517	0.014	0.008

Pre-C: Before conditioning treatment; Post-C: After conditioning treatment; Q1: Quartile 1; Q3: Quartile 3; IFN: Interferon.

and infection complications after allo-HSCT. The cytokine levels was assessed in the early period after allo-HSCT (within the first 30 d after transplantation). Before, during, and after blood sampling for cytokine determination, cytokine-producing cells were not stimulated with mitogenic substances such as lipopolysaccharide (LPS) or phytohemagglutinin (PHA). Therefore, the obtained cytokine levels and their profiles may be regarded as those which reflect real values in patients who underwent allo-HSCT. Low levels of IFN-gamma and IL-2 before and after allo-HSCT may be caused by severe pancytopenia after conditioning treatment and the use of antithymocyte globulin (ATG), which results in a deficiency of cytokine-producing cells. Moreover, immunosuppression caused impairment of the hematopoietic

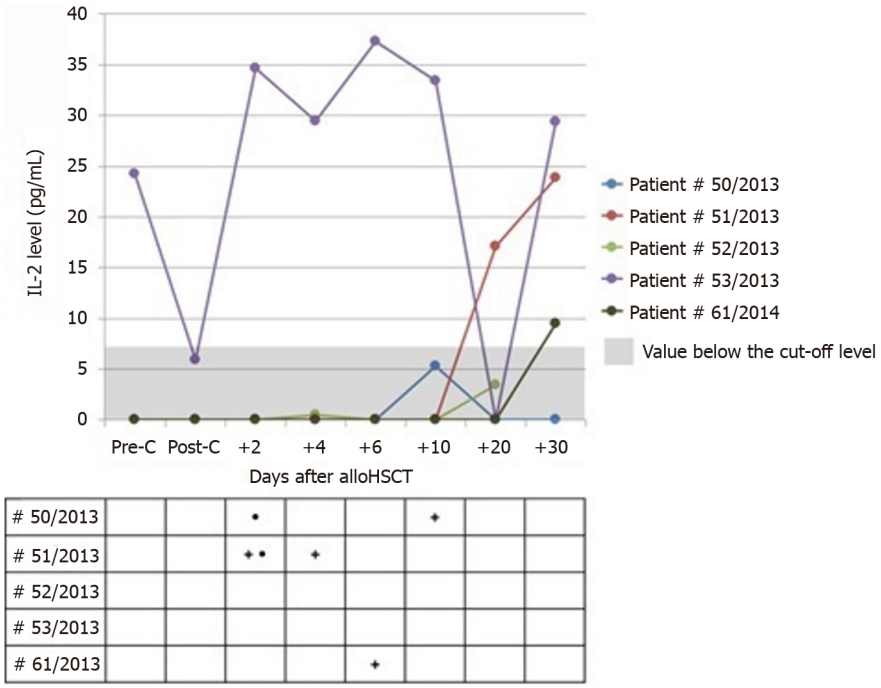

DOI: 10.4331/wjbc.v13.i4.72 **Copyright** ©The Author(s) 2022.

Figure 3 Serum levels of interleukin-2 in patients* with the value above 0 at least once in the post-transplantation period. *None of these patients presented with aGvHD. "+": Day of the occurrence of infection independent of its etiology; "•": Day of the occurrence of mucositis. Allo-HSCT: Allogeneic hematopoietic stem cell transplantation; IL-2: Interleukin-2; Pre-C: Before conditioning treatment; Post-C: After conditioning treatment.

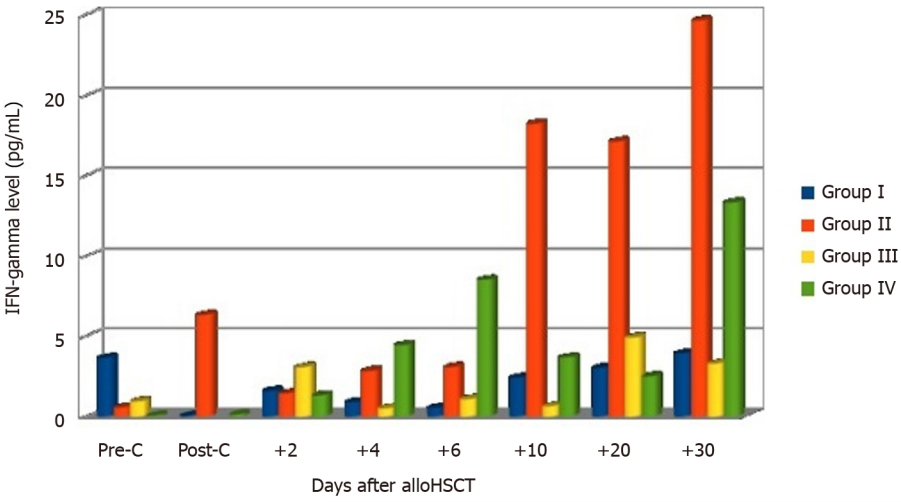

DOI: 10.4331/wjbc.v13.i4.72 **Copyright** ©The Author(s) 2022.

Figure 4 Mean levels of interferon-gamma before and after allogeneic hematopoietic stem cell transplantation in the four groups of patients. Allo-HSCT: Allogeneic hematopoietic stem cell transplantation; IFN: Interferon; Pre-C: Before conditioning treatment; Post-C: After conditioning treatment.

function and the production of cytokines. Low IFN-gamma and IL-2 levels may indicate successful immunosuppressive treatment to some extent. However, beginning with day 20 after allo-HSCT, the cytokine levels gradually increased with progressive reconstitution of the hematopoietic cells.

In the present study, the levels of the cytokines were low. In a small number of patients, they exceeded the value of the cut-off point, which was considered a positive result. This may be related to lymphocyte dysfunction caused by intensive acute myeloid leukemia (AML) treatment. In AML patients, T lymphocytes show genetic and phenotypic disorders, as well as impaired function and reduced cell count[8,9]. It was demonstrated that this could be related to an impaired function of the T lymphocyte receptor (TCR) (especially subunit ζ), whose damage causes impaired immunity in leukemia. In addition, T lymphocytes, especially with TCR Vβ, are not fully recovered after induction treatment in AML patients[10,11]. Moreover, long-term antigen stimulation of T lymphocytes leads to the "exhaustion" of these cells, which means that T lymphocytes lose their ability to secrete cytokines

such as IL-2, TNF-α, and IFN-gamma, proliferate, and induce cytotoxic reactions[12-14].

Sadeghi *et al*[15] showed a murine model of aGvHD based on conditioning with high-dose chemotherapy. The animals underwent conditioning, and were divided into two groups. Group I comprised animals that underwent allogeneic transplantation, while group II included animals with syngeneic transplantation. The authors did not use immunosuppressive treatment in the post-transplantation period. The period of bone marrow cell regeneration was varied depending on the type of transplantation; in mice after syngeneic transplantation, it was more rapid with a shorter duration (onset of recovery on day +1, peak on day +5, and the end on day +21, while in mice after allogeneic transplantation, no complete recovery was reported by day +21). Analyzing the collected blood samples, the authors examined reconstitution of the immune cells of mice and the kinetics of IFN-gamma, IL-2, and TNF-α in the early period after transplantation. The study showed that in mice after allogeneic transplantation, the proliferation and maturation of dendritic cells and CD8+ T lymphocytes of the donor were more rapid in comparison with the mice after syngeneic transplantation: Day +3 and from day +5 after transplantation, respectively. The study found a regular increase in all cytokine levels that corresponded with the rate of bone marrow cell recovery and the presence of dendritic cells and T lymphocytes in the circulation. The increase in the cytokine levels was higher in mice after allogeneic transplantation with aGvHD. While gradually increasing from low levels on the day of transplantation, the levels of the cytokines reached their peak on day +5 in mice that underwent allogeneic stem cell transplantation which developed aGvHD, followed by a decrease on subsequent days. No such phenomenon was observed in the animals after syngeneic transplantation.

In contrast to the present study, the authors of the above study based it on a murine model and did not include immunosuppressive treatment. Therefore, the kinetics of the cytokine level changes and reconstitution of bone marrow cells were deprived of the blocking effect of immunosuppressive agents on the immune cells and cytokine secretion. This is reflected by rapid recovery of bone marrow cells with a simultaneous increase in the cytokine levels. The study of Sadeghi *et al*[15] did not include the period before conditioning treatment, and the follow-up period was shorter (21 d after transplantation).

Ju *et al*[16] analyzed the cytokine expression at a molecular level and the protein expression in 30 patients after allogeneic peripheral blood stem cell transplantation (allo-PBSCT). The group of patients was not homogeneous with regard to the disease being an indication for transplantation. A myeloablative regimen of Cy+VP16+TBI was used as conditioning treatment, while ciclosporin A + and methotrexate were used as aGvHD prevention. Blood samples were collected before allo-PBSCT, during the occurrence of the first aGvHD symptoms and after pharmacological control of the disease symptoms. The samples were incubated and a solution of lipopolysaccharide and PHA was added, and the levels of IFN-gamma, IL-2, IL-4, IL-10, IL-12, and IL-18 were measured using ELISA. Of 30 patients, 16 did not develop aGvHD, 7 presented with grade I aGvHD symptoms, and 7 presented with grades II-IV aGvHD. The expression of the cytokines, especially of IL-2 and IFN-gamma, was significantly higher in patients with aGvHD at the mRNA and protein levels. The expansion of cytokines was observed with increased severity of aGvHD, and a significant decrease was reported when aGvHD symptoms were controlled. In the above study, a correlation between the protein levels of the above cytokines and aGvHD symptoms was stronger than between their mRNA expression and disease symptoms.

Unlike the authors of this paper, the authors of the above report measured the cytokine levels after stimulation with LPS and PHA, which increase cytokine secretion and result in high concentrations. Moreover, despite standard immunosuppressive treatment, high IL-2 levels (> 100 pg/mL) were observed both in the group of patients with aGvHD and in the group of patients without aGvHD symptoms. In the present study, IL-2 levels were below the detection limit in almost all patients, regardless of the presence of aGvHD symptoms, and IFN-gamma levels were higher in the group without aGvHD symptoms. Despite using standard immunosuppression, high IL-2 levels in both groups of patients with or without aGvHD indicated a possible decisive effect of LPS and PHA stimulation of the immune cells on achieving high cytokine levels. For this reason, the real picture of the kinetics of IL-2 and IFN-gamma level changes in the post-transplantation period in patients developing aGvHD is unclear in the study of Ju *et al*[16].

Visentainer *et al*[17] included 13 patients after allo-HSCT from fully matched donors in whom serum cytokine levels were determined within 15 wk after allo-HSCT using ELISA. Only the levels of IL-10 and the soluble receptor for IL-2 were significantly higher in the group of patients with aGvHD symptoms in comparison with those without. Moreover, the increase in the level of the soluble receptor for IL-2 had a direct correlation with implantation of bone marrow cells and onset of aGvHD symptoms.

In terms of the correlation between IFN-gamma and infection complications in patients after allo-HSCT, several available papers have shown contradictory results. In a study by Gayoso *et al*[18], a group of 26 patients were assessed for a correlation between the IFN-gamma level and the occurrence of cytomegalovirus (CMV) infection 6 mo after allo-HSCT. The prophylaxis of aGvHD included the use of cyclosporin and methotrexate in patients after myeloablative conditioning, and the use of cyclosporin with mycophenolate mofetil after RIC. If CMV reactivation was observed, patients were treated with valganciclovir. Blood samples were collected 6 mo after allo-HSCT. They were centrifuged and IFN-gamma levels were determined in the supernatant using ELISA. The authors proved that in patients with CMV reactivation, IFN-gamma levels were higher (> 0.2 IU/mL) than those in the group where no reactivation was observed.

Peng *et al*[19] analyzed the correlation between proinflammatory cytokines and the occurrence of invasive fungal infection in patients after allo-HSCT. Their analysis included 47 patients who underwent allo-HSCT due to various hematological diseases, and a control group (40 healthy volunteers). All the subjects were given myeloablative conditioning treatment, including 17 patients with ATG, and 30 patients without ATG. Immunosuppressive treatment for preventing aGvHD included tacrolimus with methotrexate and mycophenolate mofetil in 30 patients, and cyclosporin with methotrexate and mycophenolate mofetil in 17 patients. The levels of IL-6, IL-10, IFN-gamma, and TGF-β cytokines were determined using ELISA at 1, 2, and 3 mo after allo-HSCT. A comparison of the results in patients after allo-HSCT and the control group showed that IL-6 levels gradually increased and reached the peak value at 2 mo after allo-HSCT, and then decreased. At 3 mo, however, they were significantly higher in patients after allo-HSCT. Similarly, IL-10 levels increased in the post-transplantation period, while TGF-β levels gradually decreased. For IFN-gamma levels, no significant differences were observed between the groups. Moreover, there was no correlation between invasive fungal infection and changes in the concentrations of IFN-gamma and other cytokines.

In the above papers, their authors focused on showing a correlation between one selected infection complication and the concentration of specific proinflammatory cytokines. The study groups were not homogeneous with regard to the disease being an indication for allo-HSCT. Cytokine levels were determined in the late post-transplantation period with no regard to the effect of GvHD and other complications in the form of (bacterial) infections on the results. Contrary to our study, the above papers reflected the kinetics of cytokine level changes in a later period after allo-HSCT in relation to selected infection complications, without considering the early post-transplantation period. The present study showed a potential correlation between IFN-gamma levels and the occurrence of infection complications, while the findings reported in the above papers were inconsistent in this respect.

CONCLUSION

Higher IFN-gamma levels are more related to infection complications than the occurrence of aGvHD. IFN-gamma levels in the group of patients with acute GvHD, in the group with acute GvHD and infection, and in the group without GvHD and infection are significantly lower than those in the group of patients with infection only. Within the first 30 d after allo-HSCT, serum IL-2 levels in patients with AML are very low and diagnostically insignificant.

ARTICLE HIGHLIGHTS

Research background

Allogeneic hematopoietic stem cell transplantation (allo-HSCT) may be related to complications such as graft-versus-host disease (GvHD) and infections. GvHD is a crucial and potentially fatal complication of allo-HSCT. The pathogenesis of this complication is associated with the cytokine storm.

Research motivation

There is a small amount of medical data on the cytokine profiles in patients after allogeneic stem cell transplantation. In this report, the cytokine level was assessed in the early period after allo-HSCT (during the first 30 d after transplantation).

Research objectives

Before, during, and after blood sampling for cytokine determination, cytokine-producing cells were not stimulated with mitogenic substances. Therefore, the obtained cytokine levels and their profiles may be regarded as those which reflect real values in patients who underwent allo-HSCT.

Research methods

We enrolled 62 patients after allo-HSCT due to acute myeloid leukemia (AML). All subjects underwent standard immunosuppressive therapy based on cyclosporin and methotrexate with addition of antilymphocyte globulin in the case of unrelated donor transplantation. Peripheral blood samples were collected from each patient at the checkpoints: Before conditioning treatment, after its completion (day -1), and after transplantation on days +2 +4, +6, +10, +20, and +30, unless death occurred earlier. The samples were not stimulated with mitogenic substances. Serum levels of IL-2 and IFN-gamma were determined using ELISA.

Research results

In the final analysis, patients were divided into four groups based on the occurrence of aGvHD and infection. Significantly higher levels of IFN-gamma were found in group II on days +20 (P = 0.014) and

+30 (P = 0.008) in comparison with other groups of patients.

Research conclusions

Higher IFN-gamma levels are more related to infectious complications than the occurrence of aGvHD. Within the first 30 d after allo-HSCT, serum levels of IL-2 in patients with AML are very low and diagnostically insignificant.

Research perspectives

More studies are warranted to create a more precise cytokine profile.

FOOTNOTES

Author contributions: Rybicka-Ramos M contributed to conceptualization, methodology, investigation, data curation and analysis, original draft preparation, project administration, and fund acquisition; Markiewicz M contributed to methodology, investigation, manuscript review and editing, supervision, and fund acquisition; Dzierzak-Mietla M and Bialas K contributed to investigation; Suszka-Świtek A, Wiaderkiewicz R, and Mizia S contributed to data curation and analysis.

Institutional review board statement: The study was conducted according to the guidelines of the Declaration of Helsinki, and approved by the Ethics Committee of the Medical University of Silesia in Katowice (No. KNW/0022/KB1/71/I/12).

Conflict-of-interest statement: All the authors declare no conflict of interest for this article.

Data sharing statement: No additional data are available.

Country/Territory of origin: Poland

ORCID number: Malwina Rybicka-Ramos 0000-0002-0159-8126.

S-Editor: Liu JH
L-Editor: Wang TQ
P-Editor: Liu JH

REFERENCES

1 **Goulmy E**. Human minor histocompatibility antigens: new concepts for marrow transplantation and adoptive immunotherapy. *Immunol Rev* 1997; **157**: 125-140 [PMID: 9255626 DOI: 10.1111/j.1600-065x.1997.tb00978.x]
2 **Spierings E**, Kim YH, Hendriks M, Borst E, Sergeant R, Canossi A, Oudshoorn M, Loiseau P, Dolstra H, Markiewicz M, Leffell MS, Pereira N, Kircher B, Turpeinen H, Eliaou JF, Gervais T, Laurin D, Enczmann J, Martinetti M, Thomson J, Oguz F, Santarone S, Partanen J, Siekiera U, Alessandrino EP, Kalayoglu S, Brand R, Goulmy E. Multicenter analyses demonstrate significant clinical effects of minor histocompatibility antigens on GvHD and GvL after HLA-matched related and unrelated hematopoietic stem cell transplantation. *Biol Blood Marrow Transplant* 2013; **19**: 1244-1253 [PMID: 23756210 DOI: 10.1016/j.bbmt.2013.06.001]
3 **Pegram HJ**, Ritchie DS, Smyth MJ, Wiernik A, Prince HM, Darcy PK, Kershaw MH. Alloreactive natural killer cells in hematopoietic stem cell transplantation. *Leuk Res* 2011; **35**: 14-21 [PMID: 20719383 DOI: 10.1016/j.leukres.2010.07.030]
4 **Ferrara JL**, Reddy P. Pathophysiology of graft-versus-host disease. *Semin Hematol* 2006; **43**: 3-10 [PMID: 16412784 DOI: 10.1053/j.seminhematol.2005.09.001]
5 **Ferrara JL**. Pathogenesis of acute graft-versus-host disease: cytokines and cellular effectors. *J Hematother Stem Cell Res* 2000; **9**: 299-306 [PMID: 10894351 DOI: 10.1089/15258160050079407]
6 **Carreras E**, Diaz-Ricart M. The role of the endothelium in the short-term complications of hematopoietic SCT. *Bone Marrow Transplant* 2011; **46**: 1495-1502 [PMID: 21460864 DOI: 10.1038/bmt.2011.65]
7 **Rybicka-Ramos M**, Markiewicz M, Suszka-Switek A, Wiaderkiewicz R, Mizia S, Dzierzak-Mietla M, Bialas K. Proinflammatory cytokines as potential risk factors of acute graft-versus-host disease and infectious complications after allogeneic hematopoietic stem cell transplantation. *Am J Blood Res* 2021; **11**: 149-156 [PMID: 34079628]
8 **Govindaraj C**, Tan P, Walker P, Wei A, Spencer A, Plebanski M. Reducing TNF receptor 2+ regulatory T cells *via* the combined action of azacitidine and the HDAC inhibitor, panobinostat for clinical benefit in acute myeloid leukemia patients. *Clin Cancer Res* 2014; **20**: 724-735 [PMID: 24297862 DOI: 10.1158/1078-0432.CCR-13-1576]

9 **Billingham RE**. The biology of graft-versus-host reactions. *Harvey Lect***62**: 21-78 [PMID: 4875305]

10 **Shi L**, Chen S, Zha X, Xu Y, Xu L, Yang L, Lu Y, Zhu K, Li Y. Enhancement of the TCRζ expression, polyclonal expansion, and activation of t cells from patients with acute myeloid leukemia after IL-2, IL-7, and IL-12 induction. *DNA Cell Biol* 2015; **34**: 481-488 [PMID: 25757160 DOI: 10.1089/dna.2015.2810]

11 **Chen S**, Zha X, Shi L, Zhou L, Yang L, Li B, Wu X, Zhong J, Zhang T, Lu Y, Zhu K, Li Y. Upregulated TCRζ improves cytokine secretion in T cells from patients with AML. *J Hematol Oncol* 2015; **8**: 72 [PMID: 26081440 DOI: 10.1186/s13045-015-0170-0]

12 **Wherry EJ**. T cell exhaustion. *Nat Immunol* 2011; **12**: 492-499 [PMID: 21739672 DOI: 10.1038/ni.2035]

13 **Cooke KR**, Olkiewicz K, Erickson N, Ferrara JL. The role of endotoxin and the innate immune response in the pathophysiology of acute graft versus host disease. *J Endotoxin Res* 2002; **8**: 441-448 [PMID: 12697087 DOI: 10.1179/096805102125001046]

14 **Lan RY**, Selmi C, Gershwin ME. The regulatory, inflammatory, and T cell programming roles of interleukin-2 (IL-2). *J Autoimmun* 2008; **31**: 7-12 [PMID: 18442895 DOI: 10.1016/j.jaut.2008.03.002]

15 **Sadeghi B**, Al-Hashmi S, Hassan Z, Rozell B, Concha H, Lundmark C, Grönvik KO, Abedi-Valugerdi M, Hassan M. Expansion and activation kinetics of immune cells during early phase of GVHD in mouse model based on chemotherapy conditioning. *Clin Dev Immunol* 2010; **2010**: 142943 [PMID: 21197273 DOI: 10.1155/2010/142943]

16 **Ju XP**, Xu B, Xiao ZP, Li JY, Chen L, Lu SQ, Huang ZX. Cytokine expression during acute graft-versus-host disease after allogeneic peripheral stem cell transplantation. *Bone Marrow Transplant* 2005; **35**: 1179-1186 [PMID: 15852028 DOI: 10.1038/sj.bmt.1704972]

17 **Visentainer JE**, Lieber SR, Persoli LB, Vigorito AC, Aranha FJ, de Brito Eid KA, Oliveira GB, Miranda EC, de Souza CA. Serum cytokine levels and acute graft-versus-host disease after HLA-identical hematopoietic stem cell transplantation. *Exp Hematol* 2003; **31**: 1044-1050 [PMID: 14585368 DOI: 10.1016/j.exphem.2003.08.005]

18 **Gayoso I**, Cantisán S, Cerrato C, Sánchez-García J, Martin C, Solana R, Torres-Gomez A, Torre-Cisneros J. Clinical factors influencing phenotype of HCMV-specific CD8+ T cells and HCMV-induced interferon-gamma production after allogeneic stem cells transplantation. *Clin Dev Immunol* 2013; **2013**: 347213 [PMID: 23424600 DOI: 10.1155/2013/347213]

19 **Peng XG**, Dong Y, Zhang TT, Wang K, Ma YJ. Immune Reconstitution of CD4+T Cells after Allogeneic Hematopoietic Stem Cell Transplantation and its Correlation with Invasive Fungal Infection in Patients with Hematological Malignancies. *Asian Pac J Cancer Prev* 2015; **16**: 3137-3140 [PMID: 25921110 DOI: 10.7314/apjcp.2015.16.8.3137]

Published by **Baishideng Publishing Group Inc**
7041 Koll Center Parkway, Suite 160, Pleasanton, CA 94566, USA
Telephone: +1-925-3991568
E-mail: bpgoffice@wjgnet.com
Help Desk: https://www.f6publishing.com/helpdesk
https://www.wjgnet.com

ISSN 1949-8454 (online)

World Journal of *Biological Chemistry*

World J Biol Chem 2022 November 27; 13(5): 83-94

Published by Baishideng Publishing Group Inc

WJBC

World Journal of Biological Chemistry

Contents

Bimonthly Volume 13 Number 5 November 27, 2022

ORIGINAL ARTICLE

Case Control Study

World Journal of Biological Chemistry

Bimonthly Volume 13 Number 5 November 27, 2022

Contents

ABOUT COVER

Editorial Board Member of *World Journal of Biological Chemistry*, Mohammed Nader Shalaby, MD, PhD, Associate Professor of Biological Sciences and Sports Health Department, Faculty of Physical Education, Suez Canal University, Egypt. dr.m.nader@suez.edu.eg

AIMS AND SCOPE

The primary aim of the *World Journal of Biological Chemistry* (*WJBC*, *World J Biol Chem*) is to provide scholars and readers from various fields of biological chemistry a platform to publish high-quality basic and clinical research articles and communicate their research findings online.

WJBC mainly publishes articles reporting research results and findings obtained in the field of biological chemistry and covering a wide range of topics including bioenergetics, cell biology, chromosomes, developmental biology, DNA, enzymology, extracellular matrices, gene regulation, genomics, glycobiology, immunology, lipids, membrane biology, metabolism, molecular bases of disease, molecular biophysics, neurobiology, plant biology, protein structure and folding, protein synthesis and degradation, proteomics, and signal transduction.

INDEXING/ABSTRACTING

The *WJBC* is now abstracted and indexed in PubMed, PubMed Central, Reference Citation Analysis, China National Knowledge Infrastructure, China Science and Technology Journal Database, and Superstar Journals Database.

RESPONSIBLE EDITORS FOR THIS ISSUE

NAME OF JOURNAL
World Journal of Biological Chemistry

ISSN
ISSN 1949-8454 (online)

LAUNCH DATE
July 26, 2010

FREQUENCY
Bimonthly

EDITORS-IN-CHIEF
Vsevolod Gurevich, Jean-Marie Exbrayat, Chunpeng Craig Wan

EDITORIAL BOARD MEMBERS
https://www.wjgnet.com/1949-8454/editorialboard.htm

PUBLICATION DATE
November 27, 2022

INSTRUCTIONS TO AUTHORS
https://www.wjgnet.com/bpg/gerinfo/204

GUIDELINES FOR ETHICS DOCUMENTS
https://www.wjgnet.com/bpg/GerInfo/287

GUIDELINES FOR NON-NATIVE SPEAKERS OF ENGLISH
https://www.wjgnet.com/bpg/gerinfo/240

PUBLICATION ETHICS
https://www.wjgnet.com/bpg/GerInfo/288

PUBLICATION MISCONDUCT
https://www.wjgnet.com/bpg/gerinfo/208

ARTICLE PROCESSING CHARGE
https://www.wjgnet.com/bpg/gerinfo/242

STEPS FOR SUBMITTING MANUSCRIPTS
https://www.wjgnet.com/bpg/GerInfo/239

ONLINE SUBMISSION
https://www.f6publishing.com

E-mail: bpgoffice@wjgnet.com https://www.wjgnet.com

World Journal of Biological Chemistry

Submit a Manuscript: https://www.f6publishing.com

World J Biol Chem 2022 November 27; 13(5): 83-94

DOI: 10.4331/wjbc.v13.i5.83

ISSN 1949-8454 (online)

ORIGINAL ARTICLE

Case Control Study

Serum leptin level in Sudanese women with unexplained infertility and its relationship with some reproductive hormones

Abdullah Abdulslam Abdullah, Musa Ahmed, Adesina Oladokun, Nasir Adam Ibrahim, Shahd Nourain Adam

Specialty type: Biochemistry and molecular biology

Provenance and peer review: Unsolicited article; Externally peer reviewed

Peer-review model: Single blind

Peer-review report's scientific quality classification

Grade A (Excellent): 0
Grade B (Very good): 0
Grade C (Good): C, C
Grade D (Fair): 0
Grade E (Poor): 0

P-Reviewer: Merigo F, Italy; Zhou FT, China

Received: August 22, 2022
Peer-review started: August 22, 2022
First decision: September 26, 2022
Revised: September 30, 2022
Accepted: November 23, 2022
Article in press: November 23, 2022
Published online: November 27, 2022

Abdullah Abdulslam Abdullah, Musa Ahmed, Department of Reproductive Health Sciences, Pan African University Life and Earth Sciences Institute, University of Ibadan, Ibadan 119, Oyo, Nigeria

Abdullah Abdulslam Abdullah, Musa Ahmed, Adesina Oladokun, Department of Obstetrics and Gynecology, College of Medicine, University of Ibadan, Ibadan 119, Oyo, Nigeria

Abdullah Abdulslam Abdullah, Department of Biomedical Sciences, Faculty of Veterinary Sciences, University of Gadarif, Gadarif 208, Sudan

Musa Ahmed, Department of Veterinary Surgery, Faculty of Veterinary Medicine, AL-Salam University, Al-fula 120, West Kordofan, Sudan

Nasir Adam Ibrahim, Department of Biology, Faculty of Science, Imam Mohammed Ibn Saud Islamic University, Riyadh 13318, Saudi Arabia

Nasir Adam Ibrahim, Department of Biochemistry and Physiology, Faculty of Veterinary Medicine, University of Al-butana, Ruffaa 210, Sudan

Shahd Nourain Adam, College of Nursing, University of Bahri, Khartoum 12217, Sudan

Corresponding author: Abdullah Abdulslam Abdullah, MSc, Academic Researcher, Department of Reproductive Health Sciences, Pan African University Life and Earth Sciences Institute, University of Ibadan, Ajibode Road, 200132, Ibadan 119, Oyo, Nigeria.
bahlol32029@gmail.com

Abstract

BACKGROUND

The excessive concentration of leptin has negative effects on all aspects of female reproduction. Despite this established relationship, the exact role of leptin in women's fertility is not clear enough and needs more clarification.

AIM

To evaluate the serum leptin levels in Sudanese women and to ascertain the relationship between serum leptin levels and unexplained infertility (UI).

METHODS

A matched (age and body mass index) case-control study was conducted from March 2021 to February 2022. The study samples were 210 women with UI and

190 fertile women of reproductive age who were attending the maternity hospitals and fertility clinics in Khartoum state Sudan. The serum concentration of leptin and other serum biomarkers were determined using enzyme-linked immunosorbent assays.

RESULTS

The results showed that there was a highly statistically significant difference between the two groups ($P < 0.001$) for all examined eight biomarkers. Whereby, leptin, luteinizing hormone (LH)/follicular stimulating hormone (FSH) ratio, prolactin hormone (PRL) and testosterone (T) were significantly higher in the UI group compared with the control group. In contrast, FSH and estradiol (E2)/T ratio were significantly lower in the UI group than in the control group and the effect size test for the difference between the two groups was very large (effect size > 0.80), for leptin level, LH/FSH ratio, PRL level, and E2/T ratio, and large (effect size 0.50- ≤ 0.80) for FSH and T.

CONCLUSION

This study reveals that leptin could be a potential biomarker for UI in Sudanese women and it may be useful for identifying women with a high risk of infertility.

Key Words: Leptin; Serum level; Unexplained infertility; Sudanese women; Reproductive hormones

Core Tip: A matched (age and body mass index) case-control study was conducted to find the serum leptin levels in Sudanese women and to ascertain the relationship between serum leptin levels and unexplained infertility (UI). A total of 400 women of reproductive age were recruited for this study (210 with UI and 190 fertile women). Leptin, luteinizing hormone/follicular stimulating hormone (FSH) ratio, prolactin hormone and testosterone (T) were significantly higher in the UI group compared with the control group. In contrast, FSH and estradiol/T ratio were significantly lower in the UI group than in the control group. Thus, this study reveals that leptin could be a potential biomarker for UI in Sudanese women and it may be useful for identifying women with a high risk of infertility.

Citation: Abdulslam Abdullah A, Ahmed M, Oladokun A, Ibrahim NA, Adam SN. Serum leptin level in Sudanese women with unexplained infertility and its relationship with some reproductive hormones. *World J Biol Chem* 2022; 13(5): 83-94

URL: https://www.wjgnet.com/1949-8454/full/v13/i5/83.htm

DOI: https://dx.doi.org/10.4331/wjbc.v13.i5.83

INTRODUCTION

According to the World Health Organization, infertility is the inability of sexually active couples within 1 year who aren't under any contraceptive methods, to achieve clinically recognizable pregnancy[1]. Infertility can be due to male factors, female factors, combined factors or unknown (unexplained) factors [2,3]. Despite the discoveries and improvements in reproduction medicine, infertility prevalence seems to increase over time[4], where it is found to affect 10% of couples worldwide[1]. Nevertheless, the current knowledge and practices in infertility treatment proved a suitable treatment for almost all infertility types and their etiologies, except for unexplained infertility (UI), which is when standard-approved infertility tests have not found a clear cause for the couple's inability to achieve pregnancy[5]. Consequently, for such couples with UI, it may be very frustrating[6].

Studies from all around the world reported different prevalence's of UI (10%-37%)[1,3,7,8], whereby the highest prevalence was reported in low and middle-income countries (LMICs)[3,8]. In addition, women were reported to be responsible for at least 50% of all UI cases[1,8]. For all the above-mentioned reasons, UI has been identified as a public health priority, especially in LMICs like Sudan, which creates an urgent necessity to search and identify the unknown causes of infertility. Therefore, to achieve this goal, the reproductive system in women has been studied massively to find clear causes of UI. Studies proposed many possible causes of female UI, however, the diagnostic evidence for these proposed causes is still weak[9,10] and can't be counted on in infertility diagnosis.

Adipokines such as leptin were found to have a positive relationship with UI in females and they can be used as reliable predictive biomarkers for UI in women[11-13]. Leptin is a peptide hormone encoded in the LEP gene on chromosome 7q32.1[14]. Leptin is mainly produced by white adipocytes cells and when it is secreted in the plasma, it bonds with many binding proteins such as immunoglobulin

superfamily members siglec-6 and binds to the leptin receptor in the brain. This reaction activates the downstream signaling pathway of feeding inhibition and promotes energy expenditure, hence, it plays a key role in regulating basal metabolism, food consumption, energy expenditure and body weight[15-17].

Besides, leptin plays an important role in the physiological regulation of several neuroendocrine axes, such as hypothalamic-pituitary-gonadal, -thyroid, -growth hormone and -adrenal axes[15,16]. In particular, the effect of leptin has been studied on the hypothalamic-pituitary-ovarian (HPO) axis in females and its relationship with reproduction. These studies revealed that leptin and leptin receptors were extensively expressed in the HPO axis and this can be a strong argument about the effect of leptin on the reproduction process[18-20].

Leptin was found to have direct regulatory effects (inhibitory and stimulatory depending on its concentration) on all parts of the HPO axis[15,16]. In line with this conclusion, experimental evidence shows that the excessive concentration of leptin was found to have negative effects on all aspects of reproduction; ovarian steroidogenesis, folliculogenesis, oogenesis, and HPO axis hormones secretion [gonadotrophin-releasing hormone (GnRH), follicular stimulating hormone (FSH), luteinizing hormone (LH), prolactin hormone (PRL), anti-Mullerian hormone (AMH), estradiol (E2) as well as progesterone and testosterone (T)][16,21-23]. In addition, mice treated with anti-leptin drugs had a higher number of Graafian follicles in their ovaries compared with the non-treated group and this indicates that peripheral leptin may act as an inhibitor of ovarian follicle development and also on the HPO axis hormones[24].

Despite the established relationship between leptin and female reproduction, the exact role of leptin in women's infertility is not clear enough and a reasonable conclusion is that "we need further investigations to fill this diagnostic gap". Whereby, some studies, reported high levels of serum leptin in infertile women[25-27], other studies reported increased leptin levels in both fertile and infertile women, thus, high serum leptin levels in these patients were not a contributing factor for infertility[28]. The available findings of the role of leptin in female infertility are still contradicted, unexplained and need more clarification[29-34]. However, a meta-analysis of six studies which were conducted to find the relationship between leptin level and UI found that leptin level was higher in women with UI compared with fertile women, hence the study concludes that leptin can be used as an early predictive serum marker for UI in women[12]. Despite the many difficulties in diagnosis and treating UI, this early detection may improve pregnancy possibilities and reduce the treatment cost through increased clinical surveillance and clinical intervention for UI patients. Thus, the aim of this study was to evaluate the serum leptin levels in Sudanese women and to ascertain the relationship between serum leptin levels, UI and selected serum biomarkers between UI and fertile women.

MATERIALS AND METHODS

This matched [age and body mass index (BMI)] case-control study was conducted in Khartoum state-central Sudan during the period from March 2021 to February 2022. Study participants were recruited using the systematic random sampling technique from the largest health care facilities providing assisted conception services and modern antenatal care in the state and Sudan. In general, these hospitals and centers were purposefully selected, namely; Prof. El-Sir Abo Elhassan Fertility Center, Omdurman Maternity Hospital, Nile Fertility Center, Antenatal Care Hospital in Khartoum for Fertility, Khartoum Reproductive Health Care Center, Sudan Assisted Reproductive Clinic, University of Khartoum Fertility Center, Saad Abualila Teaching Hospital, Banoun Fertility Center and Hawwa Center for Fertility.

The required sample size of the current study (sample size to compare two means) was calculated using Open Epi software version 3.01. Based on the given inputs; 5% significance level and 80% power of the study with a mean difference of serum leptin levels of 0.97 between UI and fertile women[12], and a standard deviation of 4.29 for UI group and 2.11 for the fertile group, the minimum required sample size for the significant result was 382 (with 1:1 case-control ratio), however, to consider the non-response and attrition rates throughout the study period, a 5% have been added (5% attrition -38%). Therefore, a total of 420 Sudanese women were recruited for the study (210 infertile women with UI and 210 fertile women).

Participants' selection, recruitment, and exclusions

The current study targeted 420 Sudanese women between the age of 18 years to 44 years. The case group consisted of 210 women with UI and these cases were chosen from patients who had tried but were unable to conceive for at least a 1 year of regular unprotected sexual intercourse. In addition, they had regular menstruation, open uterine tubes, a normal size and shape of the uterine cavity according to the hysterosalpingography and no ovarian abnormalities such as fibroids and ovarian cysts according to transvaginal ultrasonography[2]. Also, of note, normal fertility tests of the woman, the male partner had a normal spermiogram "with a concentration of at least 15 million per milliliter of sperm, a motility value over 70 % and morphology of more than 4 % with normal forms"[2]. The control group consisted

of 210 fertile and non-pregnant women who had at least one healthy 2-year-old child (end of lactation).

Furthermore, study participants (cases and controls) were excluded from this study if they had any of the following illnesses; any sexual transmitted diseases, hypertension, diabetes, endocrine disorders, autoimmune/immunocompromised conditions, a history of genetic disease or severely obese (BMI of 35 kg/m^2 or more). In addition to that, women were also excluded if they were undergoing the effect of any aromatase inhibitors and/or anti-inflammatory medicines or if they were under the effects of hormonal contraception within the last 6 mo. Finally, any women who refused to sign the informed consent or withdrew during the study were excluded.

All study participants were examined by the primary investigator after obtaining written informed consent, obtaining their height (in meters) and weight (in kilograms) to find the BMI. Meanwhile, the hip measured at the level of the greater trochanter (in meter) and waist circumference measured at the level of the umbilicus (in meter) to determine the waist/hip ratio (WHR).

Serum collection and analysis

During the laboratory visits which occurred between 09:00 and 10:30 am for the women in the follicular phase of the cycle (on day 3 of the menstrual cycle) who were overnight fasting, a 5 mL sample of their peripheral blood was collected by venipuncture in a plain test tube and then the fresh blood was allowed to clot to get sera. Following the blood draw, the serum was separated by centrifuge at 3000 rpm for 5 min and immediately stored in a deep freezer at a temperature of -20 °C for subsequent analysis.

Serum levels of leptin hormone, FSH, LH, PRL, AMH, E2 and T were measured using the enzyme-linked immunosorbent assay (ELISA) method and the ELISA kits of the DRG diagnostics labs (DRG Diagnostics, Marburg Germany). All measurements were carried out in duplicate to ensure the quality of the results.

Data analysis

All data from this study were sorted and recorded in Microsoft Excel version 2016, cleaned, and then transferred to STATA software, version 16.0 (Stata Corp LLC, 77845 Texas, United States) for analysis. The data were presented as mean ± SD with a 95% confidence interval (CI), also tables and figures were used for data presentation. The normal distribution test of the study variables (Univariate, pairwise and multivariate[35]) was performed using the Shapiro Wilk test and data were considered as normally distributed if the *P* value is more than 0.05. The mean differences of the study variables (age, BMI, WHR, leptin serum level, FSH, LH, LH/FSH ratio, PRL, AMH, E2, T and E2/T ratio) between the two study groups were assessed using a two-tailed independent *t*-test for normally distributed variables (leptin serum level, LH/FSH ratio, PRL and T) and Mann-Whitney *U*-test for non-normally distributed variables (age, BMI, WHR, FSH, LH, AMH, E2 and E2/T ratio). Moreover, to magnitude the difference between the two groups we used effect sizes index for the difference between the two groups (Cohen's D for normally distributed data and rank biserial correlation for non-normally distributed data), and the threshold for interpreting these effect sizes were as follows: Small ≤ 0.20; medium ≤ 0.05; large ≤ 0.80; and very large > 0.80[36].

To better understand the study data, the association between leptin serum level and the other study variables, a correlation test was performed using Pearson's correlation for normally distributed data and Spearman's rank correlation for non-normally distributed data. Finally, to predict the serum leptin levels in Sudanese women, a multiple linear regression test was performed using the best-fit model after verifying all test assumptions. In addition, the collinearity was checked using the variance inflation factor. For all of the above-mentioned statistical tests, the threshold of significance was *P* value of < 0.05.

RESULTS

Participants' recruitment, follow-up and demographic variables

The current study recruited 420 Sudanese women (210 cases and 210 controls), of whom 20 women from the control group were removed due to the loss of the samples and the follow-up, giving a response rate of 95.2%. Finally, the study included a total of 400 women (210 women with UI as case subjects and 190 fertile women as control subjects). The study's two groups were matched by age and BMI, whereby the mean age (in years) was 28.59 and 28.44 for the case group and control group, respectively, and the mean BMI value was 24.67 and 24.41 for the case group and control group, respectively. The two groups had almost a similar mean value of WHR (0.844 for the UI group and 0.837 for the fertile group) (Table 1).

Serum biochemical parameters

Table 1 displayed the serum biomarkers investigated in this study; leptin, FSH, LH, LH/FSH ratio, PRL, AMH, E2, T and E2/T ratio. The results showed that there was a highly statistically significant difference between the two studied groups ($P < 0.001$) for all the above biomarkers. However, this statistical difference cannot be explained alone without weighting, therefore, to quantify this difference,

Table 1 Comparison of the examined variables (demographic variables and serum biochemical parameters) in the women with unexplained infertility and fertile women in Sudan

Variable	Unexplained infertility group, *n* = 210		Fertile group, *n* = 190		Effect size	*P* value
	mean ± SD	95%CI	mean ± SD	95%CI		
Age in yr	28.59 ± 5.22	27.87-29.3	28.44 ± 4.95	27.73-29.15	0.020[2]	0.731[4]
BMI in kg/m^2	24.67 ± 4.08	24.11-25.22	24.41 ± 4.38	23.78-25.03	0.046[2]	0.424[4]
WHR	0.844 ± 0.108	0.829-0.859	0.837 ± 0.114	0.821-0.854	0.032[2]	0.575[4]
Leptin in ng/mL	30.05 ± 5.22	29.34-30.76	22.89 ± 6.48	21.96-23.81	1.225[1]	< 0.001[3]
FSH in IU/L	6.42 ± 2.82	6.04-6.81	9.52 ± 2.79	9.12-9.92	0.558[2]	< 0.001[4]
LH in IU/L	10.32 ± 3.37	9.86-10.78	7.78 ± 2.19	7.46-8.09	0.423[2]	< 0.001[4]
LH/FSH ratio	1.7 ± 0.339	1.65-1.75	0.82 ± 0.075	0.81-0.83	3.502[1]	< 0.001[3]
PRL in μg/L	17.48 ± 3.434	17.01-17.95	12.52 ± 3.736	11.99-13.06	1.385[1]	< 0.001[3]
AMH in ng/mL	2.07 ± 0.418	2.01-2.13	2.43 ± 0.624	2.34-2.52	0.345[2]	< 0.001[4]
E2 in nmol/L	121.61 ± 30.54	117.46-125.77	154.86 ± 47.83	148.01-161.7	0.428[2]	< 0.001[4]
T in nmol/L	2.43 ± 0.52	2.36-2.51	2.12 ± 0.62	2.04-2.21	0.543[1]	< 0.001[3]
E2/T ratio	49.59 ± 3.97	49.05-50.13	72.69 ± 5.52	71.9-73.48	0.987[2]	< 0.001[4]

[1]Effect size is given by Cohen's d.
[2]Effect size is given by the rank biserial correlation.
[3]Student's *t*-test.
[4]Mann-Whitney *U*-test.
AMH: Anti-Mullerian hormone; BMI: Body mass index; CI: Confidence interval; E2: Estradiol; FSH: Follicular stimulating hormone; LH: Luteinizing hormone; PRL: Prolactin hormone; SD: Standard deviation; T: Testosterone; WHR: Waist/hip ratio.

Table 2 Correlation between leptin and the other variables in both the case and control groups

Variable	Unexplained Infertility group		Fertile group	
	r value	*P* value	*r* value	*P* value
Age in yr	-0.044[1]	0.524	-0.107[2]	0.142
BMI in kg/m^2	0.158[2]	0.022	0.398[2]	< 0.001[b]
WHR	0.141[1]	0.041	0.389[1]	< 0.001[b]
FSH in IU/L	-0.854[2]	< 0.001[b]	-0.723[1]	< 0.001[b]
LH in IU/L	-0.727[2]	< 0.001[b]	-0.683[1]	< 0.001[b]
LH/FSH	0.714[2]	< 0.001[b]	0.231[2]	< 0.001[a]
PRL in μg/L	0.888[2]	< 0.001[b]	0.888[2]	< 0.001[b]
AMH in ng/mL	0.928[2]	< 0.001[b]	0.917[2]	< 0.001[b]
E2 in nmol/L	0.916[2]	< 0.001[b]	0.967[2]	< 0.001[b]
T in nmol/L	0.932[2]	< 0.001[b]	0.359[2]	0.033
E2/T ratio	0.478[2]	< 0.001[b]	0.138[2]	0.057

[1]Pearson's correlation.
[2]Spearman's rank correlation.
[a]$P < 0.01$.
[b]$P < 0.001$.
AMH: Anti-Mullerian hormone; BMI: Body mass index; CI: Confidence interval; E2: Estradiol; FSH: Follicular stimulating hormone; LH: Luteinizing hormone; PRL: Prolactin hormone; T: Testosterone; WHR: Waist/hip ratio.

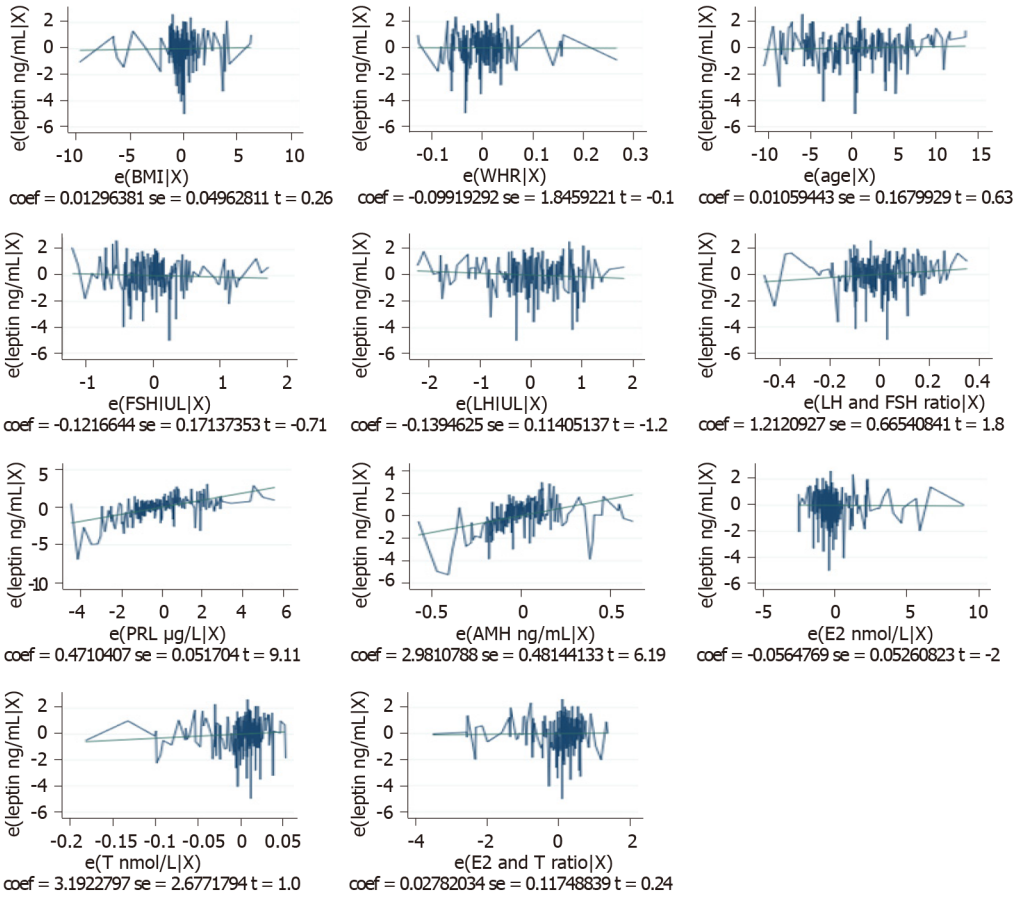

DOI: 10.4331/wjbc.v13.i5.83

Figure 1 Regression diagnostic plot for the independent predictors of serum leptin levels in Sudanese women with unexplained infertility. BMI: Body mass index; WHR: Waist/hip ratio; FSH: Follicular stimulating hormone; LH: Luteinizing hormone; PRL: Prolactin hormone; AMH: Anti-Mullerian hormone; E2: Estradiol.

an effect size test for the difference between the two groups was performed and the result found that the difference between the two groups was very large (effect size > 0.80) for leptin level, LH/FSH ratio, PRL level, and E2/T ratio, and large (effect size 0.50- ≤ 0.80) for FSH and T. To summarize the above-mentioned differences in the examined biomarkers, leptin, LH/FSH ratio, PRL and T were significantly higher in the UI group compared with the control group. In contrast, FSH, and E2/T ratio were significantly lower in the UI group than in the control group.

Association between leptin levels and other study variables

The association between leptin and other study variables in both the cases and control groups was shown in Table 2. The study results found a highly significant negative correlation between leptin levels and FSH and LH in both fertile and infertile women. On the other hand, leptin levels had a highly significant positive correlation with LH/FSH ratio, PRL, AMH, E2 and T in the two groups. However, the associations between leptin levels and E2/T ratio were positive in the two groups but statistically significant only in the UI group. This noticeable high association between leptin and other study variables requires further investigations so a multiple linear regression was performed to identify the independent predictors of serum leptin levels and the final model reveals that only PRL and AMH levels can be independent predictors ($P < 0.05$) of serum leptin level in Sudanese women with UI. The fully detailed prediction models were shown in Table 3 and Figures 1 and 2 below.

DISCUSSION

Leptin plays an important role in the function of the HPO axis by affecting the release of GnRH, gonadotrophins and aromatase enzymes from the hypothalamus, pituitary gland, and ovaries, respectively. Hence, it has a significant role in the reproductive process and reproductive hormone levels[16]. Studies on the possible relationship between leptin levels and UI showed that leptin was one of the most accurate serum biomarkers to detect UI in women[12,13,30], therefore, this study was

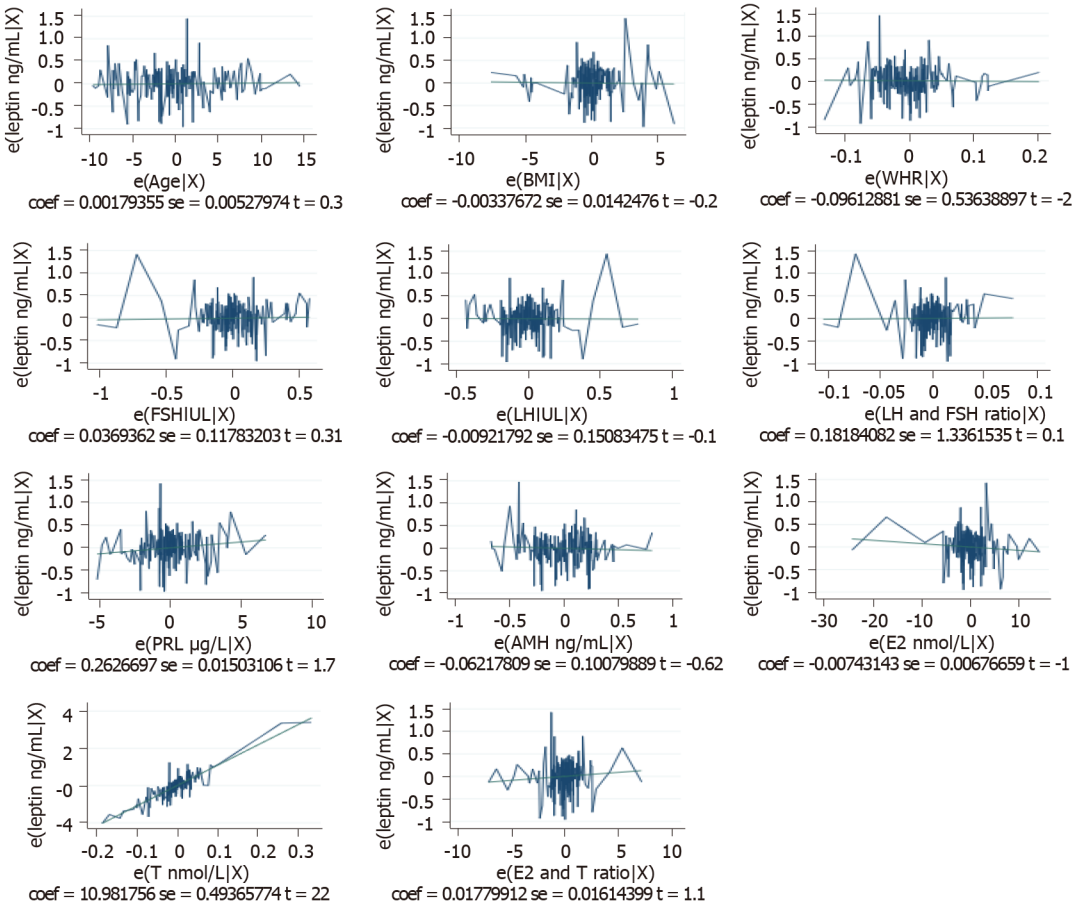

DOI: 10.4331/wjbc.v13.i5.83

Figure 2 Regression diagnostic plot for the independent predictors of serum leptin levels in fertile Sudanese women. BMI: Body mass index; WHR: Waist/hip ratio; FSH: Follicular stimulating hormone; LH: Luteinizing hormone; PRL: Prolactin hormone; AMH: Anti-Mullerian hormone; E2: Estradiol.

conducted to find the serum leptin levels in UI Sudanese women and their relationship with 4 gonadotropin biomarkers and 4 ovarian biomarkers after eliminating the effect of all possible confounding factors (age, BMI and WHR).

The current study revealed that the leptin serum level was significantly higher in women with UI compared with fertile women, 30.05 (95%CI: 29.34-30.76) and 22.89 (95%CI: 21.96-23.81), respectively, with a very large effect size of 1.225. This result is in line with the findings reported from Turkey[29], India[30], Iran[31] and Iraq[32,37], and in contrast with findings reported from Pakistan[33] and Iran [34]. The difference between the current findings reported from Sudan and other findings reported from other countries (which all were non-African countries), could be due to the difference in genetic makeup, sample sizes, age and BMI.

In this study, the four examined gonadotrophins biomarkers (LH, FSH, LH/FSH ratio and PRL) were significantly different between the two groups, whereby LH, LH/FSH ratio and PRL were significantly higher in the UI group than in the fertile group. Meanwhile, FSH was significantly lower in the UI group than in a fertile group. Furthermore, the high leptin serum level was strongly associated with the low level of FSH and LH (negative association) and the high level of LH/FSH ratio and PRL in UI women (positive association). These findings are consistent with the previous findings from Turkey [29], Iraq[32,37] and Iran[31]. However, the reported change in these biomarkers (high PRL, low LH and FSH) can be related to female infertility due to the fact that low FSH and LH levels together with the high level of PRL in females can induce ovulatory dysfunction, implantation defects and abnormal ovarian steroidogenesis[13,38]. In addition, from the examined ovarian biomarkers; AMH, E2, and E2/T ratio were significantly lower in the UI group compared with the fertile group. This low level of AMH, E2, and E2/T ratio in the UI group may affect the follicular growth and maturation[38-40]. This is in agreement with the findings of Demir *et al*[29] in Turkey, Tafvizi and Masomi[31] in Iran, Baig *et al*[33] in Pakistan and Abduljalal *et al*[37] in Iraq.

Meanwhile, similar to the results of Demir *et al*[29] in Turkey and Abduljalal *et al*[37] in Iraq, our study found that T was significantly higher in the UI group compared with the fertile group and this high T level can signal a potential female fertility problem that is mainly related to ovulatory dysfunction[41-43].

Table 3 Predictors of serum leptin levels in Sudanese women using the best-fit model

Independent variable	Model, leptin ng mL	Coefficients	*P* value	Beta, 95%CI	
				Lower	Upper
Constant	Unexplained infertility	6.812	0.274	-5.436	19.060
	Fertile	-1.076	0.527	-4.426	2.274
Age	Unexplained infertility	0.011	0.529	-0.023	0.044
	Fertile	0.002	0.734	-0.009	0.012
BMI	Unexplained infertility	0.013	0.794	-0.085	0.111
	Fertile	-0.003	0.813	-0.031	0.025
WHR	Unexplained infertility	-0.099	0.957	-3.739	3.541
	Fertile	-0.096	0.858	-1.155	0.962
FSH in IU/L	Unexplained infertility	-0.122	0.479	-0.460	0.216
	Fertile	-0.037	0.754	-0.196	0.269
LH in IU/L	Unexplained infertility	-0.139	0.223	-0.364	0.085
	Fertile	0.009	0.951	-0.307	0.288
LH/FSH	Unexplained infertility	1.212	0.070	-0.100	2.524
	Fertile	0.182	0.892	-2.455	2.819
PRL in μg/L	Unexplained infertility	0.471	< 0.001[a]	0.369	0.573
	Fertile	0.026	0.082	-0.003	0.056
AMH in ng/mL	Unexplained infertility	2.981	< 0.001[a]	2.032	3.930
	Fertile	-0.062	0.538	-0.261	0.137
E2 in nmol/L	Unexplained infertility	-0.006	0.915	-0.109	0.098
	Fertile	-0.007	0.274	-0.021	0.006
T in nmol/L	Unexplained infertility	3.192	0.235	-2.087	8.472
	Fertile	10.982	< 0.001[a]	10.008	11.956
E2/T ratio	Unexplained infertility	0.028	0.813	-0.204	0.260
	Fertile	0.018	0.272	-0.014	0.050

[a]$P < 0.05$.

AMH: Anti-Mullerian hormone; BMI: Body mass index; CI: Confidence interval; E2: Estradiol; FSH: Follicular stimulating hormone; LH: Luteinizing hormone; PRL: Prolactin hormone; T: Testosterone; WHR: Waist/hip ratio.

Despite the above, leptin was positively associated with AMH, T, and E2/T ratio and negatively associated with E2 in UI women. These results were supported by experimental findings which found that the high leptin level decreases the gene expression of the steroidogenic enzymes which leads to high T levels, low E2 and AMH levels[44]. An interesting finding in our study was that from all examined biomarkers, the strongest independent predictors of serum leptin levels in women with UI were only PRL and AMH levels, thus we can propose that leptins effect on female fertility by its cleared effect on two of the most important fertility hormones. The strength of this study was its control of all possible confounding factors and the relatively large sample size. Yet, limitations observed include that the study should have compared serum and follicular leptin levels.

CONCLUSION

The results of this study found that leptin, LH/FSH ratio, PRL, and T were significantly higher in the UI group compared with the control group. In contrast, FSH and E2/T ratio were significantly lower in the UI group than in the control group. Furthermore, this study reveals that leptin could be a potential biomarker for UI in Sudanese women and it may be useful for identifying women with a high risk of infertility. Thus, we recommend that the measuring of the leptin test should be introduced and become

one of the routine fertility tests, especially for UI cases. Finally, we recommend that further studies be carried out to clarify the exact association between leptin levels and UI in women.

ARTICLE HIGHLIGHTS

Research background

The current knowledge and practices in infertility treatment proved suitable for almost all infertility types and their etiologies, except for unexplained infertility (UI) which is when standard-approved infertility tests have not found a clear cause for the couple's inability to achieve pregnancy. Adipokines such as leptin were found to have a positive relationship with UI in females and they can be used as reliable predictive biomarkers for UI in women.

Research motivation

Despite the established relationship between leptin and female reproduction, the exact role of leptin in women's infertility is not clear enough and the reasonable conclusion is that "we need further investigations to fill this diagnostic gap". Where some studies reported high levels of serum leptin in infertile women, other studies reported increased leptin levels in both fertile and infertile women, thus, high serum leptin levels in these patients were not a contributing factor to infertility.

Research objectives

The objective of this study was to evaluate the serum leptin levels in Sudanese women and to ascertain the relationship between serum leptin levels and UI.

Research methods

A matched (age and body mass index) case-control study was conducted from March 2021 to February 2022. The study samples were 210 women with UI and 190 fertile women of reproductive age who were attending the maternity hospitals and fertility clinics in Khartoum state Sudan. The serum concentration of leptin and other serum biomarkers were determined using enzyme-linked immunosorbent assays.

Research results

The results showed that there was a highly statistically significant difference between the two groups ($P < 0.001$) for all examined eight biomarkers. Whereby, leptin, luteinizing hormone/follicular stimulating hormone (FSH) ratio, prolactin hormone and testosterone (T) were significantly higher in the UI group compared with the control group, in contrast, FSH and estradiol/T ratio were significantly lower in the UI group than in the control group.

Research conclusions

This study reveals that leptin could be a potential biomarker for UI in Sudanese women and it may be useful for identifying women with a high risk of infertility.

Research perspectives

Further studies need to be carried out to clarify the exact association between leptin levels and UI in women.

ACKNOWLEDGEMENTS

The authors would like to thank the Pan African University of Life and Earth Sciences Institute, the African Union for financial support, and the University of Ibadan for hosting this PhD program. Our appreciation also goes to data collectors and supervisors for their diligence during data collection to obtain necessary information. Our special thanks also go to participants who generously shared their thoughts and feelings despite other commitments. In addition, our thanks go to the federal ministry of health and administrators of all healthcare facilities included in this study for giving us the necessary background information to conduct this study.

FOOTNOTES

Author contributions: Abdulslam Abdullah A, Ahmed M, Oladokun A, Ibrahim NA, and Adam SN analyzed and interpreted the data, and drafted the manuscript; Abdulslam Abdullah A and Oladokun A designed the study and directed implementation and data collection; Abdulslam Abdullah A, Ahmed M, Oladokun A, Ibrahim NA, and Adam SN edited the manuscript for intellectual content and provided critical comments on the manuscript; and all

authors gave final approval of the version to be published, have agreed on the journal to which the article has been submitted, and agreed to be accountable for all aspects of the work.

Institutional review board statement: The study protocol and procedures were approved by the University of Ibadan/University College Hospital Ethics Committee (Ref. No. UI/EC/20/0438), and the Federal Ministry of Health Republic of Sudan (Ref. No. 4-12-20).

Informed consent statement: Informed consent was obtained from all the study participants, and all necessary information regarding the study (objectives, requirements of the participants, and duration of the study) were given to the prospective study participants on an information sheet in Arabic to ensure an informed decision to participate in the study. Then, the full case history of the participants was taken through clinical examinations and laboratory investigations. Ethical notions such as discretion/confidentiality, free consent of the interviewees as well as beneficence and non-maleficence to participants were scrupulously respected.

Conflict-of-interest statement: All the authors report having no relevant conflicts of interest for this article.

Data sharing statement: The datasets used during this study are available from the principal investigator upon reasonable request.

Country/Territory of origin: Sudan

ORCID number: Abdullah Abdulslam Abdullah 0000-0003-2534-4953; Musa Ahmed 0000-0003-0224-9718; Adesina Oladokun 0000-0002-5740-7608; Nasir Adam Ibrahim 0000-0001-6382-8807; Shahd Nourain Adam 0000-0002-8239-0246.

S-Editor: Wang JJ
L-Editor: Filipodia
P-Editor: Wang JJ

REFERENCES

1 **World Health Organization**. Infertility. [cited 12 March 2022]. Available from: https://www.who.int/news-room/fact-sheets/detail/infertility
2 **Mableson HE**, Okello A, Picozzi K, Welburn SC. Neglected zoonotic diseases-the long and winding road to advocacy. *PLoS Negl Trop Dis* 2014; **8**: e2800 [PMID: 24901769 DOI: 10.1371/journal.pntd.0002800]
3 **Abdullah AA**, Ahmed M, Oladokun A. Prevalence of infertility in Sudan: A systematic review and meta-analysis. *Qatar Med J* 2021; **2021**: 47 [PMID: 34650907 DOI: 10.5339/qmj.2021.47]
4 **Sun H**, Gong TT, Jiang YT, Zhang S, Zhao YH, Wu QJ. Global, regional, and national prevalence and disability-adjusted life-years for infertility in 195 countries and territories, 1990-2017: results from a global burden of disease study, 2017. *Aging (Albany NY)* 2019; **11**: 10952-10991 [PMID: 31790362 DOI: 10.18632/aging.102497]
5 **Mol BW**, Tjon-Kon-Fat R, Kamphuis E, van Wely M. Unexplained infertility: Is it over-diagnosed and over-treated? *Best Pract Res Clin Obstet Gynaecol* 2018; **53**: 20-29 [PMID: 30518485 DOI: 10.1016/j.bpobgyn.2018.09.006]
6 **Kiani Z**, Simbar M, Hajian S, Zayeri F, Shahidi M, Saei Ghare Naz M, Ghasemi V. The prevalence of anxiety symptoms in infertile women: a systematic review and meta-analysis. *Fertil Res Pract* 2020; **6**: 7 [PMID: 32313665 DOI: 10.1186/s40738-020-00076-1]
7 **Abebe MS**, Afework M, Abaynew Y. Primary and secondary infertility in Africa: systematic review with meta-analysis. *Fertil Res Pract* 2020; **6**: 20 [PMID: 33292584 DOI: 10.1186/s40738-020-00090-3]
8 **Abdelazim IA**, Purohit P, Farag RH, Zhurabekova G. Unexplained infertility: prevalence, possible causes and treatment options. A review of the literature. *J Obstet Gynecol Investigat* 2018; **1**: 17-22 [DOI: 10.5114/jogi.2018.74250]
9 **Ray A**, Shah A, Gudi A, Homburg R. Unexplained infertility: an update and review of practice. *Reprod Biomed Online* 2012; **24**: 591-602 [PMID: 22503948 DOI: 10.1016/j.rbmo.2012.02.021]
10 **Schattman GL**, Esteves S, Agarwal A. Unexplained infertility: Pathophysiology, evaluation treatment. New York: Springer, 2015
11 **Reverchon M**, Ramé C, Bertoldo M, Dupont J. Adipokines and the female reproductive tract. *Int J Endocrinol* 2014; **2014**: 232454 [PMID: 24695544 DOI: 10.1155/2014/232454]
12 **Abdullah AA**, Ahmed M, Oladokun A. Leptin levels in women with unexplained infertility: A systematic review and meta-analysis. *World J Meta-Anal* 2022; **10**: 37-45 [DOI: 10.13105/wjma.v10.i1.37]
13 **Qu T**, Yan M, Shen WJ, Li L, Zhu P, Li Z, Huang J, Han T, Hu W, Zhou R, Li P, Xu L, Huang T, Zhong Y, Gu J. Predictive serum markers for unexplained infertility in child-bearing aged women. *Am J Reprod Immunol* 2020; **83**: e13194 [PMID: 31585484 DOI: 10.1111/aji.13194]
14 LEP leptin [Homo sapiens (human)]. [cited 13 March 2022]. Available from: https://www.ncbi.nlm.nih.gov/gene/3952

15 **Mantzoros CS**, Magkos F, Brinkoetter M, Sienkiewicz E, Dardeno TA, Kim SY, Hamnvik OP, Koniaris A. Leptin in human physiology and pathophysiology. *Am J Physiol Endocrinol Metab* 2011; **301**: E567-E584 [PMID: 21791620 DOI: 10.1152/ajpendo.00315.2011]

16 **Khan SM**, Hamnvik OP, Brinkoetter M, Mantzoros CS. Leptin as a modulator of neuroendocrine function in humans. *Yonsei Med J* 2012; **53**: 671-679 [PMID: 22665330 DOI: 10.3349/ymj.2012.53.4.671]

17 **Mitchell M**, Armstrong DT, Robker RL, Norman RJ. Adipokines: implications for female fertility and obesity. *Reproduction* 2005; **130**: 583-597 [PMID: 16264089 DOI: 10.1530/rep.1.00521]

18 **Herrid M**, Palanisamy SK, Ciller UA, Fan R, Moens P, Smart NA, McFarlane JR. An updated view of leptin on implantation and pregnancy: a review. *Physiol Res* 2014; **63**: 543-557 [PMID: 24908087 DOI: 10.33549/physiolres.932674]

19 **Siawrys G**, Smolinska N. In vitro effects of luteinizing hormone, progesterone and oestradiol-17β on leptin gene expression and leptin secretion by porcine luteal cells obtained in early pregnancy. *J Physiol Pharmacol* 2013; **64**: 513-520 [PMID: 24101399]

20 **Maleszka A**, Smolinska N, Nitkiewicz A, Kiezun M, Chojnowska K, Dobrzyn K, Szwaczek H, Kaminski T. Adiponectin Expression in the Porcine Ovary during the Oestrous Cycle and Its Effect on Ovarian Steroidogenesis. *Int J Endocrinol* 2014; **2014**: 957076 [PMID: 24790602 DOI: 10.1155/2014/957076]

21 **Fornari MC**, Sarto A, Berardi VE, Martínez MA, Rocha MG, Pasqualini S, Diez RA. Effect of ovaric hyper-stimulation on blood lymphocyte subpopulations, cytokines, leptin and nitrite among patients with unexplained infertility. *Am J Reprod Immunol* 2002; **48**: 394-403 [PMID: 12607776 DOI: 10.1034/j.1600-0897.2002.01128.x]

22 **Hausman GJ**, Barb CR, Lents CA. Leptin and reproductive function. *Biochimie* 2012; **94**: 2075-2081 [PMID: 22980196 DOI: 10.1016/j.biochi.2012.02.022]

23 **Avelino-Cruz JE**, Flores A, Cebada J, Mellon PL, Felix R, Monjaraz E. Leptin increases L-type Ca2+ channel expression and GnRH-stimulated LH release in LbetaT2 gonadotropes. *Mol Cell Endocrinol* 2009; **298**: 57-65 [PMID: 18834922 DOI: 10.1016/j.mce.2008.09.003]

24 **Panwar S**, Herrid M, Kauter KG, McFarlane JR. Effect of passive immunization against leptin on ovarian follicular development in prepubertal mice. *J Reprod Immunol* 2012; **96**: 19-24 [PMID: 22989496 DOI: 10.1016/j.jri.2012.07.004]

25 **Barcz E**, Milewski L, Radomski D, Dziunycz P, Kamiński P, Roszkowski PI, Malejczyk J. A relationship between increased peritoneal leptin levels and infertility in endometriosis. *Gynecol Endocrinol* 2008; **24**: 526-530 [PMID: 18958774 DOI: 10.1080/09513590802288200]

26 **Dayer D**, Nikbakht R, Kadkhodai Elyaderani M. Comparison of leptin concentrations between infertile women with polycystic ovary syndrome and fertile women. *Iran J Reprod Med* 2013; **11**: 1033-1034 [PMID: 24639732]

27 **Kucera R**, Babuska V, Ulcova-Gallova Z, Kulda V, Topolcan O. Follicular fluid levels of anti-Müllerian hormone, insulin-like growth factor 1 and leptin in women with fertility disorders. *Syst Biol Reprod Med* 2018; **64**: 220-223 [PMID: 29595066 DOI: 10.1080/19396368.2018.1450906]

28 **Wertel I**, Gogacz M, Polak G, Jakowicki J, Kotarski J. Leptin is not involved in the pathophysiology of endometriosis-related infertility. *Eur J Obstet Gynecol Reprod Biol* 2005; **119**: 206-209 [PMID: 15808381 DOI: 10.1016/j.ejogrb.2004.08.004]

29 **Demir B**, Guven S, Guven ES, Atamer Y, Gunalp GS, Gul T. Serum leptin level in women with unexplained infertility. *J Reprod Immunol* 2007; **75**: 145-149 [PMID: 17485120 DOI: 10.1016/j.jri.2007.04.001]

30 **Kumari P**, Jaiswar SP, Shankhwar P, Deo S, Ahmad K, Iqbal B, Mahdi AA. Leptin as a Predictive Marker in Unexplained Infertility in North Indian Population. *J Clin Diagn Res* 2017; **11**: QC28-QC31 [PMID: 28511457 DOI: 10.7860/JCDR/2017/22444.9567]

31 **Tafvizi F**, Masomi M. Comparison of Serum Leptin Level in Women with Unexplained Infertility and Fertile Women in Iran. *J Obstet Gynaecol India* 2016; **66**: 466-470 [PMID: 27651647 DOI: 10.1007/s13224-016-0843-9]

32 **Al-Fartosy AJM**, Awad NA, Mahmood RA. A comparative study of leptin, oxidant/antioxidant status and some trace elements in women of healthy control and unexplained infertility in Basrah-Iraq. *Indone Biomed J* 2019; **11**: 327-337 [DOI: 10.18585/inabj.v11i3.915]

33 **Baig M**, Azhar A, Rehman R, Syed H, Tariq S, Gazzaz ZJ. Relationship of Serum Leptin and Reproductive Hormones in Unexplained Infertile and Fertile Females. *Cureus* 2019; **11**: e6524 [PMID: 32025443 DOI: 10.7759/cureus.6524]

34 **Kamyabi Z**, Gholamalizade T. A Comparative Study of Serum and Follicular Fluid Leptin Concentrations among Explained Infertile, Unexplained Infertile and Fertile Women. *Int J Fertil Steril* 2015; **9**: 150-156 [PMID: 26246872 DOI: 10.22074/ijfs.2015.4235]

35 **Keselman HJ**, Othman AR, Wilcox RR. Preliminary testing for normality: Is this a good practice? *J Modern Appl Statist Methods* 2013; **12**: 1-19 [DOI: 10.22237/jmasm/1383278460]

36 **Sullivan GM**, Feinn R. Using Effect Size-or Why the P Value Is Not Enough. *J Grad Med Educ* 2012; **4**: 279-282 [PMID: 23997866 DOI: 10.4300/JGME-D-12-00156.1]

37 **Abduljalal MH**, Chilmeran SK, Ali Z, Salih SA. Evaluation of serum leptin level, lipid profile and sex hormones in infertile females of unknown cause. *Biochem Cell Arch* 2021; **21**: 4473-4477

38 **Murto T**, Bjuresten K, Landgren BM, Stavreus-Evers A. Predictive value of hormonal parameters for live birth in women with unexplained infertility and male infertility. *Reprod Biol Endocrinol* 2013; **11**: 61 [PMID: 23844631 DOI: 10.1186/1477-7827-11-61]

39 **Grynnerup AG**, Lindhard A, Sørensen S. Anti-Müllerian hormone levels in salpingectomized compared with nonsalpingectomized women with tubal factor infertility and women with unexplained infertility. *Acta Obstet Gynecol Scand* 2013; **92**: 1297-1303 [PMID: 24032634 DOI: 10.1111/aogs.12234]

40 **Seckin B**, Tokmak A, Yumusak OH. The role of anti-Müllerian hormone in prediction of pregnancy in young and older women with unexplained infertility undergoing intrauterine insemination. *J Chin Med Assoc* 2019; **82**: 300-304 [PMID: 30946209 DOI: 10.1097/JCMA.0000000000000023]

41 **Barbieri RL**, Sluss PM, Powers RD, McShane PM, Vitonis A, Ginsburg E, Cramer DC. Association of body mass index, age, and cigarette smoking with serum testosterone levels in cycling women undergoing in vitro fertilization. *Fertil Steril*

2005; **83**: 302-308 [PMID: 15705366 DOI: 10.1016/j.fertnstert.2004.07.956]

42 **Olooto WE**, Amballi AA, Banjo TA. A review of Female Infertility; important etiological factors and management. *J Microbiol Biotech Res* 2017; **2**: 379-385

43 **Rashid BM**, Mahmoud TJ, Nore BF. Hormonal study of primary infertile women. *J Zankoy Sulaimani-Part A* 2013 [DOI: 10.17656/jzs.10253]

44 **Masarwi M**, Shamir R, Phillip M, Gat-Yablonski G. Leptin stimulates aromatase in the growth plate: limiting catch-up growth efficiency. *J Endocrinol* 2018; **237**: 229-242 [PMID: 29615477 DOI: 10.1530/JOE-18-0028]

Published by **Baishideng Publishing Group Inc**
7041 Koll Center Parkway, Suite 160, Pleasanton, CA 94566, USA
Telephone: +1-925-3991568
E-mail: bpgoffice@wjgnet.com
Help Desk: https://www.f6publishing.com/helpdesk
https://www.wjgnet.com